PH.D. THESIS

# Thermo-Ecological Cost assessment for renewable energy systems

*Author:*
Agnieszka SZOSTOK

*Supervisor:*
Wojciech STANEK


Scientific discipline: Environmental Engineering, Mining and Energy

Gliwice, Poland, 2025

**Author:**
Agnieszka Szostok, M.Sc.
Silesian University of Technology
Faculty of Energy and Environmental Engineering
Department of Thermal Technology
Konarskiego 22, 44-100 Gliwice, Poland

**Supervisor:**
Wojciech Stanek, Prof.
Professor at Silesian University of Technology
Faculty of Energy and Environmental Engineering
Department of Thermal Technology
Konarskiego 22, 44-100 Gliwice, Poland
e-mail: wojciech.stanek@polsl.pl

**Polish title:**
Ocena kosztu termo-ekologicznego systemów energetycznych wykorzystujących odnawialne źródła energii

# Acknowledgements

I would like to express my sincere gratitude to my supervisor, Prof. Wojciech Stanek, for his continuous guidance, encouragement, and dedication throughout my academic journey – from the first and second degree of studies to the completion of this Ph.D. thesis. His expertise, patience, and insightful feedback have been invaluable at every stage of my work. I am deeply thankful for his mentorship, which has helped me grow both academically and personally.

My sincere thanks also go to all the people I have met along my professional path. I am grateful for their contributions and collaboration, which have supported my development in many ways. I am especially thankful to my family and friends for their constant support, patience, and motivation throughout this journey.

# Contents

# List of monothematic publications

The thesis consists of three monothematic papers listed below. The full texts of these papers can be found in the Appendices chapter. The papers are referred by the Roman numerals through the thesis.

I. Agnieszka Szostok, Wojciech Stanek, Thermo-ecological analysis - The comparison of collector and PV to PV/T system, Renewable Energy, Volume 200, 2022, Pages 10-23, ISSN 0960-1481, https://doi.org/10.1016/j.renene.2022.09.070.

II. Agnieszka Szostok, Wojciech Stanek, Thermo-ecological analysis of the power system based on renewable energy sources integrated with energy storage system, Renewable Energy, Volume 216, 2023, 119035, ISSN 0960-1481, https://doi.org/10.1016/j.renene.2023.119035.

III. Wojciech Stanek, Agnieszka Szostok, Thermo-ecological assessment of microgrid supported with renewable energy, Energy, Volume 314, 2025, 134256, ISSN 0360-5442, https://doi.org/10.1016/j.energy.2024.134256.

# Nomenclature

| | | |
|---|---|---|
| **A** | Surface | [$m^2$] |
| **B** | Exergy | [MJ] |
| **$\dot{B}$** | Exergy stream | [MJ/h] |
| **CHP** | Combined Heat and Power | |
| **COP** | Coefficient of performance | |
| **DHW** | Domestic hot water | |
| **ΔT** | Difference of temperature | [K] |
| **E** | Energy | [kW] |
| **EMS** | Energy management system | |
| **ES** | Energy storage system | |
| $I_\beta$ | Solar radiation | [kW/$m^2$] |
| **LCA** | Life cycle assessment | |
| $\dot{m}$ | Mass stream | [kg/s] |
| **P** | Power | [kW] |
| **PV** | Photovoltaic | |
| **PV** | Photovoltaic system | |
| **PV/T** | Photovoltaic-Thermal hybrid system | |
| **Q** | Heat | [kW] |
| **RES** | Renewable energy sources | |
| **STEPS** | Stated policies scenario | |
| **T** | Temperature | [K] |
| **t** | Temperature | [°C] |
| **TEA** | Thermo-economic analysis | |
| **TEC** | Thermo-ecological cost | [MJ/MJ] |
| **VRE** | Variable renewable energy | |
| **ε-NTU** | Effectiveness–Number of Transfer Units | |
| **η** | Efficiency | |
| $\dot{W}$ | Heat capacity of stream | [kW/s] |
| **Subscripts** | | |
| **0** | Environment | |
| **C** | Collector | |

| | |
|---|---|
| **d** | Demand |
| **E** | Electrolyser |
| **FC** | Fuel cell |
| **G** | Grid |
| **PV** | Photovoltaic system |
| **PV/T** | Photovoltaic-Thermal hybrid system |
| **ref** | Reference |
| **s** | Stored |
| **W** | Wind turbine |

## Chapter 1

# Introduction

## 1.1. Background

Between 2013 and 2023, global demand for energy has increased by 15.0%. In the Stated Policies Scenario (STEPS) developed by the International Energy Agency, global electricity demand nearly doubles by 2050, rising from 26 000 TWh in 2023 to 50 000 TWh in 2050 [1]. This highlights that the challenges facing the energy sector related to increased energy production will continue to grow. In 2023, global primary energy consumption reached an all-time high of 620 exajoules (EJ). Global fossil fuel consumption also hit a record level, amounting to 505 EJ [2].

The combustion of fossil fuels gives rise to a range of environmental and social challenges. The energy sector is currently the largest emitter of carbon dioxide globally. By 2023, it was responsible for 36.0% of global energy-related $CO_2$ emissions. Methane, primarily, fugitive emissions from oil, gas, and coal, accounted for 18.0% of greenhouse gas emissions in 2019. Limiting warming to well below 2°C will require significant changes to the energy system over the next 30 years. This includes reduced fossil fuel use, increased production from low-emission and zero-emission energy sources, and increased use of alternative energy carriers and electricity [3].

A second critical issue is the limited availability of fossil fuel resources. Geopolitical tensions and armed conflicts, such as Russia's aggression against Ukraine and escalating hostilities in the Middle East, further exacerbate the instability of fossil fuel markets. The transition away from fossil fuels is accompanied by a shift towards renewable energy sources [1, 2, 4]. The fastest growth is observed in solar PV and wind power. . Between 2010 and 2023, global PV capacity increased fortyfold, and wind power capacity increased sixfold. Growth was concentrated in the European Union, the United States, China and Japan. Other renewable energy technologies have also expanded: hydropower grew by a factor of 1.4 and bioenergy capacity increased two and a half times. In 2023, the total installed capacity of solar PV and wind was about 550 GW. According to the STEPS scenario, more than 800 GW will be added each year by 2040 [1].

As the world moves toward a more electrified and renewable-rich energy system, new threats to energy security are emerging, highlighting certain needs related to these systems. Power system flexibility—necessary to balance wind and solar power with changing demand patterns—will quadruple by 2050, even as the retirement of fossil fuel generation capacity reduces conventional sources of flexibility. Rapid electrification across all sectors makes electricity even more crucial to energy security worldwide than it is today. This transformation requires a significant increase in the use of all sources of flexibility: batteries, demand response systems, and low-emission, flexible power plants, supported by smarter and more digital electricity grids [5, 6].

An energy system powered by green energy technologies is fundamentally different from one that relies conventional hydrocarbon resources. Wind farms, solar photovoltaic (PV) plants and electric

vehicles typically require significantly larger amounts of minerals to build than systems based on fossil fuels. Since 2010, mineral demand for each new unit of power generation has grown by 50%. This rise is due to the growing share of renewables in new energy investments. Meeting climate goals with more low-carbon energy will also lead to the energy sector needing minerals tripling by 2040 [7].

At the same time, the final stage of the life cycle of energy components poses significant challenges. Waste generated during the development and use of renewable energy infrastructure is resource-rich. It contains rare earth elements in addition to other valuable materials such as copper, steel, and glass. Recovering and reintroducing materials into the production cycle presents several challenges. These include complex logistics, such as high volumes and the need to recover materials from remote locations. Another issue is product design that does not account for end-of-life management or recyclability. Additionally, the presence of hazardous substances complicates the recovery process [8].

The growing role of renewable energy sources and the challenges posed by grids based on them encourage the search for new assessment methods. This PhD thesis presents the Thermo-Ecological Cost (TEC) Assessment. TEC expresses the cumulative consumption of non-renewable exergy per unit of any product considered useful. It is an application of exergy analysis proposed by Szargut [9], which allows for the integration of exergy and ecology. The method accounts for the cumulative exergy consumption of non-renewable resources throughout the entire life cycle of a product – from raw material extraction, through production and use, to activities related to environmental protection and reclamation. TEC should also include the consumption of non-renewable exergy for environmental protection or compensation for the negative effects of harmful emissions in production processes [10].

Thermo-Ecological Cost is expressed not in monetary units but in exergy units, and it does not replace or supplement classical economics. The method could be useful in developing concepts such as a pro-ecological tax proportional to the Thermo-Ecological Cost of a given market product [11]. TEC enables the comparison of renewable and non-renewable energy sources, showing the importance of introducing RES in the context of non-renewable resource conservation, while at the same time indicating the challenges of these technologies. Renewable energy sources also carry a certain Thermo-Ecological Cost, as the production of the necessary equipment requires the consumption of non-renewable resources [10].

## 1.2. Literature survey

### 1.2.1. Thermo-Ecological Cost (TEC) Assessment

The Thermo-Ecological Cost (TEC), calculated annually, serves as a tool for assessing how efficiently natural resources are managed. It combines exergy—reflecting the quality of resources—with cumulative calculations, and by accounting for non-renewable resources through cumulative exergy consumption, it provides a measure of overall exergy-ecological performance [12–14]. It should be stressed that the Thermo-Ecological Cost, as a systems-oriented approach, plays an important role in the comparison of different energy systems. One possible way of presenting the physical and ecological burden of each product (reflecting the total use of natural resources at the stage of their extraction from nature) is the Thermo-Ecological Cost (TEC). This measure accounts for the exergy consumption of non-renewable resources obtained directly from nature, such as freshwater, fuels, and mineral ores. TEC is defined (according to Szargut [9]) as: “cumulative consumption of non-renewable exergy associated with the production of a specific product, including additionally the consumption required

to offset environmental losses caused by the release of harmful waste into the environment". The main applications of TEC include [9,15,16]:

- Assessing the influence of operating parameters of energy systems on fossil fuel resource depletion.
- Estimating the effect of releasing harmful substances into the environment on the reduction of non-renewable resources.
- Optimizing operating parameters, the production structure of a given utility product, and designing parameters that contribute to minimizing non-renewable resource depletion.
- Choosing technologies that ensure the lowest possible depletion of non-renewable resources.
- Analysing the effect of interregional exchange on the depletion of non-renewable resources.
- Estimating the degree of sustainable development.
- Determining the influence of individual consumer products on non-renewable resource depletion over their entire life cycle.
- Calculating the amount of eco-tax that could replace existing taxation.

**1.2.2. Idea of TEC balance equation**

TEC may also rise as a result of the consumption of by-products exchanged between different branches of the system. In this context, the Thermo-Ecological Cost of pollutants is not determined as chemical exergy, but rather as the amount of energy required to prevent their release into the environment. A typical example is the use of exergy in emission reduction installations. When preventing the emission of such pollutants is not possible, the Thermo-Ecological Cost should be expressed as the exergy needed to mitigate the negative impacts caused by wastes introduced into the environment [17, 18]. In certain processes, by-products may substitute the main product in other applications, thereby lowering the TEC value of the primary product under analysis [9, 19, 20]. The specific Thermo-Ecological Cost can be defined by three components (Eq.(1)):

- The first component refers to the exergy of non-renewable natural resources directly consumed in the process $b_{sj}$.
- The second component includes the Thermo-Ecological Cost of harmful substances $\zeta_k$ generated by the process. Both of these elements contribute to an increase in the TEC value.
- The last component of the specific Thermo-Ecological Cost, a0ssociated with by-products $f_{ij}$ can reduce volume of the index of operational TEC $\rho_i$or increase it when the consumption of the i-th material per unit of the j-th main product is significant [9, 15, 16, 19, 21].

$$\rho_j = \sum_s b_{sj} + \sum_k p_{kj}\zeta_k - \sum_i (f_{ij} - a_{ij})\rho_i \tag{1}$$

Where:

$b_{sj}$ exergy of *s*-th non-renewable natural resource immediately consumed in the process under consideration per unit of *j*-th product [MJ/kg],

$\zeta_k$ Thermo-Ecological Cost of *k*-th harmful substance [MJ/kg].

$p_{kj}$ amount of *k*-th harmful substance from *j*-th process [kg],

$f_{ij}$ coefficient of by-production of *i*-th product per unit of *j*-th main product [kg/kg or kg/MJ],

$a_{ij}$ coefficient of consumption of *i*-th material per unit of *j*-th main product [kg/kg or kg/MJ],

$\rho_i$ specific Thermo-Ecological Cost of *i*-th product [MJ/kg].

The schematic representation of the Thermo-Ecological Cost (TEC) balance is shown in **Figure *1*.**

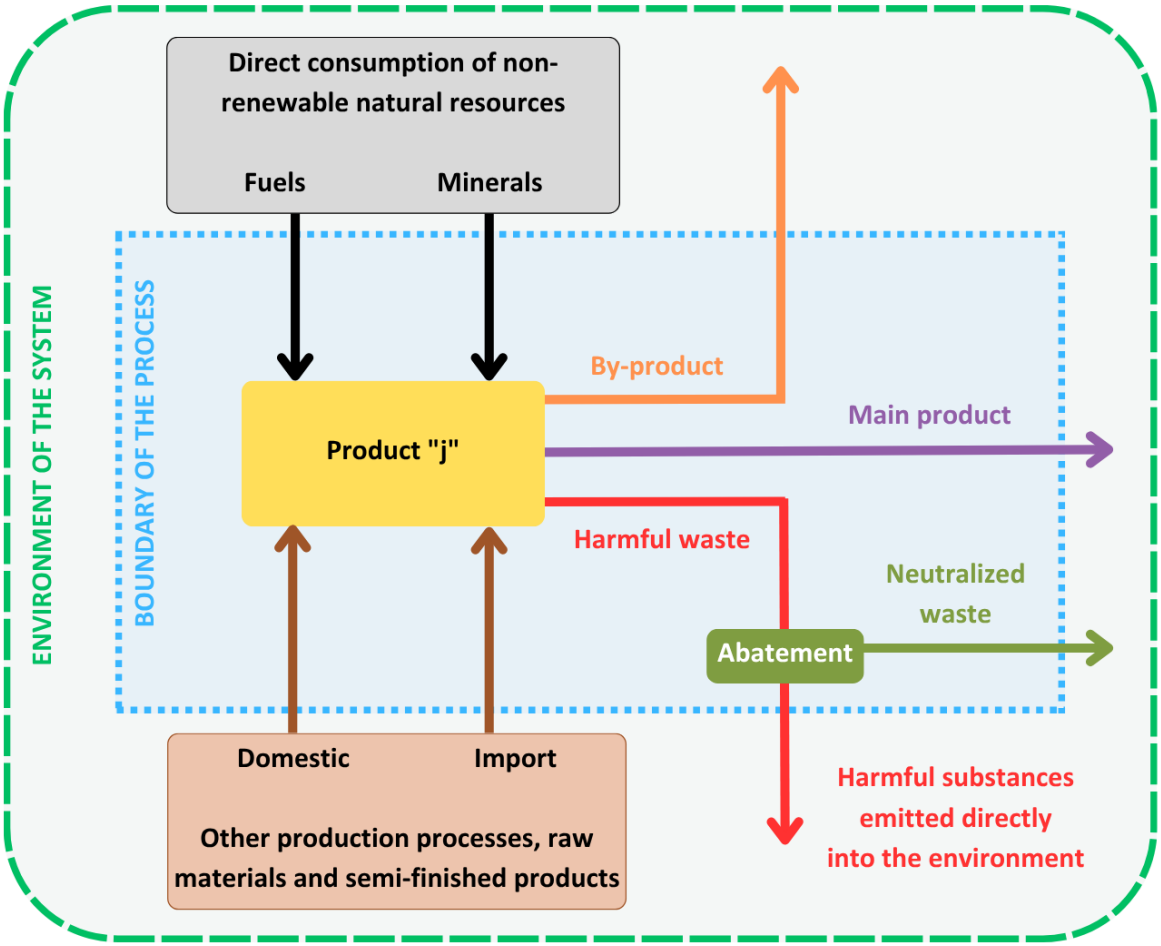


**Figure 1. Concept of the TEC balance equation**

It should be emphasised that the above equation describes only the operational stage; however, in the case of power technologies, other phases of the life cycle may also be significant. The general equation for calculating TEC throughout the entire life cycle, formulated by Szargut [9] and applied in the analysis of the exergetic life cycle of a solar collector system by Szargut and Stanek [19] is presented by Eq.(2):

$$\rho_j^{LCA} = \theta_n \left( \sum_i \dot{G}_i \rho_i + \sum_k \dot{P}_k \zeta_k - \sum_u \dot{G}_u \rho_j s_{ju} \right) + \frac{1}{\tau_j} \left( \sum_l G_l \rho_l (1 - u_l) + \sum_r G_r \rho_r \right) \quad (2)$$

Where:

$\theta_n$ average annual time of exploitation of *j*-th considered machine, device, installation or building, in other words annual operation time with nominal capacity [h/year],

$\dot{G}_i$ nominal stream of *i*-th material used in *j*-th production process [kg/h],

$\dot{P}_k$ nominal stream of *k*-th waste product released to the environment from *j*-th production process [kg/h],

$\dot{G}_u$ nominal stream of *u*-th by-product manufactured simultaneously with *j*-th product within the production process [kg/h],

$s_{ju}$ replacement index of by-product *u* by main product *j*,

$\tau_j$ nominal lifetime of *j*-th machine, device, installation or building, years,

$G_l$ amount of *l*-th material used for the construction of *j*-th considered machine, device, installation or building [kg],

$u_l$ expected recovery rates of *l*-th material after the end of operation phase of *j*-th considered machine, device, installation or building [kg/kg],

$G_r$ amount of *r*-th material used for the maintenance of *j*-th considered machine, device, installation or building [kg].

### 1.2.3. Applications of the TEC method

The TEC algorithm was introduced by Szargut in 1986 in the paper "Application of exergy for the calculation of ecological cost" [14, 22]. Subsequent studies have focused on the analysis of the TEC method proposed by Professor Szargut and present numerous computational examples of using exergy analysis to assess ecological impacts. These studies address issues related to renewable energy sources, including solar energy [19, 23], wind energy [24–26], biomass and biofuels [27, 28], heat pumps [29], as well as the integration of various RES [30–33]. The studies also presented the application of the TEC method in the analysis of nuclear energy systems [34, 35]. Several publications on the implementation of the TEC method also address the analysis of fossil fuel-based energy systems [36–40] as well as hybrid systems combining fossil fuels and renewable energy sources [41–43]. The presented examples of applying exergy analysis to assess ecological impacts also include studies on individual components of energy systems [44] as well as research focused on the development of specific elements of the TEC algorithm [45–53].

### 1.2.4. Thermo-Economic Analysis (TEA)

The purpose of thermo-economic analysis is to assess, optimise, and diagnose energy-intensive systems by combining exergy-based evaluation (grounded in the Second Law of Thermodynamics) with economic considerations [54]. TEA analysis results provide valuable information on system performance and can assist in improving efficiency. Such modifications may include, for example, design improvements or operational strategies. Optimization can also focus on minimizing exergy losses or finding a balance between them [55, 56].

This approach is particularly important in energy-intensive sectors. A prime example is the energy sector, where reducing exergy losses and improving cost efficiency are crucial for operational efficiency and long-term sustainability [57]. By measuring irreversibility and resource use, TEA helps design economically viable systems that are also environmentally friendly. In the case studied, this method demonstrated significant potential for reducing emissions and conserving resources while simultaneously improving system reliability [58, 59].

## 1.3. Motivation and objectives

Increasing energy demand and climate change call for more sustainable methods of assessing energy systems. Standard efficiency indicators do not fully account for environmental impacts and resource depletion. The main objective of this thesis is to develop and apply the Thermo-Ecological Cost (TEC) method for the assessment of energy systems based on renewable energy sources. To achieve this overall goal, the following specific objectives are defined:

- To determine the TEC value for a photovoltaic-thermal PV/T system. These data have not been previously reported in the literature, and their determination is essential for further research on grids that include a PV/T component.
- To develop a method for allocating the Thermo-Ecological Cost in hybrid systems such as PV/T.
- To compare solar technologies (PV, solar collector, PV/T) in terms of their Thermo-Ecological Cost and consumption of non-renewable resources.
- To simulate and analyse a microgrid based on multiple renewable energy sources, including integration with an energy storage system.
- To determine TEC values for a microgrid producing electricity, heat, and useful cooling.
- To identify energy mix configurations for the microgrid that minimize the Thermo-Ecological Cost and maximize independence from the external power grid.
- To indicate the environmental and resource-related benefits resulting from the integration of different renewable energy sources and energy storage technologies.

## 1.4. Subject of the study

The following section of this chapter presents a detailed characterization of an energy system based on renewable energy sources (RES). The system comprises various technologies, including wind turbines, photovoltaic (PV) panels, hybrid PV/T modules, solar collectors, a biogas-powered combined heat and power (CHP) unit, heat pumps, and an energy storage system consisting of an electrolyser and fuel cells. The chapter describes the generation of electricity, heat, and cooling. The description includes information about the individual components of the system and an operational analysis of the various elements, taking into account their interactions and impact on the overall system efficiency.

The analysed microgrid is a trigeneration system composed of energy, heat, and cooling sources. Energy storage is implemented to allow the system to operate autonomously for as long as possible, and various energy sources are used to reduce dependence on a single weather variable. The schematic diagram of the analysed microgrid is presented in the figure below (**Figure *2***).

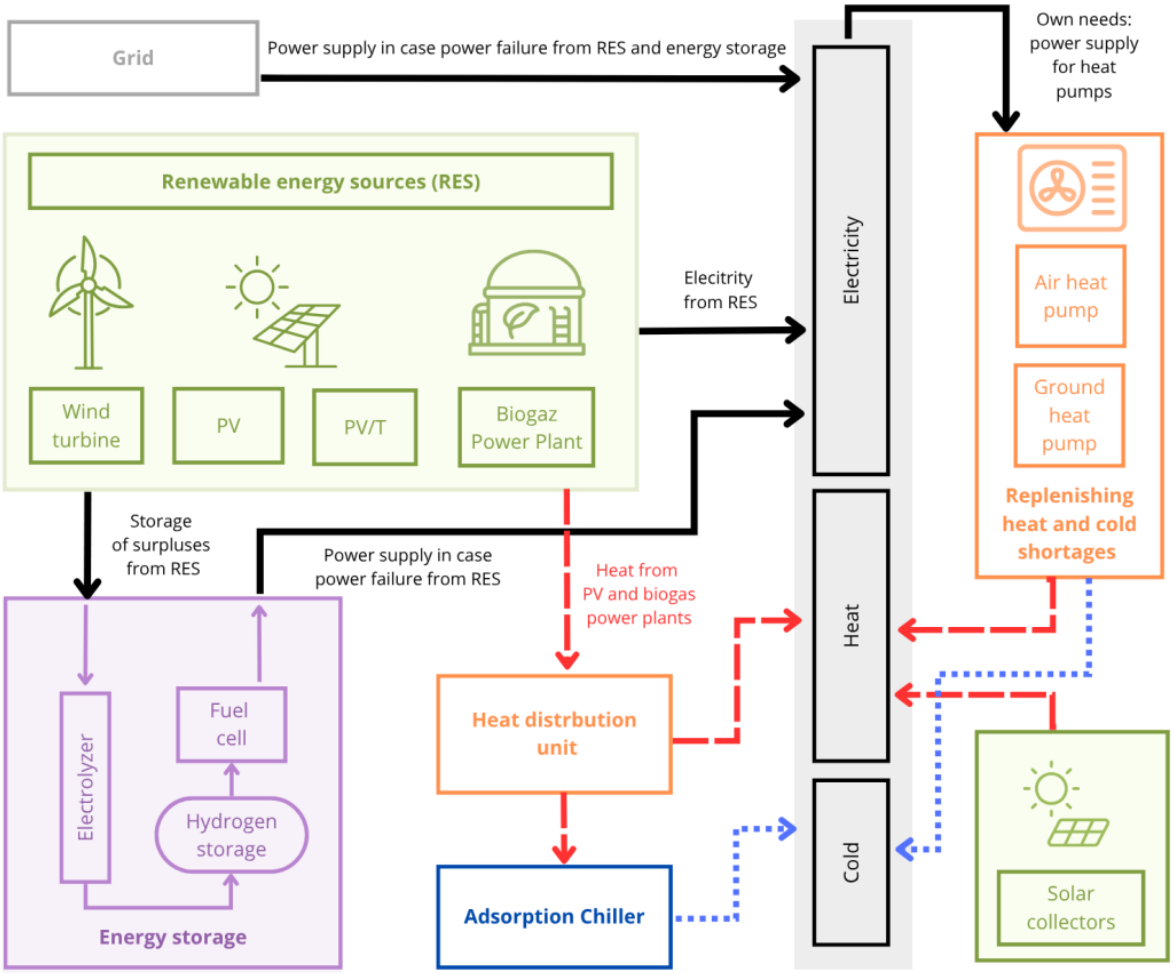


**Figure 2. Schematic diagram of a microgrid – description**

In the microgrid, electrical energy is generated by a wind turbine, photovoltaic panels, PV/T panels, and a CHP engine powered by biogas (biogas power plant). Electrical energy from renewable energy sources (RES) is first supplied to meet the current demand of end users. Surplus energy produced by RES is directed to an energy storage system, consisting of an electrolyser, hydrogen storage, and a fuel cell. When renewable energy sources do not cover the current microgrid demand, energy is drawn from the storage system. If this is insufficient and current consumption exceeds the combined production from RES and available energy in storage, electricity is supplied from the grid.

Heat is also produced in the system. It is obtained from the PV/T system and the biogas power plant. The system also includes solar collectors that provide domestic hot water production (mainly in summer months). Heat from the PV/T system and the biogas power plant can also be used for cooling purposes through the use of adsorption chillers in the system. In cases where heat generated within the system does not meet current demand, heat pump systems (air and ground source) are utilised. Their application allows for compensating deficits in both heat and cooling. The operation of the individual components was simulated under real weather conditions characteristic of Katowice (Poland) [60]. **Figure *3*** presents the exergy flows through the analysed system.

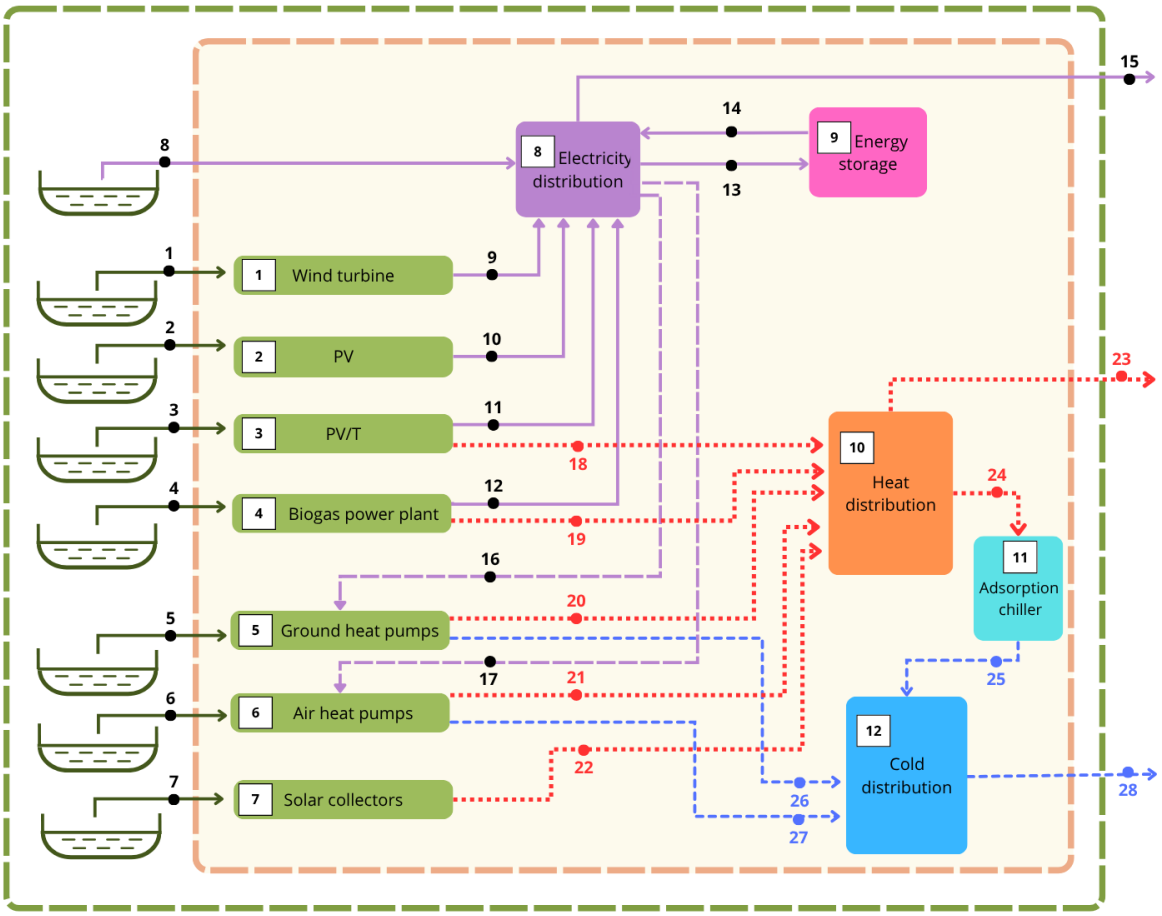


**Figure 3. Exergy streams in the analysed system**

**Table *1*** presents the fuel and product for each component of the system. Streams 1–8 represent exergy flows supplied from outside the system:

- $B_1$ – wind energy used for generation in the wind turbine,
- $B_2$ – solar radiation stream used for electricity production by PV panels,
- $B_3$ – solar radiation stream used for electricity production by the hybrid PV/T module,
- $B_4$ – chemical exergy used to generate biogas and subsequently heat and electricity in the CHP engine,
- $B_5$ – ground heat used in the ground-source heat pump,
- $B_6$ – atmospheric air heat used in the air-source heat pump,
- $B_7$ – solar radiation stream used for heat production by the collector,
- $B_8$ – electrical energy from the external grid (supplied to the system in case of shortage).

The described streams are directed to the following components: wind turbine (1), PV (2), PV/T (3), biogas plant with CHP module (4), ground-source heat pump (5), air-source heat pump (6), solar collector (7), and the electrical energy stream from the grid to component number 8. Component number 8 consists of a set of devices and energy management technologies that enable the distribution of electrical energy within the microgrid. This system includes electrical switchboards, automatic switches, and an Energy Management System (EMS). The system ensures stability and optimization of energy production and consumption, guaranteeing energy availability at all times, even under variable weather conditions and different levels of renewable energy production. The following streams enter component number 8:

- $B_8$ – electrical energy stream from the external grid (supplied to the system in case of shortage),
- $B_9$ – electrical energy generated by the wind turbine,
- $B_{10}$ – electrical energy generated by the PV system,
- $B_{11}$ – electrical energy generated by the PV/T system,
- $B_{12}$ – electrical energy generated by the biogas-powered CHP,
- $B_{14}$ – electrical energy generated by the energy storage system.

In addition to the described RES components (1–7), energy from the energy storage system (component 9) is directed to the energy distribution system. The streams exiting the energy distribution system are as follows:

- $B_{13}$ – electrical energy supplying the energy storage system,
- $B_{15}$ – electrical energy supplied to end consumers,
- $B_{16}$ – electrical energy supplying the ground-source heat pump,
- $B_{17}$ – electrical energy supplying the air-source heat pump.

The next component of the system is the heat management (distribution) system. The heat streams are:

- $B_{18}$ – heat from the PV/T module,
- $B_{19}$ – heat from the biogas-powered CHP engine,
- $B_{20}$ – heat from the ground-source heat pump,
- $B_{21}$ – heat from the air-source heat pump,
- $B_{22}$ – heat from the solar collectors.

Heat is directed to end users (stream $\dot{B}_{23}$) or, if there is a need for cooling generation, to the adsorption chiller (stream $\dot{B}_{24}$). The adsorption chiller (component number 11 of the system) generates stream $\dot{B}_{25}$, which is the useful cooling stream directed to component 12 (useful cooling distribution). Three streams enter component 12:

- $B_{25}$ – useful cooling from the adsorption chiller,
- $B_{26}$ – useful cooling from the ground-source heat pump,
- $B_{27}$ – useful cooling from the air-source heat pump.

The stream leaving component number 12 (cooling distribution) is stream $B_{28}$ – useful cooling directed to end users.

The described relationships are presented using equations in the table below (***Table 1***).

**Table 1. Fuel and product equations for the system components**

| No. | Component | Fuel | Product |
|---|---|---|---|
| 1 | Wind turbine | $F_1 = \dot{B}_1$ | $P_1 = \dot{B}_9$ |
| 2 | PV | $F_2 = \dot{B}_2$ | $P_2 = \dot{B}_{10}$ |
| 3 | PV/T | $F_3 = \dot{B}_3$ | $P_1 = \dot{B}_{11} + \dot{B}_{18}$ |
| 4 | Biogas plant with CHP engine | $F_4 = \dot{B}_4$ | $P_3 = \dot{B}_{12} + \dot{B}_{19}$ |
| 5 | Ground-source heat pump | $F_5 = \dot{B}_5 + \dot{B}_{16}$ | $P_5 = \dot{B}_{20} + \dot{B}_{26}$ |
| 6 | Air-source heat pump | $F_6 = \dot{B}_6 + \dot{B}_{17}$ | $P_6 = \dot{B}_{21} + \dot{B}_{37}$ |
| 7 | Solar collector | $F_7 = \dot{B}_7$ | $P_7 = \dot{B}_{32}$ |
| 8 | Electrical energy distribution | $F_8 = \dot{B}_8 + \dot{B}_9 + \dot{B}_{10} + \dot{B}_{11} + \dot{B}_{12} + \dot{B}_{14}$ | $P_8 = \dot{B}_{13} + \dot{B}_{15} + \dot{B}_{16} + \dot{B}_{17}$ |
| 9 | Energy storage | $F_9 = \dot{B}_{13}$ | $P_9 = \dot{B}_{14}$ |
| 10 | Heat distribution | $F_{10} = \dot{B}_{18} + \dot{B}_{19} + \dot{B}_{20} + \dot{B}_{21} + \dot{B}_{22}$ | $P_{10} = \dot{B}_{23} + \dot{B}_{24}$ |
| 11 | Adsorption chiller | $F_{11} = \dot{B}_{25}$ | $P_{11} = \dot{B}_{21}$ |
| 12 | Cooling distribution | $F_{12} = \dot{B}_{25} + \dot{B}_{26} + \dot{B}_{27}$ | $P_{12} = \dot{B}_{28}$ |

### 1.4.1. Description and characterization of the demand for electrical energy

Hourly data were used in the analysis [61]. An example of the daily distribution of electricity consumption is shown in **Figure *4***.

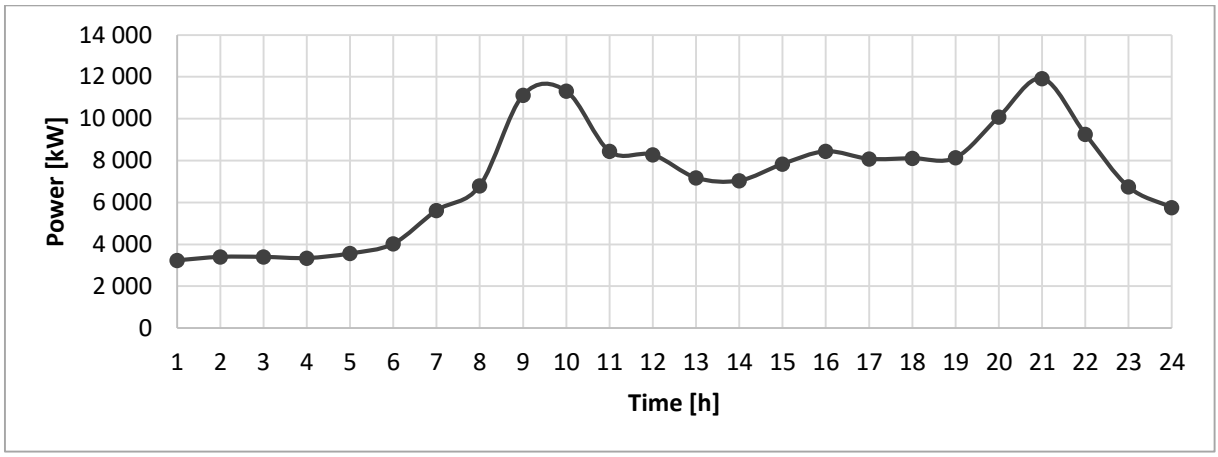


**Figure 4. Example of the daily electricity consumption profile (based on [61])**

The maximum instantaneous demand of the system during the analysed year reached 15 MW. Consequently, for the purposes of the analysis, the total installed capacity of the energy sources in the system was set to 15 MW.

### 1.4.2. Description and characterization of heat and cooling demand

The heat demand for space heating was calculated according to the following equation (3).

$$\frac{Q_g}{Q_{g,max}} = \frac{t_w - t_z}{t_w - t_{z,min}} \quad (3)$$

Where:
$Q_g$ – heat demand [kW],
$Q_{g,max}$ – maximum heat demand [kW] obtained from calculations in the PURMO software,
$t_w$ – indoor temperature [°C],
$t_z$ – outdoor temperature [°C],
$t_{z,min}$ – minimum outdoor temperature [°C].

For the calculations, a daily repetitive domestic hot water (DHW) demand profile based on [62], was adopted, as shown in **Figure *5***.

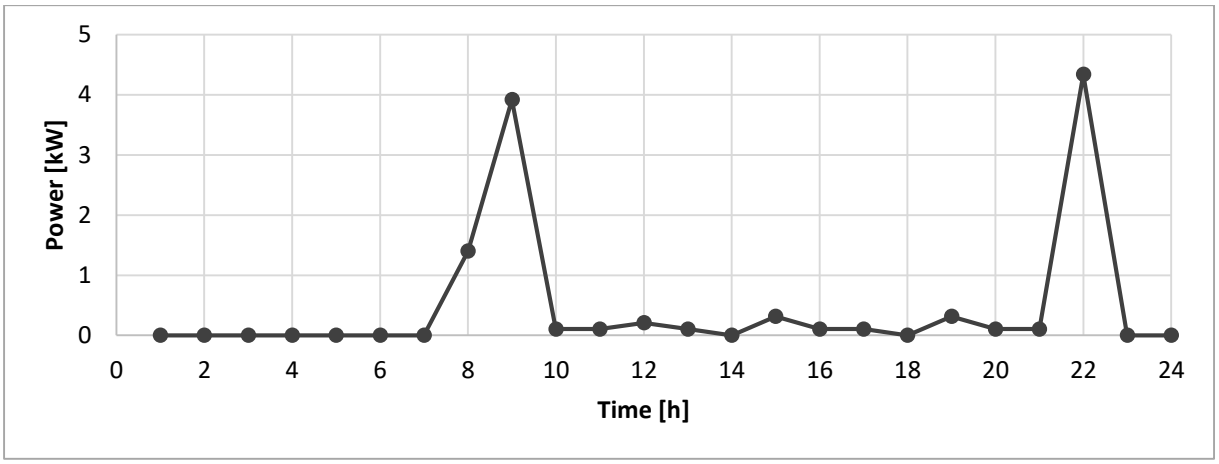


**Figure 5. Example of the domestic hot water (DHW) consumption profile (based on [62])**

The total amount of heat was calculated based on the following equation (4).

$$Q = Q_g + Q_{hotwather} \tag{4}$$

An example of the daily heat consumption profile is presented in **Figure *6***.

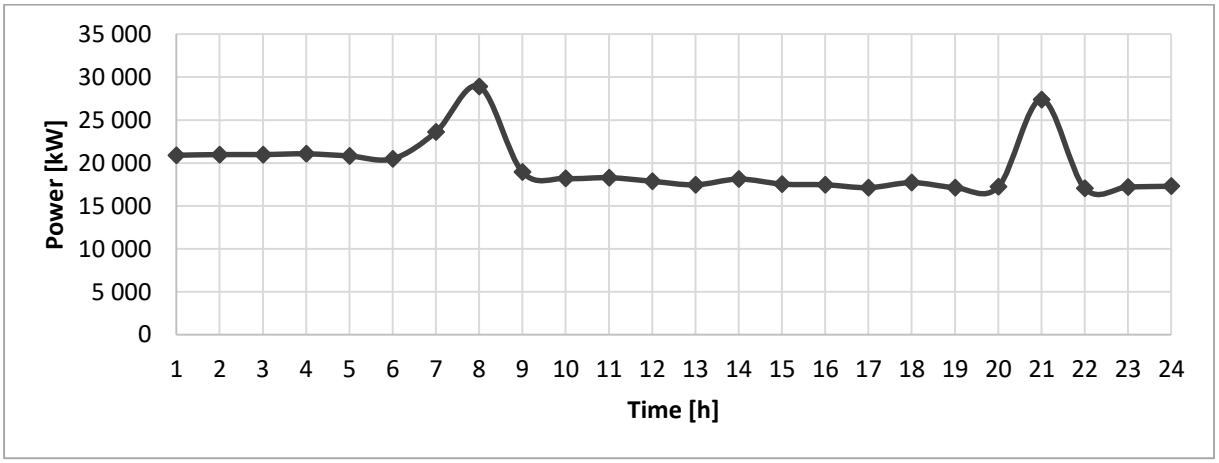


**Figure 6. Example of the daily heat consumption profile (based on [61])**

The cooling demand was determined based on the following equation (5).

$$\sum Q_{ji} = Q_{jL} + Q_{oc} + Q_{r,i} + Q_{ps,i} + Q_{losses,i} \tag{5}$$

Where:
$Q_{jL}$ – internal heat gain from occupants [kW],
$Q_{oc}$ – internal heat gain from equipment and lighting [kW],
$Q_{r,i}$ – solar heat gain (depending on the total solar radiation intensity during a given hour of the year) [kW],
$Q_{ps,i}$ – rate of heat flow from fresh air [kW],
$Q_{losses,i}$ – heat losses through building partitions depending on outdoor temperature tab [kW].

The heat gain from occupants was calculated assuming a simultaneous occupancy factor ϕ and a unit heat gain $q_j$ according to Eq. (6).

$$Q_L = \varphi \cdot n \cdot q_j \tag{6}$$

Where:
$\varphi$ – simultaneous occupancy factor [-],
n – number of occupants [-],
$q_j$ – unit heat gain [kW].

The heat gain from equipment and lighting was determined using Eq. (7).

$$Q_{oc} = F \cdot N \cdot [\beta + (1 - \alpha - \beta) \cdot k_o] \cdot \Phi \tag{7}$$

Where:
F – floor area [m²],
N – installed lighting power per unit floor area [W/m²],
β – fraction of convective heat transferred to the room air relative to the installed power [-],
α - fraction of convective heat released to the air flowing through ventilated luminaires relative to the installed power (for non-ventilated luminaires α = 0) [-],
$k_o$ - accumulation factor [-],
Φ - simultaneity factor of installed power utilization [-],

The solar heat gain (depending on the total hourly solar radiation) was calculated according to Eq. (8):

$$Q_{r,i} = Q_{r,obl} \cdot \frac{I_{c,i}}{I_{c,max}} \tag{8}$$

Where:
$Q_{r,i}$ – calculated solar heat gain under given conditions [W],
$I_{c,i}$ – solar radiation intensity in a given hour of the year [W/m²],
$I_{c,max}$ – maximum annual solar radiation intensity [W/m²].

The reference solar heat gain was determined according to Eqs. (9), (10) and (11).

$$Q_{r,obl} = Q_{winN} + Q_{winE} + Q_{winS} + Q_{winW} + Q_{wall} \tag{9}$$

$$Q_{winX} = A_{winX} \cdot \left[\Phi_1 \cdot \Phi_2 \cdot \Phi_3 \cdot \left(k_{cX} \cdot R_s \cdot I_{c,maxX}\right) + U_{win} \cdot (t_{ab} - t_{room})\right] \tag{10}$$

$$Q_{wall} = F \cdot K \cdot \Delta tr \tag{11}$$

Where:
$A_{winX}$ – total window area on wall with orientation X [m²],
$\phi_1$ – window correction factor [-],

$\Phi_2$ – altitude correction factor [-],
$\Phi_3$ – factor accounting for glazing type and shading devices [-],
$U_{win}$ – window heat transfer coefficient [W·(m²·K)$^{-1}$],
$R_s$ – share of solar-exposed window area [-],
$k_{cx}$ – accumulation coefficient for 12-hour operation [-],
F – opaque wall area [m²],
K – wall heat transfer coefficient [W·(m²·K)$^{-1}$],
Δtr – equivalent temperature difference [°C].

The heat gain from ventilation air was calculated according to Eq. (12).

$$Q_i = 1.163 \cdot 0.24 \cdot V_i \cdot \gamma(t_{out} - t_{room}) \tag{12}$$

Where:
$V_i$ – infiltrating air volume flow rate [m³/h],
γ – specific weight of air [kg/m³],
$t_{out}$ – outdoor air temperature [°C],
$t_{room}$ – indoor air temperature [°C].

The heat losses through building partitions, depending on outdoor temperature, $Q_{losses,i}$ were calculated using Eq. (13):

$$Q_{losses,i} = Q_{losses,cal} \cdot \frac{t_{room} - t_{out,i}}{t_{room} - t_{out}} \tag{13}$$

$Q_{losses,cal}$ – design heat losses through partitions [W],
$t_{room}$ – indoor air temperature [°C],
$t_{out}$ – design outdoor temperature [°C],
$t_{out,i}$ – actual outdoor temperature at time i [°C].

An example of the daily cooling demand profile is shown in **Figure 7**.

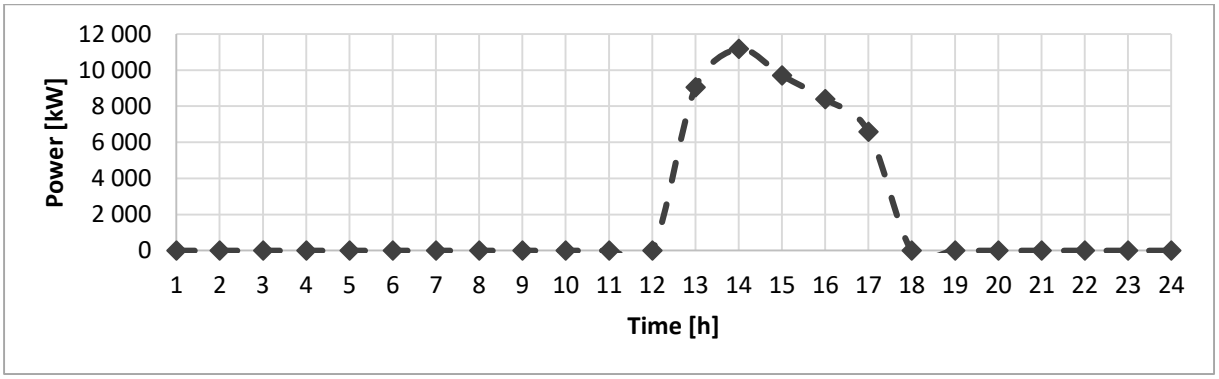


**Figure 7. Example of the daily cooling demand profile [61]**

### 1.4.3. System Components

Conventional power generation, which relies on non-renewable sources such as coal, gas, or oil, is a major source of greenhouse gas emissions released into the atmosphere during combustion processes [63–66]. The transition to energy systems based on renewable energy sources (RES) represents response to the accelerating depletion of fossil fuel resources and the ongoing climate crisis [67–69]. However, although RES offers an advantages, they also pose significant challenges. The main difficulties arise from the nature of their sources [70]. Renewable energy relies on natural phenomena such as: solar radiation, wind and water flows. They depend on weather and climate conditions, and are therefore marked by considerable temporal and spatial variability [71–75]. This variability can make planning more challenging. Solutions enabling energy generation with lower greenhouse gas emissions and reduced environmental impacts, including renewable energy sources and microgrids, are essential for sustainable development [76].

In energy systems based on Variable Renewable Energy (VRE), such as solar (PV, PV/T) and wind power (wind turbines), a key issue to consider is the inherently intermittent nature of the main renewable generation sources. Therefore, leveraging system complementarity is essential to meet demand and reduce electricity supply risks [77]. The planning of power systems dominated by low-flexibility generation must account for spatial, temporal, and technical factors to enable coordinated dispatch of generating units. Without predictable generation sources (such as conventional power plants), models may overestimate the integration of renewable energy and underestimate the need for flexible resources [78]. A system that combines various renewable energy sources within a microgrid, equipped with smart meters and capable of sharing and trading energy, is referred to as a smart microgrid or smart grid [79].

VRE must address variability through solutions such as energy storage. Another option for adjustment involves backup generators or firm-capacity sources, including nuclear, natural gas, hydroelectric, bioenergy, and geothermal power [80]. The primary approach to VRE integration is Energy Storage (ES), which can be realized in various forms. Mechanical storage methods include pumped hydro and compressed air storage, while electrochemical systems comprise advanced lead-acid, sodium-sulphur, lithium-ion, and nickel–sodium-chloride batteries. Hydrogen production via electrolysis, with subsequent utilization in fuel cells, also represents a storage pathway. In recent years, novel approaches such as water splitting have emerged. New prospects for renewable-based hydrogen production involve catalytic conversion of bioethanol in the presence of steam [81]. Hydrogen-enriched natural gas has also become an important topic [82]. Although many storage methods exist, this thesis focuses on the electrolysis/fuel cell system [83, 84].

#### *1.4.3.1. Photovoltaics*

The first photovoltaic cell, designed and developed in 1877, had an efficiency of only about 0.5%, and selenium was the material used for its construction. A significant improvement in efficiency was achieved with the use of silicon, which enabled the development of the technology—the first historical application of a solar cell took place in 1955. One of the driving forces behind the new technology was the space race—photovoltaic energy sources became an important system in space projects. Today, photovoltaic technology is an important element of the energy transition. [85]. The conversion of sunlight into electricity in solar cells occurs through electronic semiconductors, particularly—but not

exclusively—crystalline silicon (c-Si) or thin-film semiconductor materials. Incoming photons knock electrons loose, and the built-in electric field within the cell structure directs their flow, generating direct current [86, 87]. The amount of solar radiation converted into electrical energy by a photovoltaic panel can be calculated using the following equation (14):

$$E_{PV} = \eta_{e_{PV}} I_\beta A_{PV} \quad (14)$$

The effectiveness of converting solar radiation into energy depends on the amount of radiation incident on the panel as well as on the temperature. Therefore, the calculations of energy efficiency values were carried out using efficiency ranges obtained from the literature [88, 89]. An example range of efficiency is presented in **Figure *8***.

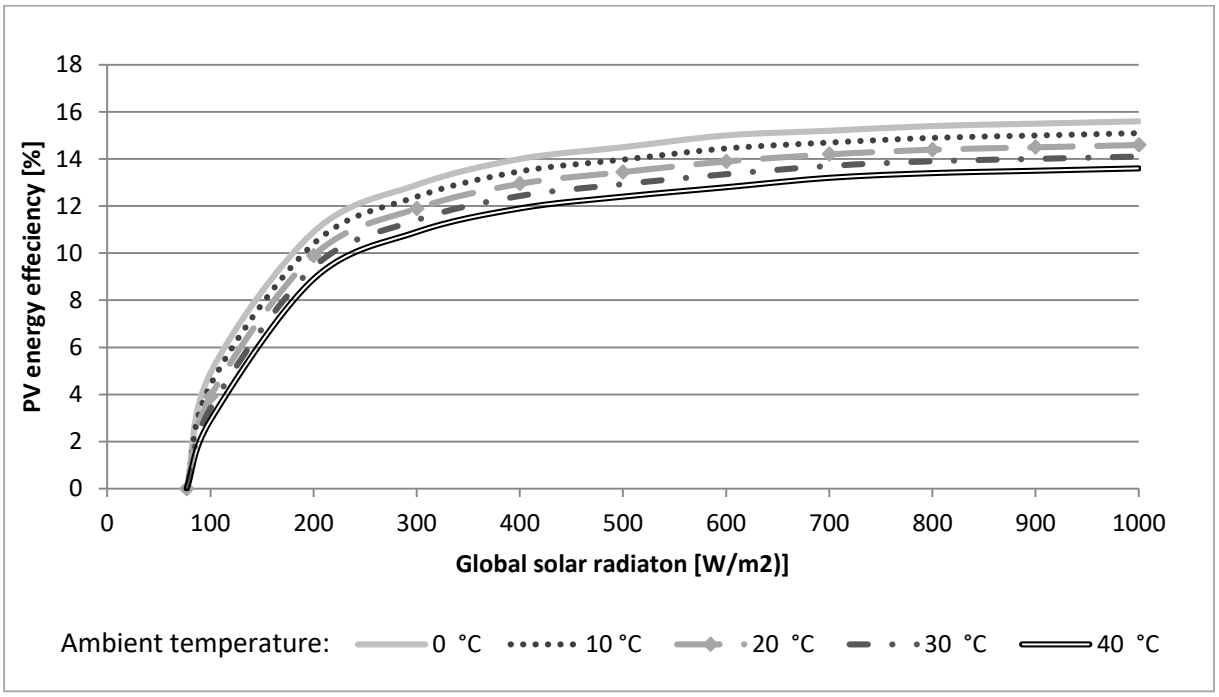


**Figure 8. The relationship between global radiation, ambient temperature, and the energy efficiency of a photovoltaic panel (based on [90])**

***1.4.3.2. Solar collectors***

Solar thermal collectors are devices that convert incident solar radiation into useful heat. The most common technologies include flat-plate and evacuated tube collectors, both using selective surfaces and insulation to minimize thermal losses [91]. Depending on the design and operating conditions, solar collectors typically achieve efficiencies in the range of 40–70% and are widely applied in domestic hot water supply and large-scale solar thermal systems [92, 93].

The amount of solar radiation converted into heat by a solar collector can be calculated using equation (15).

$$Q_c = \eta_{th_c} I_\beta A_C \quad (15)$$

The thermal efficiency of the collector $\eta_{th_c}$ was determined from equation (16) [94]:

$$\eta_{th_C} = \eta_{th_{C_0}} - \frac{k_1 \Delta T}{I_\beta} - \frac{k_2 - \Delta T^2}{I_\beta} \quad (16)$$

where the temperature difference $\Delta T$ is given by equation (17):

$$\Delta T = T_O - T_C \quad (17)$$

The calculations of energy efficiency values were carried out for efficiency ranges commonly reported in the literature [94]. An example efficiency range is presented in **Figure *9***.

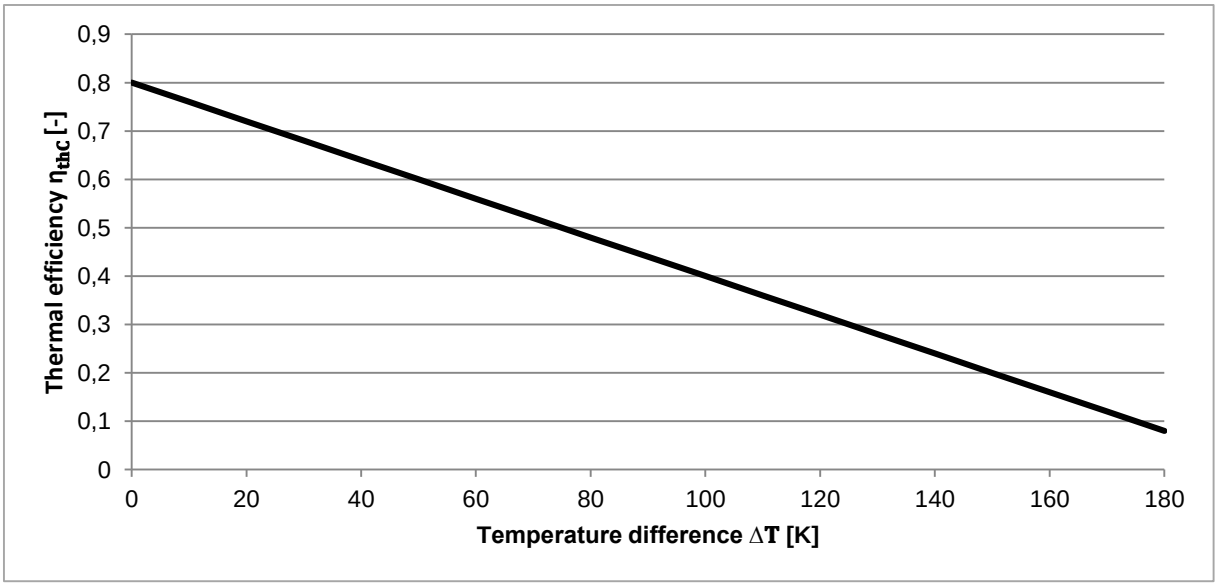


**Figure 9. Thermal efficiency of a solar collector as a function of operating conditions (based on [94])**

The value of $\eta_{th_{C_0}}$ was assumed, and the obtained heat loss coefficients are summarized in **Table *2*.**

**Table 2. Heat loss coefficients of a solar collector (based on [94])**

| | **Heat loss coefficients $k_1$** | **Heat loss coefficients $k_2$** |
|---|---|---|
| | W/(m$^2$K) | W/(m$^2$K$^2$) |
| Flat-plate | 4 | 0.1 |

***1.4.3.3. Photovoltaic-Thermal system***

Photovoltaic-thermal (PV/T) systems combine photovoltaic modules and solar collectors. This allows them to simultaneously generate electricity and heat, improving overall energy efficiency compared to standalone photovoltaic or thermal systems [95]. Their performance depends strongly on design parameters: mass flow rate, absorber design, coolant type. Studies report thermal efficiencies in the range of 40-65% and electrical efficiencies 10-15% under standard test conditions. These systems are very useful where space is limited, because a single panel can deliver both thermal and electrical outputs [96]

First, for the PV/T system, the amount of heat generated from solar radiation was calculated. It was assumed that the heat from the PV/T installation was transferred through a heat exchanger to a water storage tank. The cooling process started when the cell temperature exceeded the assumed value of 30 °C. The estimated module temperature was calculated using equation (18):

$$t_{PV} = t_O + \frac{(t_{NOCT} - 20) I_\beta}{800} \quad (18)$$

Where:
$t_{PV}$ – the module temperature [°C],
$I_\beta$ – the solar radiation incident on the module [W·m$^{-2}$],
$t_O$ – the ambient temperature [°C],
$t_{NOCT}$ – the nominal operating cell temperature (44–48 °C) [97-99].

For the calculations, the following assumptions were adopted:

- the cooling process starts when the cell temperature exceeds 30°C,
- the temperature of the cooling water from the domestic hot water tank is constant ($T_{w\ in}$ = 10°C),
- the cooling fluid in the PV/T circuit is heat transfer fluid (Ergolid), $c_e$ = 3.17 [kJ/(kg·K)],
- the mass flow rate of water and heat transfer fluid is 0.02 kg/s,
- heat losses in the pipes are neglected.

**Figure *10*** presents the simplified schematic diagram of the PV/T installation.

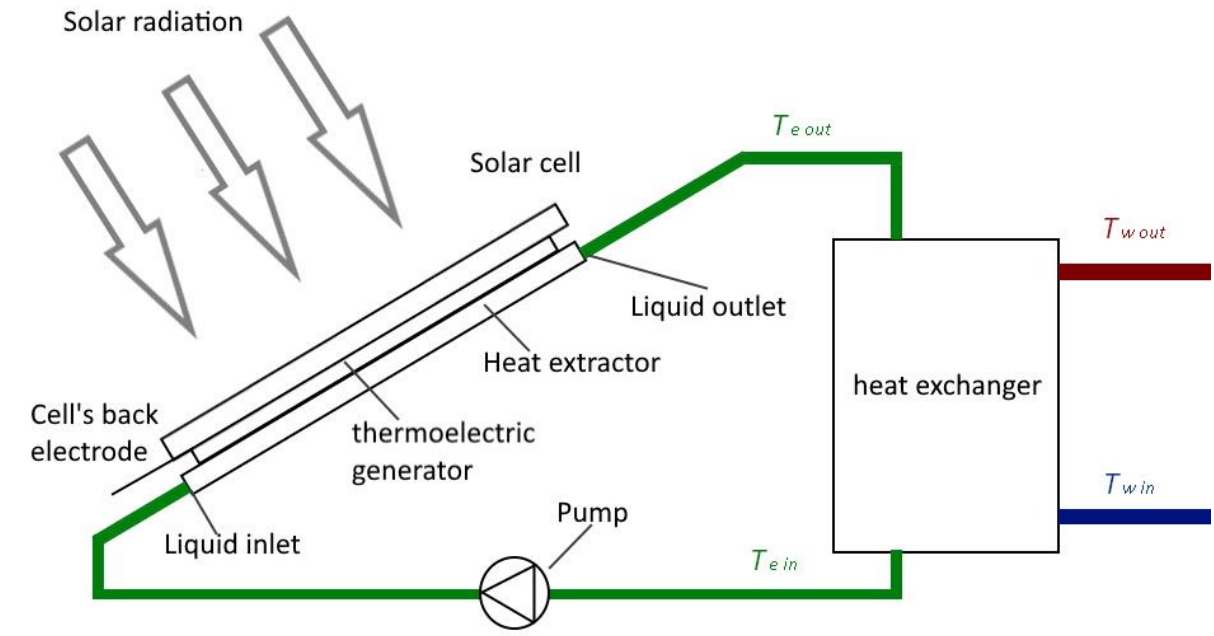


**Figure 10. Simplified schematic of the PV/T installation (based on [100])**

To determine the thermal efficiency of the PV/T system, equation (19) was applied [97].

$$\eta_{th} = \eta_0 - \frac{\alpha\left(T_{eg_{out}} - T_O\right)}{I_\beta} \tag{19}$$

Where:

$\eta_{th}$ – the thermal efficiency of the PV/T system [-],

$\eta_0$ = 0.6099 [-],

$\alpha$ – the heat transfer coefficient, $\alpha$ = 5.8343 [W/(m²·K)],

$T_{(eg\ out)}$ – the outlet temperature of the working medium from the PV/T panel (heat transfer fluid outlet temperature). The dependence of thermal efficiency on operating conditions is shown in **Figure *11***.

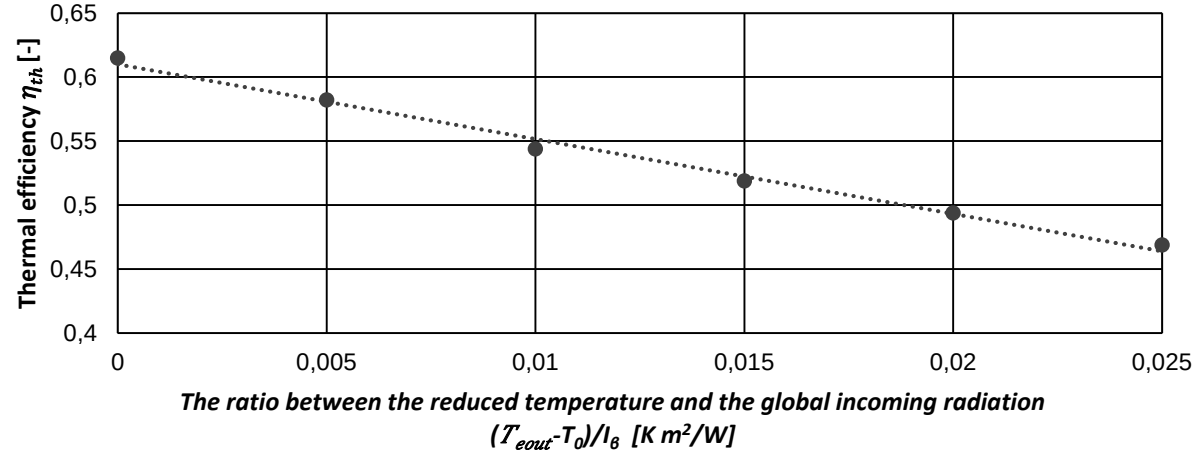


**Figure 11. Thermal efficiency of the PV/T system (based on [101])**

In equation (19), all values except for the heat transfer fluid temperature are known. The inlet heat transfer fluid temperature at the start of cooling was assumed to be equal to the ambient temperature and was subsequently calculated using heat exchanger analysis based on the ε–NTU method – equation (20).

$$\dot{Q}_{PVT} = \eta_{th_{PVT}} I_\beta A_{PVT} \tag{20}$$

Where:

$\eta_{th_{PVT}}$ – the thermal efficiency of PV/T [-],

$I_\beta$ – the incident solar radiation [W·m⁻²],

$A_{PVT}$ – the surface area of the PV/T panel [m²].

The ε-NTU method is applied to determine the heat transfer fluid and supply water temperatures and is one of the standard approaches for heat exchanger analysis. It uses dimensionless thermal parameters, enabling calculations when inlet temperatures and heat exchanger characteristics are known. The dimensionless parameters R, S, p, and φ were determined according to the values presented in **Table *3*.**

**Table 3. Methodology of dimensionless ε-NTU parameters (based on [102,103])**

| | | |
|---|---|---|
| R | $R = \frac{W_w}{W_{eg}}$ | 1.32 |
| S | $S = k\frac{A_W}{W_{eg}}$ | 1.44 |
| p | $p = \left(\frac{1 - e^{[-S(1-1R)]}}{R - e^{[-S(1-1R)]}}\right)$ | 0.478 |
| ϕ | $\phi = pR$ | 0.633 |

The indices in **Table *3*** include heat capacities of the fluid streams, calculated using equations (21) and (22).

$$\dot{W_w} = \dot{m}_w c_w \quad (21)$$

$$\dot{W_{eg}} = \dot{m}_{eg} c_{eg} \quad (22)$$

The outlet temperatures of the working medium from the PV/T panel were determined using equations (23) (24) (25) and (26).

$$t_{e_{gout}} = \frac{\dot{Q}_{PVT}}{\dot{m}_{eg} \cdot c_{eg}} + t_{eg_{in}} \quad (23)$$

$$t_{eg_{in}} = t_{eg_{out}} - \phi\left(t_{w_{in}} - t_{w_{out}}\right) \quad (24)$$

$$t_{w_{in}} = const. \quad (25)$$

$$t_{eg_{in}} = p\left(t_{eg_{out}} - t_{w_{in}}\right) + t_{w_{in}} \quad (26)$$

Where:`

$T_{eg_{out}}$– outlet temperature of the working medium (heat transfer fluid) from the PV/T panel [K],

$T_{eg_{in}}$– inlet temperature of heat transfer fluid [K],

$T_{w_{out}}$– outlet water temperature from the heat exchanger [K],

$T_{w_{in}}$– inlet water temperature to the heat exchanger [K].

The useful heat for domestic hot water production was calculated with equation (27).

$$\dot{Q} = \dot{m}_w c_w \left(t_{w_{out}} - t_{w_{in}}\right) \quad (27)$$

For the PV/T system, the amount of generated solar energy was determined using equation (28).

$$E_{PVT} = \eta_{e_{PVT}} I_\beta A_{PVT} \quad (28)$$

The energy efficiency of the PV/T system was evaluated based on the relationship shown in **Figure *12*** [97] [101].

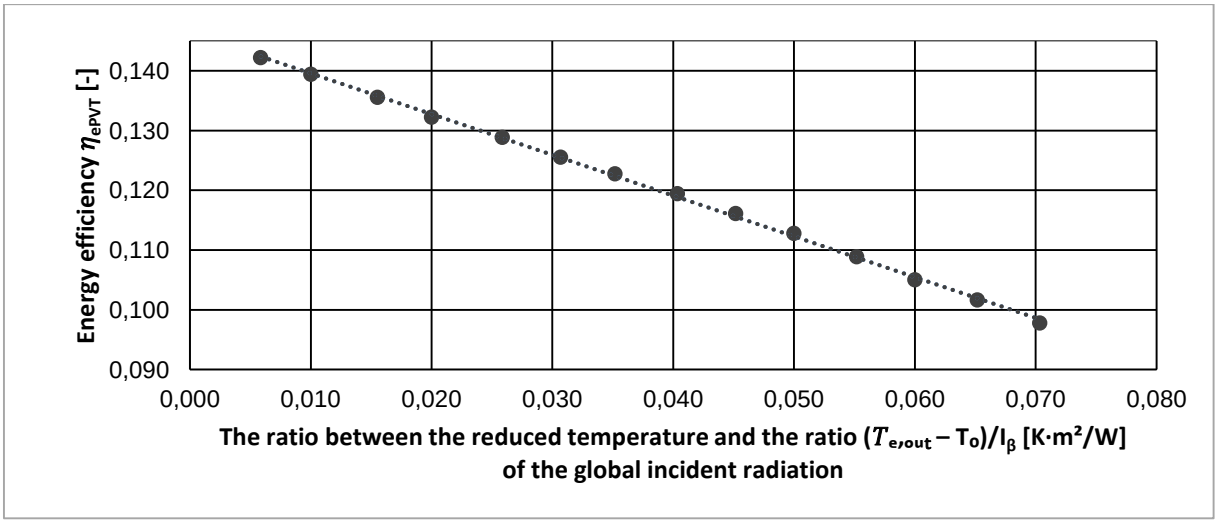


**Figure 12. Energy efficiency of the PV/T system (based on [97, 101])**

The energy efficiency of the PV/T system was calculated using equation (29):

$$\eta_{e_{PVT}} = 0.1464 \frac{T_{eg_{out}} - T_O}{I_\beta} - 0.6828 \quad (29)$$

Where $T_O$ is the ambient temperature, and $T_{eg_{out}}$ is the outlet temperature of the working medium from the PV/T panel.

#### *1.4.3.4. Wind turbine*

Wind turbines convert the kinetic energy of wind into mechanical power and then into electricity via a generator, making them a cornerstone technology in renewable energy systems [104]. Their performance depends critically on: rotor and blade design, wind speed distribution, pitch control, and hub height [105]. They are widely deployed in both onshore and offshore settings as a mature and scalable solution for large-scale renewable power generation [106, 107].

In determining the amount of energy produced by the wind turbine, the relationships shown in **Figure *13*** were used. The figure illustrates the wind turbine characteristic, presenting the relationship between wind speed v and wind turbine power $P_w$. The curve is based on performance data for the V90-3.0 MW turbine [108].

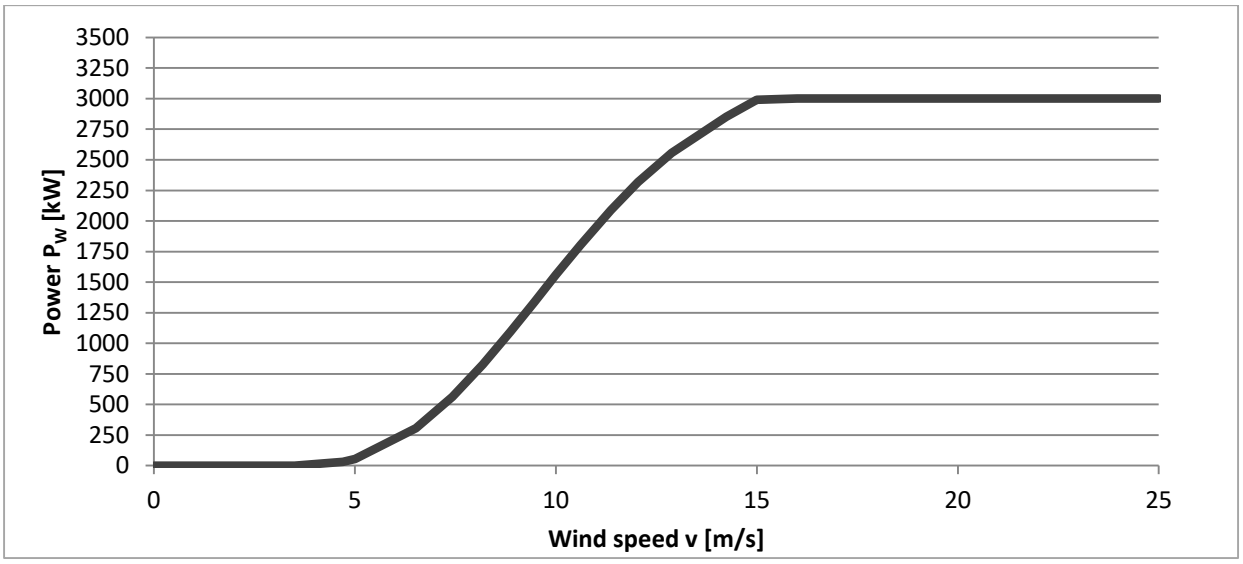


**Figure 13. Power curve of a wind turbine as a function of wind speed (based on [108])**

The power of the wind turbine was determined using the equation (30).

$$P_w = 0.06136v^5 - 2.81942v^4 + 45.26322v^3 - 287.49133v^2 + 789.72637v - 794.68233 \quad (30)$$

Where:
$P_w$ – wind turbine power [kW],
v – wind speed [m/s].

In the calculations, the following assumptions were made:

- Cut-in wind speed: 5 m/s,
- Cut-out wind speed: 15 m/s.

#### *1.4.3.5. Heat pump*

Heat pumps transfer thermal energy from a low-temperature source (air, ground, or water) to a higher-temperature sink using a vapour-compression or alternative thermodynamic cycle, converting electrical work into useful heat with high efficiency [109, 110]. Their performance depends strongly on cycle design, working fluid, source/sink temperature difference and system integration [111]. Typical seasonal or operating COP values for modern residential and commercial units are commonly in the range of about 3–5, although real-world COP varies with ambient conditions and load. Heat pumps are widely deployed for space heating, hot-water production and industrial low-temperature heat recovery, and are considered a key technology for decarbonizing heating when coupled with low-carbon electricity and waste-heat sources [112, 113]. In the system, two options were considered—both an air-source heat pump and a ground-source heat pump were analysed. The characteristics of both types of devices are presented below.

***Air source heat pump***

**Figure *14*** shows the performance characteristics of an air-to-water heat pump [114]. It illustrates the relationship between the inlet air temperature and the heat output, as well as the electrical power consumption of the heat pump.

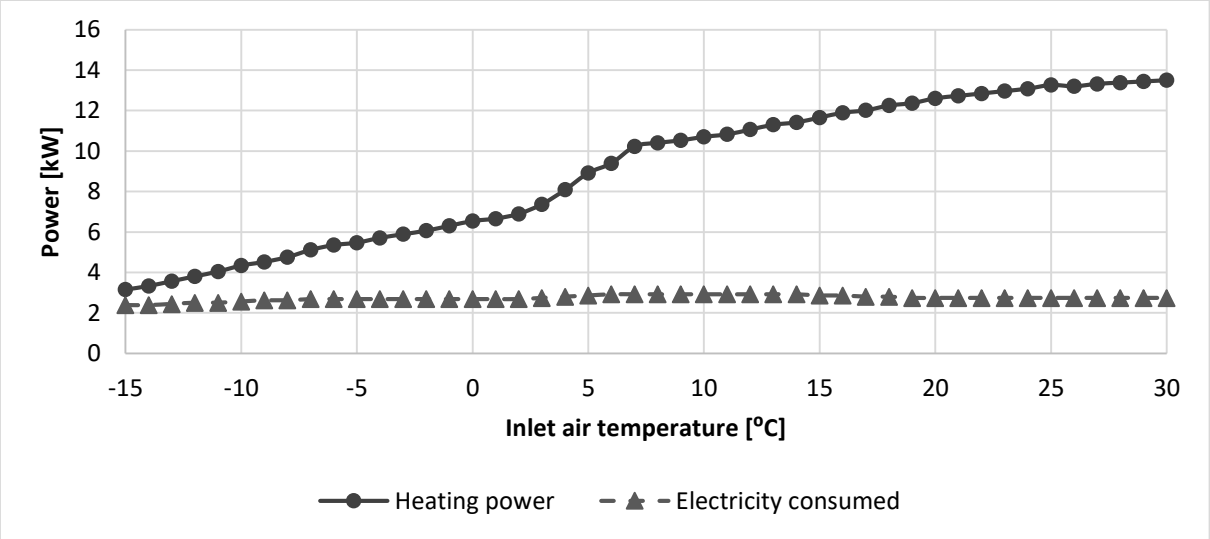


**Figure 14. Performance characteristics of an air source heat pump in heating mode (based on [114])**

The heat supplied by the air-to-water heat pump was calculated using equation (31).

$$Q_{AHP} = -0.0002{t_{in}}^3 + 0.0023{t_{in}}^2 + 0.3289t_{in} + 6.9917 \quad (31)$$

Where:

$Q_{AHP}$ – heat generated by the air-to-water heat pump [kW]

$t_{in}$ – inlet air temperature [°C]

The electrical power consumption of the air-to-water heat pump was determined using equation (32).

$$P_{AHP} = 0.000003{t_{in}}^3 - 0.000697{t_{in}}^2 + 0.015054t_{in} + 2.763814 \quad (32)$$

Where:

$P_{AHP}$ – electrical power consumption of the air-to-water heat pump [kW]

A heat pump can also provide cooling. **Figure *15*** shows the performance characteristics of an air-to-water heat pump [114]. It illustrates the relationship between the inlet air temperature and the cooling capacity, as well as the electrical power consumption of the air-to-water heat pump.

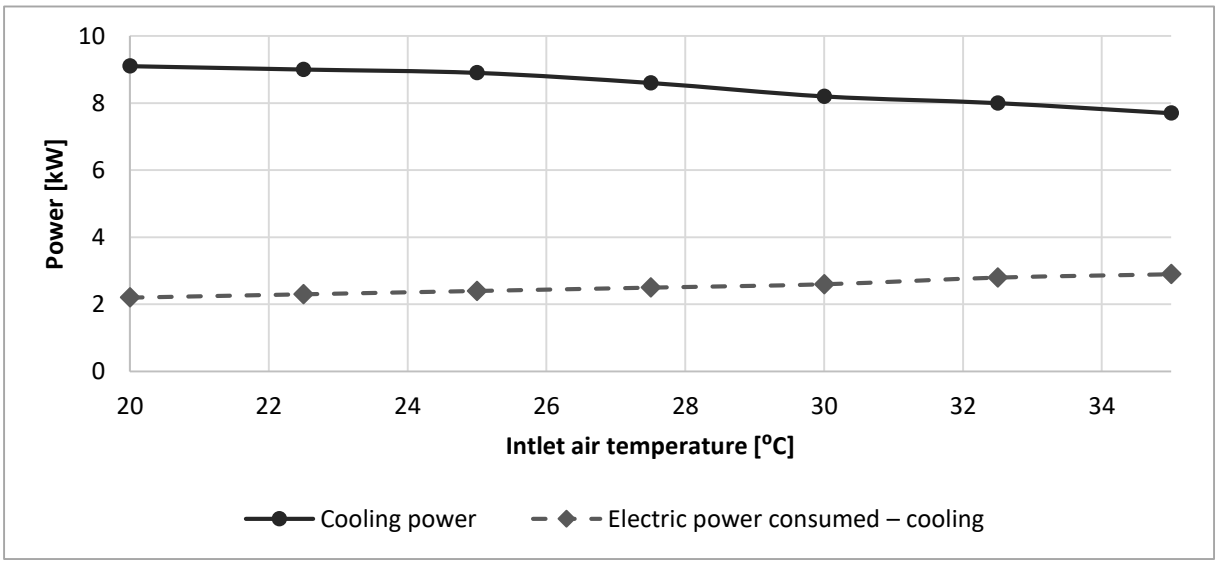


**Figure 15. Performance characteristics of an air source heat pump in cooling mode (based on [114])**

The cooling capacity of the air-to-water heat pump was calculated using equation (33).

$$Q_{AHP-C} = -0.0032{t_{in}}^2 + 0.0795t_{in} + 8.8429 \quad (33)$$

Where:

$Q_{AHP-C}$ – cooling capacity of the air-to-water heat pump [kW],

$t_{in}$ - inlet air temperature [°C].

The electrical power consumption of the air-to-water heat pump in cooling mode was determined using equation (34).

$$P_{AHP-C} = 0.001{t_{in}}^2 - 0.0052t_{in} + 1.9286 \quad (34)$$

Where:

$P_{AHP-C}$ -– electrical power consumption of the air-to-water heat pump [kW].

***Ground-source heat pump***

In the first stage of calculations for the ground-source heat pump, the soil temperature was determined. Soil temperature varies according to properties such as thermal conductivity and heat capacity (which themselves depend on environmental variables, e.g. latent heat of condensation (phase-change heat), solar radiation, and soil water evaporation). These factors determine the thermal flux in the soil profile according to Fourier's law – equation (35):

$$F = -\lambda \frac{\partial T}{\partial z} \quad (35)$$

Where:

F [W·m$^{-2}$]— heat flux at depth z [m],

λ — soil thermal conductivity [W·m$^{-1}$·K$^{-1}$],

$\frac{\partial T}{\partial z}$ — temperature gradient with depth [K·m⁻¹].

Assuming homogeneous soil properties and that heat conduction occurs mainly in the vertical direction along the steepest temperature gradient, the soil temperature variation at a given depth, under known initial and boundary conditions and over time, can be described by a sinusoidal curve representing both diurnal and annual temperature cycles – equation (36):

$$T_S(z,t) = \overline{T_0} + A_0 e^{-z\left(\frac{\omega}{2k_s}\right)^{\frac{1}{2}}} sin\left(\omega t - z\left(\frac{\omega}{2k_s}\right)^{1/2}\right) \quad (36)$$

Where:
ω — angular frequency [rad·s⁻¹],
$T_0$ — mean surface temperature [K],
$A_0$ — amplitude of surface temperature fluctuations [K],
$k_s$ — thermal diffusivity of the soil [m²·s⁻¹],
z — depth [m].

Besides the soil thermal properties, other factors (e.g. vegetation cover and litter) affect soil temperature by attenuating incoming solar radiation. The fraction of radiation reaching the soil surface can be described by Beer's–Lambert law. An empirical model is used in calculations to estimate soil temperature at a given depth from air temperature [115]. The temperature of the working fluid leaving the ground heat exchanger, $T_{B2}$, was calculated using equation (37) :

$$T_{B2} = T_s - (T_s - T_{B1}) \cdot e^{\frac{-U_d \cdot AS}{\dot{m}_{HT} \cdot Cp_{HT}}} \quad (37)$$

Where:

$T_{B2}$ — outlet temperature of the working fluid from the ground heat exchanger [K],
$T_{B1}$ — inlet temperature of the working fluid to the ground heat exchanger [K],
$T_S$ — soil temperature [K],
$U_d$ — overall heat transfer coefficient for the buried pipe [W·m⁻²·K⁻¹]
$AS$ - tube surface area [m²],
$\dot{m}_{HT}$ — mass flow rate of the heat-transfer medium [kg·s⁻¹],
$Cp_{HT}$ — specific heat capacity of the heat-transfer medium [J·kg⁻¹·K⁻¹].

To compute $T_{B2}$ information about the working fluid was used: mass flow $\dot{m}_{HT}$ and heat capacity [116, 117]. Another set of required data concerns the ground heat-exchanger construction, such as tube surface area $AS$ [118] and the pipe heat transfer coefficient $U_d$ (see equations (38)–(41)):

$$AS = \frac{Q_o}{q_s} \quad (38)$$

$$Q_o = Q_C \cdot \frac{COP - 1}{COP} \tag{39}$$

Where:
$q_s$ — ground heat flux density [W·m⁻²],
$Q_c$ — heat produced by the heat pump [kW],
$Q_o$ — required power of the ground heat source [kW],
$COP$ — coefficient of performance [-].

$$U_d = \left( \frac{1}{2 \cdot \pi} \cdot \frac{1}{\lambda} \cdot ln \frac{\frac{d_o}{2}}{\frac{d_i}{2}} + \frac{1}{\alpha} \right)^{-1} \tag{40}$$

Where:
$U_d$ — pipe overall heat transfer coefficient [W·m⁻²·K⁻¹],
$d_o$ — outer pipe diameter [m],
$d_i$ — inner pipe diameter [m],
λ — thermal conductivity of the pipe material [W·m⁻¹·K⁻¹],
α— convective heat transfer coefficient on the pipe internal side [W·m⁻²·K⁻¹].

The internal convective coefficient α is estimated as – Wq. (41):

$$\alpha = \left( 4.13 + 0.23 \cdot \frac{\theta_m}{100} - 0.0077 \cdot \left( \frac{\theta_m}{100} \right)^2 \right) \cdot \frac{V_B^{0.75}}{d_i^{0.25}} \tag{41}$$

Where $\theta_m$ is the arithmetic mean temperature of the working fluid at the inlet and outlet of the heat exchanger.

According to the literature [119], equation (41) can be simplified by assuming that the arithmetic mean temperature of the working fluid equals the inlet temperature to the exchanger. A fully accurate value of $\theta_m$ can be obtained iteratively, but the simplified approach yields sufficiently precise results for practical calculations. The heat flux that can be extracted from the ground $Q_S$ is computed as Eq. (42):

$$Q_S = AS \cdot U_d \cdot \left( T_s - \frac{T_{HT1} + T_{HT2}}{2} \right) \tag{42}$$

where $T_{HT1}$ is the inlet temperature of the working fluid, determined from Eq. (43).

$$\dot{Q}_s = \dot{m}_{HT} cp_{HT} (T_{HT2} - T_{HT1}) \tag{43}$$

Here $T_s$ denotes the soil temperature on the n-th day, $T_{HT1}$ the working fluid inlet temperature, and $T_{HT2}$the working fluid outlet temperature.

To start the above calculations, initial temperature assumptions were adopted: the initial soil temperature $T_{s-1}$ was taken as 281.15 K (8 °C) and the initial working-fluid inlet temperature $T_{HT1}$ was also 281.15 K (8 °C). Subsequent values of$T_{s-1}$ and $T_{HT1}$ were then computed using the methods described above (**Figure *16***) [120].

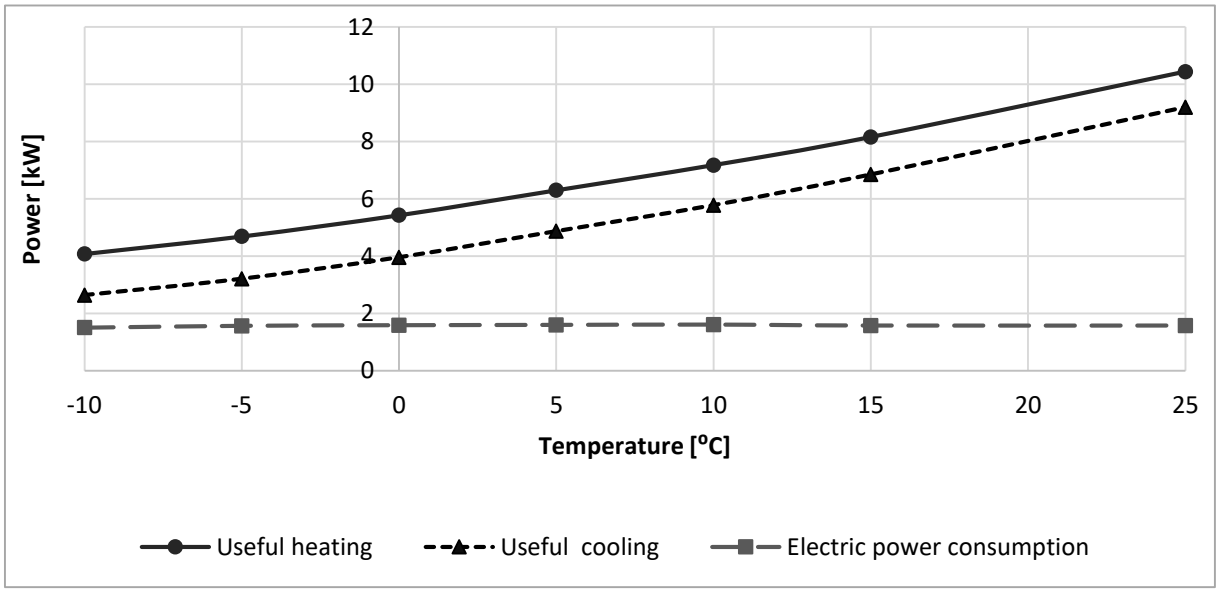


**Figure 16. characteristics of the ground-source heat pump (based on [120])**

The heat/cooling and electrical power streams were then approximated using the linear relations (44) (45) and (46).

$$Q_{GHP} = 0.1813t_{in} + 5.5754 \quad (44)$$

$$Q_{GHP-C} = 0.188t_{in} + 4.1415 \quad (45)$$

$$P_{GHP} = 0.0015t_{in} + 1.5689 \quad (46)$$

Where:
$Q_{GHP}$ — heat generated by the ground-source heat pump [kW],
$Q_{GHP-C}$ — cooling produced by the ground-source heat pump [kW],
$t_{in}$ — inlet air temperature [°C],
$P_{GHP}$ — electrical power consumption of the ground-source heat pump [kW].

### *1.4.3.6. Adsorption chiller*

An additional component ensuring cooling during shortage periods is the adsorption chiller. Adsorption chillers are thermally driven cooling devices that use a solid adsorbent (e.g. silica gel) and a working fluid (commonly water) instead of relying primarily on electricity for compression cycles [121] The adsorption chiller is powered by heat derived from renewable energy sources. The coefficient of performance (COP) of this device depends on the temperature of the water supplying heat to the adsorption chiller [122] , and its performance characteristics are shown in **Figure *17***.

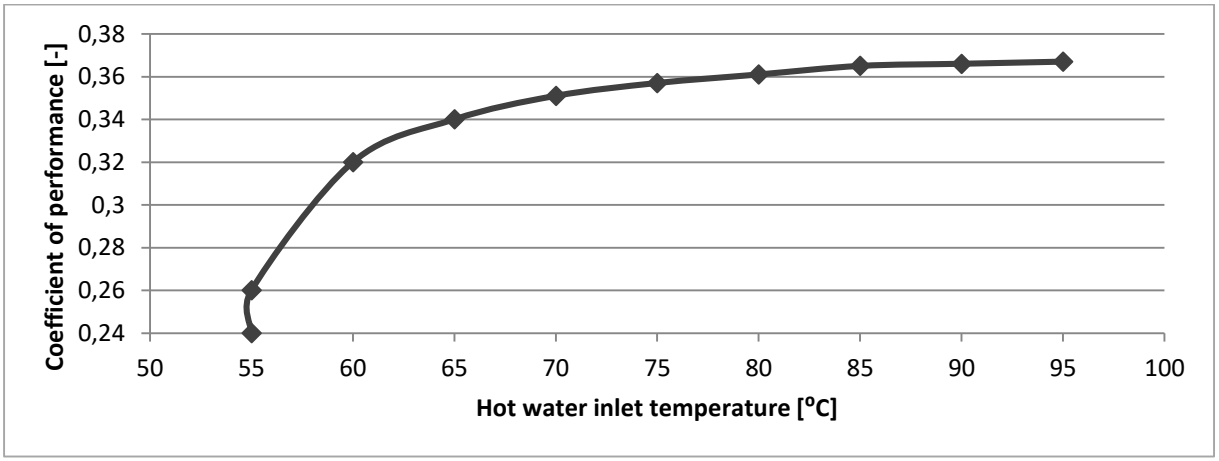


**Figure 17. Performance characteristics of an adsorption chiller as a function of heat source temperature (based on [122])**

In the calculations, a constant COP value was assumed, and the cooling output was determined using equation (47).

$$Q_{Ads} = COP \cdot Q_{ads-in} \tag{47}$$

Where:

$Q_{Ads}$ – cooling output generated by the adsorption chiller [kW],

$Q_{ads\text{-}in}$ – heat supplied to the adsorption chiller [kW].

### *1.4.3.7. Energy storage – electrolyser and fuel cell*

Electrolyser–fuel cell systems enable storage of surplus electrical energy by converting it into hydrogen and then reconverting that hydrogen back into electricity, offering a potential solution for long-duration energy storage [123, 124]. In the next step, the parameters of the energy storage unit were determined, consisting of two main components: an electrolyser and a fuel cell. **Figure *18*** presents the electrolyser characteristics, illustrating the relationship between reduced power and electrolyser efficiency.

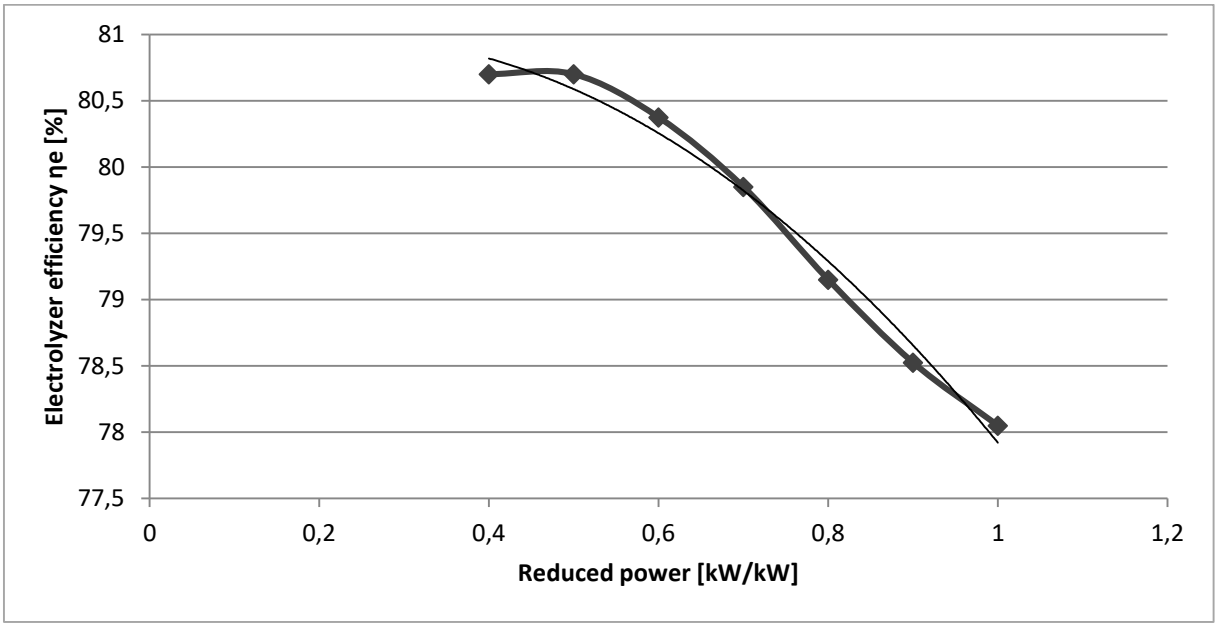


**Figure 18. Efficiency of the electrolyser as a function of reduced power (based on: [125])**

The hydrogen mass flow generated during electrolysis was calculated using equation (48):

$$\dot{m}_{h_2} = \frac{\eta_e P_{AC}}{Q_{wH_2}} \tag{48}$$

Where:
$\dot{m}_{h_2}$ – mass flow of hydrogen produced during electrolysis [kg/h],
$\eta_e$ – electrolyser efficiency [-],
$P_{AC}$ – power supplied to the hydrogen generator [kW],
$Q_{wH_2}$ – hydrogen calorific value [kWh/kg].

The second main component of the storage system is the fuel cell, whose performance is characterised by the relationship between reduced power and fuel cell efficiency. **Figure *19*** presents this dependency.

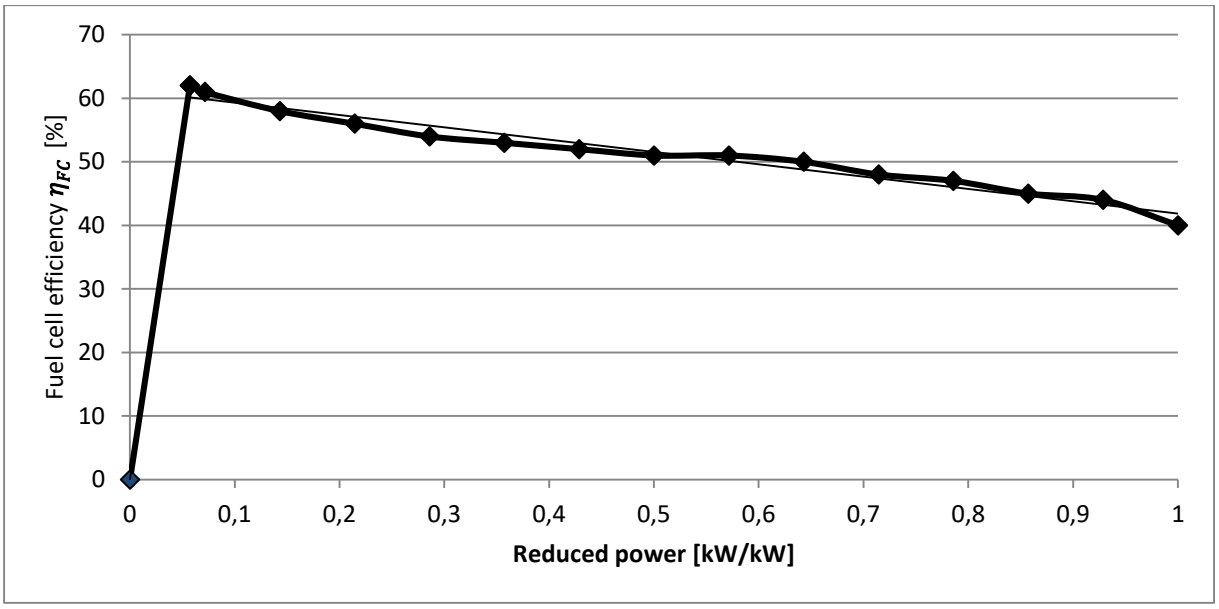


**Figure 19. Efficiency of the fuel cell as a function of reduced power (based on: [125])**

The power output of the fuel cell used to supply the microgrid was calculated using equation (49).

$$P_{el} = \eta_{FC} \dot{m}_{h_2} Q_{wH_2} \tag{49}$$

Where:

$\eta_{FC}$ – fuel cell efficiency [-].

Surplus energy generated from RES is directed to the electrolyser, where hydrogen is produced. The hydrogen is stored and, in the case of supply shortages, reconverted into electricity via the fuel cell.

## 1.5. Scope

The thesis consists of the following chapters:

**Chapter 1** sets the stage for this thesis by explaining the background, motivation, and theoretical framework. It begins with a discussion of global energy demand and the growing importance of renewable energy sources (RES). The chapter then introduces the Thermo-Ecological Cost (TEC) methodology, outlining its definition, balance equations, and practical applications. The chapter also presents demand profiles for electricity, heating, and cooling which form the basis for the technical and ecological analysis conducted in the following chapters. Finally, the main components of the microgrid are described, including photovoltaic (PV) panel, solar collector, photovoltaic-thermal (PV/T) module, wind turbines, heat pump, adsorption chiller and energy storage.

**Chapter 2** presents the first stage of the thesis research. It is based on the article " Thermo-ecological analysis - The comparison of collector and PV to PV/T system" (attached as Appendix 2). This chapter introduces the determination of the Thermo-Ecological Cost (TEC) for a PV/T system (which has not been previously described in the literature). The study illustrates the application of Thermo-Ecological methodology to evaluate hybrid PV/T technology and compares it with conventional PV and collector systems. It then discusses fuel splitting methods between heat and electricity, assesses energy efficiency, and highlights the environmental benefits of PV/T. These results provide the basis for integrating the PV/T system into the microgrid model analysed later in the thesis.

**Chapter 3** is based on the article " Thermo-ecological analysis of the power system based on renewable energy sources integrated with energy storage system – Paper II" (attached as Appendix 2). This chapter focuses on the analysis of various renewable energy configurations in a microgrid. The study assessed the system's performance under specific climatic conditions, taking into account the use of an energy storage system. Using Thermo-Ecological Cost (TEC), the chapter compares single-source and multi-source configurations to demonstrate the optimal combination in terms of resilience and environmental efficiency. The results highlight the benefits of combining complementary resources and storage.

**Chapter 4** builds on the article " Thermo-ecological assessment of microgrid supported with renewable energy – Paper III" (attached as Appendix 3). In this section, the scope of the analysis is expanded to include electricity, heating, and cooling in a multigenerational microgrid based on RES. Two tools are used: Thermo-Economic analysis (TEA), which combines exergy and cost efficiency, and Thermo-Ecological Cost (TEC), which reflects the environmental burden resulting from resource use. The chapter presents an analysis of exergy flow, seasonal and diurnal system operation variability, and fuel splitting factors for cogeneration units. The results demonstrate how TEC better reflects the sustainability of multigenerational microgrids (emphasising resource optimization, emission reduction, and improved resilience) compared to TEA.

**Chapter 5** summarizes the results of the thesis, emphasising the role of Thermo-Ecological Cost (TEC) as a coherent tool for assessing various renewable energy technologies and microgrid configurations. The results highlight the advantages of hybrid renewable energy systems, the importance of seasonal complementarity, and the benefits of energy storage for system resilience and sustainability.

Finally, a list of the literature cited in the thesis (Bibliography), a summary of the thesis (Abstract), and a summary in Polish (Streszczenie) have been appended to the PhD thesis.

## Chapter 2

# Comparison of collector and PV to PV/T system – Paper I

The determination of the TEC value for the PV/T system was established as a first research activity within this thesis. The chapter illustrates the practical application of the thermo-ecological methodology in the assessment of hybrid technology. The study was the first step in creating the thesis, as no value for the PV/T system was found in the literature review. Therefore, in order to use this component in the microgrid and subject the system to further analyses, it was necessary to carry out calculations for this component. The article analyses and presents methods of division of allocation of fuel between heat and electricity.

Solar energy can be used in a variety of ways: can be converted into other energy, such as mechanical, electrical, chemical, etc. The conversion of solar energy into useful energy is generally recognized in two main ways: solar-thermal conversion using solar collectors and through the use of the photovoltaic effect by means of photovoltaic cells [126].

Solar radiation incident on the Earth's surface is approximately 120 000 TW. That greatly exceeds global demand, which makes it a key candidate for large-scale energy supply [127]. Solar energy is therefore highly promising and is harnessed through photovoltaic (PV) systems, which generate electricity, and solar thermal technologies, which produce heat [128]. A key limitation of PV modules is their low efficiency, influenced by shading, mismatch losses, and environmental factors [129–134]. Only a relatively small fraction of the incident solar radiation is converted into electricity, while most becomes heat, raising cell temperature and reducing efficiency by 0.40–0.65 percentage points per degree [135]. This efficiency loss coincides with peak irradiance, when heat losses are highest. Photovoltaic–thermal (PV/T) systems address this by simultaneously producing electricity and heat [136, 137]. This is crucial in the EU, where space and water heating account for almost 79% of household energy use [138]. However, PV/T faces technical and financial barriers [139].

In terms of exergy, RES systems remain less efficient than fossil-based ones: PV achieves 11.6–14.8%, while coal BAT (best available techniques) and NGCC (natural gas combined-cycle), reach 45.9% and 57.7%, respectively [15]. Thus, Thermo-Ecological Cost (TEC) analysis becomes essential, highlighting ecological benefits of RES despite lower efficiency. Since pure energy analysis is insufficient—cogeneration with fossil fuels achieves 80–95% [140]. exergy analysis is necessary, as it accounts for the quality of energy carriers and their ability to perform work [9, 12].The study therefore compares PV, solar thermal, and hybrid PV/T systems in the context of non-renewable energy.

## 2.1. Energy analysis of PV, collector and PV/T

Simulation results indicate that annual PV/T energy production amounts to 267.07 kWh (**Table *4***). It is roughly 1.5 times higher than the output from PV modules alone (183.62 kWh per year). This increase is mainly due to module cooling, which improves PV cell efficiency. Monthly electricity generation from PV/T and PV is summarized in **Table *4*** and illustrated in **Figure *20***.

**Table 4. The quantity of electricity and heat from PV/T and PV/collector per 1 year**

| Parameter | The amount of electricity per year | The amount of heat per year |
|---|---|---|
| Unit | [kWh] | [kWh] |
| PV | 183.62 | - |
| collector | - | 2191.49 |
| PV/T | 267.07 | 540.84 |

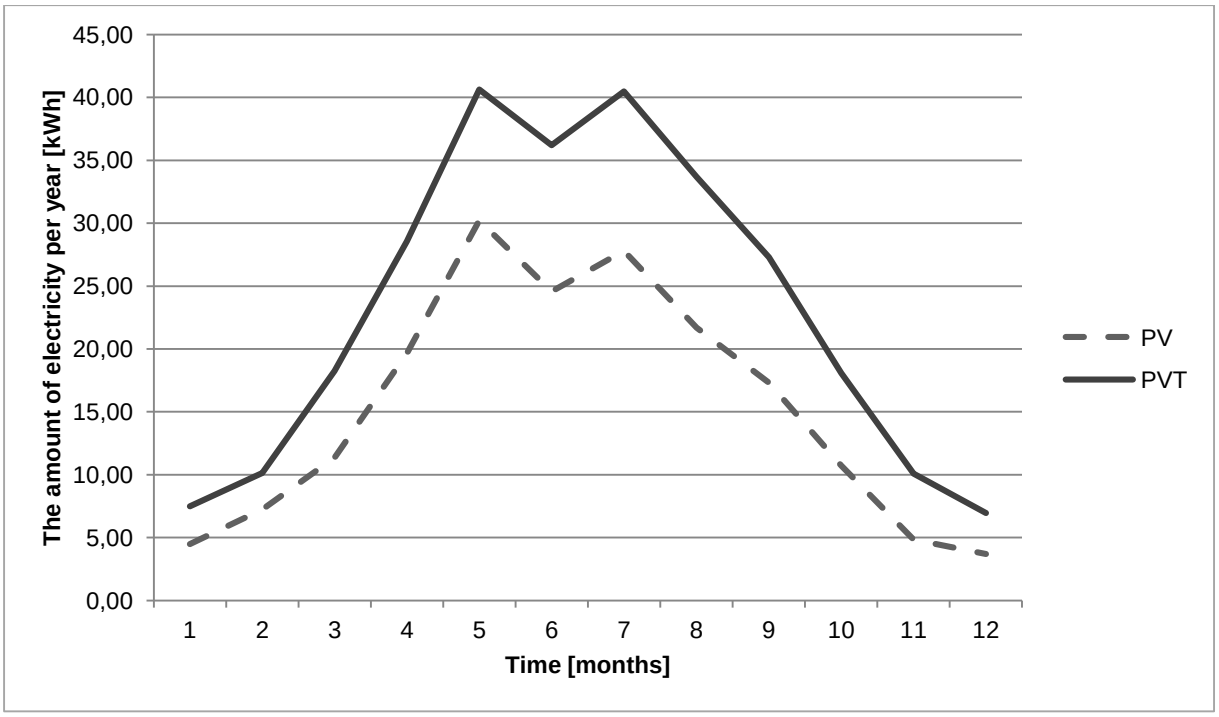


**Figure 20. Electricity from PV/T and PV by months**

When considering the annual heat production, the separated system performs better, as shown in **Figure *21***. The solar collector generates 2.191.49 kWh of heat per year, while the PV/T system produces 540.84 kWh. The substantial difference results partly from the assumption that cooling of the PV/T module begins only once its temperature exceeds 30 °C.

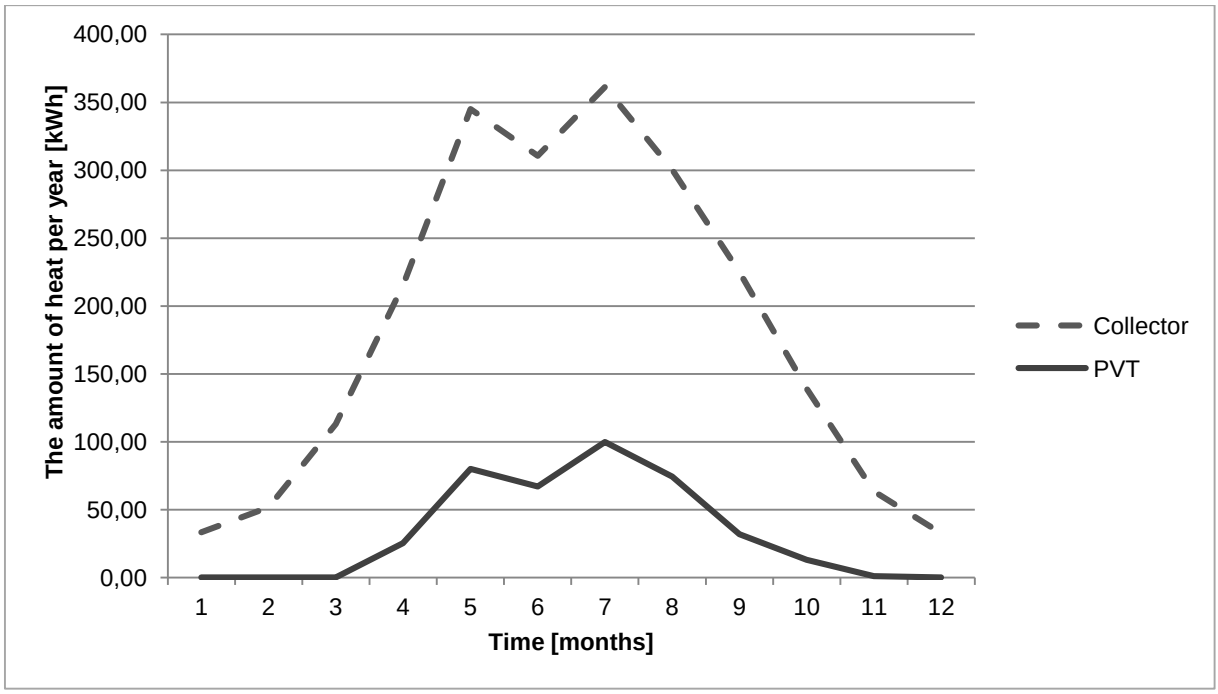


**Figure 21. Heat from PV/T and PV by months**

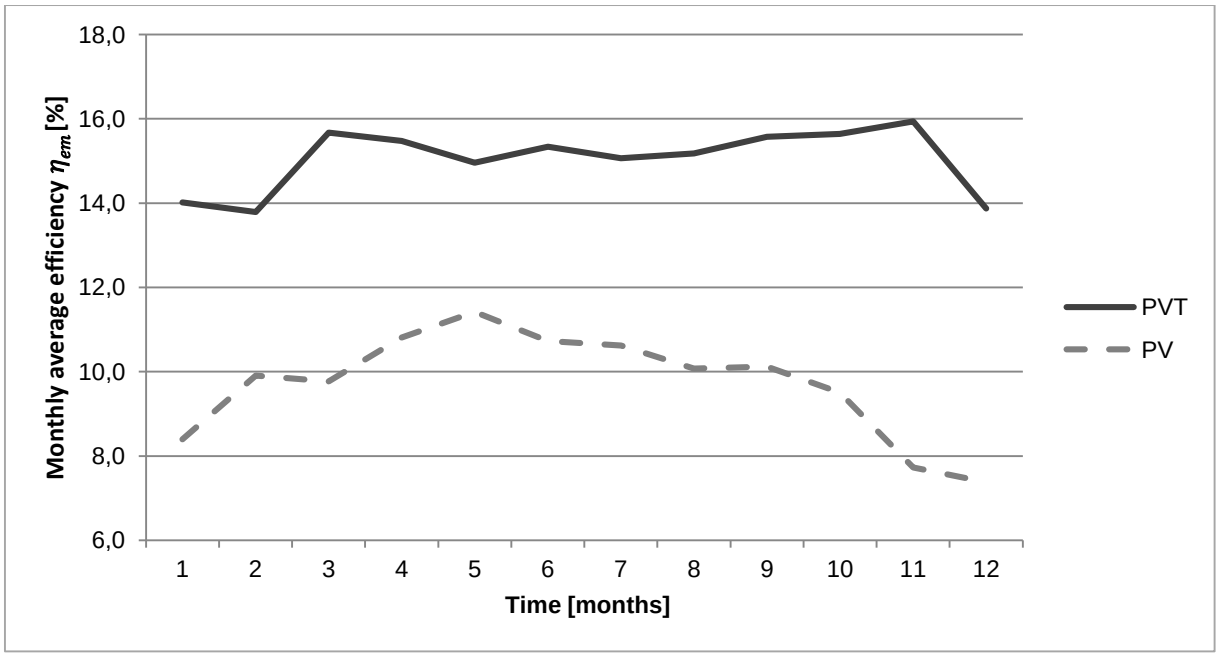


**Figure 22. Monthly average energy efficiency of PV/T and PV**

**Figure *22*** shows that the monthly average efficiency of the PV/T system consistently exceeds that of the PV system across the year. The simulation outcomes serve as the foundation for the TEC analysis discussed in the following section.

## 2.2. Thermo-Ecological Cost of the materials

The calculations considered the Thermo-Ecological Cost of the materials used for constructing the collector, as well as the Thermo-Ecological Cost of the additional equipment. They also take into account the service life of the installation (τ) and the potential for material recovery after decommissioning (u – material recovery coefficient) [19]. **Table *5*** presents the results of the exergy calculations for the applied materials, the expected operating lifetime of the installation, and the product stream.

**Table 5. Exergy results for materials used, expected service life, and product stream of the installation**

| Parameter | Value | Unity |
|---|---|---|
| Total exergy of used materials | 10234.2 | MJ/unit |
| Life time of the PV/T | 25 | years |
| Total exergy of electricity | 979.3 | MJ/year |
| Total exergy of heat | 640.6 | MJ/year |
| Total solar radiation | 6452.9 | MJ/year |
| *unit* refers to a single PV/T installation | | |

Due to cogeneration (simultaneous production of electricity and heat by PV/T), the calculation algorithm also incorporates the allocation of Thermo-Ecological Costs, as presented below.

## 2.3. The division of Thermo-Ecological Costs in cogeneration system

In this calculation, the allocation of fuel between heat and electricity was based on the exergetic cost. The exergetic cost (k*) is defined as the total exergy consumption associated with the useful product. In the case of the PV/T process, this implies that Eq.(50) [19]:

$$k_{PVT}^{*} = \frac{B_{F,PVT}}{B_{P,PVT}} = \frac{B_{F,PVT}}{E_{PVT} + Q_{PVT}\dfrac{\left(T_{e,m} - T_a\right)}{T_{e,m}}} \tag{50}$$

Where:

$B_{F,PVT}$ – total exergy of fuel feeding the PV/T system [MJ],

$B_{P,PVT}$ – total exergy of useful products of the cogeneration unit [MJ],

$T_{e,m}$ – temperature of of the working fluid [K],

$T_a$ – ambient temperature [K].

Based on the specific cost of PV/T, the solar energy input assigned to the production of heat and electricity in the PV/T system can be determined as follows Eqs.(51) - (58) [19]:

$$B_{F,PVT,ele} = E_{PVT} k_{PVT}^{*} \tag{51}$$

$$B_{F,PVT,heat} = Q_{PVT}\frac{\left(T_{e,m} - T_a\right)}{T_{e,m}}k^*_{PVT} \tag{52}$$

$$y_{PVT,ele} = \frac{B_{F,PVT,ele}}{B_{F,PVT}} \tag{53}$$

$$y_{PVT,heat} = \frac{B_{F,PVT,heat}}{B_{F,PVT}} \tag{54}$$

$$TEC_{PVT,mat} = \frac{B_{materials}}{\tau} = \frac{B_{materials}}{\tau} \tag{55}$$

$$TEC_{PVT} = \frac{TEC_{PVT,mat}}{B_{P,PVT}} \tag{56}$$

$$TEC_{PVT,ele} = y_{PVT,ele}TEC_{PVT} \tag{57}$$

$$TEC_{PVT,heat} = y_{PVT,heat}TEC_{PVT} \tag{58}$$

The second division method proposed in this article applies the Thermo-Ecological Cost (TEC) approach, using the proportional TEC indicators of conventional (replaced) technologies. In order to produce electricity and heat in conventional systems—such as coal-fired power plants and heating plants—the total TEC ($TEC_{\sum}$ ) is expressed as Eq. (59) :

$$TEC_{\sum} = TEC_1 + TEC_2 = B_{ele}TEC_{elex} + B_{heat}TEC_{heatx} \tag{59}$$

Where: $TEC_{elex}$ and $TEC_{heatx}$ represent the TEC of electricity from a coal-fired power station and heat from a coal heating plant, respectively. The division coefficients were determined according to the following relations - Eqs. (60) and (61) :

$$\mu_{TEC,ele} = \frac{TEC_1}{TEC_{\sum}} \tag{60}$$

$$\mu_{TEC,heat} = \frac{TEC_2}{TEC_{\sum}} \tag{61}$$

The total TEC of the PV/T system is then expressed as Eqs. (62) - (64):

$$TEC_{PVT,mat} = \frac{B_{materials}}{\tau} = \frac{B_{materials}}{\tau} \tag{62}$$

$$TEC_{PVT,ele} = \frac{\mu_{TEC,ele}TEC_{PVT}}{B_{ele}} \tag{63}$$

$$TEC_{PVt,heat} = \frac{\mu_{TEC,heat} TEC_{PVT}}{B_{heat}} \quad (64)$$

The monthly TEC of electricity and heat generated by the PV/T system according to this second division method is shown in **Figure *23***.

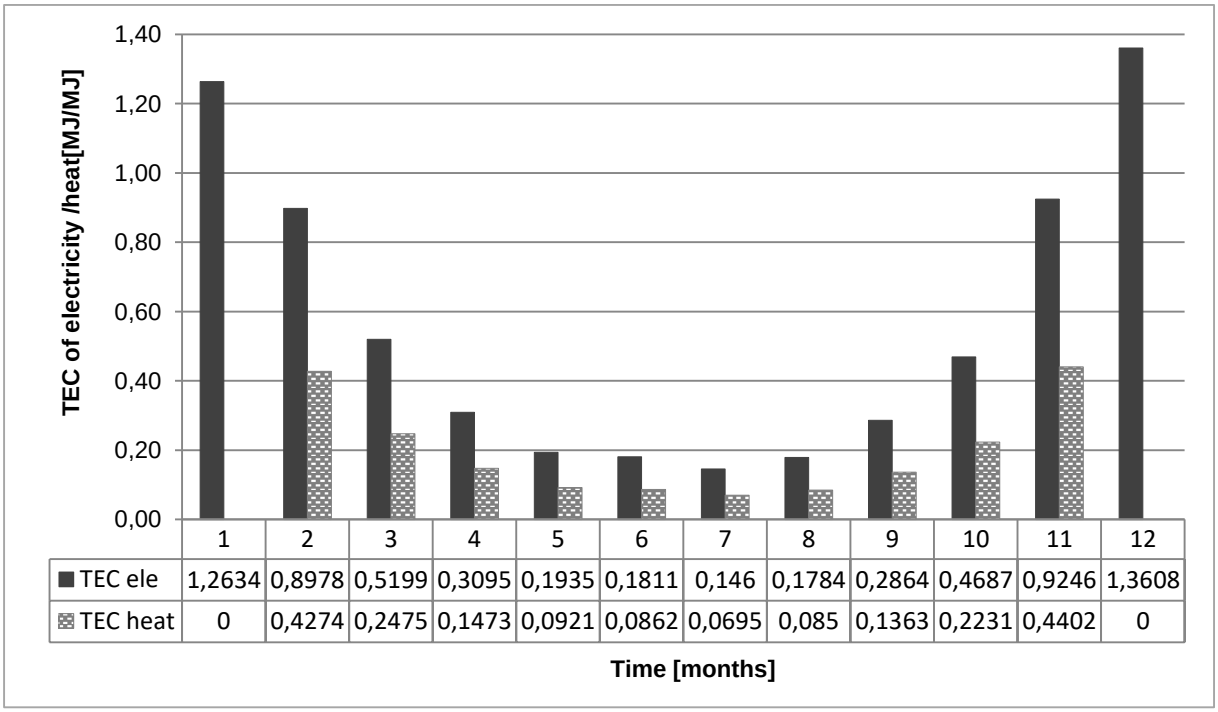


| | 1 | 2 | 3 | 4 | 5 | 6 | 7 | 8 | 9 | 10 | 11 | 12 |
|---|---|---|---|---|---|---|---|---|---|---|---|---|
| TEC ele | 1,2634 | 0,8978 | 0,5199 | 0,3095 | 0,1935 | 0,1811 | 0,146 | 0,1784 | 0,2864 | 0,4687 | 0,9246 | 1,3608 |
| TEC heat | 0 | 0,4274 | 0,2475 | 0,1473 | 0,0921 | 0,0862 | 0,0695 | 0,085 | 0,1363 | 0,2231 | 0,4402 | 0 |

**Figure 23. Monthly TEC of electricity and heat produced by PV/T – the division 2**

The annual average TEC of electricity for the PV/T system, as presented in the **Table *6***, does not exceed 0.2. For the first division method, it equals 0.153, while for the second it is 0.193. Both values are below the TEC of electricity produced by a PV system (0.26) [141]. **Table *6*** presents the calculated TEC values for PV/T, PV, and solar collectors, as well as conventional systems for comparison.

**Table 6. Thermo-Ecological Cost (TEC) analysis of PV and PV/T (based on: [89], [141])**

| TEC [MJ/MJ] | PV | PV/T | | Coal power station | Coal Heating plant | Combined heat and power plant (coal-fired) |
|---|---|---|---|---|---|---|
| | | first division | second division | | | |
| Thermo-Ecological Cost of the electricity | 0.26 | 0.153 | 0.193 | 4.39 | | 4.67 |
| Thermo-Ecological Cost of the useful heat | - | 0.100 | 0.060 | - | 2.09 | 1.31 |

**Figure *24***, **Figure *25***, **Figure *26*** and **Figure *27*** illustrate representative days in spring, summer, autumn, and winter. For each season, four characteristic days were selected, which makes it possible to observe variations in TEC values depending on atmospheric conditions (solar radiation and temperature). In the figures, (1) indicates the first allocation method (the allocation of fuel between heat and electricity was based on the exergetic cost), while (2) represents the second allocation method.

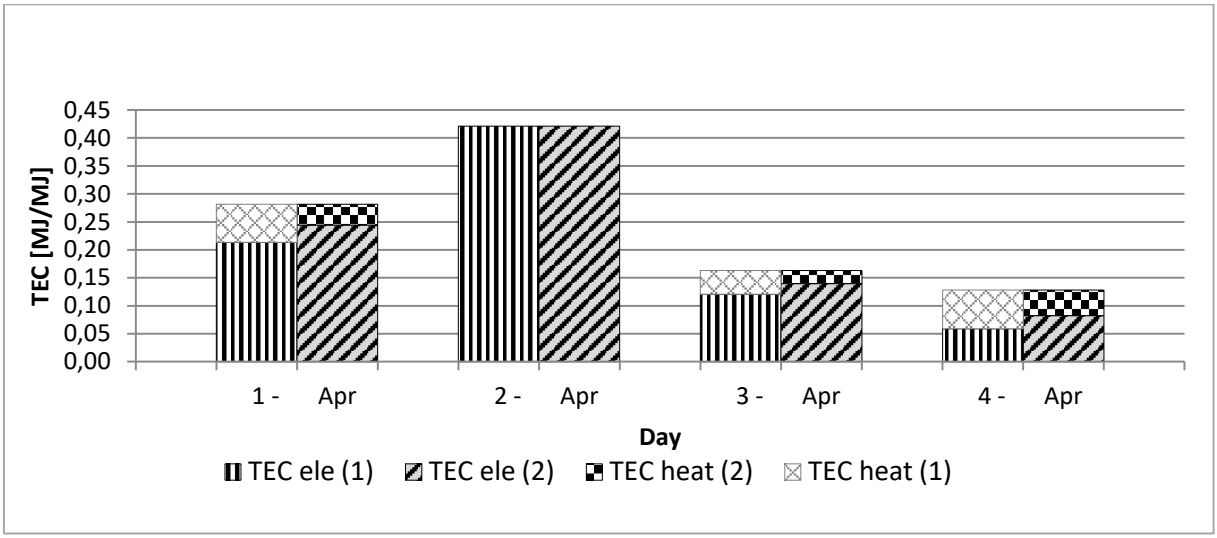


**Figure 24. Daily TEC for selected days in spring of electricity and heat produced by PV/T**

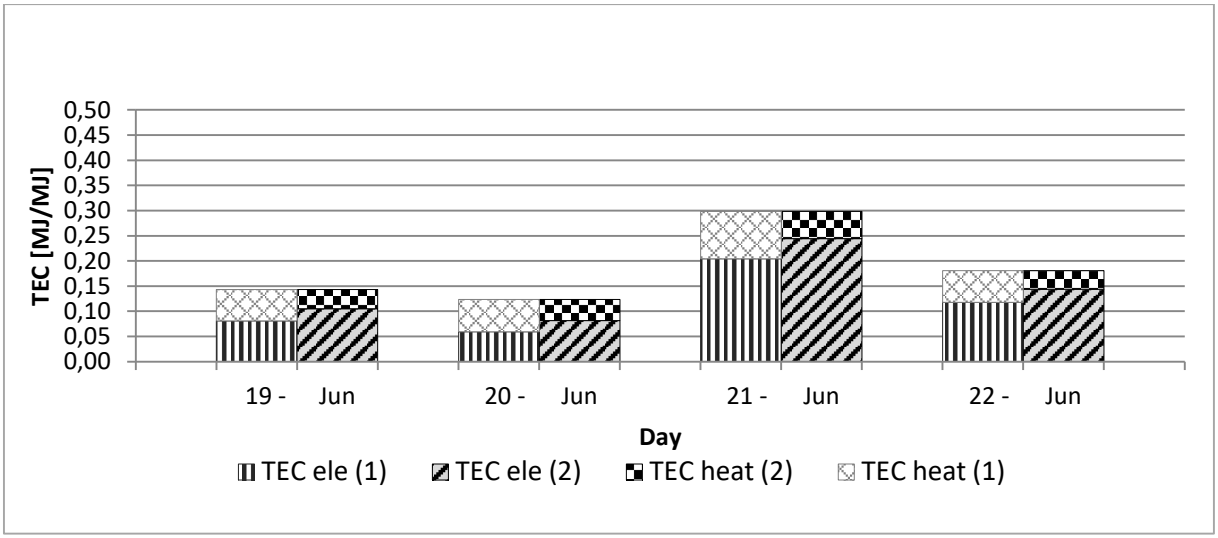


**Figure 25. Daily TEC for selected days in summer of electricity and heat produced by PV/T**

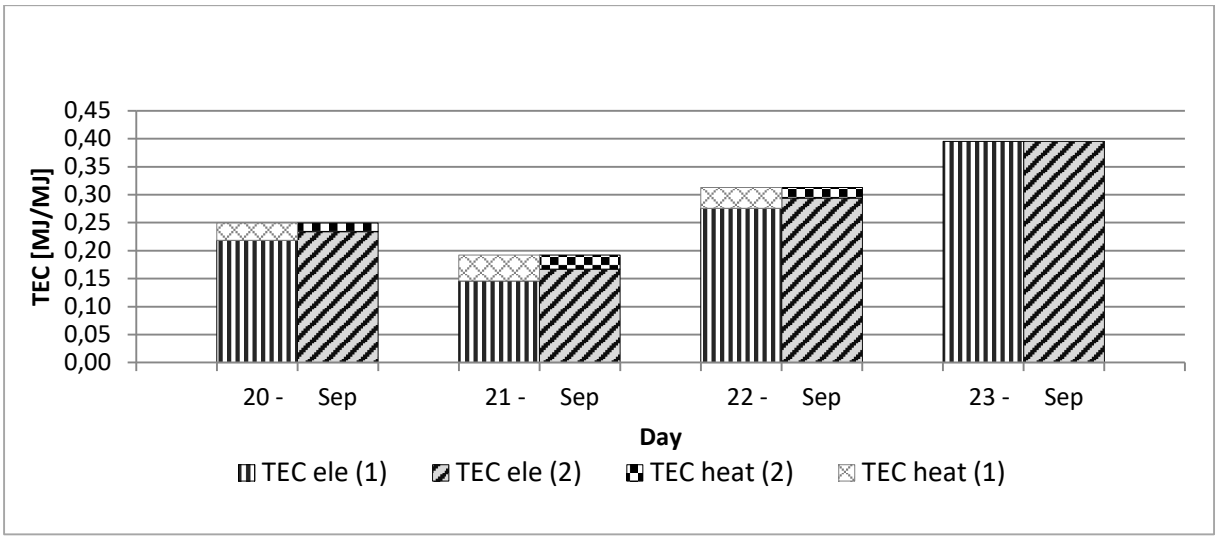


**Figure 26. Daily TEC for selected days in autumn of electricity and heat produced by PV/T**

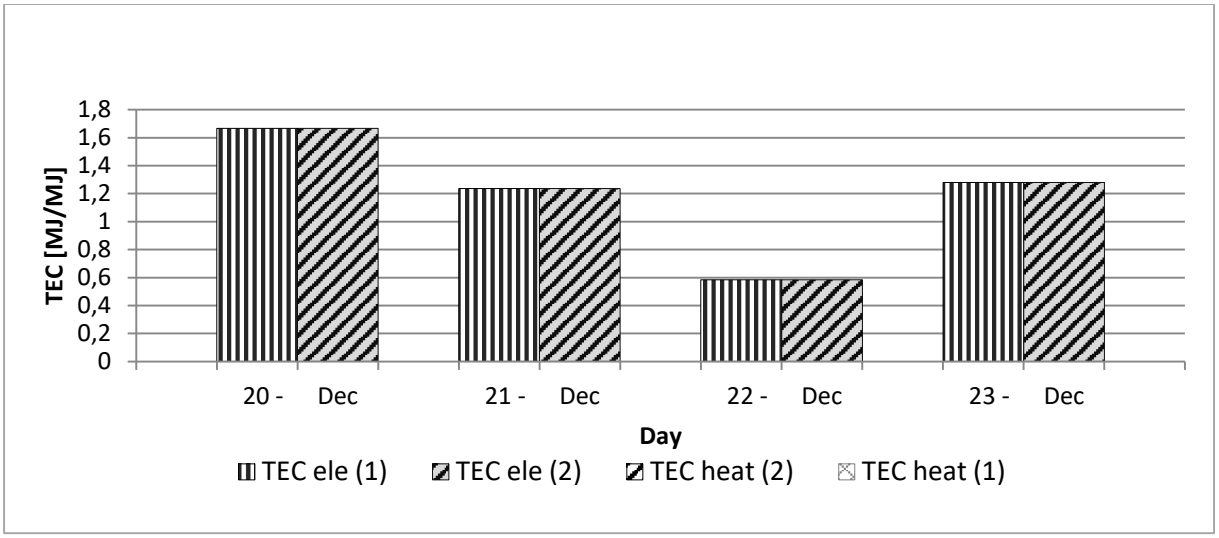


**Figure 27. Daily TEC for selected days in winter of electricity and heat produced by PV/T**

In summer days with high solar irradiation, TEC values remain low (e.g., June 19–22: 0.06 for electricity). In winter (December 20–23), the opposite is observed—TEC for electricity exceeds 1 (1.67 in both divisions), while no heat is generated due to insufficient irradiation and low collector temperature. In spring and autumn, values vary but do not exceed 0.5, with both low TEC days and periods without heat production. The comparison of PV and PV/T showed that the hybrid system is more efficient, with annual average electricity efficiency of 15.18% versus 10.24% for PV. PV/T also generates useful heat, although four times less than a solar collector, since cooling is primarily used to enhance electricity production.

TEC analysis confirmed the environmental advantage of PV/T. The Thermo-Ecological Cost of electricity in PV/T is 0.153 (0.193 in the second division), lower than PV (0.26) and significantly below coal-based systems. The first division method (exergetic cost) gave high TEC values in low-heat months, whereas the second method (proportional to conventional technologies) proved more reliable. The TEC analysis indicated that PV/T systems make more efficient use of resources and have a lower environmental cost compared to separate PV, collector, or fossil-based systems.

## Chapter 3

# Thermo-Ecological Cost of various RES energy mix options – Paper II

The second part of the thesis is focused on the analysis of cooperation between various renewable energy installations within a microgrid. The study compares different energy mixes to find the best configuration for supplying the microgrid. Analysed microgrid includes a photovoltaic system (PV), a hybrid photovoltaic/thermal system (PV/T), a wind turbine, and a biogas-fuelled CHP engine. The analysis also includes the use of stored energy (based on an electrolyser, hydrogen storage tank, and fuel cell) and presents the potential for integrating energy storage technologies into various energy mix scenarios. In the research Katowice was selected as the reference location.

Given the central issue that conventional energy production based on fossil fuels (coal, gas, oil) is a major source of greenhouse gas emissions [63–66] and that the transition to renewable energy systems (RES) is an important response to the climate crisis [67–69, 127] implementing RES-based grids is crucial [76]. However, RES pose challenges due to their dependence on natural conditions - their production is time-varying [71–75]. Variable renewable energy sources (RES), such as PV, PV/T, and wind, are intermittent and require more careful system planning and integration with flexible resources [77, 78]. Solutions such as smart microgrids (supported by energy storage and smart meters) enable improved balancing [79]. Storage can include various technologies, such as batteries, pumped-storage hydropower, compressed air, and hydrogen systems [80–84]. The analysed microgrid combined photovoltaic (PV) systems, photovoltaic-TV systems, wind turbines, a biogas plant, and storage systems. Various system configurations were compared against demand profiles, and the Thermo-Ecological Cost (TEC) was used as an evaluation metric.

### 3.1. Hour-by-hour analysis

The studied microgrid is based on renewable energy sources, whose operational characteristics were presented in the Chapter 1. The analysis was performed on an hourly time step for a full year (in order to capture temporal variability). Electricity from RES primarily covers the current demand. Any surplus goes to an electrolyser to produce hydrogen, which is stored for later use. During low generation periods, the hydrogen is converted back into electricity through a fuel cell.

In cases where the output from RES is insufficient to meet the demand (e.g., due to unfavourable meteorological conditions), the required balance is supplied from the energy storage unit. In practice, this means that even on cloudy winter days, the system can maintain supply. If the available storage capacity is depleted or inadequate, the remaining electricity demand is satisfied by the power grid. The configuration of the integrated system is schematically illustrated in **Figure *28***.

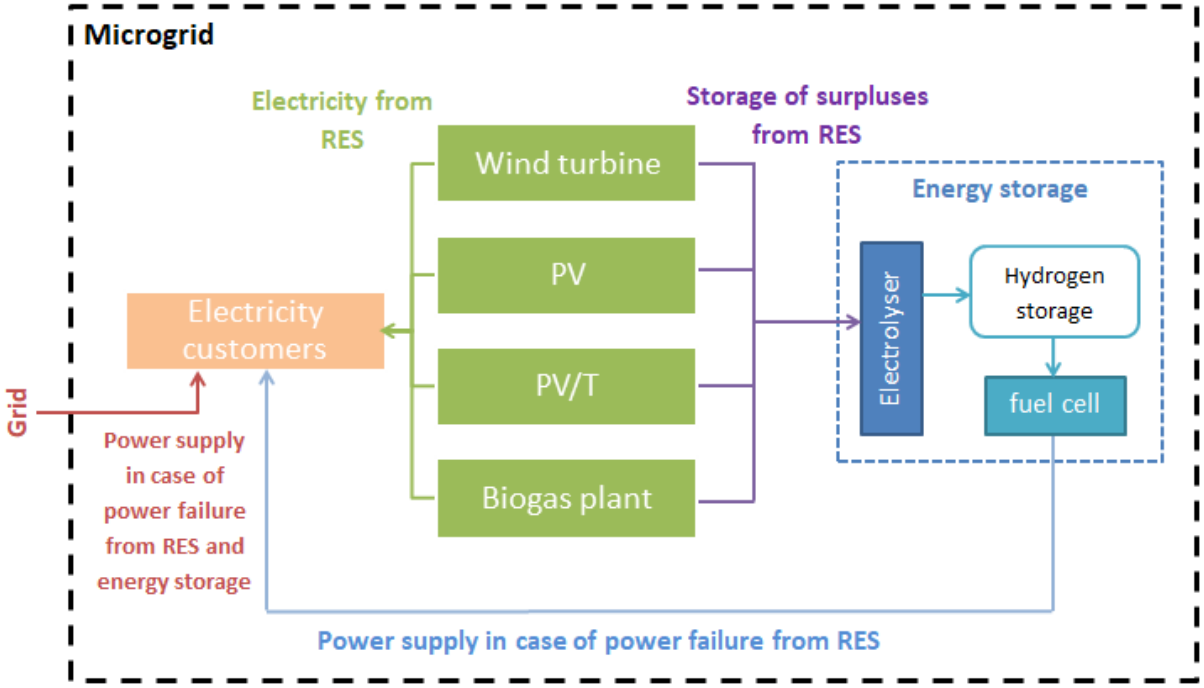


**Figure 28. Power system (microgrid) consisting of renewable sources, energy storage, and emergency power supply from the grid**

The performance of each renewable energy source and storage system was analysed on the basis of hourly resolution data. Simulations were carried out using climatic inputs for a representative location in Poland (Katowice). In the following section, aggregated monthly energy balances are presented, while below selected representative days are shown to illustrate the interplay between generation and demand.

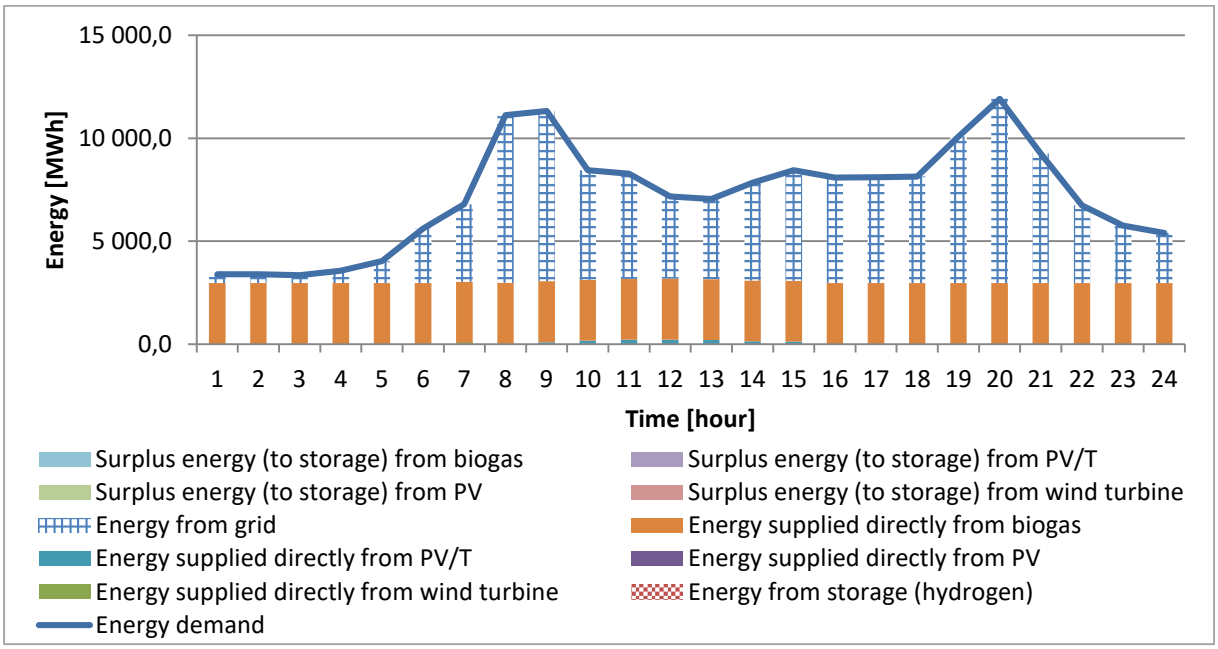


**Figure 29. Hourly consumption and generation for a winter day with low renewable generation (January 3)**

**Figure *29*** illustrates a winter day characterized by low renewable generation, limited hydrogen storage, and high demand. In this case, the majority of the required electricity had to be supplied from the grid. The contrasting situation is presented in **Figure *30***.

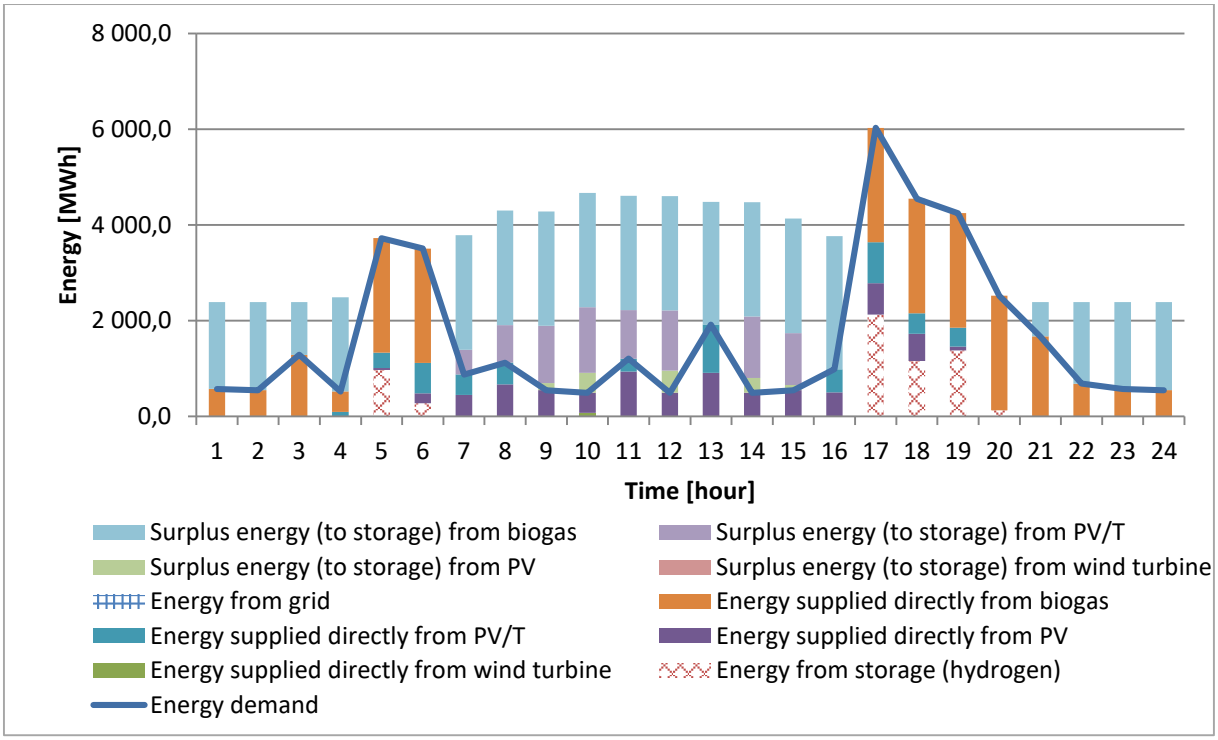


**Figure 30. Hourly consumption and generation for a summer day with high renewable generation**

**Figure *30*** depicts a summer day with high renewable output, eliminating the need for grid supply. During periods of partial mismatch between demand and renewable supply (e.g., in the morning or afternoon), the deficit was covered by the storage system. These results were obtained for the scenario including four renewable energy sources operating simultaneously (4.0 MW wind turbine, 4.0 MW PV/T, 4.0 MW PV, and 3.0 MW biogas). In subsequent sections, the performance of alternative energy mix configurations is analysed.

## 3.2. Energy mix options

The analysis considered various renewable energy mix configurations—starting with single installations and subsequently extending to combinations of two, three, and four sources. For each individual source (PV, PV/T, wind turbine, and biogas), operation was assessed at a nominal capacity of 15 MW. The following observations were made for each technology and their combinations:

- PV and PV/T systems generated electricity primarily during summer months. The higher efficiency of PV/T enabled complete coverage of demand in July through direct supply and storage utilization.
- The wind turbine delivered its highest output in winter, but under the analysed climatic conditions its annual effectiveness remained limited.
- The biogas plant provided the most stable and weather-independent generation, although it did not fully exploit the storage capacity.

Representative results for single, dual, and triple configurations are presented in the article included in Appendix 2. Below, a detailed example is provided for the four-source configuration.

For two-source mixes (e.g., PV/T + wind or biogas + PV/T), improved seasonal complementarity was observed. The PV/T + biogas system covered demand almost year-round, with only small amounts of electricity drawn from the grid. Adding a third source improved performance further. Three-source systems (such as PV + PV/T + biogas or PV/T + wind + bio-gas) demonstrated even higher resilience, although shortages were still recorded during winter when storage capacity was insufficient. The best results were achieved with the four-source setup. The four-source configuration (PV, PV/T, wind turbine, and biogas) yielded the most favourable outcome. Grid supply was required only in early and late winter, when the hydrogen storage was either not yet sufficiently charged or had been depleted**.** **Figure *31*** presents the cooperation of four renewable energy sources within the microgrid.

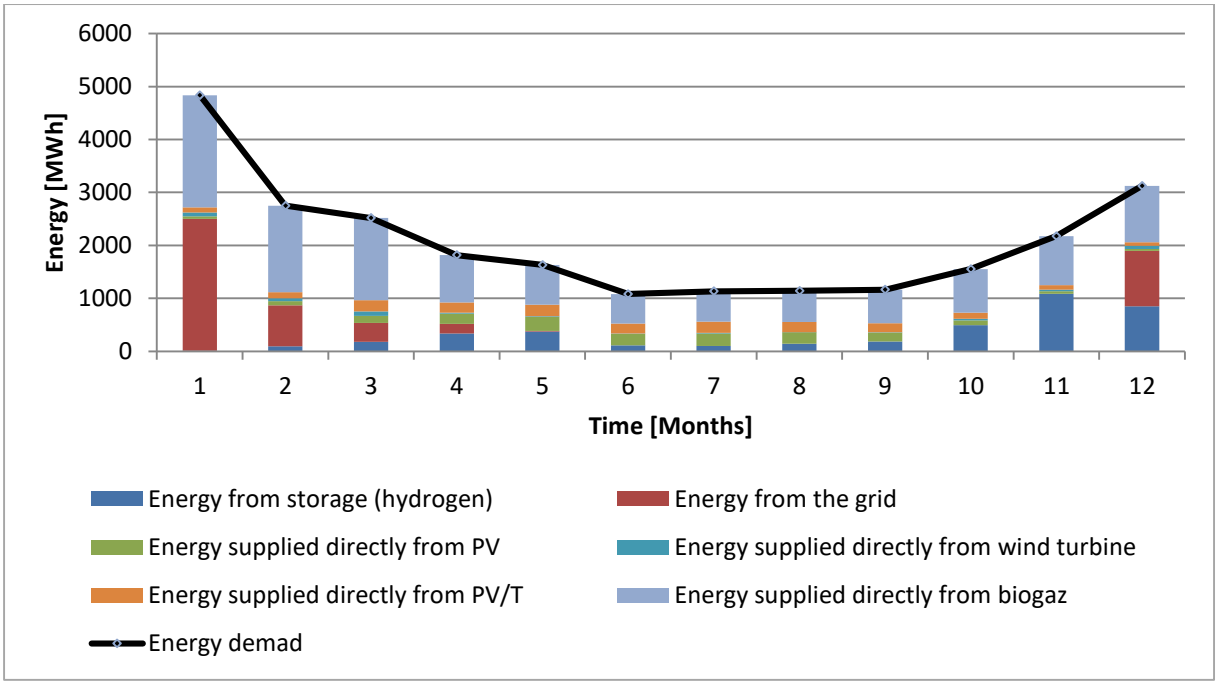


**Figure 31. Energy mix option – electricity generation based on four renewable energy sources (4.0 MW wind turbine, 4.0 MW PV/T, 4.0 MW PV, and 3.0 MW biogas)**

## 3.2. Thermo-Ecological Cost (TEC) of energy mix options

In the first stage of the assessment, the Thermo-Ecological Cost (TEC) was calculated for systems based on a single renewable source. Single-source systems was: photovoltaic panels (PV), photovoltaic–thermal collectors (PV/T), a wind turbine or a biogas plant. The PV-based system showed the lowest TEC values during summer, reflecting high renewable output and effective storage utilization. A similar seasonal pattern was observed for PV/T, but with even lower summer TEC due to higher system efficiency. In the wind-based system, TEC values remained relatively high throughout the year, with a local minimum in March when wind conditions were most favourable. By contrast, the biogas-based system achieved the lowest annual TEC, as the energy demand was entirely met by a stable renewable source. The slight increase in TEC toward the end of the year was caused by storage-related efficiency losses.

In the second stage, dual-source systems were analysed. The PV/T + wind configuration still exhibited relatively high TEC values due to frequent grid supplementation, with improvements only during summer peaks of PV/T production. In the PV/T + biogas configuration, TEC gradually decreased as RES contribution and storage use increased. The wind + biogas system recorded the lowest TEC values in summer and maintained favourable performance in autumn due to previously stored energy.

In the third stage, triple-source configurations were evaluated. The wind + PV/T + biogas mix achieved TEC values below 1 for most of the year, indicating strong complementarity. The PV + PV/T + wind mix showed higher TEC due to persistent reliance on grid supply. The PV + PV/T + biogas mix delivered the best performance, with TEC below 1 for 11 months and dropping below 0.2 between May and November.

Finally, the four-source configuration (PV, PV/T, wind, and biogas) demonstrated consistently low TEC values throughout the year (**Figure *32***). Only in January did TEC exceed 1.5, reflecting substantial grid imports during periods of low renewable output and uncharged hydrogen storage. In December, TEC rose close to 1 due to depleted storage.

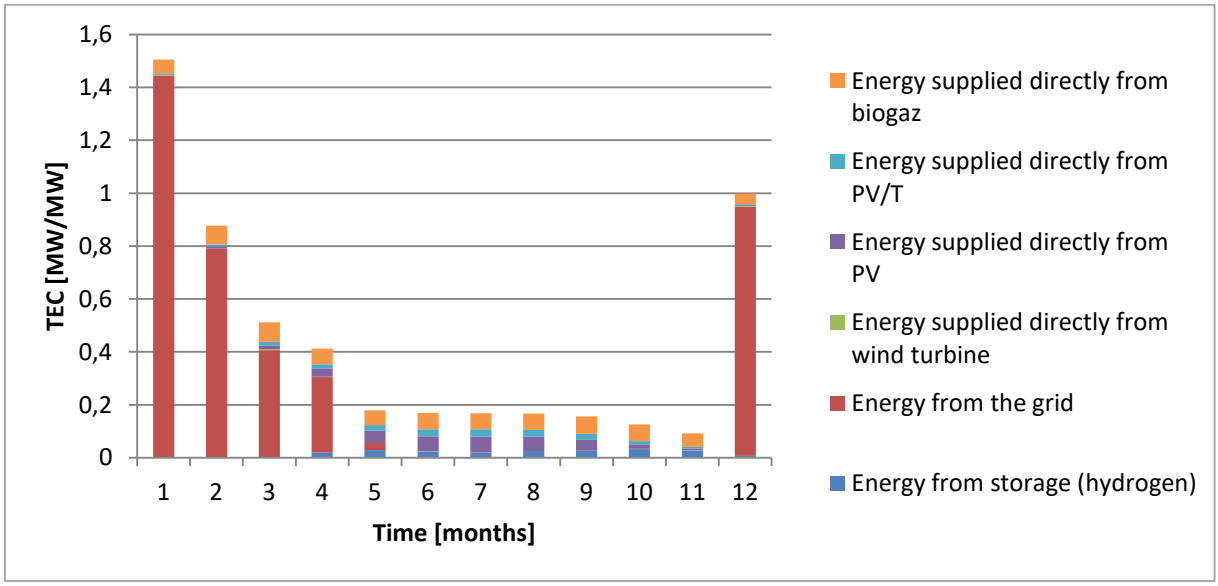


**Figure 32. Thermo-Ecological Cost (TEC) – energy production based on four renewable energy sources (4.0 MW wind turbine, 4.0 MW PV/T, 4.0 MW PV, and 3.0 MW biogas)**

The comparative analysis of different renewable energy configurations within a microgrid was tailored to local demand and climatic conditions. It enabled the identification of scenarios with the highest resilience and the lowest Thermo-Ecological Cost. The results show that optimal integration of renewable sources provides a range of benefits. First, the study emphasises that optimal integration ensures seasonal complementarity. Second, it positively affects effective energy storage management and reduces dependence on the external grid. As a result, the system becomes more self-sufficient, and its environmental impact decreases.

## Chapter 4

# Local and global evaluations of microgrid supported by RES – Paper III

In the next stage of the research, the analysis was extended beyond electricity to include heat and cooling, both demanded and generated within the microgrid. Two evaluation tools were employed: Thermo-Economic Analysis (TEA) and Thermo-Ecological Cost (TEC). In hybrid systems, TEA may misleadingly suggest a preference for maximizing the use of external resources (without regard to their origin) and minimizing internal energy conversion. In contrast, TEC provides a clearer assessment of the actual resources supplied to the system. This study highlights the importance of considering both the origin and the efficiency of resources in microgrid applications. A comprehensive multigeneration system based on a mix of renewable energy sources was therefore analysed.

Energy is a key driver of economic and social development, and ensuring its sustainable supply while minimizing environmental impacts has become a global priority [143]. Achieving this goal requires a shift toward clean, affordable, and renewable sources [144]. Declining costs of renewable energy technologies and the integration of smart energy systems are pivotal in facilitating this transition [145]. Among modern solutions, microgrids are recognized as a promising approach to renewable integration, improving energy use and reducing transmission losses [146].

A microgrid, composed of distributed resources and loads, can operate both grid-connected and islanded, offering flexibility and resilience [147, 148]. Its reliance on renewable sources makes it a sustainable alternative to conventional systems [149, 150], while its role in the smart grid highlights efficiency and reliability [151]. However, energy management is challenging due to variability in renewable output and market conditions [152], which necessitates the use of storage systems and advanced management strategies [153, 154].

Variable Renewable Energy (VRE) sources like PV, PV/T, and wind are inherently intermittent, requiring system complementarity to balance demand [155, 156]. Effective planning must consider technical and temporal details to avoid underestimating flexibility needs [78] smart microgrids, equipped with meters and energy-sharing capabilities, address these challenges [79]. Storage technologies, including hydrogen via electrolysis/fuel cells, play a key role [83, 84]. Other options, such as electric vehicles integration [157], pumped hydro [158], or optimised sizing of RES and storage [159–161] further enhance stability and efficiency.

Advanced control and embedded systems are increasingly important in optimizing multigeneration microgrids and ensuring sustainable operation [162].Thermo-Ecological Cost (TEC) analysis provides an effective framework for assessing environmental performance of both renewable and hybrid systems. Studies demonstrate the value of its application in multigeneration systems [163, 164]. Its use in wind energy [26, 165] and Carnot batteries [166] also appears promising. Previous works additionally indicate a range of benefits from applying the Thermo-Ecological Cost (TEC) methodology

in energy mix optimization [23, 31, 32, 167]. The analysed studies emphasise the importance of a global resource assessment, particularly for systems based on renewable energy sources. In the study presented below, the TEC method was applied to evaluate a renewable-based microgrid. The obtained results indicate resource optimization, emission reduction, and improved system resilience.

## 4.1. Thermo-Economic analysis – methodology

The first step in TEA is to define the system boundaries and identify all components, such as turbines, boilers, and compressors. Each component is modelled using input–output relationships for energy, exergy, and cost. Clearly establishing the system boundaries is essential for both the energetic and economic assessment [54–56].

TEA applies exergy analysis to evaluate how effectively each component utilises available energy, identifying losses due to irreversibilities (e.g., friction, heat transfer). Fuel and product are the two central concepts. The product is determined by the function of the component, while the fuel refers to the resources consumed to achieve that function. For instance, in a steam turbine the reduction in steam exergy constitutes the fuel, while the work output represents the product. In all cases, fuel exceeds product, with the difference accounting for irreversibility – Eq. (65).

$$F_i = P_i + I_i \tag{65}$$

Where:
$F_i$ – fuel of component (i) [W],
$P_i$ – product of component (i) [W],
$I_i$ – irreversibility rate, of component (i) [W],

It should be emphasised that the exergy cost refers exclusively to the exergy entering the analysed system. As a result, it does not account for upstream transformation processes, which clearly distinguishes it from the Thermo-Ecological Cost (TEC).

Within TEA, the economic implications of exergy destruction (or losses) are assessed to quantify the contribution of component inefficiencies to the overall system cost. The exergetic cost is defined as the ratio of total fuel exergy consumed to the useful product exergy. It is expressed in equation (66) [19]:

$$k^* = \frac{B_F}{B_P} \tag{66}$$

Where:
$k^*$ - exegetic cost [-],
$B_P$ – exergy of product [MJ],
$B_F$ – exergy of fuel [MJ].

## 4.2. Exergy flow analysis

In this study, an analysis of 28 exergy flows was performed. Among them, eight streams represent inputs to the system, while three correspond to output flows of electricity, heating, and cooling delivered to end users. The overall configuration of the analysed flows is illustrated in **Figure *33***.

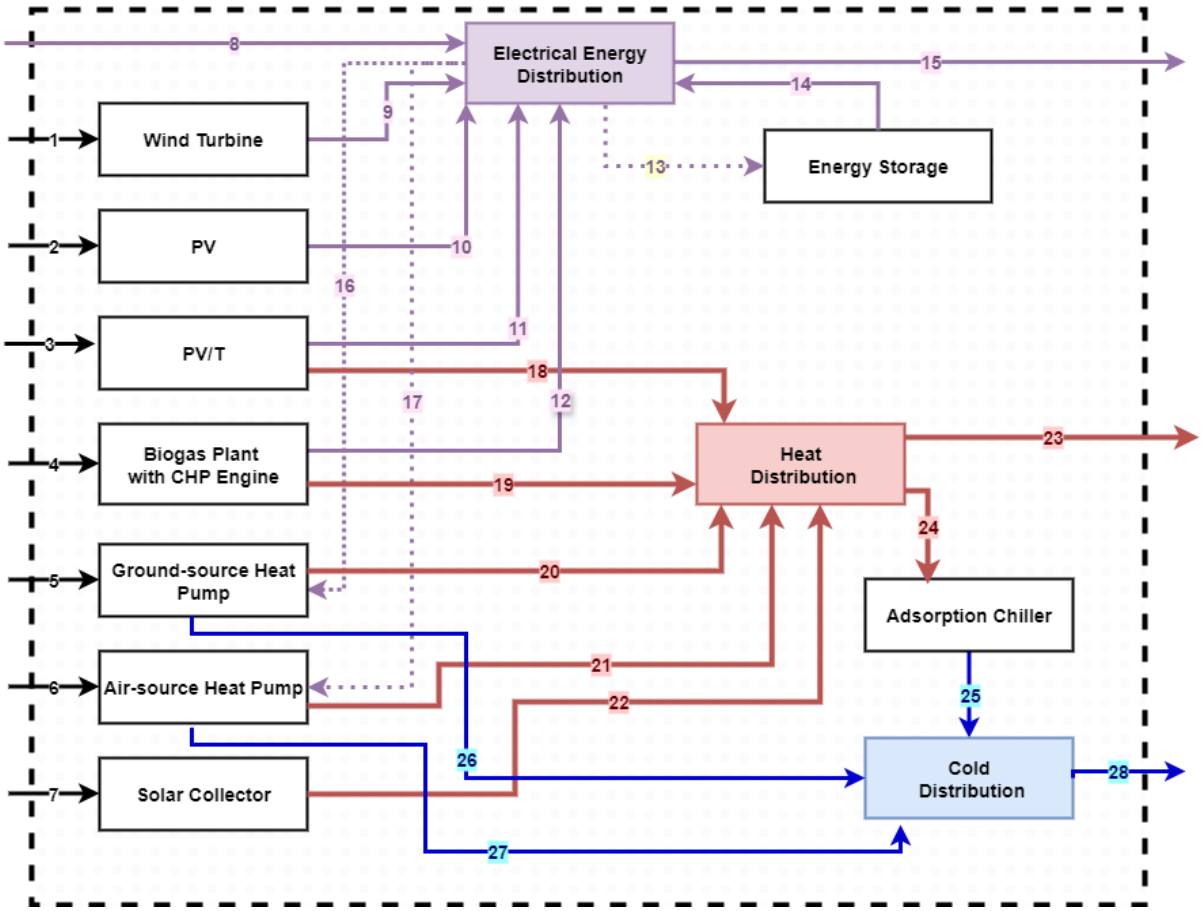


**Figure 33. Exergy flows in the analysed system**

The descriptions of the individual exergy flows are presented in **Table *7***. A comprehensive explanation of the system's operation is provided in Chapter 1 of this thesis.

**Table 7. Designations and explanations of exergy flows in the analysed system**

| Flow | Description |
|---|---|
| $\dot{B}_1$ | wind energy used for generation in the wind turbine |
| $\dot{B}_2$ | solar radiation flow used for electricity production by PV panels |
| $\dot{B}_3$ | solar radiation flow used for electricity production by the hybrid PV/T module, |
| $\dot{B}_4$ | chemical energy used to generate biogas and subsequently heat and electricity in the CHP engine |
| $\dot{B}_5$ | ground heat used in the ground-source heat pump |
| $\dot{B}_6$ | atmospheric air heat used in the air-source heat pump |

| Flow | Description |
|---|---|
| $\dot{B}_7$ | solar radiation stream used for heat production by the collector |
| $\dot{B}_8$ | electrical energy stream from the external grid (supplied to the system in case of shortage |
| $\dot{B}_9$ | electrical energy generated by the wind turbine, |
| $\dot{B}_{10}$ | electrical energy generated by the PV system |
| $\dot{B}_{11}$ | electrical energy generated by the PV/T system |
| $\dot{B}_{12}$ | electrical energy generated by the biogas-powered CHP |
| $\dot{B}_{13}$ | electrical energy supplying the energy storage system, |
| $\dot{B}_{14}$ | electrical energy generated by the energy storage system. |
| $\dot{B}_{15}$ | electrical energy supplied to end consumers |
| $\dot{B}_{16}$ | electrical energy supplying the ground-source heat pump |
| $\dot{B}_{17}$ | electrical energy supplying the air-source heat pump |
| $\dot{B}_{18}$ | heat from the PV/T module |
| $\dot{B}_{19}$ | heat from the biogas-powered CHP engine |
| $\dot{B}_{20}$ | heat from the ground-source heat pump |
| $\dot{B}_{21}$ | heat from the air-source heat pump, |
| $\dot{B}_{22}$ | heat from the solar collectors |
| $\dot{B}_{23}$ | heat is directed to end users |
| $\dot{B}_{24}$ | heat is directed to adsorption chiller |
| $\dot{B}_{25}$ | useful cooling from the adsorption chiller, |
| $\dot{B}_{26}$ | useful cooling from the ground-source heat pump |
| $\dot{B}_{27}$ | useful cooling from the air-source heat pump |

The conducted analysis enables the presentation of the system's state—expressed in terms of exergy flow values—for each hour of the year. **Table *8*** provides an example dataset for a single representative hour (April 3rd, 8:00 AM). The table illustrates how energy and exergy flows are managed at this moment, reflecting both generation and consumption patterns in the microgrid. These results are essential for understanding the balance between renewable energy generation, storage, and demand coverage.

**Table 8. Example exergy - 3rd April, 8 am**

| Name | F | P | $\eta_B$ | I | k* | (TEC) |
|---|---|---|---|---|---|---|
| - | kW | kW | - | kW | - | - |
| **Electricity** | | | | | | |
| PV | 13 233.2 | 1 621.5 | 0.1 | 11 611.8 | 8.2 | 0.3 |
| PV/T | 13 233.2 | 2 082.7 | 0.2 | 11 150.6 | 6.4 | 0.2 |
| Wind turbine | 36 087.6 | 10 465.4 | 0.3 | 25 622.2 | 3.4 | 0.1 |
| Biogas CHP plant | 1 459.1 | 830.6 | 0.6 | 628.5 | 1.8 | 0.7 |
| Gird (Polish grid energy mix) | 0.0 | 0.0 | - | - | - | 2.8 |
| Energy Storage (from ES) | 0.0 | 0.0 | - | - | - | 0.3 |
| Energy Storage (into ES) | 9 328.1 | 7 531.5 | 0.8 | 1 796.6 | 1.2 | 0.1 |
| **Heat** | | | | | | |
| PV/T | 0.0 | 0.0 | - | - | - | 0.1 |
| Solar collector | 1 320.0 | 209.2 | 0.2 | 1 110.9 | 6.3 | 0.6 |
| Biogas CHP plant | 505.3 | 305.5 | 0.6 | 199.8 | 1.7 | 0.3 |
| Air heat pump | 2 559.6 | 486.9 | 0.2 | 2 072.7 | 5.3 | 4.0 |
| Ground heat pump | 1 424.4 | 445.4 | 0.3 | 979.0 | 3.2 | 2.4 |
| **Cold** | | | | | | |
| Adsorption Chiller | 0.0 | 0.0 | - | - | - | 4.6 |
| Air heat pump | 0.0 | 0.0 | - | - | - | 0.0 |
| Ground heat pump | 0.0 | 0.0 | - | - | - | 0.0 |

## 4.3. Fuel division indicators

Using the adopted TEC indicators of the replaced processes, the fuel division indicators for the combined heat and power (CHP) unit were determined between its two products—heat and electricity—according to equations (67) and (68):

$$\mu_Q = \frac{Q_{CHP} TEC_{Q,rep}}{\left(E_{el,CHP} TEC_{el,rep} + Q_{CHP} TEC_{Q,rep}\right)} \quad (67)$$

$$\mu_{el} = \frac{E_{el,CHP} TEC_{el,zast}}{\left(E_{el,CHP} TEC_{el,zast} + Q_{CHP} TEC_{Q,zast}\right)} \quad (68)$$

Where:

$u_Q$ – share of heat production in fuel consumption in CHP [-],

$u_{ele}$ – share of electricity production in fuel consumption in CHP [-],

$TEC_{Q,rep}$ – TEC of heat produced in CHP (of the replaced processes) [MJ/MJ] [168]

$TEC_{ele,rep}$ – TEC of electricity produced in CHP(of the replaced processes) [MJ/MJ] [168],

The specific fuel consumption rates with TEC distribution for each product are then calculated from equations (69) and (70):

$$x_Q = \frac{\mu_Q E_{ch,CHP}}{Q_{CHP}} \tag{69}$$

$$x_{el} = \frac{\mu_{el} E_{ch,CHP}}{E_{el,CHP}} \tag{70}$$

Where:
$x_Q$ - specific fuel consumption indicator with TEC section for heat [-],
$x_{ele}$ - specific fuel consumption indicator with TEC section for electricity [-],
$E_{ch,CHP}$ - chemical energy consumed by CHP [kW].

Finally, for the determined values of $x_Q$ and $x_{ele}$, the TEC indicators for heat and electricity are calculated as follows - Eqs. (71) and (72):

$$TEC_{Q,CHP} = x_Q TEC_{FUEL} \tag{71}$$

$$TEC_{el,CHP} = x_{el} TEC_{FUEL} \tag{72}$$

Where:
$TEC_{FUEL}$– TEC of the fuel consumed by the CHP unit [MJ/MJ],

## 4.3. Analysis of seasonal and diurnal variability in microgrid operation

The study examined microgrid operation across selected days and hours of the year. Both seasonal variability in renewable energy generation and diurnal fluctuations (e.g., variation in solar irradiance throughout the day) were taken into account. The analysis also incorporated seasonal differences in the demand for electricity, heat, and cooling (which depend on both the time of year and the time of day).To illustrate these dynamics several representative hours of the year were selected.

The first representative case corresponds to April 3rd at 8:00 AM**.** At this moment, the primary source of electricity was the wind turbine. The system generated a surplus of electricity, which was directed into the energy storage unit. Heat production was mainly provided by the biogas-fuelled combined heat and power (CHP) engine, supplemented by the heat pump and solar thermal collector (used primarily for domestic hot water). At this time of year, there was no demand for cooling, and therefore no cooling output was recorded.

**Figure *34*** and **Figure *35*** illustrate the system operation on April 3rd at 8:00 AM. **Figure *34*** resents the exergy values corresponding to the analysed hour, while **Figure *35*** depicts the inflows and outflows of exergy within the system. It can be observed that, at this moment in the year, the system accumulated energy: the total incoming exergy significantly exceeded the outgoing flows, resulting in surplus storage.

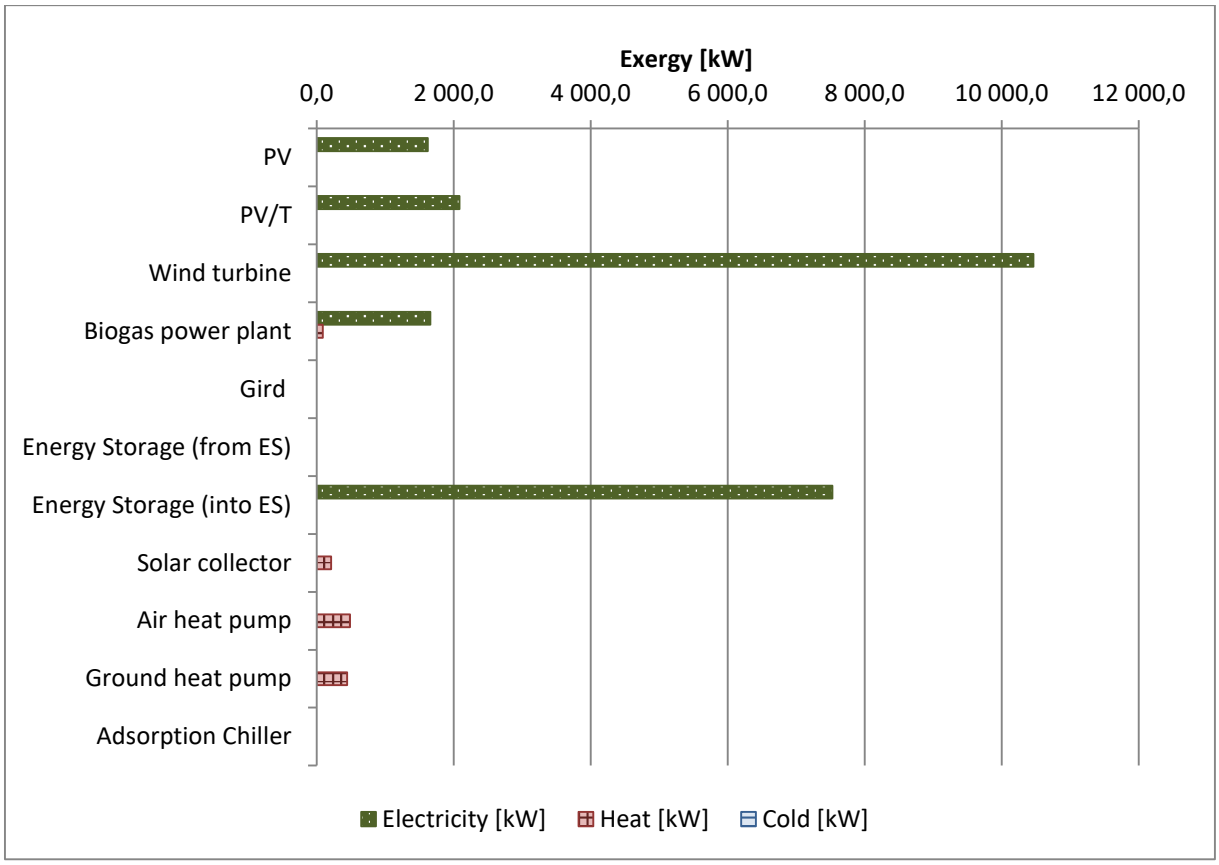


**Figure 34. Exergy values for 3rd April, 8 am**

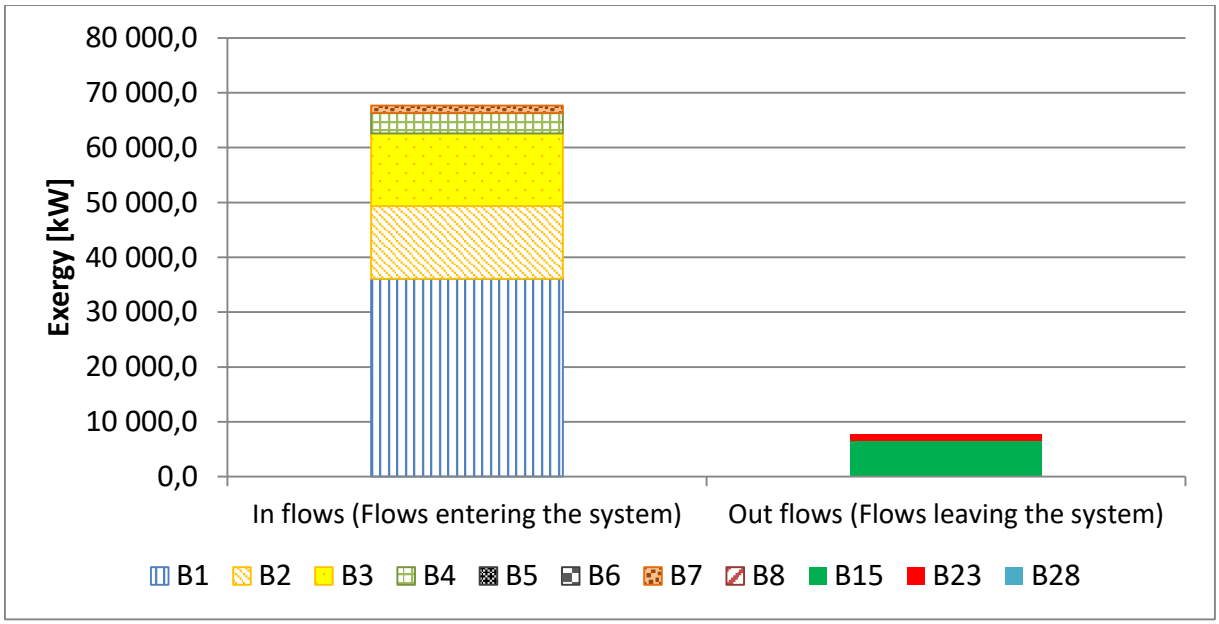


**Figure 35 In flows and out flows for 3rd April, 8 am**

Additional examples of daily operation plots are presented in the article included in Appendix 3. To illustrate the variability of the system under different seasonal conditions, three representative cases were selected.

The second case corresponds to July 28th at 2:00 PM, a summer day with high solar irradiance. At this time, electricity generation was primarily provided by PV and PV/T systems, supported by the biogas-fuelled CHP engine. Heat production originated from solar-based technologies (PV/T and solar thermal collectors) as well as from the CHP unit. Importantly, part of the generated heat—beyond its use for domestic hot water—was directed to an adsorption chiller, enabling cooling production. Additional cooling demand was also met by heat pumps, demonstrating the system's ability to integrate renewable-driven cooling into the overall energy balance.

The third case refers to October 6th at 3:00 PM. On this autumn day, electricity was generated by PV and PV/T systems in combination with the biogas CHP engine. However, total output was insufficient to meet demand, necessitating supplementation from the external grid. Heat generation was provided by multiple sources, including the PV/T system, the CHP unit, solar thermal collectors, and heat pumps. At this time of year, no cooling was required, and thus none was produced.

The final scenario illustrates a winter night-time condition on December 15th at 10:00 PM. At this moment, neither the wind turbine nor solar-based renewable systems (PV, PV/T, and solar collectors) were operational due to the absence of wind and sunlight. Electricity was therefore provided almost exclusively by the biogas-fuelled CHP engine, with the remaining demand covered by the energy storage system and the external grid. Heat production was ensured by the CHP unit in combination with the heat pumps, highlighting their crucial role in maintaining energy supply during periods of limited renewable availability.

## Chapter 5

# Summary and conclusions

This chapter summarizes the PhD thesis and the key findings of the research. The main objective of the study was to develop the applicability of the Thermo-Ecological Cost (TEC) concept and to demonstrate its significance in the assessment of energy systems. The TEC analysis was presented as a tool enabling a comprehensive evaluation of the environmental costs associated with the operation of energy systems. Its application allowed for the inclusion of not only economic aspects but also the impact on natural resources and pollutant emissions.

The research was conducted in several stages. Initially, after a literature review, research gaps were identified. The review revealed a lack of comprehensive studies on the application of TEC to the analysis of multigeneration microgrids based on renewable energy sources. On this basis, the research was planned. In the first stage, a grid based on renewable energy sources was designed to generate electricity, heat, and cooling. Subsequently, possible demand scenarios for the various energy services were analysed. The literature review provided a range of data on TEC values for different energy systems and identified a lack of such data for the photovoltaic-thermal (PV/T) system. Therefore, a key stage of the research involved a detailed analysis of this system and the determination of its TEC value.

After obtaining the TEC value for the PV/T system, further analyses of the system were conducted. Various configurations of renewable energy source (RES) cooperation were examined. The daily and seasonal variability of energy production was identified. Based on the observed challenges, a configuration of RES cooperation was proposed to ensure the most stable energy generation. The possibility of electricity storage was also taken into account. To assess environmental impacts and optimise resource management, TEC analysis was applied. The research on the application of TEC analysis for a multigeneration system was divided into two parts – the first focused solely on the analysis of electricity, while the second extended the scope to include heat and cooling. A series of simulations was performed to identify optimal energy mixes, and the application of TEC analysis for multigeneration systems was developed.

The first stage of the research, focused on solar technologies, highlighted the advantages of PV/T as a more efficient system compared to the separate configuration (i.e., PV and thermal collector). The simulations showed that the improvement in efficiency resulted mainly from the increased electricity generation efficiency due to the cooling of PV/T modules. The Thermo-Ecological Cost analysis demonstrated that electricity and heat produced in the PV/T system have a TEC coefficient below 1. Thus, the exergy of the resources used to produce the products is lower than the exergy value of the products themselves. Another important conclusion from the first stage of the study was the significance of fuel allocation between heat and electricity for determining the TEC indicator. Two allocation methods were proposed. The first suggested using exergy cost allocation, which resulted in very high TEC values for months with low heat production. The second approach used the proportion

of TEC indicators for conventional/replaced technologies. Although the monthly TEC values exceeded the annual average, they did not deviate as drastically as in the first approach.

It should be emphasised that due to the continued presence of non-renewable resource input in the final product, as well as pollution, it is not possible for any currently known energy generation technology to achieve a zero TEC coefficient. However, the conducted research showed that the PV/T system significantly reduces the TEC value compared to the separated system (PV and collector). The obtained results also clearly indicated that when comparing different energy systems (renewable and conventional), global analysis (determining the Thermo-Ecological Cost) allows for proper assessment and comparison of systems. The TEC makes it possible to explicitly determine the impact of a process on the depletion of non-renewable resources. For example, the TEC of electricity and heat for a coal-fired combined heat and power plant is significantly higher than for a PV/T system.

It is important to note that such clarity is lacking in local analyses, where comparisons of energy efficiency indicators suggest better performance for conventional systems. The research indicated that even when comparing similar energy systems (such as PV and PV/T), TEC is a more advantageous analytical tool. It captures the impact of renewable energy sources on non-renewable resources and more accurately reflects the environmental impact of the system. In contrast, traditional efficiency analysis only enables the evaluation of the process itself, without placing it in the broader environmental context (Earth).

Therefore, determining the TEC constitutes a key method for the proper evaluation of energy production systems and their impact on the depletion of non-renewable resources. This issue becomes even more evident when combining different RES systems within a microgrid. Such conclusions emerged from the stage of research involving microgrid simulations. In local evaluations, such grids show lower efficiency compared to conventional power systems and face challenges such as production randomness and instability. However, the conducted study demonstrated that these challenges can be significantly mitigated. The first key conclusion drawn from the research is the necessity to integrate individual RES into a local conditions and analyse their daily and seasonal variability. The results showed which energy mix ensured the best conditions for microgrid stability while minimizing resource consumption. The second crucial finding emphasised the role of energy storage. The use of Thermo-Ecological analysis provided insights into how to effectively design an energy mix to minimize environmental impact and resource depletion. By combining sources with different characteristics (annual production profiles, stability, etc.), the best values of Thermo-Ecological Cost indicators were achieved.

Another significant conclusion concerns the limited applicability of traditional Thermo-Economic Analysis (TEA). TEA proves effective in minimizing internal process irreversibilities in conventional power plants but is not an appropriate approach for assessing systems with diverse external resource inputs, especially renewable sources. In hybrid systems, TEA results may misleadingly suggest maximizing external resource use (without considering their origin) and minimizing internal energy transformation. In contrast, the proposed Thermo-Ecological Cost (TEC) provides a clear assessment of the resources supplied to the system.

The findings demonstrate the potential of TEC as an important tool for evaluating and optimizing energy systems, representing a significant contribution to the development of analytical approaches that incorporate a broader context—the environment (Earth). The data obtained through this analysis enable the positioning of studied systems within a planetary perspective. This makes it possible to identify the environmental implications of a system in a wider context. Many contemporary challenges require such an approach. Among them is resource depletion, which, due to the complexity of supply chains, is increasingly difficult to monitor and control. This necessitates the integration of data on material, energy, and emission flows on a global scale. Likewise, combating climate change requires a broad, systemic perspective, as the effects of greenhouse gas emissions are not confined to local areas but impact the entire Earth system. There are many such challenges: increasing energy demand, dependence on imported raw materials, environmental degradation, and others. They require comprehensive research and process optimisation on a planetary scale. The presented Thermo-Ecological analysis responds to these needs by providing a global framework.

Furthermore, the obtained data may be used in the development of public policies concerning the efficient use of resources, renewable energy sources, and energy storage systems. The presented research also sheds new light on the design of sustainable microgrids. It provides guidelines for designing flexible systems based on sources subject to daily and seasonal variability.

The discussed issues also reveal important limitations of the presented study. One of the main limitations is the focus on a single region. The analysed application of TEC to location made it possible to capture specific local conditions. In the future, it would be worthwhile to extend the research to other locations and conduct a comparative analysis of the obtained TEC results. This would enable a better understanding of regional differences and the identification of the most sustainable solution patterns. Further studies should also consider climate change and its impact on microgrids. This would allow evaluation the of benefits of applying TEC analysis to energy systems under changing climatic conditions, providing valuable insights for adaptive planning and the design of resilient energy infrastructure.

In the context of the presented findings, future research could also focus on methods of achieving the lowest possible TEC values. Achieving a TEC of 0 is unrealistic due to dependence on non-renewable resources and environmental costs; however, further studies aimed at finding the most sustainable options and energy mixes are extremely important. Future analyses could be expanded to include the optimisation of renewable energy integration and storage technologies. Promising directions include more sustainable production of energy components and efficient recovery and recycling processes. Another interesting line of research would involve incorporating social aspects of the energy transition into the analysis. Among the potential topics worth considering are social acceptance of new technologies, the impact of energy investments on local communities, and the fairness of the transition. Including these factors could significantly enrich the assessment of the effectiveness and sustainability of implemented solutions.

# Bibliography


[1] International Energy Agency, “World Energy Outlook 2024,” Paris: IEA, 2024. [online]. Accessed: 1 October 2025, https://www.iea.org/reports/world-energy-outlook-2024.

[2] Energy Institute, “Statistical Review of World Energy 2023,” [online]. Accessed: 27 October 2025, https://www.energyinst.org.

[3] The Intergovernmental Panel on Climate Change (IPCC), “Sixth Assessment Report (AR6),” [online]. Geneva: Intergovernmental Panel on Climate Change, 2025. Accessed: 10 July 2025, https://www.ipcc.ch/report/sixth-assessment-report-cycle/.

[4] Bukowski, M., “ ClimeNous Project. Geopolitics of the energy transition, Part 1: Six challenges for the international balance of power arising from the departure from fossil fuels (in Polish),” [online]. Accessed: 27 April 2025, www.ine.org.pl Instytut Nowej Europ.

[5] International Energy Agency, “Net Zero by 2050,” Paris: IEA, 2021. Accessed: 27 October 2025, https://www.iea.org/reports/net-zero-by-2050.

[6] International Energy Agency, “Renewables 2023,” [online]. Paris: IEA, 2024. Accessed: 27 October 2025, https://www.iea.org/reports/renewables-2023.

[7] International Energy Agency, “The Role of Critical Minerals in Clean Energy Transitions,” [online]. Paris: IEA, 2021. Accessed: 27 October 2025, https://www.iea.org/reports/the-role-of-critical-minerals-in-clean-energy-transitions.

[8] European Environment Agency, “Emerging Waste Streams: Opportunities and Challenges of the Clean-Energy Transition from a Circular Economy Perspective,” Briefing No. 07/2021. Luxembourg: Publications Office of the European Union, 2021.

[9] Szargut, J., Exergy Method: Technical and Ecological Applications. Developments in Heat Transfer, vol. 18. Silesian University of Technology, Poland: WIT Press, 2005. ISBN: 978-1-85312-753-3.

[10] Szargut, J., “Exergy around us (in Polish).,” *ACADEMIA. Magazine of the Polish Academy of Sciences,* , no. 3 (2005), pp. 31–33. Polish Academy of Sciences, Warsaw.

[11] Szargut, J., Stanek, , “W. Influence of the pro-ecological tax on the market prices of fuels and electricity,” *Energy,* vol. 33, no. 2, pp. 137–143, 2008. doi: 10.1016/j.energy.2007.07.003. [online].

[12] Stanek, W., Gazda, W., Kostowski, W. , “Thermo-ecological assessment of CCHP (combined cold-heat-and-power) plant supported with renewable energy.,” *Energy,* 2015. doi.org/10.1016/j.energy.2015.02.005.

[13] Stanek, W. , Exergy Analysis in Theory and Practice, Silesian University of Technology Publishing House, 2016. ISBN 978-83-7880-415-4.

[14] Stanek, W., Czarnowska, L., “Thermo-ecological cost – Szargut's proposal on exergy and ecology connection,” vol. 165, part B, pp. 1050–1059, Dec. 2018. doi: 10.1016/j.energy.2018.10.040., Energy.

[15] Stanek W., “Method of Evaluation of Ecological Effects in Thermal Processes with the Application of Exergy Analysis,” Silesian University of Technology Press, 2009 (in Polish).

[16] Szargut, J., Ziębik, A. and Stanek, W., “Depletion of the non-renewable natural exergy resources as a measure of the ecological cost,” Energy Convers. Manag. 43 (9-12) (2002) 1149-1163. https://doi.org/10.1016/S0196-8904(02)00005-5.

[17] Czarnowska, L., “Thermo-ecological cost of products with emphasis on external environmental costs,” Gliwice: Silesian University of Technology, 2014.

[18] Faist Emmenegger, M., Heck, T., Jungbluth, N. Erdgas., Swiss Centre for Life Cycle Inventories. Final Report Ecoinvent No. 6-V. Dübendorf: Swiss Centre for Life Cycle Inventories, [online] Accessed: 27 October 2025, http://www.ecoinvent.org/database/olderversions/ecoinvent-version-2/reports-on-ecoinvent-2/reports-on-ecoinvent2.html.

[19] Szargut J., Stanek W., “Thermo-ecological optimization of a solar collector,” *Energy,* 2007, vol. 32, nr 4, s.584-590. doi:10.1016/j.energy.2006.06.010.

[20] Szargut, J., “Optimization of the design parameters aiming at the minimization of the depletion of non-renewable resources,” *Energy*, Volume 29, Issues 12–15,2004, pp. 2161-2169,ISSN 0360-5442,https://doi.org/10.1016/j.energy.2004.03.019.

[21] Stanek, W., Czarnowska, L., “ Environmental externalities and their effect on the cost of consumer products,” *International Journal of Environmental and Sustainable Development, p*p. 50–63 11(1), 50–63, 2012. https://doi.org/10.1504/IJESD.2012.049142.

[22] Szargut, J., “Application of Exergy for the Calculation of Ecological Cost,” Bulletin of the Polish Academy of Sciences: Technical Sciences, vol. 7–8, 1986, pp. 475–480.

[23] Szostok A., Stanek W., “Thermo-ecological analysis - the comparison of collector and PV to PV/T system,” *Renewable Energy,* 2022, vol. 200, pp.10-23. doi:10.1016/j.renene.2022.09.070.

[24] Stanek W., Mendecka B., Lombardi L., et al., “Environmental assessment of wind turbine systems based on thermo-ecological cost,” *Energy,* 2018, vol. 160, s.341-348. doi:10.1016/j.energy.2018.07.032.

[25] Simla T., Stanek W., Czarnowska L., “Thermo-ecological cost of electricity generated in wind turbine systems,” *Journal of Energy Resources Technology-Transactions of the Asme,* 2019, vol. 141, nr 3, s.1-7, Numer artykułu:031201doi:10.1115/1.4041612.

[26] Mendecka, B.; Lombardi, L.; Stanek, W., “Analysis of life cycle thermo-ecological cost of electricity from wind and its application for future incentive mechanism,” https://doi.org/10.1016/j.enconman.2018.05.084, *Energy Conversion and Management*, Volume 170, 2018, Pages 73-81.

[27] Piekarczyk W., Czarnowska L. Ptasiński K., et al., “Thermodynamic evaluation of biomass-to-biofuels production systems,” *Energy,* 2013, vol. 62, s.95-104. doi:10.1016/j.energy.2013.06.072.

[28] Stanek W., Czarnowska L., Kalina J., “Application of life cycle thermo-ecological cost methodology for evaluation of biomass integrated gasification gas turbine based cogeneration,” *Applied Thermal Engineering,* 2014, vol. 70, nr 1, s.1007-1017 doi:10.1016/j.applthermaleng.2014.06.029.

[29] Stanek W., Simla T., Gazda W.,”Exergetic and thermo-ecological assessment of heat pump supported by electricity from renewable sources"*, Renewable Energy,* 2019, vol. 131, s.404-412, doi:10.1016/j.renene.2018.07.084.

[30] Stanek, W., Gazda, W., Kostowski, W., “Thermo-ecological assessment of CCHP (combined cold-heat-and-power) plant supported with renewable energy,” *Energy,* 2015. doi.org/10.1016/j.energy.2015.02.005.

[31] Stanek W., Czarnowska L., Gazda W., Simla T., “Thermo-ecological cost of electricity from renewable energy sources,” *Renewable Energy,* 2018, vol. 115, s.87-96. https://doi.org/10.1016/j.renene.2017.07.074.

[32] Szostok A., Stanek W., “Thermo-ecological analysis of the power system based on renewable energy sources integrated with energy storage system,” *Renewable Energy*, vol. 216, 2023, pp. 1–20. Article number: 119035. doi: 10.1016/j.renene.2023.119035.

[33] Stanek W., Szostok A. , “Thermo-ecological assessment of microgrid supported with renewable energy,” *Energy,* Volume 314, 2025, 134256, ISSN 0360-5442, https://doi.org/10.1016/j.energy.2024.134256.

[34] Stanek W., Szargut J., Kolenda Z.,et al., “Thermo-ecological evaluation of a nuclear power plant within the whole life cycle,” *International Journal of Applied Thermodynamics,* 2015, vol. 18, nr 2, s.121-131, doi:10.5541/ijot.72035.

[35] Mendrela P., Stanek W. Simla T., “Sustainability assessment of hydrogen production based on nuclear energy,” *International Journal of Hydrogen Energy,* 2024, vol. 49, nr Pt A, s.729-744. doi:10.1016/j.ijhydene.2023.07.156.

[36] Stanek W., Pluta Ł., “The termo-ecological cost of liquid fuels producted by direct coal liquefaction (in polish) ,” *Archiwum Energetyki,* 2010, vol. 40, nr 1/2, s.141-159.

[37] Kostowski, W., Usón, S., Stanek, W., et al., “Thermoecological Cost of Electricity Production in the Natural Gas Pressure Reduction Process,” *Energy,* vol. 76, 2014, pp. 1018. doi: 10.1016/j.energy.2014.01.045.

[38] Stanek W., Czarnowska L. Pikoń K. et al., “Thermo-ecological cost of hard coal with inclusion of the whole life cycle chain,” *Energy,* 2015, vol. 92, s.341-348. doi:10.1016/j.energy.2015.05.042.

[39] Gładysz P., Stanek W., Czarnowska L. et al., “Thermo-ecological evaluation of an integrated MILD oxy-fuel combustion power plant with CO2 capture, utilisation, and storage - case study in Poland,” *Energy,* 2018, vol. 144, s.379-392. doi:10.1016/j.energy.2017.11.133.

[40] Stanek W., Simla T., Rutczyk B., et al., “Thermo-ecological assessment of Stirling engine with regenerator fed with cryogenic exergy of liquid natural gas (LNG),” *Energy,* 2019, vol. 185, s.1045-1053, doi:10.1016/j.energy.2019.07.116.

[41] Usón S., Kostowski W., Stanek W., et al., “Thermoecological cost of electricity, heat and cold generated in a trigeneration module fuelled with selected fossil and renewable fuels,” *Energy,* 2015, vol. 92, pt. 3, s.308-319. doi:10.1016/j.energy.2015.05.020.

[42] Stanek W. , “Thermo-Ecological Cost (TEC) - comparison of energy-ecological efficiency of renewable and non-renewable energy technologies,” *Energy,* 2022, vol. 261, nr Pt. A, s.1-10, doi:10.1016/j.energy.2022.125152.

[43] Mendrela P. Stanek W., Simla T., “ Thermo-ecological cost – system evaluation of energy-ecological efficiency of hydrogen production from renewable and non-renewable energy resources,” *International Journal of Hydrogen Energy,* 2024, vol. 50 nr Pt B, s.1-14. doi:10.1016/j.ijhydene.2023.06.150.

[44] Czarnowska L., Litwin W., Stanek W., “Selection of numerical methods and their application to the thermo-ecological life cycle cost of heat exchanger components,” *Journal of Sustainable Development of Energy, Water and Environment Systems,* 2016, vol. 3, nr 2, s.131-139. doi:10.13044/j.sdewes.2015.03.0010.

[45] Simla T., Gazda W., Stanek W., “System evaluation of hydrogen energy – thermo-ecological cost analysis,” *International Journal of Hydrogen Energy,* 2023, vol. 48, no. 48, pp. 18187-18200. doi:10.1016/j.ijhydene.2023.01.331.

[46] Szargut J., Stanek W., “Fuel part and mineral part of the thermoecological cost,” *International Journal of Applied Thermodynamics,* 2012, vol. 15, nr 4, s.187-190. doi:10.5541/ijot.1034000419.

[47] Dominguez A., Czarnowska L., Valero A., et al., “ Thermo-ecological and exergy replacement costs of nickel processing,” *Energy,* 2014, vol. 72, s.103-114. doi:10.1016/j.energy.2014.05.013.

[48] Stanek W., Blacha L., Szega M., Metalurgija, “Thermo-ecological cost (TEC) evaluation of metallurgical processes,” *Metalurgija,* 2015, vol. 54, nr 1, s.270-272.

[49] Stanek W., Gładysz P., Czarnowska L., et al., “Thermo-ecology : Exergy as a measure of sustainability,” *Academic Press,* 2019, 228 s., ISBN 978-0-12-813142-8.

[50] Ziębik A., Stanek W., Szega M., “Energy and Ecological Efficiency: A Methodological Guide for Thermodynamic and Thermoecological Analyses (in polish), ” 2022, Politechnika Śląska, 281 s., ISBN 978-83-7880-791-9.

[51] Szargut J., “Application of exergy for the determination of the pro-ecological tax replacing the actual personal taxes,” *Energy ,* Int J 2002;27(4):379-89. doi: 10.1016/S0360-5442(01)00092-5.

[52] Szargut, J. and Stanek, W., “Thermo-climatic cost of the domestic consumption products.,” *Energy,* 2010, 35(2), 1196–1199. https://doi.org/10.1016/j.energy.2009.04.025.

[53] Stanek W., “Ecological cost index of domestic export. Energy. Problems of Energy and Fuel Economy (in Polish),” *Energetyka. Problemy Energetyki i Gospodarki Paliwowo-Energetycznej,* 2001, vol. 49, no. 10, pp. 2-7. [in Polish].

[54] Valero A, Lozano MA, Serra L, Tsatsaronis G, Pisa J, Frangopoulos CA, et al., “CGAM problema: definition and conventional solution,” *Energy ,* 1994;19(3): 279e86. https://doi.org/10.1016/0360-5442(94)90112-0.

[55] Valero A., Torres C., Thermoeconomic analysis, Oxford, UK: EOLSS Publishers, 2006.

[56] Tsatsaronis G, Winhold M., “Exergoeconomic analysis and evaluation of energy conversion plants e I. A new general methodology,” *Energy,* 1985;10:69e80. https://doi.org/10.1016/0360-5442(85)90020-9.

[57] Picallo-Pérez, A.; Sala, J.M.; Portillo, L.d.; Vidal, R. Delving Into Thermoeconomics: A Brief Theoretical Comparison of Thermoeconomic Approaches for Simple Cooling Systems. Frontiers in Sustainability 2021, 2, 656818. https://doi.org/10.3389/frsus.2021.

[58] Tsatsaronis, G., “Exergoeconomic and Exergoenvironmental Analysis,” in *Thermodynamics and the Destruction of Resources*, 2011, pp. 377–401.

[59] Bejan, A., Tsatsaronis, G., Moran, M., Thermal Design and Optimization, New York: Wiley, 1996.

[60] Data Bank of the Institute of Meteorology and Water Management, “Data Bank,” [online]. Accessed: 8 August 2021, https://bank-danych.imgw.pl/home.

[61] EKONTROL, “Ekontrol – Remote Device Monitoring System,” (in Polish) [online]. Accessed: 11 January 2020, https://ekontrol.pl/pl/demo/8.

[62] Teraz Środowisko, “Guide to Preparing Hot Water,” (in Polish) [online]. Accessed: 11 January 2020, https://www.teraz-srodowisko.pl/media/pdf/aktualnosci/1406-Poradnik-przygotowania-cieplej-wody.pdf.

[63] The European Youth Portal, “What is climate change?,” [online]. Accessed: 8 August 2021, https://europa.eu/youth/get-involved/sustainable%20development/what-climate-change_pl.

[64] Intergovernmental Panel on Climate Change (IPCC), “Climate Change 2021. The Physical Science Basis,” [online]. Geneva: IPCC, 2021. Accessed: 27 October 2025, https://www.ipcc.ch/report/ar6/wg1/downloads/report/IPCC_AR6_WGI_Full_Report.pdf.

[65] BP p.l.c., “Statistical Review of World Energy,” [online]. 2021. Accessed: 27 October 2025, https://www.bp.com/en/global/corporate/energy-economics/statistical-review-of-world-energy.html.

[66] Chao, C., Deng, Y., Dewil, R., Baeyens, J., Fan, X. , “Post-combustion carbon capture,” 138 (2021), 110490. https://doi.org/10.1016/j.rser.2020.110490, Renewable and Sustainable Energy Reviews.

[67] Gomez-Navarro, T., Brazzini, T., Alfonso-Solar, D., Vargas-Salgado, C., “Analysis of the potential for PV rooftop prosumer production: Technical, economic and environmental assessment for the city of Valencia (Spain),” *Renewable Energy,* 170 (2021), 1114–1126, https://doi.org/10.1016/j.renene.2021.04.049.

[68] Bevilacqua, P., Perrella, S., Bruno, R., Arcuri, N. An accurate thermal model for the PV electric generation prediction: long-term validation in different climatic conditions. Renewable Energy, 162 (2020), 1455–1470, https://doi.org/10.1016/j.renene.2020.08.051.

[69] Intergovernmental Panel on Climate Change, , “Climate Change 2021. The Physical Science Basis,” [online]. Accessed: 25 October 2022, https://www.ipcc.ch/report/ar6/wg1/downloads/report/IPCC_AR6_WGI_Full_Report.pdf, 2021.

[70] Das, P., Kanudia, A., Bhakar, R., Mathur, J., “Intra-regional renewable energy resource variability in long-term energy system planning,” Energy, https://doi.org/10.1016/j.energy.2022.123302, Volume 245, 2022, 123302, ISSN 0360-5442.

[71] Jurasz, J., Canales, F.A., Kies, A., Guezgouz, M., Beluco, “A review on the complementarity of renewable energy sources: Concept, metrics, application and future research directions,” Solar Energy,Pages 703-724,ISSN 0038-092X, https://doi.org/10.1016/j.solener.2019.11.087, Volume 195, 2020.

[72] Kan, A., Zeng, Y., Meng, X., Wang, D., Xina, J., Yang, X., Tesren, L., “The linkage between renewable energy potential and sustainable development: Understanding solar energy variability and photovoltaic power potential in Tibet, China,” Sustainable Energy Technologies and Assessments, https://doi.org/10.1016/j.seta.2021.101551., Volume 48, 2021, 101551, ISSN 2213-1388.

[73] Khamlich, I., Zeng, K., Flamant, G., Baeyens, J., Zou, C., Li, J., Yang, X., He, X., Liu, Q., Yang, H., Yang, Q., Chen, H., “Technical and economic assessment of thermal energy storage in concentrated solar power plants within a spot electricity market,” *Renewable and Sustainable*

*Energy Reviews,* Volume 139, 2021, 110583, ISSN 1364-0321, tps://doi.org/10.1016/j.rser.2020.110583.

[74] Flamant, G., Grange, B., Wheeldon, J., Siros, F., Valentin, B., Bataille, F., Zhang, H., Deng, Y., Baeyens, J., "Opportunities and challenges in using particle circulation loops for concentrated solar power applications, Progress in Energy and Combustion Science, Volume 94, 2023, 101056, ISSN 0360-1285".

[75] Fernandes, D., Pitié, F., Cáceres, G., Baeyens, J., "Thermal energy storage: "How previous findings determine current research priorities", Energy," Volume 39, Issue 1,2012, Pages 246-257, ISSN 0360-5442, https://doi.org/10.1016/j.energy.2012.01.024.

[76] Jiménez-Vargas, I.; Rey, J.M.; Osma-Pinto, G., "Sizing of hybrid microgrids considering life cycle assessment," https://doi.org/10.1016/j.renene.2022.11.1, Renewable Energy, Volume 202, 2023, Pages 554-565.

[77] Maimó-Far, A., Homar, V., Tantet, A., Drobinski, P., "The effect of spatial granularity on optimal renewable energy portfolios in an integrated climate-energy assessment model," Sustainable Energy Technologies and Assessments, https://doi.org/10.1016/j.seta.2022.102827, Volume 54, 2022, 102827, ISSN 2213-1388.

[78] Jain, A.; Yamujala, S.; Gaur, A.; Das, P.; Bhakar, R.; Mathur, J., "Power sector decarbonization planning considering renewable resource variability and system operational constraints," *Applied Energy,* Volume 331, 2023, 120404, https://doi.org/10.1016/j.apenergy.2022.120404.

[79] Sitharthan, R., Vimal, S., Verma, A., Karthikeyan, M., Dhanabalan, S.S., Prabaharan, N., Rajesh, M., Eswaran, T., "Smart microgrid with the internet of things for adequate energy management and analysis," *Computers and Electrical Engineering,* Volume 106, 2023, 108556,https://doi.org/10.1016/j.compeleceng.2022.108556.

[80] Dowling, J.A., Rinaldi, K.Z., Ruggles, T.H., Davis, S.J., Yuan, M., Tong, F., Lewis, N.S., Caldeira, K., "Role of Long-Duration Energy Storage in Variable Renewable Electricity Systems," Joule, https://doi.org/10.1016/j.joule.2020.07.007, Volume 4, Issue 9, 2020, Pages 1907-1928, ISSN 2542-4351.

[81] Deng, Y., Li, S., Appels, L., Zhang, H., Sweygers, N., Baeyens, J., Dewil, R., "Steam reforming of ethanol by non-noble metal catalysts," *Renewable and Sustainable Energy Reviews*, Volume 175,2023,113184,ISSN 1364-0321,https://doi.org/10.1016/j.rser.2023.113184.

[82] Deng, Y., Dewil, R., Appels, L., Van Tulden, F., Li, S., Yang, M., Baeyens, "Hydrogen-enriched natural gas in a decarbonization perspective," *Fuel,* Volume 318, 2022, 123680,ISSN 0016-2361,https://doi.org/10.1016/j.fuel.2022.123680.

[83] Oliveira, L., Messagie, M., Mertens, J., Laget, H., Coosemans, T., Van Mierlo, J., "Environmental performance of electricity storage systems for grid applications, a life cycle approach," *Energy*

*Conversion and Management,* Volume 101, 2015, Pages 326-335, ISSN 0196-8904 https://doi.org/10.1016/j.enconman.2015.05.063.

[84] Jiao, Y., Månsson, D., "Greenhouse gas emissions from hybrid energy storage systems in future 100% renewable power systems – A Swedish case based on consequential life cycle assessment," Journal of Energy Storage, https://doi.org/10.1016/j.est.2022.106167, Volume 57, 2023,106167,ISSN 2352-152X.

[85] Marques Lameirinhas, R.A., Torres, J.P.N., de Melo Cunha, J.P., "Photovoltaic Technology Review: History, Fundamentals and Applications," *Energies,* vol. 15, 2022, article 1823. doi: 10.3390/en15051823.

[86] Al-Ezzi, A.S., Ansari, M.N.M., "Photovoltaic Cells: A Review," *Applied System Innovation,* vol. 5, 2022, article 67. doi: 10.3390/asi5040067.

[87] Vodapally, S.N., Ali, M.H., "A comprehensive review of photovoltaic (PV) technologies, architectures and their applications for efficiency improvement," *Energies,* 16 (2023), 319. https://doi.org/10.3390/en16010319.

[88] Akyuz, E., Coskun, C., Oktay, Z., Dincer, I., "Hydrogen production probability distributionsfor a PV-electrolyser system," *International Journal of Hydrogen Energy ,* Volume 36, Issue 17, 2011, Pages 11292-11299, ISSN 0360-3199, https://doi.org/10.1016/j.ijhydene.2010.11.125.

[89] Stanek, W., "Assessment of energy and ecological efficiency of the TETIP transformation toward electroprosumerism in the exergy paradigm environment – thermo-ecological cost: electroprosumerism vs WEK-PK energy sector (in Polish)," Accessed: 27 October 2025 [onilne] https://ppte2050.pl/platforman/bzppte/static/uploads/Ocena%20efektywno%C5%9Bci%20energetycznej%20i%20ekologicznej%20transformacji%20TETIP%20do%20elektroprosumeryzmu.pdf.

[90] Newman, S., Shiozawa, K., Follum, J., Barrett, E., Douville, T., Hardy, T., Solana, A., " A comparison of PV resource modeling for sizing microgrid components," *Renewable Energy,* Volume 162, 2020, Pages 831-843, ISSN 0960-1481, 10.1016/j.renene.2020.08.074.

[91] Tian, Y., Zhao, C.Y., "A review of solar collectors and thermal energy storage in solar thermal applications," *Applied Energy,* 104 (2013), 538–553. https://doi.org/10.1016/j.apenergy.2012.11.051.

[92] Duffie, J.A., Beckman, W.A., Solar Engineering of Thermal Processes., Wiley, 2013. ISBN 978-0-470-87366-3.

[93] Kalogirou, S.A., "Solar thermal collectors and applications," *Progress in Energy and Combustion Science,* 30 (3) (2004), 231–295. https://doi.org/10.1016/j.pecs.2004.02.001.

[94] Viessmann Academy Poland, Architect, Designer and Installer Manual – Solar Collectors, [online]. Wrocław: Viessmann Werke, Allendorf (Eder), 2013. Accessed: 27 October 2025,

https://www.viessmann.poznan.pl/images/design/pdf/podrccznik-architekta-projektanta-i-instalatora-kolektory-soneczne.pdf.

[95] Aggour, H.S., Atia, D.M., Farghally, H.M., et al., Electrical and Thermal Performance Analysis of Hybrid Photovoltaic/Thermal Water Collector Using Meta-Heuristic Optimization, Journal of Electrical Systems and Information Technology, vol. 11, 2024, article 20. https://doi.org/10.1186/s43067-024-00146-0.

[96] Kong, X., Zhang, Y., Wu, J., Pan, S., "Numerical study on the optimization design of photovoltaic/thermal (PV/T) collector with internal corrugated channels," *International Journal of Photoenergy,* 2022, Article 8632826. https://doi.org/10.1155/2022.

[97] Anderson, T.N., Duke, M., Morrison, G.L., Carson, J.K., "Performance of a building integrated photovoltaic/thermal (BIPVT) solar collector," International Solar Energy Society, 2020.

[98] Gagliano, A., Tina, G.M., Nocera, F., Grasso, A.D., Aneli, S., "Description and performance analysis of a flexible photovoltaic/thermal (PV/T) solar system," Renewable Energy, 2017.

[99] Chow, T.-T., Ji, J., "Environmental Life-Cycle Analysis of Hybrid Solar Photovoltaic/Thermal Systems for Use in Hong Kong," *International Journal of Photoenergy,* 2012 , 101968, 9 stron, 2012. https://doi.org/10.1155/2012/101968.

[100] Shakouri, M., Ebadi, H., Gorjian, S., "Chapter 4 - Solar photovoltaic thermal (PVT) module technologies," Photovoltaic Solar Energy Conversion Technologies, Applications and Environmental Impacts, 2020, Pages 79-116.

[101] Mert Cuce, P., "Novel, practical and reliable analytical models to estimate electrical efficiency of buildingintegrated photovoltaic/thermal (BIPVT) collectors and systems," Uludağ University Journal of The Faculty of Engineering, Vol. 23, No. 3, 2018.

[102] Smith, E.M., " Effectiveness-NTU relationships for tubular exchangers," *International Journal of Heat and Fluid Flow,* Volume 1, Issue 1, 1979, Pages 43-46, ISSN 0142-727X, https://doi.org/10.1016/0142-727X(79)90024-9.

[103] Shah, Ramesh K. & Sekulić, Dušan P. , Fundamentals of Heat Exchanger Design, (2003). Hoboken, NJ: John Wiley & Sons, Inc.

[104] Chaudhuri, A., Datta, R., Kumar, M.P., Davim, J.P., Pramanik, S., Energy Conversion Strategies for Wind Energy System: Electrical, Mechanical and Material Aspects, Materials, vol. 15, 2022, article 1232. doi: 10.3390/ma15031232.

[105] Jouchi, A.A., Pourrajabian, A., Rahgozar, S., et al., Performance Appraisal of a Small Wind Turbine Under the Use of Three Rotor Hub Configurations, Clean Technologies and Environmental Policy, vol. 25, 2023, pp. 1509–1523. doi: 10.1007/s10098-022-02451-6.

[106] Liu, S., Janajreh, I., Development and Application of an Improved Blade Element Momentum Method Model on Horizontal Axis Wind Turbines, International Journal of Energy and Environmental Engineering, vol. 3, 2012, article 30. doi: 10.1186/2251-6832-3-30.

[107] Gambier, A., "Pitch Control of Three Bladed Large Wind Energy Converters—A Review," *Energies,* vol. 14, 2021, article 8083. doi: 10.3390/en14238083.

[108] Śmigielski, Z., "Wind Farm (in Polish)," [online]. 2020. Accessed: 23 October 2021, http://zet10.ipee.pwr.wroc.pl/record/18/files/Wind%20Farm.doc.pdf.

[109] Lund, H., Werner, S., Wiltshire, R., Svendsen, S., Thorsen, J.E., Hvelplund, F., Mathiesen, B.V. , "4th Generation District Heating (4GDH): Integrating smart thermal grids into future sustainable energy systems," *Energy,* 68, 1–11, 2014, https://doi.org/10.1016/j.energy.2014.02.089.

[110] Hepbasli, A., "A key review on exergetic analysis and assessment of renewable energy resources for a sustainable future," *Renewable and Sustainable Energy Reviews,* 12(3), 593–661, 2008. https://doi.org/10.1016/j.rser.2006.10.001.

[111] International Energy Agency., The Future of Heat Pumps. World Energy Outlook Special Report, Revised version December 2022., [online]. Accessed: 18 September 2025 https://iea.blob.core.windows.net/assets/4713780d-c0ae-4686-8c9b-29e782452695/TheFutureofHeatPumps.pdf.

[112] Arpagaus, C., Bless, F., Uhlmann, M., Schiffmann, J., Bertsch, S.S., "High temperature heat pumps: Market overview, state of the art, research status, refrigerants, and application potentials," *Energy,* 152, 985–1010, 2018, https://doi.org/10.1016/j.energy.2018.03.166.

[113] Bobbo, S.; Lombardo, G.; Menegazzo, D.; Vallese, L.; Fedele, L. A , "Technological Update on Heat Pumps for Industrial Applications.," *Energies ,* 2024, 17, 4942. https://doi.org/10.3390/en17194942.

[114] Viessmann Sp. z o.o. 241.A, "VITOCAL 242-S Typ AWT-AC," [online] Accessed: 18 September 2020 http://www.viessmann.com/web/poland/PDF-90.nsf/7a38371490532f7bc125727b002d5e9e/8668cc3dc77c947ac1257b48001ff04f/$FILE/WP%20Vitocal%20200-S,%20222-S,%20242-S%20(05-2011).pdf.

[115] Liang, L. L. , Riveros-Iregui, D. A., Emanuel, R. E. , McGlynn B. L., "A simple framework to estimate distributed soil temperature from discrete air temperature measurements in data-scarce regions," *Journal of Geophysical Research: Atmospheres,* 2013 Volume 119, Issue 2. https://doi.org/10.1002/2013JD020597.

[116] Boryszew ERG, "Why Use Ergolid? (in polish)," [online] Accessed: 18 September 2025 https://www.boryszewerg.com.pl/wp-content/uploads/2019/05/dlaczego-warto-stosowac%CC%81-ergolid.pdf.

[117] Viessmann Sp. z o.o., “Split-Type Heat Pump 222-G, VITOCAL,” [online]. Accessed: 17 December 2025 https://www.viessmann.pl/pl/budynki-mieszkalne/pompy-ciepla/pompy-ciepla-powietrzewoda-w-wersji-split/vitocal-222s.html?utm_source=google&utm_medium=paid_search&utm_campaign=1711677766_&utm_term=&utm_content=3590544530.

[118] Kopeć, P., “Calculations and Selection of a Ground Heat Exchanger for a Heat Pump (in Polish),” *Journal of Civil Engineering, Environment and Architecture,* vol. XXXII, no. 62 (2/15), April–June 2015, pp. 167–177.

[119] Polish Committee for Standardization., “PN-EN 15241:2007+AC:2011 Ventilation for buildings. Calculation methods for energy losses due to ventilation and infiltration in buildings. (in polish),” (2011). Warsaw: PKN.

[120] Romicki Eko System, “Heat Pumps – Projects,” [online] Accessed: 17 April 2020, http://romicki-ekosystem.pl/pl.

[121] Marlinda; Uyun, A.S.; Miyazaki, T.; Ueda, Y.; Akisawa, “A. Performance analysis of a double-effect adsorption refrigeration cycle with a silica gel/water working pair,” *Energies,* 2010, 3, pp. 1704–1720. https://doi.org/10.3390/en3111704.

[122] Gado, M.; Elgendy, E.; Elsayed, K.; Fatouh, M., “Parametric study of an adsorption refrigeration system using different working pairs”.*Aerospace Sciences & Aviation Technology Conference.* doi: 10.21608/asat.2017.22455

[123] Gulraiz A, Al Bastaki AJ, Magamal K, Subhi M, Hammad A, Allanjawi A, Zaidi SH, Khalid HM, Ismail A, Hussain GA, Said Z., “Energy advancements and integration strategies in hydrogen and battery storage for renewable energy systems,” *iScience,* Vol. 28(3), 111945, Feb. 2025. doi: 10.1016/j.isci.2025.111945.

[124] Wagner, E., Delp, E., Mishra, R., “ Energy Storage with Highly-Efficient Electrolysis and Fuel Cells: Experimental Evaluation of Bifunctional Catalyst Structures,” *Top Catal ,* 66, 546–559 (2023). https://doi.org/10.1007/s11244-022-01771-7.

[125] Kotowicz, J., Jurczyk, M., Węcel, D., Ogulewicz, W., “Analysis of Hydrogen Production in Alkaline Electrolyzers,” *Journal of Power Technologies,* 2016 vol. 96, no. 3, pp. 149–156.

[126] Alam, T., Balam, N.B., Kulkarni, K.S., Siddiqui, M.I.H., Kapoor, N.R., Meena, C.S., Kumar, A., Cozzolino, R., “Performance Augmentation of the Flat Plate Solar Thermal Collector: A Review,” *Energies,* vol. 14, 2021, article 6203. doi: 10.3390/en14196203.

[127] Bevilacqua, P., Perrella, S., Bruno, R., Arcuri, N., “An accurate thermal model for the PV electric generation prediction: long-term validation in different climatic conditions,” *Renewable Energy,* 162 (2020), 1455–1470. https://doi.org/10.1016/j.renene.2020.08.051.

[128] Othman, M.Y.; Ibrahim, A.; Jin, G.L.; Ruslan, M.H.; Sopian, K., "Photovoltaic-thermal (PV/T) technology – The future energy technology," *Renewable Energy,* Volume 49, 2013, Pages 171-174, ISSN 0960-1481, https://doi.org/10.1016/j.renene.2012.01.038.

[129] Teo, J.C.; Tan, R.H.G.; Mok, V.H.; Ramachandaramurthy, V.K.; Kwang, C., "Impact of Partial Shading on the P-V Characteristics and the Maximum Power of a Photovoltaic String," *Energie,* 2018 , 11 (7), 1860; https://doi.org/10.3390/en11071860.

[130] Taherbaneh, M.; Rezaie, H.; Ghafoorifard, H.; Rahimi, K.; Menhaj, M.B.; Bhattacharya, R.N., "Maximizing Output Power of a Solar Panel via Combination of Sun Tracking and Maximum Power Point Tracking by Fuzzy Controllers," *International Journal of Photoenergy,* 2011 https://doi.org/10.1155/2010/312580.

[131] Siddique, A.A.; Nahri, A.M.S.M., "Effects of Surface Temperature Variations on Output Power of Three Commercial Photovoltaic Modules," *International Journal of Engineering Research & Technology (IJERT),* Vol. 5 Issue 11, November-2016.

[132] Wurster, T.S.; Schubert, M.B., "Mismatch loss in photovoltaic systems," *Solar Energy,* Volume 105, July 2014, Pages 505-511, https://doi.org/10.1016/j.solener.2014.04.014.

[133] Dhass, A.D.; Beemkumar, N.; Harikrishnan, S.; Ali, H.M.; Álvarez-Gallegos, A., "A Review on Factors Influencing the Mismatch Losses in Solar Photovoltaic System," *International Journal of Photoenergy,* Volume 2022, Article ID 2986004, https://doi.org/10.1155/2022/2986004.

[134] Zhang, F.; Han, C.; Wu, M.; Hou, X.; Wang, X.; Li, B., "Global sensitivity analysis of photovoltaic cell parameters based on credibility variance," *Energy Reports,* Volume 8, November 2022, Pages 7582-7588 https://doi.org/10.1016/j.egyr.2022.05.280.

[135] Kalateh, M.R.; Kianifar, A.; Sardarabadi, M., "Energy, exergy, and entropy generation analyses of a water-based photovoltaic thermal system equipped with clockwise counter-clockwise twisted tapes: An indoor experimental study," *Applied Thermal Engineering,* Volume 215, 2022, 118906, ISSN 1359-4311, https://doi.org/10.1016/j.applthermaleng.2022.118906.

[136] Bigorajski, J.; Chwieduk, D., "Analysis of a micro photovoltaic/thermal e PV/T system operation in Analysis of a micro photovoltaic/thermal e PV/T system operation in," *Renewable Energy,* Volume 137, 2019, Pages 127-136, ISSN 0960-1481, https://doi.org/10.1016/j.renene.2018.01.116.

[137] Osma-Pinto, G.; Ordonez-Plata, G., "Dynamic thermal modelling for the prediction of the operating temperature of a PV panel with an integrated cooling system," *Renewable Energy,* Volume 152, 2020, Pages 1041-1054, ISSN 0960-1481, https://doi.org/10.1016/j.renene.2020.01.132.

[138] Chwieduk, B.; Chwieduk, D., "Analysis of operation and energy performance of a heat pump driven by a PV system for space heating of a single family house in polish conditions," *Renewable*

*Energy,* Volume 165, Part 2, 2021, Pages 117-126, ISSN 0960-1481, https://doi.org/10.1016/j.renene.2020.11.026.

[139] Mostakim, K.; Hasanuzzaman, M., "Global prospects, challenges and progress of photovoltaic thermal system," *Sustainable Energy Technologies and Assessments,* Volume 53, Part A, October 2022, 102426 https://doi.org/10.1016/j.seta.2022.102426.

[140] Polskie Towarzystwo Elektrociepłowni Zawodowych, "Report on cogeneration (in Polish). 2019.," [Online]. Accessed: 17 April 2020 https://ptec.org.pl/wp-content/uploads/2023/08/Raport-o-kogeneracji-w-cieplownictwie-PTEZ-Pazdziernik-2019.pdf.

[141] Szargut J., Stanek W., "Thermo-ecological optimization of a solar collector," *Energy,* 2007, vol. 32, nr 4, s.584-590. doi:10.1016/j.energy.2006.06.010.

[142] Xu, J.; Lv, T.; Hou, X.; Deng, X.; Liu, F., "Provincial allocation of renewable portfolio standard in China based on efficiency and fairness principles," *Renewable Energy,* Volume 179,2021,Pages 1233-1245,ISSN 0960-1481,https://doi.org/10.1016/j.renene.2021.07.101.

[143] Yang, J., Changqi S., "Robust optimization of microgrid based on renewable distributed power generation and load demand uncertainty," *Energy,* 2021, vol. 223(C)., doi: 10.1016/j.energy.2021.120043.

[144] Østergaard, P.A.; Duic, N.; Noorollahi, Y.; Kalogirou, S.A., "Advances in renewable energy for sustainable development," *Renewable Energy,* Vol. 219, Part 1, 119377, 2023. https://doi.org/10.1016/j.renene.2023.119377.

[145] Mérida García, A.; Gallagher, J.; Rodríguez Díaz, J.A.; McNabola, A., "n economic and environmental optimization model for sizing a hybrid renewable energy and battery storage system in off-grid farms.," *Renewable Energy,* Vol. 220, 119588, 2024. https://doi.org/10.1016/j.renene.2023.119588.

[146] Long, Y.; Liu, X., "Optimal green investment strategy for grid-connected microgrid considering the impact of renewable energy source endowment and incentive policy.," *Energy,* Vol. 295(C), 2024. https://doi.org/10.1016/j.energy.2024.131073.

[147] Mansouri, S.A.; Ahmarinejad, A.; Nematbakhsh, E.; Javadi, M.S.; Nezhad, A.E.; Catalão, J.P.S., *A sustainable framework for multi-microgrids energy management in automated distribution network by considering smart homes and high penetration of renewable energy resources,*" *Energy, Elsevier, vol. 245(C).,* doi: 10.1016/j.energy.2022.123228.

[148] John, T.; Sarantakos, I.; Teo, T.T., "Stacking different services of an energy storage system in a grid-connected microgrid," *Renewable Energy,* Volume 195, 2022, Pages 357-365, https://doi.org/10.1016/j.renene.2022.06.035.

[149] Jiménez-Vargas, I.; Rey, J.M.; Osma-Pinto, G., “Sizing of hybrid microgrids considering life cycle assessment,” *Renewable Energy,* Vol. 202, pp. 554–565, 2023. https://doi.org/10.1016/j.renene.2022.11.103.

[150] Hirsch, A.; Parag, Y.; Guerrero, J., “Microgrids: A review of technologies, key drivers, and outstanding issues,” *Renewable and Sustainable Energy Reviews,* Vol. 90, pp. 402–411, 2018. https://doi.org/10.1016/j.rser.2018.03.040.

[151] Liu, F.; Mo, Q.; Zhao, X. , “Two-level optimal scheduling method for a renewable microgrid considering charging performances of heat pump with thermal storages,” *Renewable Energy,* Vol. 203, pp. 102–112, 2023 https://doi.org/10.1016/j.renene.2022.12.031.

[152] Zandrazavi, S.F.; Guzman, C.P.; Pozos, A.T.; Quiros-Tortos, J.; Franco, J.F., “Stochastic multi-objective optimal energy management of grid-connected unbalanced microgrids with renewable energy generation and plug-in electric vehicles,” *Energy,* Elsevier, vol. 241(C). doi: 10.1016/j.energy.2021.122884.

[153] Ouédraogo, S.; Faggianelli, G.A.; Notton, G.; Duchaud, J.L.; Voyant, C., “ Impact of electricity tariffs and energy management strategies on PV/Battery microgrid performances,” *Renewable Energy,* Vol. 199, pp. 816–825, 2022. https://doi.org/10.1016/j.renene.2022.09.042.

[154] Restrepo, M.; Cañizares, C.A.; Simpson-Porco, J.W.; Su, P.; Taruc, J., “Optimization- and rule-based energy management systems at the Canadian Renewable Energy Laboratory microgrid facility,” *Applied Energy,* Vol. 290, 116760, 2021. ISSN 0306-2619, https://doi.org/10.1016/j.apenergy.2021.116760.

[155] Gomes, G.J.; Xu, H.J.; Yang, Q.; Zhao, C.Y., “An optimization study on a typical renewable microgrid energy system with energy storage,” *Energy,* Vol. 234(C), 2021. https://doi.org/10.1016/j.energy.2021.121210.

[156] Maimó-Far, A., Homar, V., Tantet, A., Drobinski, P., “The effect of spatial granularity on optimal renewable energy portfolios in an integrated climate-energy assessment model,” *Sustainable Energy Technologies and Assessments,* 2022. https://doi.org/10.1016/j.seta.2022.102827.

[157] Güven, A.F., “Integrating electric vehicles into hybrid microgrids: A stochastic approach to future-ready renewable energy solutions and management,” *Energy,* Vol. 303, 131968, 2024. https://doi.org/10.1016/j.energy.2024.131968.

[158] Alharbi, T.; Abo-Elyousr, F.K.; Abdelshafy, A.M. , “Efficient coordination of renewable energy resources through optimal reversible pumped hydro-storage integration for autonomous microgrid economic operation,” *Energy,* Vol. 304, 131910, 2024. https://doi.org/10.1016/j.energy.2024.131910.

[159] Sady, H.; Rashidi, S.; Rafee, R., “Towards a net-zero-energy building with smart control of Trombe walls, underground air ducts, and optimal microgrid composed of renewable energy systems,” *Energy,* Vol. 294, 130703, 2024. https://doi.org/10.1016/j.energy.2024.130703.

[160] Ibrahim, N.N.; Jamian, J.J.; Md Rasid, M., " Optimal multi-objective sizing of renewable energy sources and battery energy storage systems for formation of a multi-microgrid system considering diverse load patterns," *Energy,* Vol. 304, 131921, 2024.https://doi.org/10.1016/j.energy.2024.131921.

[161] Roldán-Blay, C.; Escrivá-Escrivá, G.; Roldán-Porta, C.; Dasí-Crespo, D., "Optimal sizing and design of renewable power plants in rural microgrids using multi-objective particle swarm optimization and branch and bound methods," *Energy,* Vol. 284, 129318, 2023. 129318. https://doi.org/10.1016/j.energy.2023.129318.

[162] Kozák, Š., "State-of-the-art in control engineering," *Journal of Electrical Systems and Information Technology,* Vol. 1, pp. 1–9, 2014. https://doi.org/10.1016/j.jesit.2014.03.002.

[163] Ünal, C.; Açıkkalp, E.; Balta, M.T.; Hepbasli, A., "Dynamic thermo-ecological cost assessment and performance analyses of a multi generation system," *International Journal of Hydrogen Energy,* Volume 46, Issue 40, 2021, Pages 21198-21211, https://doi.org/10.1016/j.ijhydene.2021.03.208.

[164] Stanek, W., Gazda, W., Kostowski, W., "Thermo-ecological assessment of CCHP (combined cold-heat-and-power) plant supported with renewable energy," *Energy,* 2015. doi.org/10.1016/j.energy.2015.02.005.

[165] Lombardi L., Mendecka B., Carnevale E., "Environmental impacts of electricity production of micro wind turbines with vertical axis," *Renewable Energy,* 2017, vol. 128, pt. B, s.553-564. doi:10.1016/j.renene.2017.07.010.

[166] Tosun, D.C.; Açıkkalp, E.; Altuntas, O.; Hepbasli, A.; Palmero-Marrero, A.I.; Borge-Diez, D., "Dynamic performance and sustainability assessment of a PV driven Carnot battery," *Energy,* Volume 278, 2023, 127769. https://doi.org/10.1016/j.energy.2023.127769.

[167] Simla, T., Stanek, W., "Reducing the impact of wind farms on the electric power system by the use of energy storage," *Renewable Energy,* 2020, vol. 145, s.772-782. doi:10.1016/j.renene.2019.06.028.

[168] Gładysz, P., Saari, J. and Czarnowska, L., "Thermo-ecological cost analysis of cogeneration and polygeneration energy systems - Case study for thermal conversion of biomass," *Renewable Energy,* Volume 145, 2020, Pages 1748-1760, ISSN 0960-1481, https://doi.org/10.1016/j.renene.2019.06.088.

# Abstract

In an era of increasing energy demand, it is crucial to develop methods that account for both the complexity of energy systems and their impact on the natural environment. Identifying appropriate tools is particularly important in the context of ongoing climate change and the need for more sustainable resource management. In response to these challenges, this PhD thesis proposes new applications of the Thermo-Ecological Cost (TEC), enabling a comprehensive assessment of energy systems.

The research was conducted in several stages, encompassing different implementations of the Thermo-Ecological analysis. The main focus of the study was on renewable energy sources: wind turbines, solar energy systems (photovoltaic panels, solar collectors, and hybrid photovoltaic-thermal PV/T systems), a biogas-fuelled cogeneration engine, and heat pumps (ground- and air-source). The analysis also considered the possibility of electricity storage. In the first stage, the application of TEC analysis was developed for a single system, the PV/T system.

Subsequently, a microgrid based on renewable energy sources was designed. The analysis of the energy systems' operation was based on real meteorological data for the selected location. The designed grid was a multigeneration system producing electricity, heat, and useful cooling, corresponding to the real demand profiles for each energy service. In the next stage, the operation of the described microgrid was evaluated using TEC analysis, initially focusing on electricity production. In the final stage, the analysis was extended to include heat and cooling.

The results demonstrated that TEC analysis enables a cross-sectional assessment of energy systems. Compared to other commonly used indicators, such as energy efficiency, it better reflects the system's environmental impact. Furthermore, it allows for a clear assessment of the systems' influence on resource depletion and incorporates a broader environmental context (planet Earth). This makes TEC a tool suitable for analysing energy systems in the face of global challenges such as climate change and resource degradation.

Another important conclusion from the conducted analyses is the applicability of TEC in the design and study of microgrids. It allowed for the selection of energy source configurations that minimize non-renewable resource consumption while ensuring the best energy stability. The results also indicated that conventional methods, such as Thermo-Economic Analysis (TEA), may incorrectly suggest the benefits of systems that intensively utilise external resources. The application of TEC provided a significantly more accurate evaluation of systems in terms of sustainable resource use and offered valuable guidance for designing stable grids.

The presented research contributes to the advancement of knowledge in sustainable design of energy systems based on renewable sources. TEC analysis was adapted and expanded as a tool enabling a comprehensive assessment of systems' impact on non-renewable resources. The results also provide a basis for practical applications, indicating optimal configurations of renewable energy mixes and supporting the design of sustainable grids.

# Streszczenie

W dobie rosnącego zapotrzebowania na energię kluczowe staje się opracowanie metod uwzględniających zarówno złożoność systemów energetycznych, jak i ich wpływ na środowisko naturalne. Znalezienie odpowiednich narzędzi jest szczególnie istotne w kontekście postępującej zmiany klimatu oraz potrzeby bardziej zrównoważonego gospodarowania zasobami. W odpowiedzi na te wyzwania w niniejszej rozprawie doktorskiej zaproponowano nowe zastosowania Kosztu Termoekologicznego (TEC), który umożliwia kompleksową ocenę systemów energetycznych.

Badania przeprowadzono w kilku etapach, obejmujących różne implementacje Analizy Termoekologicznej. Głównym przedmiotem badań był system oparty na odnawialnych źródłach energii, tj. turbina wiatrowa, systemy wykorzystujące energię słoneczną (panele fotowoltaiczne, kolektory słoneczne, systemy hybrydowe fotowoltaiczno-termiczne PV/T), kogeneracyjny silnik zasilany biogazem oraz pompy ciepła (gruntowe i powietrzne). W analizie uwzględniono również możliwość magazynowania energii elektrycznej. W pierwszym etapie opracowano zastosowanie analizy TEC dla jednego komponentu układu, jakim był system fotowoltaiczno-termiczny PV/T.

Następnie zaprojektowano mikrosieć opartą na odnawialnych źródłach energii. Analiza działania systemów energetycznych została oparta na rzeczywistych danych meteorologicznych dla wybranej lokalizacji. Zaprojektowana sieć była układem multigeneracyjnym, który produkował energię elektryczną, ciepło oraz chłód użytkowy. Układ odpowiadał rzeczywistym charakterystykom zapotrzebowania na poszczególne usługi energetyczne. W kolejnym etapie prac zbadano działanie opisanej mikrosieci za pomocą analizy termoekologicznej, koncentrując się początkowo na produkcji energii elektrycznej. W końcowym etapie rozszerzono analizę również na ciepło i chłód.

Wyniki badań wykazały, że Koszt Termoekologiczny umożliwia przekrojową ocenę systemów energetycznych. Lepiej niż inne standardowo stosowane wskaźniki, takie jak sprawność energetyczna, odzwierciedla wpływ systemu na środowisko. Ponadto pozwala na jednoznaczną ocenę wpływu systemów na wyczerpywanie zasobów i uwzględnia szerszy, globalny kontekst środowiskowy. Sprawia to, że TEC jest narzędziem odpowiadającym na potrzeby analizy systemów energetycznych w dobie globalnych wyzwań, takich jak zmiana klimatu czy degradacja zasobów.

Kolejnym istotnym wnioskiem z przeprowadzonych analiz jest możliwość wykorzystania analizy TEC do projektowania i badań mikrosieci. Dzięki niej możliwe było dobranie konfiguracji źródeł energii o najniższym zużyciu zasobów nieodnawialnych wraz z jednoczesnym zapewnieniem stabilności sieci. Wyniki pokazały również, że klasyczne metody, takie jak analiza termoekonomiczna (TEA), mogą błędnie sugerować korzystność układów intensywnie wykorzystujących zasoby zewnętrzne. Zastosowanie Kosztu Termoekologicznego pozwoliło na znacznie lepszą ocenę systemów pod kątem zrównoważonego wykorzystania zasobów, a także dostarczyło istotnych wskazówek dla projektowania stabilnych sieci. Zaprezentowane badania przyczyniają się do rozwoju wiedzy w zakresie zrównoważonego projektowania systemów energetycznych opartych na odnawialnych źródłach energii.

Koszt Termoekologiczny został zaadaptowany i rozwinięty jako narzędzie umożliwiające kompleksową ocenę wpływu systemów na zasoby nieodnawialne. Wyniki badań stanowią podstawę do zastosowań praktycznych, pozwalając na wskazanie optymalnych konfiguracji miksów odnawialnych źródeł energii oraz wspierając projektowanie zrównoważonych sieci energetycznych.

# Appendices

In this Chapter, the full-text papers that were briefly described in Chapters 2 - 4 are presented. The papers are listed in the following order:

I. Agnieszka Szostok, Wojciech Stanek, Thermo-ecological analysis - The comparison of collector and PV to PV/T system, Renewable Energy, Volume 200, 2022, Pages 10-23, ISSN 0960-1481, https://doi.org/10.1016/j.renene.2022.09.070.

II. Agnieszka Szostok, Wojciech Stanek, Thermo-ecological analysis of the power system based on renewable energy sources integrated with energy storage system, Renewable Energy, Volume 216, 2023, 119035, ISSN 0960-1481, https://doi.org/10.1016/j.renene.2023.119035.

III. Wojciech Stanek, Agnieszka Szostok, Thermo-ecological assessment of microgrid supported with renewable energy, Energy, Volume 314, 2025, 134256, ISSN 0360-5442, https://doi.org/10.1016/j.energy.2024.134256.

# Paper I: Comparison of collector and PV to PV/T system

Renewable Energy 200 (2022) 10–23

Contents lists available at ScienceDirect

Renewable Energy

journal homepage: www.elsevier.com/locate/renene

## Thermo-ecological analysis - The comparison of collector and PV to PV/T system

Agnieszka Szostok [a,*], Wojciech Stanek [b]

[a] Environmental Analysis Eko-precyzja/Zakład Analiz Środowiskowych Eko-Precyzja, Poland
[b] Silesian University of Technology, Department of Thermal Technlogy, Poland

ARTICLE INFO

*Keywords:*
Photovoltaic thermal collectors thermo-ecological cost

ABSTRACT

The use of solar radiation energy is one of the important elements to achieve energy transformation. This potential can be utilized by generating electricity with PV modules or heat from collectors. It is also possible to combine these elements into one system and more efficient use of solar radiation, as is the case with the Photovoltaic thermal collectors (PV/T system), which is considered in the article below. The amounts of produced electricity and heat are compared and the energy efficiency of electricity production by PV or PV/T. Local energy analysis from the point of view of resource efficiency, however, becomes insufficient, because it ignores the issue of the quality of individual energy carriers, therefore also in the rest of the article presents an exergo-ecological analysis using the TEC concept (thermo-ecological cost). It has been demonstrated that the TEC for generated carrier (electricity/heat) produced from solar radiation is lower for combined systems and depends on a few factors: the type of generated carrier and implementation of division of allocation of fuel between heat and electricity (for combined systems). Local analysis leads to conclusions other than the global one, as demonstrated by the results presented in the article.

### 1. Introduction

Energy has played a key role in all of human society's economic and social development. The number of global electricity generation increased from 9880.0 to 26823 TWh (between 1985 and 2020) [1]. This trend is a response to the ever-growing demand. According to the International Energy Agency report the rise in electricity demand in 2021 is 4,5% [2] and electricity generation increased by 6.2% [3]. At the current rate, electricity consumption is growing year by year [4]. The projections from the United States Energy Information Administration (EIA), forecast that the global electricity generation will increase by 45% by the year 2040 [5]. Today's humankind stands in an era that is experiencing unprecedented social inequalities and environmental issues, and climate change is the most difficult. The dependence on fossil fuels has led to a steadily increasing greenhouse gas emission rate. Conventional energy generation based on sources such as natural coal, gas, oil or coal is a source of greenhouse gas emissions, which are released into the atmosphere during combustion processes. According to IPCC (The Intergovernmental Panel on Climate Change) Report, AR6 Climate Change 2021: 'The Physical Science Basis human impact on climate change' refers to human activities that lead or contribute to climate responses, such as human-induced greenhouse gas emissions. The greenhouse gases (e.g. carbon dioxide) change the radiative properties of the atmosphere, warming the climate. Between 2010 and 2019 average annual anthropogenic carbon dioxide emissions reached the highest levels in human history [2,6,7].Each of the last four decades has been successively warmer than any decade preceding it since 1850 [7]. Switching to energy based on renewable energy sources (RES) is currently the only viable solution in the face of the climate crisis and increasingly depleting fossil fuel resources. In the case of renewable energies TEC is mainly due to material inputs to construction It should also be emphasized that the lack of emission of harmful substances from RES systems results in the reduction of their TEC (thermo-ecological cost) values [4].. In the [8] the TEC wsas used fot analisys of the multi-generation system consisting of an internal combustion engine fueled by natural gas, a heat pump, a reverse osmosis desalination plant and a magnesium-chlorine (Mg–Cl) thermochemical (TC) water splitting cycle. Results showed that TEC is an effective method of assessing the environmental performance of various energy systems and comparing them with each other [8].

Another important argument in favour of the growing importance of renewable energy sources is improving the resilience of the electric

* Corresponding author.
*E-mail addresses:* agnieszka.szostok@eko-precyzja.eu (A. Szostok), wojciech.stanek@polsl.pl (W. Stanek).

https://doi.org/10.1016/j.renene.2022.09.070
Received 7 July 2022; Received in revised form 12 July 2022; Accepted 19 September 2022
Available online 24 September 2022

power system. Decentralized system based on local resources represents both the system's ability to adapt to changing conditions and therefore ensuring the continuity of services that might otherwise be disrupted [9]. The Earth's surface receives about 120.000 TW of solar radiation, which is a thousand times more than the energy demand of the entire planet [10]. For this reason solar energy is one of the most promising branches of renewable energy. Solar energy can broadly be divided into two parts. Firstly, photovoltaic technology, that is derived from solar cell technology and transformed into electricity. The second part is thermal solar technology, that is derived from a thermal collector and converts solar energy into heat [11].

The relatively low efficiency of solar energy conversion into electricity in most of the photovoltaic modules available on the market is one of the major problematic issues limiting the wide application of this technology.

It should also be mentioned environmental and operational factors affecting the operation of photovoltaic systems as partial shading, photovoltaic output power variations and mismatch losses discussing their characteristics. Photovoltaic systems are very prone to partial shading. The maximum power of a PV system can reduce drastically when partial shading takes place. The susceptibility of partial shading may vary depending on the shading heaviness, partial shading patterns, and the configuration employed in connecting all the PV modules in the photovoltaic system [12]. The maximum output power of a solar panel depends on the environmental conditions and load profile. PV cell performance is very vulnerable to cell surface temperature. This temperature is determined by weather parameters like ambient temperature, humidity, wind velocity, cell structure, material and solar irradiance [13,14]. The efficiency of the photovoltaic modules decrease because of mismatch and ohmic losses. Based on the availability of incident solar radiation, the mismatch effect can be reduced by adding an appropriate connection configuration. For small PV systems there is no need for the end user to consider parameter matching since this is done by the module manufacturer. For larger PV systems, nevertheless, where several PV strings are connected in parallel to increase the system power, parameter matching becomes a significant issue [15–17].

Almost half of the solar radiation absorbed by photovoltaic thermal systems is converted into heat, which leads to high operating temperature, damage to the cell structure and reduced service life; therefore, efficient cooling of the photovoltaic units is essential [18]. Usually 5–18% of solar radiation falling on a photovoltaic module is converted into electricity [3]. Two parameters which influence the performance of a photovoltaic device can be distinguished: operating cell temperature and the incident solar radiation. A small percentage of the incident solar radiation actually is converted into electricity. Most of the solar energy absorbed by the photovoltaic module is converted into heat which has the effect of increasing the operating temperature of the cells. As a consequence of this process the module efficiency decreases. The decrease is almost linearly with the increase in temperature: between 0.40 and 0.65% points for each degree of temperature growth, in relation to the considered photovoltaic technology [10]. In addition, it should be emphasized that the efficiency decrease occurs at times of greatest solar radiation availability. Thus, the in the best conditions not only the module efficiency is low, but also large amounts of heat are lost to the environment. A good way to partially avoid this loss is recovering the lost heat from the photovoltaic cells. The technology using this solution is called: photovoltaic thermal PV/T technology [10,11,19,20].

A Solar Photovoltaic Thermal (PV/T) system enables the simultaneous conversion of solar radiation into electricity and heat. Results published in 2001 by S A. Kalogirou on the simulation of a hybrid photovoltaic thermal plant installed in Cyprus using TRNSYS (simulation program used in the fields of renewable energy engineering) showed that a PV/T system can increase the average annual efficiency of a PV system from 2.8% to 7.7%. Furthermore, it can meet the demand of a home's hot water needs to 49%, thus enhancing the average annual system efficiency to 31.7% [21]. What is important especially in the context of heat households needs: home heating accounts for 64.1% of total final energy consumption in European Union. Water and space heating together represents as many as 78.9% [22]. The challenges of PV/T systems should also be mentioned: especially technical barriers (i. e. energy loss effects, weight problems, tracking systems, load distribution) and financial barriers (i.e. high initial costs, payback period and life cycle cost) [23].

The values of the exergy efficiency of RES (PV, PV/T) are at a low level compared to systems based on fossil fuels. The average efficiency of power plants in Poland is 36.7%, and the exergy efficiency of the BAT (best available techniques) coal-fired power plant is 45.9%. Even higher values are achieved by NGCC (natural gas combined-cycle), which in the case of BAT reaches 57.7%. Against this background, the PV system ranks poorly as regards the values of the exergy efficiency between 11.6 and 14.8% [24]. That is why it is so important to introduce TEC diagnostics (global), which, despite the low efficiency of renewable energy sources, indicates their advantage over conventional systems.

Focusing only on pure energy analysis it can be concluded that renewable sources are much less efficient than non-renewable. Cogeneration evaluated as the energy efficiency as presented above still achieves low values (the energy efficiency of heat and electricity generation in cogeneration with the combustion of non-renewable fuels is 80–95%) [25]. Therefore the energy evaluation is insufficient or even not acceptable, and certainly it is not able to determine the thermodynamic degree of perfection of the mentioned processes. To deepen the analysis and make it more accurate it is worth introducing exergy analysis. The exergy analysis allows us to evaluate different qualities of energy carriers. Exergy can be defined as the maximum ability of an energy carrier to perform work in respect to the common environment or in other words the minimum theoretical work required to obtain the substance with given parameters and composition [26,27].

The overall purpose of this article is to compare the separate systems: photovoltaic technology and thermal solar technology with the hybrid photovoltaic thermal PV/T technology system in the context of non-renewable energy.

## 2. Methodology

### 2.1. Description and characteristic of the analysed PV and collector system

Quantity of transformed a solar radiation into electricity by photovoltaic panel can be calculated from equation (1)

$$\boldsymbol{E_{PV}} = \eta_{e_{PV}} \boldsymbol{I_\beta A_{PV}} \tag{1}$$

As already mentioned, the efficiency of converting solar radiation into energy depends on the amount of radiation that falls on the panel and temperature. Therefore, the value of energy efficiency is determined based on the diagram [28,29] presented in Fig. 1.

Quantity of transformed a solar radiation into heat by thermal collector can be calculated from equation (2)

$$\boldsymbol{Q_e} = \eta_{th_C} \boldsymbol{I_\beta A_C} \tag{2}$$

Thermal efficiency of collector $\eta_{th_C}$ is calculated from equation (3) [30]:

$$\eta_{th_C} = \eta_{th_{C_0}} - \frac{\boldsymbol{k_1}\,\boldsymbol{\Delta T}}{\boldsymbol{I_\beta}} - \frac{\boldsymbol{k_2} - \boldsymbol{\Delta T}^2}{\boldsymbol{I_\beta}} \tag{3}$$

where:

The temperature difference $\Delta T$ is calculated from relation (4):

$$\Delta T = T_O - T_C \tag{4}$$

Optical efficiency $\eta_{th_{C_0}}$ is designated with the diagram [30] presented in Fig. 2 and the received values of are heat loss coefficients are presented in Table 1.

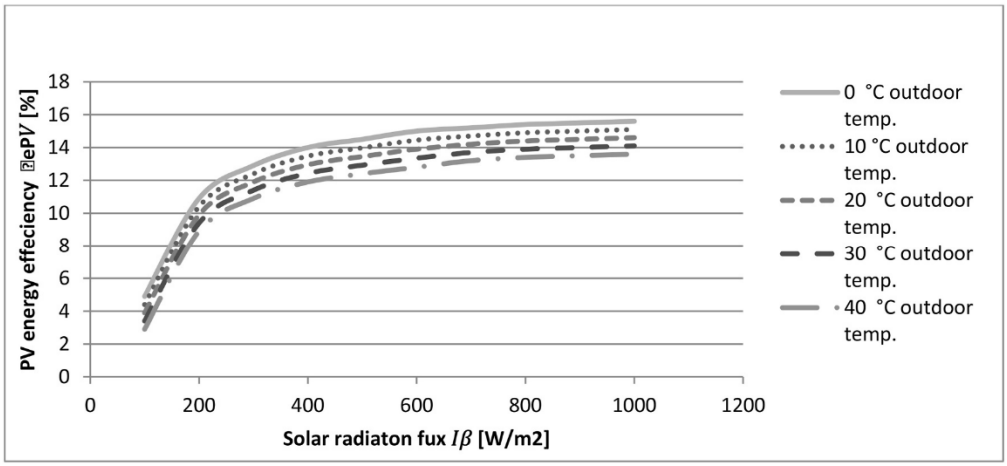


**Fig. 1.** Graph of the relation of global radiation, outdoor temperature and energy efficiency of PV panel (based on [17]).

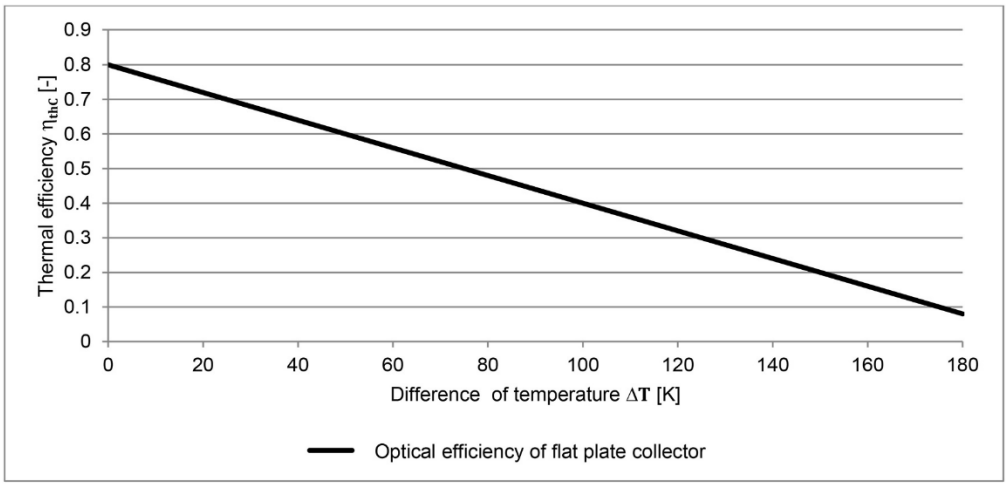


**Fig. 2.** Optical efficiency graph (based on [30]).

**Table 1**
Values of are heat loss coefficients of collector (based on [30]).

| | heat loss coefficients $k_1$ | heat loss coefficients $k_2$ |
|---|---|---|
| | W/(m$^2$K) | W/(m$^2$K$^2$) |
| flat-plate collector | 4 | 0.1 |

### 2.2. Description and characteristic of the analysed PV/T system

First for the PV/T system the amount of generated heat from solar radiation is calculated. The heat from PV/T installation is transferred through the exchanger to the water tank. The cooling process begins when the cell temperature exceeds the assumed temperature of 30 °C. Estimate module temperature is calculated using eq. (5):

$$t_{PV} = t_O + \frac{(t_{NOCT} - 20) I_\beta}{800} \tag{5}$$

where $t_{PV}$ is module temperature, $I_\beta$ is solar radiation on the module, $t_O$ is the temperature of the environment and $t_{NOCT}$ is Normal Operating Cell Temperature (44–48 °C) [31].

For the purposes of the calculations, the following assumptions where made.

- the cooling process begins when the cell temperature exceeds the assumed temperature of 30 °C,
- cooling water temperature from the domestic hot water tank is constant ($T_{w_{in}} = 10$ °C),
- the refrigerant in the PV/T circuit is ergolide ($c_e = 3.17$ kJ/(kg·K)),
- mass stream of water and ergolide is 0.02 kg/s,
- heat losses in pipelines are ignored.

Fig. 3 presents the simplified diagram of PV/T installations.

The purpose of determining PV/T thermal efficiency is used with features that where created based on [30].

$$\eta_{th} = \eta_0 - \frac{\alpha (T_{eg\ out} - T_O)}{I_\beta} \tag{6}$$

where $\eta_{th}$ is PV/T thermal efficiency; $\eta_0$ is 0.6099. α is heat transfer coefficient (α = 5.8343 W/(m$^2$K)), $T_{eg\ out}$ is temperature of the working medium flowing out the PV/T panel (outlet temperature ergolide).

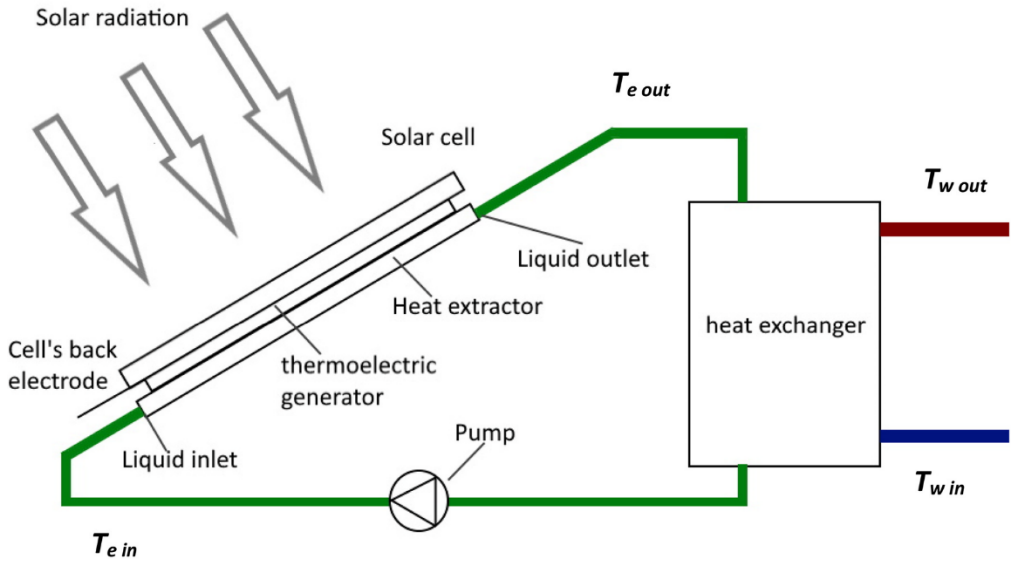


**Fig. 3.** Simplified diagram of PV/T installations (based on [32]).

Thermal efficiency of PV/T is presented in Fig. 4.

In the equation (6). except for the temperature of ergolide, other values are known. The temperature of ergolide at the moment of starting the cooling process is assumed as the ambient temperature, then it is calculated from the heat exchanger analysis using the ε-NTU method.

$$\dot{Q}_{PVT} = \eta_{th_{PVT}}\, I_\beta A_{PVT} \tag{7}$$

where $\eta_{th_{PVT}}$ is thermal efficiency of PV/T, $I_\beta$ is solar radiation and $A_{PVT}$ is PV/T panel surface.

The ε-NTU method is used to determine ergolide and feed water temperatures. The ε-NTU method is one method in which a heat exchanger is analysed. For this purpose, thermal equations in dimensionless form are used [33]. The method enables thermal calculations for the exchanger when the inlet temperatures of the factors and the exchanger parameters are known. The dimensionless parameters R, S, p, φ where determined as presented in Table 2.:

The indicators presented in Table 2 contain the heat capacity of streams, which were calculated using equations (8) and (9).

**Table 2**
Methodology of dimensionless parameters ε-NTU.

| | | |
|---|---|---|
| R | $R = \frac{W_w}{W_{eg}}$ | 1.32 |
| S | $S = k\,\frac{A_W}{W_{eg}}$ | 1.44 |
| p | $p = \left(\frac{1 - e^{[-s(1-1R)]}}{R - e^{[-s(1-1R)]}}\right)$ | 0.478 |
| φ | $\varphi = pR$ | 0.633 |

$$\dot{W}_w = \dot{m}_w c_w \tag{8}$$

$$\dot{W}_{eg} = \dot{m}_{eg} c_{eg} \tag{9}$$

$$t_{e_{gout}} = \frac{\dot{Q}_{PVT}}{\dot{m}_{eg} * c_{eg}} + t_{eg_{in}} \tag{10}$$

$$t_{eg_{in}} = t_{eg-out} - \varphi(t_{w_{in}} - t_{w_{out}}) \tag{11}$$

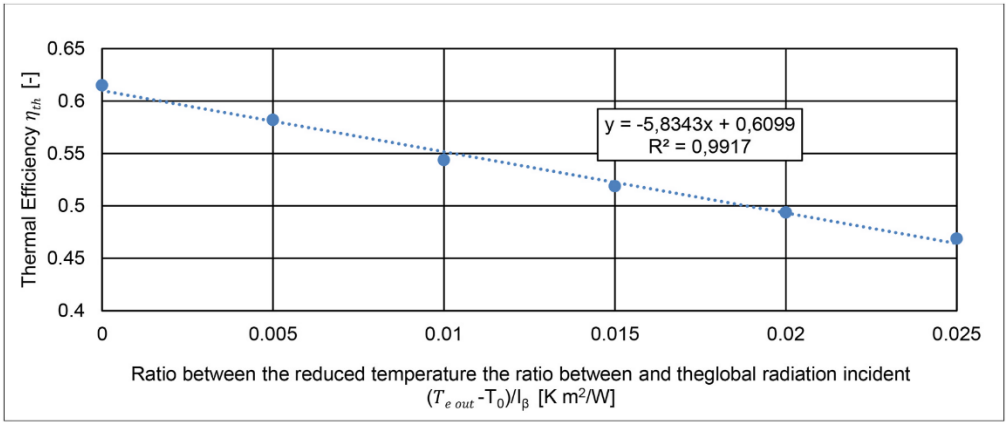


**Fig. 4.** Thermal efficiency of PV/T (based on [17]).

$$t_{w_{in}} = const. \tag{12}$$

$$t_{eg_{in}} = p\left(t_{eg\ out} - t_{w_{in}}\right) + t_{w_{in}} \tag{13}$$

where $T_{eg\ out}$ [K] is temperature of the working medium flowing out the PV/T panel (outlet temperature ergolide).

$T_{eg\ in}$ [K] is temperature of the working medium flowing in the PV/T panel (intake temperature ergolide).

$T_{w\ out}$ [K] is temperature of water flowing out the heat exchanger (outlet temperature water).

$T_{w\ in}$ [K]is temperature of water flowing in the heat exchanger (intake temperature water).

Useful heat to support hot water calculated using equation (14)

$$\dot{Q} = \dot{m}_w c_w (t_{w_{out}} - t_{w_{in}}) \tag{14}$$

For the PV/T system, the amount of generated energy from solar radiation is calculated from equation (15):

$$E_{PVT} = \eta_{e_{PVT}}\ I_\beta\ A_{PVT} \tag{15}$$

Energy efficiency of PV/T is determined based on the Fig. 5 [31,34].

PV/T energy efficiency therefore is calculated from equation (16):

$$\eta_{e_{PVT}} = 0.1464 \frac{T_{eg\ out} - T_O}{I_\beta} - 0.6828 \tag{16}$$

where $T_O$ is the temperature of the environment and $T_{eg_{out}}$ is temperature of the working medium flowing out the PV/T panel (outlet temperature ergolide).

### 2.3. The comparative energy analysis of PV, collector and PV/T

The results of the simulations show that PV/T energy generation is 267.07 kWh annually (see Table 3). That's about one and a half more than energy generation from PV (which is 183.62 kWh per year). These results show the positive effect of module cooling, which directly translates into higher energy gains. The quantity of electricity from PV/T and PV by months is presented in Table 4 and in Fig. 6.

If we take into account the amount of heat produced per year, the divided system is better (the quantity of heat from PV/T and PV by months as can be seen in Table 5 and Fig. 7). The collector will generate 2191.49 kWh per year. The amount of heat produced by PV/T throughout a year is 540.84 kWh. One of the reasons for such a significant difference is the assumption that we start cooling the PV/T module when the module temperature is 30 °C.

Efficiency of solar energy conversion into electricity in the case of PV/T is higher than that of PV. To compare the values, the average monthly value of energy efficiency is calculated by the formula (16) and the results are presented in the Table 6 and Fig. 8. As demonstrated, the energy efficiency for each month is higher for PV/T. The difference between PV/T and PV ranges from 3.8 to 8.2% points. The average annual value of PV/T 's energy efficiency is 15.2%, and as regards to PV – 10.2%.

**Table 3**
The quantity of electricity and heat from PV/T and PV/collector per 1 year.

| Parameter | The amount of electricity per year | The amount of heat per year |
|---|---|---|
| Unit | [kwh] | [kwh] |
| PV | 183.62 | – |
| collector | – | 2191.49 |
| PV/T | 267.07 | 540.84 |

**Table 4**
The quantity of electricity from PV/T and PV by months.

| Months | | PV | | PV/T | |
|---|---|---|---|---|---|
| Lp. | Unit | kWh | MJ | kWh | MJ |
| 1 | **January** | 4.49 | 16.16 | 7.50 | 27.00 |
| 2 | **February** | 7.22 | 26.00 | 10.06 | 36.20 |
| 3 | **March** | 11.35 | 40.86 | 18.20 | 65.53 |
| 4 | **April** | 19.66 | 70.76 | 28.15 | 101.33 |
| 5 | **May** | 30.23 | 108.84 | 39.59 | 142.52 |
| 6 | **June** | 24.57 | 88.43 | 35.11 | 126.40 |
| 7 | **July** | 27.81 | 100.12 | 39.46 | 142.05 |
| 8 | **August** | 21.70 | 78.12 | 32.69 | 117.69 |
| 9 | **September** | 17.31 | 62.31 | 26.65 | 95.92 |
| 10 | **October** | 10.73 | 38.63 | 17.66 | 63.57 |
| 11 | **November** | 4.85 | 17.47 | 10.01 | 36.05 |
| 12 | **December** | 3.70 | 13.33 | 6.96 | 25.07 |
| **SUMA:** | | **183.62** | **661.03** | **277.90** | **272.03** |

$$\eta_{e_m} = \frac{\sum E_{PV,PVT}}{\sum I_\beta A_{PV,PVT}} \tag{17}$$

where $\eta_{e_m}$ is monthly energy efficiency of PV or PV/T, $\sum E_{PV,PVT}$ is monthly sum of the amount of energy of PV or PV/T, $\sum I_\beta$ ismonthly sum of the amount solar radiation and $A_{PV,PVT}$ is PV or PV/T panel surface.

As can be seen in Fig. 8, the monthly average efficiency of a PVT system is higher than that of a PV system throughout the year. The results obtained as a result of the simulation are the basis for the TEC analysis presented below in the article.

## 3. Thermo-ecological cost (TEC) – methodology

The yearly thermo-ecological cost (TEC) is an evaluation tool dedicated to measure the efficiency of natural resources management. It contains exergy (as a resource's quality indicator) and he cumulative calculus. TEC can be a measure of global exergy-ecological efficiency by depicting non-renewable resources by cumulative exergy consumption

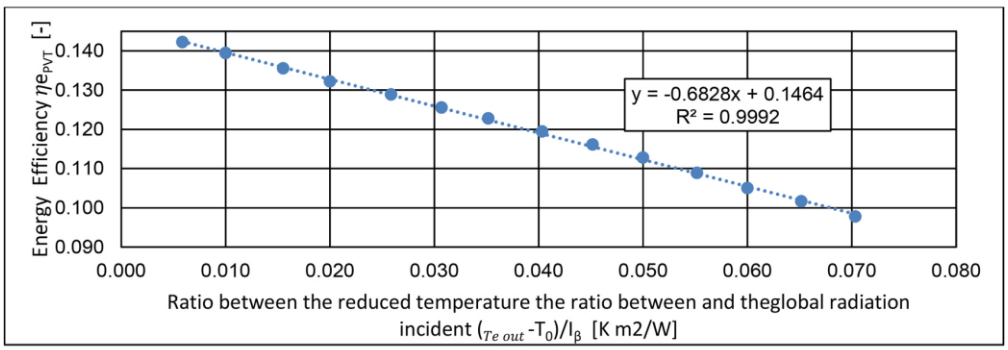


**Fig. 5.** Energy efficiency of PV/T (based on [31,34]).

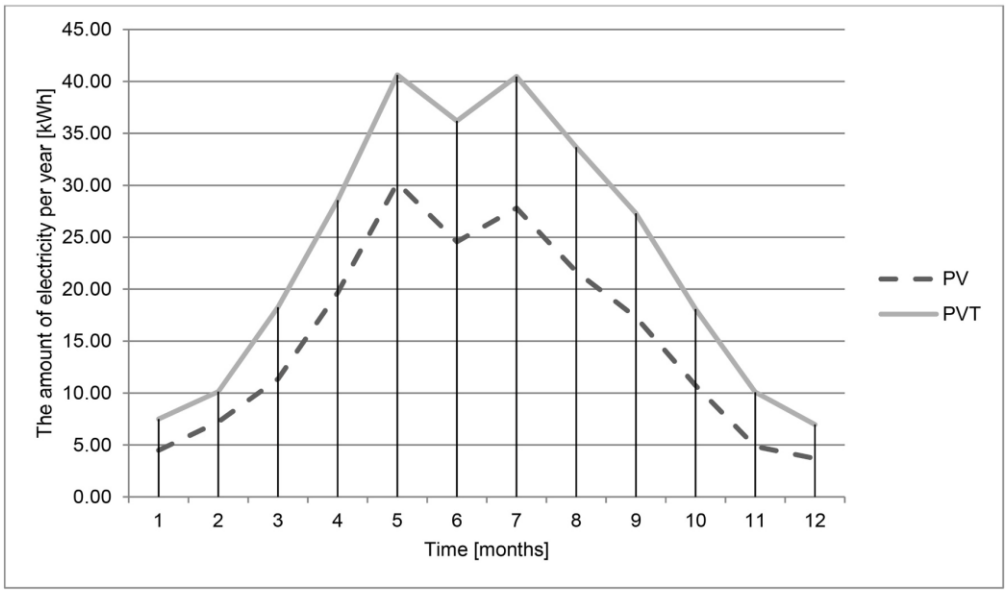


**Fig. 6.** Electricity from PV/T and PV by months.

**Table 5**
The quantity of heat from PV/T and collector by months.

| Months | | collector | | PV/T | |
|---|---|---|---|---|---|
| Lp. | Unit | kWh | MJ | kWh | MJ |
| 1 | **January** | 33.41 | 120.26 | 0.00 | 0.00 |
| 2 | **February** | 51.79 | 1.37 | 4.94 | 1.37 |
| 3 | **March** | 113.16 | 0.89 | 3.22 | 0.89 |
| 4 | **April** | 215.15 | 34.95 | 125.81 | 34.95 |
| 5 | **May** | 345.07 | 102.72 | 369.81 | 102.72 |
| 6 | **June** | 310.62 | 94.70 | 340.92 | 94.70 |
| 7 | **July** | 361.39 | 129.32 | 465.56 | 129.32 |
| 8 | **August** | 300.52 | 103.99 | 374.37 | 103.99 |
| 9 | **September** | 225.02 | 48.64 | 175.10 | 48.64 |
| 10 | **October** | 139.21 | 22.12 | 79.63 | 22.12 |
| 11 | **November** | 63.61 | 2.13 | 7.68 | 2.13 |
| 12 | **December** | 32.55 | 0.00 | 0.00 | 0.00 |
| **SUMA:** | | **2191.49** | **7889.38** | **540.84** | **1947.03** |

[27,35,36]. It should be also underlined that the thermo-ecological cost as a systemic approach is crucial when comparing different energy systems.

One way to present the physical and ecological cost of each product that accounts for the total consumption of natural resources at the level of their extraction from nature is the TEC - thermo-ecological cost. TEC includes the exergy consumption of non-renewable resources directly obtained from nature, such as fuels, mineral ores, freshwater and mineral ores. TEC can be defeated (according to Szargut [26]) as: cumulative consumption of non-renewable exergy related to the production of a given product with additional consideration of the consumption resulting from the need to compensate for environmental losses caused by the rejection of harmful waste substances into the environment. The main applications of thermo-ecological cost are:

- Assessment of the impact of the operational parameters of energy systems on the depletion of fossil fuels.
- Optimization of operating parameters, the structure of production of a given useful product and design parameters ensuring minimization of the depletion of non-renewable resources.
- Choice of technology that ensures minimal depletion of non-renewable resources.
- Estimating the impact of discharging harmful substances into the environment on the depletion of non-renewable resources.
- Determining the impact of individual useful goods on the depletion of non-renewable resources during their full life cycle.
- Analysis of the impact of interregional exchange on the depletion of non-renewable resources.
- Estimating the degree of sustainable development.
- Determining the size of the pro-ecological tax replacing the existing taxes [24,26,37].

The thermo-ecological cost can be also generated by the consumption of by-products which are exchanged between the branches of the system. In this case TEC of pollution is not calculated as the chemical exergy, but as the amount of exergy needed to prevent releasing the pollution to the environment. As an example can be given using exergy in abatement installations. On condition when it is impossible to prevent releasing these pollutants to the environment the TEC should be determined as the amount of exergy needed to need to decrease the negative effects caused by the discards which are introduced into the environment [38,39]. In some processes by-products can replace main in other processes and hence the value of the thermo-ecological cost of a considered main product is decreased [40]. In the case of combined processes, such as the generation of electricity and heat in the case of a PV/T system, a very important influence on the TEC values is the method of dividing the thermo-ecological costs between the products. This issue is also considered in the article, presenting two ways of dividing the TEC of PV/T.

The specific thermo-ecological cost can be defined by three components. Firstly, the component related to exergy of non-renewable natural resources immediately consumed in the process $b_{sj}$. Nextly, the component contains the thermo-ecological cost of harmful substances $\zeta_k$ of the described process. Both of the mentioned elements increase the volume of TEC. The last component of specific thermo-ecological cost described specific thermo-ecological of by-products $f_{ij}$ can reduce volume of the index of operational TEC $\rho_i$ or increase when the consumption of i-th material per unit of j-th main product is high [24,26,37,40,41]:

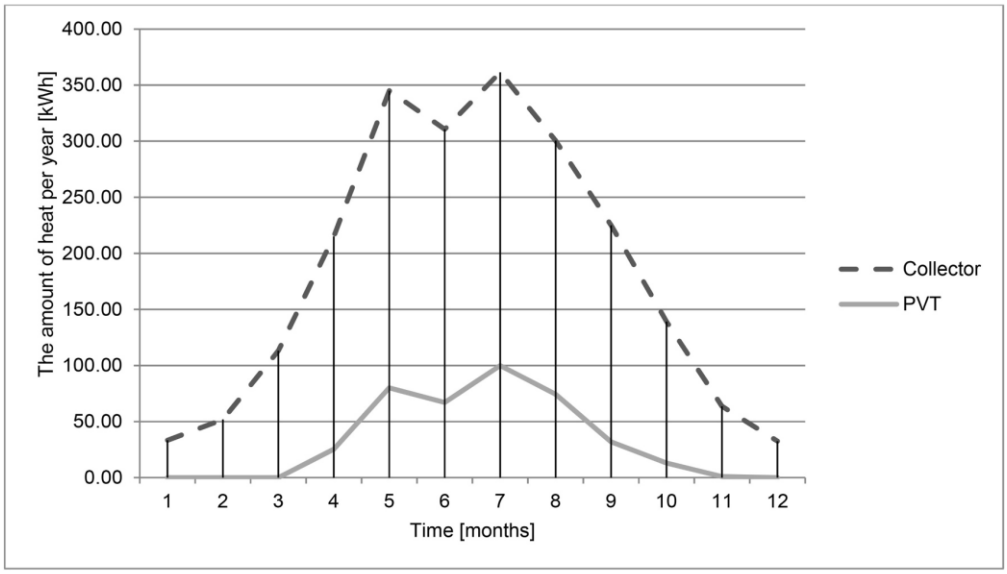


**Fig. 7.** Heat from PV/T and PV by months.

**Table 6**
Monthly average energy efficiency of electricity generation of PV/T and PV.

| Months | | PV/T | PV |
|---|---|---|---|
| | | Monthly average efficiency | Monthly average efficiency |
| Lp | Unit | % | % |
| 1 | **January** | 14.02 | 8.39 |
| 2 | **February** | 13.79 | 9.90 |
| 3 | **March** | 15.67 | 9.77 |
| 4 | **April** | 15.48 | 10.81 |
| 5 | **May** | 14.95 | 11.42 |
| 6 | **June** | 15.33 | 10.73 |
| 7 | **July** | 15.06 | 10.62 |
| 8 | **August** | 15.18 | 10.07 |
| 9 | **September** | 15.57 | 10.12 |
| 10 | **October** | 15.64 | 9.50 |
| 11 | **November** | 15.94 | 7.72 |
| 12 | **December** | 13.87 | 7.38 |
| **YEAR** | | **15.18** | **10.24** |

$$\rho_j = \sum_s b_{sj} + \sum_k p_{kj}\zeta_k - \sum_i (f_{ij} - a_{ij})\rho_i \tag{18}$$

where:

$b_{sj}$ exergy of $s$-th non-renewable natural resource immediately consumed in the process under consideration per unit of $j$-th product, MJ/kg.

$p_{kj}$ amount of $k$-th harmful substance from $j$-th process, kg.

$\zeta_k$ thermo-ecological cost of $k$-th harmful substance, MJ/kg.

$a_{ij}$ coefficient of consumption of $i$-th material per unit of $j$-th main product, e.g. in kg/kg or kg/MJ,

$f_{ij}$ coefficient of by-production of $i$-th product per unit of $j$-th main product, e.g. in kg/kg or kg/MJ,

$\rho_i$ specific thermo-ecological cost of $i$-th product, e.g. in MJ/kg.

The balance of TEC is schematically presented in Fig. 9.

However, the above equation only describes the operational part but when the power technologies are considered also other phases of the life cycle can be important. The general equation to calculate the thermo-ecological cost in the whole life cycle (formulated by Szargut [26] and used in analysing the exergetic life cycle of solar collector system by Szargut and Stanek [40]) is presented by eq. (19):

$$\rho_j^{LCA} = \theta_n\left(\sum_i \dot{G}_i\rho_i + \sum_k \dot{P}_k\zeta_k - \sum_u \dot{G}_u\rho_j s_{ju}\right) + \frac{1}{\tau_j}\left(\sum_l G_l\rho_l(1-u_l) + \sum_r G_r\rho_r\right) \tag{19}$$

where:

$\theta_n$ average annual time of exploitation of $j$-th considered machine, device, installation or building, in other words annual operation time with nominal capacity, h/year.

$\dot{G}_i$ nominal stream of $i$-th material used in $j$-th production process, kg/h.

$\dot{P}_k$ nominal stream of $k$-th waste product released to the environment from $j$-th production process, kg/h.

$\dot{G}_u$ nominal stream of $u$-th by-product manufactured simultaneously with $j$-th product within the production process, kg/h, $s_{ju}$ replacement index of by-product $u$ by main product $j$.

$s_{ju}$ replacement index of by-product u by main product j.

$\tau_j$ nominal lifetime of $j$-th machine, device, installation or building, years.

$G_l$ amount of $l$-th material used for the construction of $j$-th considered machine, device, installation or building, kg.

$u_l$ expected recovery rates of $l$-th material after the end of operation phase of $j$-th considered machine, device, installation or building, kg/kg.

$G_r$ amount of $r$-th material used for the maintenance of $j$-th considered machine, device, installation or building, kg.

The annual thermo-ecological cost of the materials used in an installation equipped with a PV/T system may be expressed as follows:

$$K_{TE} = \frac{1}{\tau}\sum_{i=1}^{n} G_n\,\rho_n\,(1-u_n) \tag{20}$$

where:

$G$ amount of material used to construct the collector, kg

$\rho$ specific thermo-ecological cost, J/kg, J/W, J/J

$u$ coefficient of recovery of the material;-

$n$ kind of material or equipment.

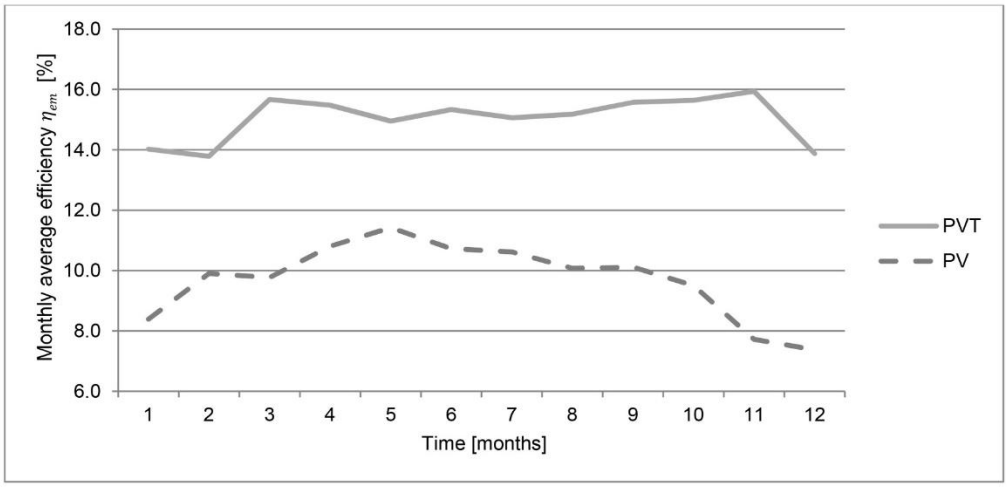


**Fig. 8.** Monthly average energy efficiency of PV/T and PV.

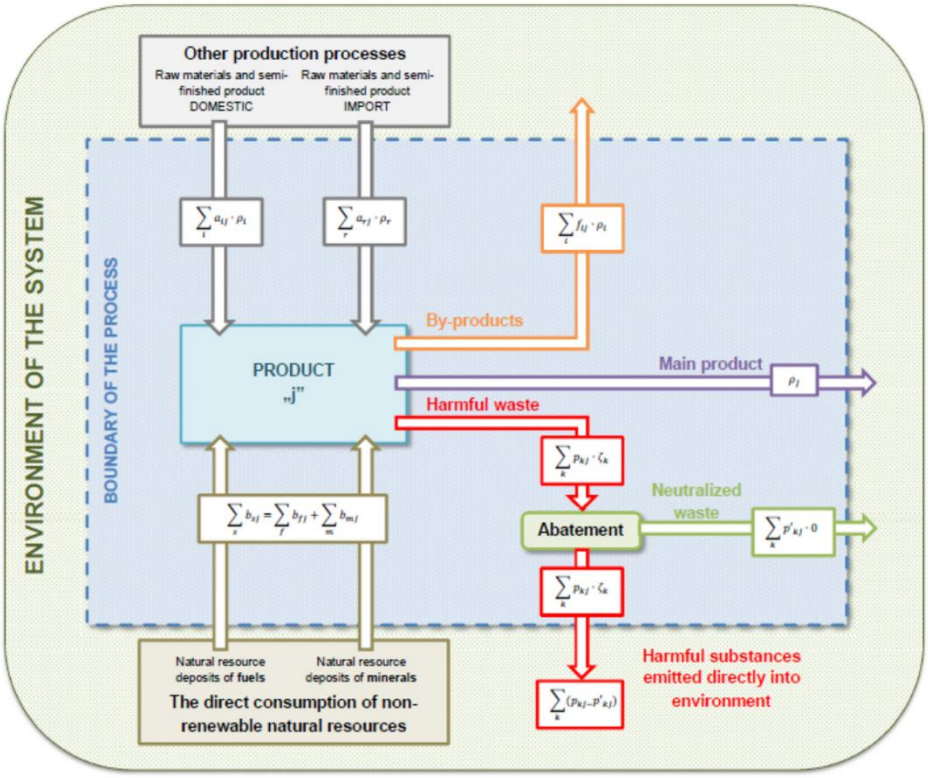


**Fig. 9.** Idea of TEC balance equation.

### 3.1. *Thermo-ecological cost of the materials*

Presented equation containing the Thermo-ecological cost of the materials used for the construction of the collector and the thermo-ecological cost of the additional equipment (n – listed in Table 7 materials and equipment). The calculations take into account the lifetime τ of the installation and the possibility to utilize some materials after the end of the exploitation of the installation(u coefficient of recovery of the material) [40]. Table 8 presents the results of calculating the exergy of the materials used, the planned service life of the installation and the product stream.

**Table 7**
Material parameters of PV/T (based on [38,42,43]).

| n | G | ρ | TEC | u | TEC (with u) |
|---|---|---|---|---|---|
| Unit | kg/ unit | MJ/kg | MJ | – | MJ |
| solar glass, low-iron, at regional storage | 11 kg | 14.63 | 288.2 | 0.5 | 144.1 |
| glass wool mat, at plant | 19.7 kg | 29.46 | 49.8 | | 49.8 |
| aluminium | 1.69 kg | 190.6 | 3488.0 | 0.5 | 1744.0 |
| aluminium | 18.3 kg | 190.6 | 339.3 | 0.5 | 169.6 |
| photovoltaic cell, multi-Si, at plant | 1.78 kg | 1827.35 | 2028.4 | | 2028.4 |
| hot water tank 600l, at plant | 1.11 | 13 375.30 | 4458.4 | 0.5 | 2229.2 |
| glass wool mat, at plant | 1 unit | 29.46 | 46.5 | | 46.5 |
| aluminium | 1.58 kg | 190.6 | 184.1 | 0.5 | 92.1 |
| Copper (kg) | 0.966 kg | 151 | 664.4 | 0.5 | 332.2 |
| glass wool mat, at plant | 4.4 kg | 29.46 | 1.8 | | 1.8 |
| slanted-roof construction, mounted, on roof | 0.063 kg | 539.23 | 539.2 | 0.5 | 269.6 |
| inverter, 500W, at plant | 14.2 kg | 565.96 | 566.0 | | 566.0 |
| electric installation, photovoltaic plant, at plant | 1 unit | 2560.85 | 2560.8 | | 2560.8 |
| solar glass, low-iron, at regional storage | 1 unit | 14.63 | 288.2 | 0.5 | 144.1 |

**Table 8**
Basic parameters obtained from the simulation.

| Parameter | value | unity |
|---|---|---|
| Total exergy of used materials | 10234.2 | MJ/unit |
| Life time of the PV/T | 25 | years |
| Total exergy of electricity | 979.3 | MJ/year |
| Total exergy of heat | 640.6 | MJ/year |
| Total solar radiation | 6452.9 | MJ/year |

Due to the cogeneration (production electricity and heat by PV/T), the calculation algorithm also includes the division of Thermo-ecological costs, which is presented later in the article.

### 3.2. The division of thermo-ecological costs in cogeneration system

In this calculation for the allocation of fuel between heat and electricity was applied the exegetic cost. The exegetic cost can be defined as the total exergy consumption of exergy of useful product. In the case of PV/T process it means that [44]:

$$k^*_{PVT} = \frac{B_{F,PVT}}{B_{P,PVT}} = \frac{B_{F,PVT}}{E_{PVT} + Q_{PVT}\frac{(T_{e,m}-T_a)}{T_{e,m}}} \tag{21}$$

where $B_{F,PVT}$ – total exergy of fuel feeding the PV/T system, $B_{P,PVT}$ – total exergy of useful products of the cogeneration unit, $T_{e,m}$ - - temperature of ergolide, $T_a$ – ambient temperature.

Using the specific cost of PV/T the solar energy of fuel burdening respectively production of heat and electricity in PV/T can be determined as follows [44]:

$$B_{F,PVT,ele} = E_{PVT}\, k^*_{PVT} \tag{22}$$

$$B_{F,PVT,heat} = Q_{PVT}\frac{(T_{e,m}-T_a)}{T_{e,m}}\; k^*_{PVT} \tag{23}$$

$$y_{PVT,ele} = \frac{B_{F,PVT,ele}}{B_{F,PVT}} \tag{24}$$

$$y_{PVT,heat} = \frac{B_{F,PVT,heat}}{B_{F,PVT}} \tag{25}$$

$$TEC_{PVT,mat} = \frac{B_{materials}}{\tau} = \frac{B_{materials}}{\tau} \tag{26}$$

$$TEC_{PVT} = \frac{TEC_{PVT,mat}}{B_{P,PVT}} \tag{27}$$

$$TEC_{PVT,ele} = y_{PVT,ele}\; TEC_{PVT} \tag{28}$$

$$TEC_{PVT,heat} = y_{PVT,heat}\; TEC_{PVT} \tag{29}$$

Monthly TEC of electricity and heat produced by PV/T for the division 1 is presented in Fig. 10.

The second, proposed in this article, form of division, TEC, uses the proportion of TEC indicators for classic/replaced technologies. To produce electricity and heat by conventional power plant or heating plant should be used:

$$TEC_{sum} = TEC_1 + TEC_2 = B_{ele}TEC_{elex} + B_{heat}TEC_{heatx} \tag{30}$$

where $TEC_{elex}$ and $TEC_{heatx}$ is the Thermo-ecological cost of a conventional coal power station and coal heating plant (coal-fired). The division coefficients were assumed according to the dependence:

$$\mu_{TEC,ele} = \frac{TEC_1}{TEC_{sum}} \tag{31}$$

$$\mu_{TEC,heat} = \frac{TEC_2}{TEC_{sum}} \tag{32}$$

Total cost TEC of PV/T:

$$TEC_{PVT,mat} = \frac{B_{materials}}{\tau} = \frac{B_{materials}}{\tau} \tag{33}$$

$$TEC_{PVT,ele} = \frac{\mu_{TEC,ele}TEC_{PVT}}{B_{ele}} \tag{34}$$

$$TEC_{PVt,heat} = \frac{\mu_{TEC,heat}TEC_{PVT}}{B_{heat}} \tag{35}$$

Monthly TEC of electricity and heat produced by PV/T for the division 2 is presented in Fig. 11.

The annual average TEC of the electricity for PV/T, as can be seen in the table above, does not exceed 0.2. For the first presented division it is 0.153. while for the second one it is 0.193. This is below the TEC for the electricity produced by PV (the TEC is 0.26) [40]. The values of the Thermo-ecological cost of PV/T are presented in Table 9. There are also indicators for PV and collector as well as conventional systems for comparison.

Fig. 12. 12. 14 and 15 show selected days during: spring, summer, autumn and winter. For each figure four representative days were chosen which are characteristic of their seasons. This makes it possible to observe changes in TEC values in relation to atmospheric conditions: radiation and temperature. It can also be observed how important the division of TEC between products is.

The Figs. 12–15 present the TEC of selected days during the year (12 selected days in spring, 13 – summer, 14 – autumn, 15 – winter). It can be seen that in the case of summer days with high solar radiation values, the TEC is low. The summer graph shows the period from June 19 to June 22. The lowest TEC values for electricity during these four days were 0.06 (0.08 - second division), and for heat 0.06 (0.04 - second division). The opposite situation is for winter days - from 20 to 23 December. Two points can be noted here. First, the highest volume of TEC for electricity peaked above 1 (1.67 for both divisions). The second issue is the lack of TEC of heat - for the mentioned days the heat TEC was not determined because no useful heat was generated by the PV/T system. Both issues result from very low insolation and thus small amounts of electricity produced and low collector temperatures, which excludes the possibility of heat generation by PV/T.

In the intermediate periods represented in the graphs by spring 1–4

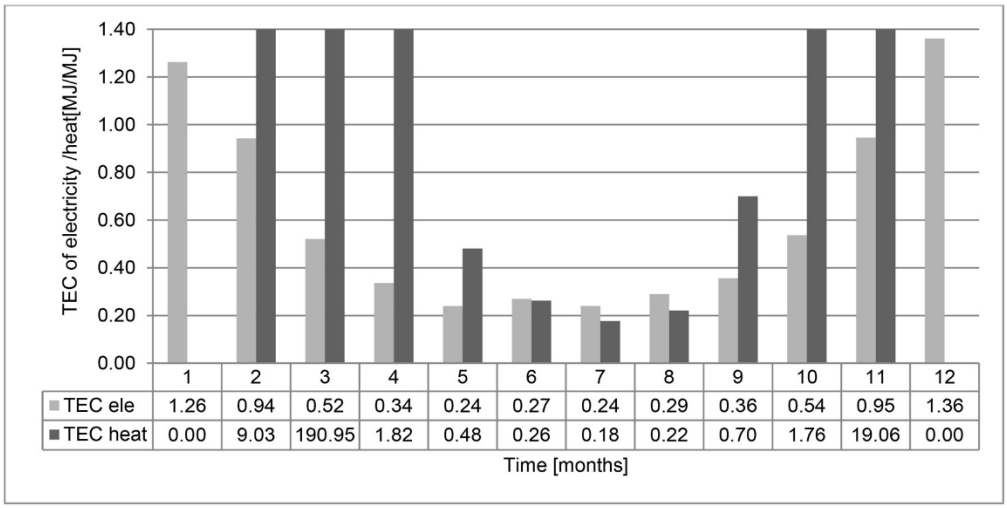


**Fig. 10.** Monthly TEC of electricity and heat produced by PV/T – the division 1.

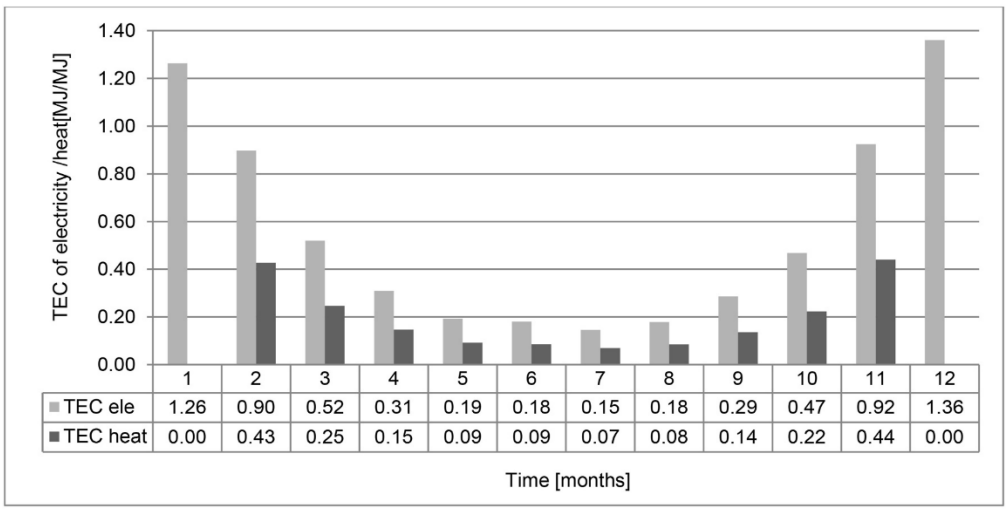


**Fig. 11.** Monthly TEC of electricity and heat produced by PV/T – the division 2.

**Table 9**
TEC analysis (based on: [29,40]).

| TEC [MJ/MJ] | PV | PV/T | | Coal power station | Coal Heating plant | Combined heat and power plant (coal-fired) |
|---|---|---|---|---|---|---|
| | | first division | second division | | | |
| thermo-ecological cost of the electricity | 0.26 | 0.153 | 0.193 | 4.39 | | 4.67 |
| thermo-ecological cost of the useful heat | – | 0.100 | 0.060 | – | 2.09 | 1.31 |

April and autumn 20–23 April, the TEC values are very diverse, but they do not exceed 0.5. There are both days with low TEC indexes (such as April 4 or September 21), but also days where heat production did not take place and TEC indicators for electricity are very high, e.g. on April 2 and September 23.

The article presents two ways of comparing solar electricity production systems - PV and PV/T. Both local and global comparisons pointed to PV/T as the more efficient system. However, it should be emphasized that only the determination of the thermo-ecological cost allows to show the actual impact of both installations on non-renewable resources and thus to determine the legitimacy of choosing a given installation as more profitable in the context of sustainable use of non-renewable resources.

## 4. Summary and conclusions

The efficiency comparison of collector and PV to PV/T system showed that the combined system (PV/T) is more efficient for electricity

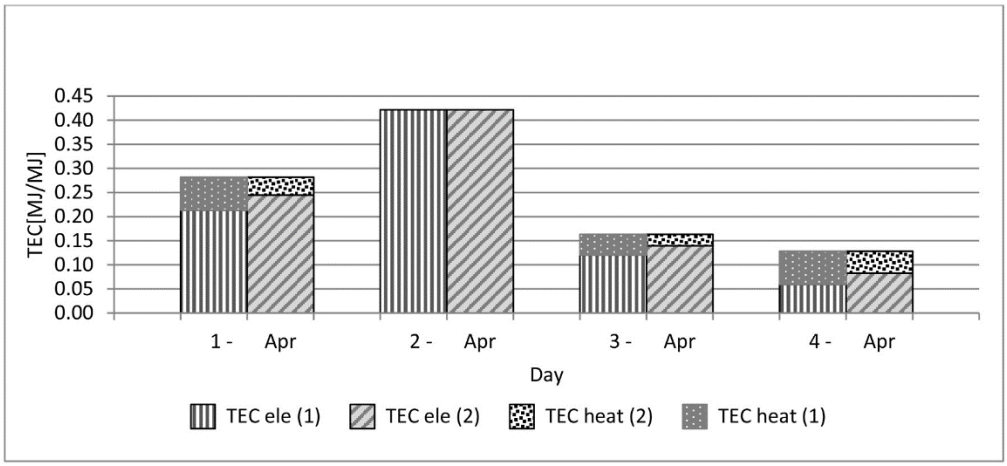


**Fig. 12.** Daily TEC for selected days in spring of electricity and heat produced by PV/T.

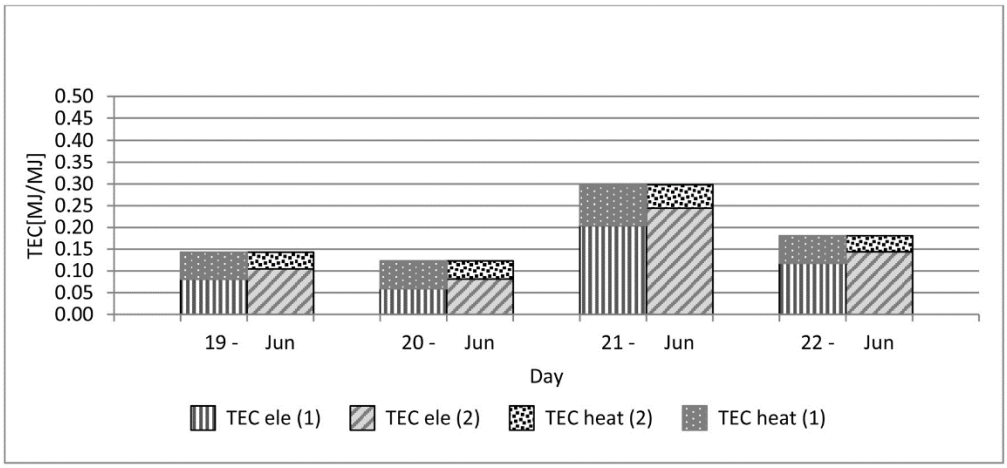


**Fig. 13.** Daily TEC for selected days in summer of electricity and heat produced by PV/T.

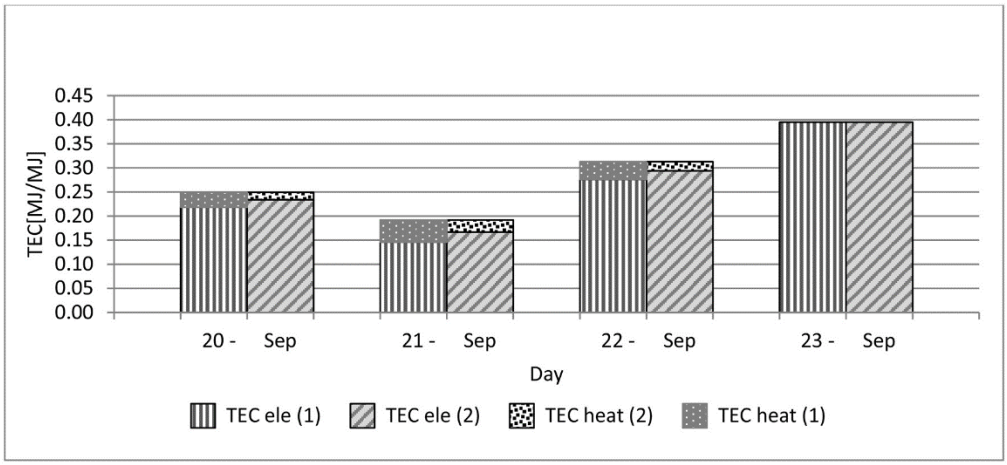


**Fig. 14.** Daily TEC for selected days in autumn of electricity and heat produced by PV/T.

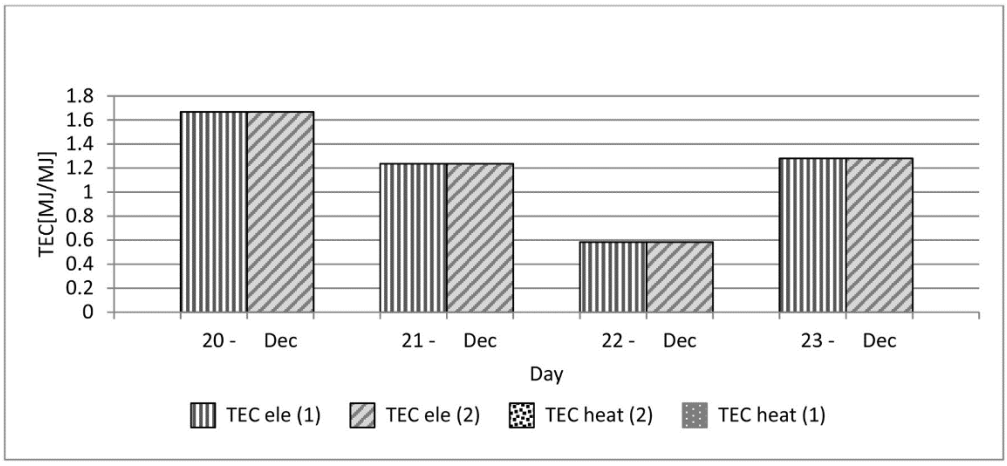


**Fig. 15.** Daily TEC for selected days in winter of electricity and heat produced by PV/T.

production than separate production. This is mainly due to the increase in efficiency it produces electricity by cooling PV/T modules. As shown by the calculations, annual average efficiency of electricity production for PV/T was 15.18%, while for PV only 10.24%. This difference results from the use of heat, which in the case of PV is lost to the environment and affects the system's operating parameters. In the case of PV/T, heat management takes place, accompanied by a significant increase in the efficiency of the system.

According to the presented calculations, the heat production from PV/T is about four times lower than the amount produced from the collector. This is caused, among other things, by the assumption of the temperature at which the cooling of the panels begins, and thus the production from the PV/T system. It should be emphasized that cooling the PV/T system is primarily used to increase efficiency and the heat obtained is only an indirect benefit. Therefore, the small amounts of heat produced by the PV/T system should not be taken as a disadvantage, and the additional benefit of combining the two systems and as a side effect of increasing the efficiency of electricity production by the combined system. This very simple comparison based on the amount of heat and electricity produced and the efficiency shows the significant advantages in favour of the PV/T system. A clear increase in parameters can be noticed in the area of electricity production with the accompanying additional product in the form of useful heat.

In the further part of the study calculations of the thermo-ecological cost for the PV/T system were carried out, taking into account the thermo-ecological cost of the materials used to build the collector and the thermo-ecological cost of additional equipment. The conducted thermo-ecological cost analysis showed the electricity and heat produced from the PV/T system have a TEC below 1. Thus, the exergy of resources used to produce the product is lower than the exergy value of this product. In the case of production from non-renewable resources (e.g. for coal power station, coal heating plant, combined heat and power plant coal-fired) the product TEC under unity. This shows another important point that the article tries to prove - TEC gives a clear comparison between renewable and non-renewable systems. It should be emphasized that it is not possible for any known system to achieve a TEC value of a different zero, i.e. neutral for the ecosystem, because each of the systems, including renewable energy systems, consumes raw materials, e.g. as it is presented in this article on the example of PV/T, raw materials for production. However, the TEC makes a clear distinction where the environmental impact is very significant (over zero for non-energy systems).

In the following of study, a challenge was encountered, which was the separation of TEC into two products, electricity and heat. Calculations have shown that in the case of combined processes, the division of the fuel between heat and electricity is very important in determining TEC. The article presents two division options. In the first one, the division was proposed using the exergetic cost. Using the specific cost of PV/T the solar energy of fuel burdening respectively production of heat and electricity in PV/T was determined which resulted in very high TEC values for months with low heat production. Therefore, with this method of energy cost allocation, further caution should be exercised, especially for aggregated time periods such as e.g. monthly values. For smaller time periods of such day specific TECs, no such drastic split results were observed.

Due to the observed disadvantages in the first presented method of division in the article, the division was carried out in a different way. The second device uses the proportion of TEC indicators for classic/replaced technologies. Despite reaching the monthly TEC values above the annual average, they did not deviate as drastically from the average as in the case of the first division. This argues for the validity of the use of the second method of division as a more reliable one.

By reason of the still existing share of non-renewable resources in the final product as well as the pollution, for any currently known power generation technology it is not possible to achieve a TEC of zero, but calculations have shown that the PV/T system significantly reduces the TEC value compared to a split system. The calculated thermo-ecological cost of the electricity in the case of PV/T is 0.153 (in the second division 0.193), therefore the value is lower than in the case of PV - 0.26. This additionally confirms the advantage of using a combined system - in the case of PV/T we use less material than in the production of systems separate from the benefits obtained, i.e. heat and electricity. Therefore, the TEC value drops and thus we obtain a more environmentally friendly system.

It should be emphasized that when comparing different energy systems (RES and conditional systems), the global analysis, i.e. the determination of the thermo-ecological cost, allowed for a proper assessment and comparison of the systems. Thanks to the TEC, it is possible to clearly define the impact of the process on the depletion of non-renewable resources (the TEC of electricity and heat for combined heat and power plant coal-fired is much greater than for the PV/T system). There is no such clarity in the local analysis, in which the comparison of energy efficiency indicators indicates a better operation of conventional systems. Also when comparing similar energy systems (such as PV and PV/T), it is preferable to choose a TEC that covers the impact of RES on non-convertible resources. In the case of efficiency, it is only the possibility to evaluate the process itself, not placing it in the context of a wider system such as the environment (Earth). Thus, the

determination of the thermo-ecological cost is a key method in the proper assessment of energy production systems and their influence on depletion of non-renewable resources.

## CRediT authorship contribution statement

**Agnieszka Szostok:** Methodology, Writing – original draft, creation, presentation of the published work. **Wojciech Stanek:** formulation or evolution of overarching research goals and aims, .

## Declaration of competing interest

The authors declare that they have no known competing financial interests or personal relationships that could have appeared to influence the work reported in this paper.

## Nomenclatures

| | |
|---|---|
| E | energy [kW] |
| $I_\beta$ | solar radiation [kW/m$^2$] |
| A | surface [m$^2$] |
| Q | heat [kW] |
| k | heat loss coefficients[-] |
| T | temperature [K] |
| t | temperarure[°C] |
| $\dot{W}$ | heat capacity of stream [kW/s] |
| $\dot{m}$ | mass stream [kg/s] |
| k | heat transfer coefficient in the exchanger[W/(m2·K)] |
| $K_{TE}$ | annual thermo-ecologicalcost [−] |
| G | amount of material used to construct the collector[kg] |
| ρ | specific thermo-ecological cost[MJ/kg] |
| u | coefficient of recovery of the material[-] |
| k* | exergetic cost[MJ/MJ] |
| B | exergy[MJ] |
| TEC | cost of thermo-ecological[MJ/MJ] |
| ΔT | difference of temperature [K] |

*Greek symbols*

| | |
|---|---|
| $\eta$ | efficiency |
| τ | time, hours |

*Indices*

| | |
|---|---|
| C | applies to the collector |
| PV | applies to the PV system |
| PV/T | applies to the PV/T system |
| 0 | applies to the environment |
| b | exergy |
| e | Energy |
| th | thermal |

## References

[1] bp p.l.c., „Statistical Review of World Energy, 2021 (Ful Raport)" https://www.bp.com/content/dam/bp/business-sites/en/global/corporate/pdfs/energy-economics/statistical-review/bp-stats-review-2021-full-report.pdf, pages 65, 2021.

[2] International Energy Agency, „Electricity Market Report - July 2021", pages 5-9, https://iea.blob.core.windows.net/assets/01e1e998-8611-45d7-acab-5564bc22575a/ElectricityMarketReportJuly2021.pdf, 2021.

[3] p.l.c. bp, „Statistical review of world energy. https://www.bp.com/content/dam/bp/business-sites/en/global/corporate/pdfs/energy-economics/statistical-review/bp-stats-review-2021-full-report.pdf, 2021, 6-12.

[4] Tomas Gomez-Navarro, Tommaso Brazzini, David Alfonso-Solar, Carlos Vargas-Salgado, Analysis of the potential for PV rooftop prosumer production: technical, economic and environmental assessment for the city of Valencia (Spain), Renew. Energy (2021) 372–381, https://doi.org/10.1016/j.renene.2021.04.049".

[5] Mauricio Carmona, , Alberto Palacio Bastos, Jose Doria García, „Experimental Evaluation of a Hybrid Photovoltaic and Thermal Solar Energy Collector with Integrated Phase Change Material (PVT-PCM) in Comparison with a Traditional Photovoltaic (PV) Module, „Renewable Energy, 2021, pp. 680–696, https://doi.org/10.1016/j.renene.2021.03.022".

[6] The European Youth Portal, What is climate change?, website, https://europa.eu/youth/get-involved/sustainable%20development/what-climate-change_pl. (Accessed 8 August 2021).

[7] Intergovernmental Panel on Climate Change, Climate change 2021. The physical science basis, pages TS-46 SPM-52021, https://www.ipcc.ch/report/ar6/wg1/downloads/report/IPCC_AR6_WGI_Full_Report.pdf.

[8] Canberk Ünal, Emin Açıkkalp, Mustafa Tolga Balta, Arif Hepbasli, „Dynamic thermo-ecological cost assessment and performance analyses of a multi generation system. https://doi.org/10.1016/j.ijhydene.2021.03.208, 2011. Volume 46, Issue 40, pages 21198-21211.

[9] Sarah Newman, Kaymie Shiozawa, b Jim Follum, Emily Barrett, Douville Travis, Trevor Hardy, Solana Amy, „A Comparison of PV Resource Modeling for Sizing Microgrid Components, Renewable Energy, 2020, pp. 831–843, https://doi.org/10.1016/j.renene.2020.08.074.

[10] Piero Bevilacqua, Stefania Perrella, Roberto Bruno, Natale Arcuri, An accurate thermal model for the PV electric generation prediction: long-term validation in different climatic conditions, Renew. Energy (2020) 1092–1112, https://doi.org/10.1016/j.renene.2020.07.115.

[11] Mohd Yusof Othman, Adnan Ibrahim, Goh Li Jin, Mohd Hafidz Ruslan, Kamaruzzaman Sopian, Photovoltaic-thermal (PV/T) technology e the future energy technology, Renew. Energy (2012) 171–174, https://doi.org/10.1016/j.renene.2012.01.038.

[12] Tan 1, ID J.C. Teo, H.G. Rodney, V.H. Mok, Vigna K. Ramachandaramurthy, ChiaKwang, Impact of partial shading on the P-V characteristics and the maximum power of a photovoltaic string, Energies (2018) 2–5, https://doi.org/10.3390/en11071860.

[13] Mohsen Taherbaneh, H. Rezaie H. Ghafoorifard, K. Rahimi, M.B. Menhaj, Raghu N. Bhattacharya, Maximizing output power of a solar panel via combination of sun

tracking and maximum power point tracking by fuzzy controllers, Int. J. Photoenergy (2011) 1–2, https://doi.org/10.1155/2010/312580.
[14] Adnan Ahmed Siddique, Akram Mohiuddin, Syed Mohammed Nahri, Effects of surface temperature variations on output power of three commercial photovoltaic modules, Int. J. Eng. Res. Technol. 5 (11) (November-2016) 12–16, https://doi.org/10.17577/IJERTV5IS110009.
[15] Thomas S. Wurster, Markus B. Schubert, Mismatch loss in photovoltaic systems, Sol. Energy 105 (July 2014) 505–511, https://doi.org/10.1016/j.solener.2014.04.014.
[16] A.D. Dhass, N. Beemkumar, S. Harikrishnan, Hafiz Muhammad Ali, Alberto Álvarez Gallegos, A review on factors influencing the mismatch losses in solar photovoltaic system, |Article ID 2986004, Int. J. Photoenergy (2022) 20–21, https://doi.org/10.1155/2022/2986004.
[17] Feng Zhang, Cheng Han, Mingying Wu, Xinting Hou, Xinhe Wang, Bingqiang Li, Global sensitivity analysis of photovoltaic cell parameters based on credibility variance, November, Energy Rep. 8 (2022) 7582–7588, https://doi.org/10.1016/j.egyr.2022.05.280.
[18] Mohammad Reza Kalateh, Kianifar Ali, Mohammad Sardarabadi, Energy, exergy, and entropy generation analyses of a water-based photovoltaic thermal system equipped with clockwise counter-clockwise twisted tapes: an indoor experimental study, Applied Thermal Engineering Available 215 (2022) 1, https://doi.org/10.1016/j.applthermaleng.2022.118906.
[19] Jarosław Bigorajski, Dorota Chwieduk, „Analysis of a micro photovoltaic/thermal e PV/T system operation in Analysis of a micro photovoltaic/thermal e PV/T system operation in", pages 1-12 January 2018E3S Web of Conferences vol. 70:01002, doi: 10.1051/e3sconf/20187001002.
[20] German Osma-Pinto, Gabriel Ordonez-Plata, Dynamic thermal modelling for the prediction of the operating temperature of a PV panel with an integrated cooling system, Renew. Energy 152 (2020) 1041–1054, https://doi.org/10.1016/j.renene.2020.01.132.
[21] Gagliano, Antonio Tina, M. Giuseppe, Nocera, Francesco, Grasso, Alfio Dario, Stefano Aneli, Description and performance analysis of a flexible photovoltaic/thermal (PV/T) solar system, Renewable Energy, Elsevier 137 (C) (2019) 144–156, https://doi.org/10.1016/j.renene.2018.04.057, 2019.
[22] Bartosz Chwieduk, Dorota Chwieduk, „Analysis of operation and energy performance of a heat pump driven by a PV system for space heating of a single family house in polish conditions. https://doi.org/10.1016/j.renene.2020.11.026, 2021. Volume 165, Part 2, pages 117-126.
[23] Khodadad Mostakim, M. Hasanuzzaman, Global prospects, challenges and progress of photovoltaic thermal system, page 1, Sustain. Energy Technol. Assessments 53 (2022), 102426, https://doi.org/10.1016/j.seta.2022.102426. Part A.
[24] W. Stanek, Method of Evaluation of Ecological Effects in Thermal Processes with the Application of Exergy Analysis, Silesian University of Technology Press, 2009, pp. 53–139, in Polish.
[25] Polskie Towarzystwo Elektrociepłowni Zawodowych, http://ptez.pl/files/news_attachment/129/raport_o_kogeneracji_w_cieplownictwie_ptez_pazdziernik_2019.pdf, „Report on cogeneration in heating", page 5, 2019 (in polish).
[26] J. Szargut, Exergy Analysis: Technical and Ecological Applications, Wit press, 2005, pp. 91–119, 1-72.
[27] Wojciech Stanek, Wiesław Gazda, Wojciech Kostowski, Thermo-ecological assessment of CCHP (combined cold-heat-and-power) plant supported with renewable energy, Energy 92 (3) (2015) 279–289, https://doi.org/10.1016/j.energy.2015.02.005.
[28] E. Akyuza, C. Coskuna, Z. Oktaya, I. Dincer, Hydrogen production probability distributionsfor a PV-electrolyser system, Int. J. Hydrogen Energy 36 (17) (2011) 11292–11299.
[29] W. Stanek, Assessment of energy efficiency and ecological transformation of TETIP to electroprosumerism in the environment of the exergy paradigm - thermoecological cost: electroprosumerism vs WEK-PK energy (in polish), https://ppte2050.pl/platforman/bzppte/static/uploads/Ocena%20efektywno%C5%9Bci%20energetycznej%20i%20ekologicznej%20transformacji%20TETIP%20do%20elektroprosumeryzmu.pdf, 2021, 9-11.
[30] Akademia Viessmann Polska, "Architect, Designer and Installer Manual - Solar Collectors, Wrosław: Viessmann Werke, Allendorf (Eder), 2013, pp. 20–26, in polish.
[31] T.N. Anderson, M. Duke, G.L. Morrison, J.K. Carson, „Performance of a Building Integrated Photovoltaic/thermal (BIPVT) Solar Collector, International Solar Energy Society, 2009, pp. 45–55, https://doi.org/10.1115/ES2014-6455.
[32] Mahdi Shakouri, Hossein Ebadi, Shiva Gorjian, „Chapter 4 - Solar Photovoltaic Thermal (PVT) Module Technologies", Photovoltaic Solar Energy Conversion Technologies, Applications and Environmental Impacts, 2020, pp. 79–116, https://doi.org/10.1016/B978-0-12-819610-6.00004-1.
[33] T. Aysar, Jarullah, Heat exchanger effectiveness (NTU method), website, https://ceng.tu.edu.iq/ched/images/lectures/chem-lec/st3/c2/Lec23.pdf. (Accessed 4 July 2022).
[34] Pinar Mert Cuce, „Novel, practical and reliable analytical models to estimate electrical efficiency of buildingintegrated photovoltaic/thermal (BIPVT) collectors and systems, Uludağ University Journal of The Faculty of Engineering 23 (No. 3) (2018) 191–206, https://doi.org/10.17482/uumfd.404598.
[35] Wojciech Stanek, „Exergy Analysis in Theory and Practice" Wydawnictwo Politechniki Śląskiej, 2016, pp. 11–266, in polish.
[36] Wojciech Stanek, Lucyna Czarnowska, „Thermo-ecological cost – szargut's proposal on exergy and ecology connection, Energy Volume 165 (15 December 2018) 1050–1059, https://doi.org/10.1016/j.energy.2018.10.040. Part B.
[37] J. Szargut, A. Ziębik, W. Stanek, „Depletion of the non-renewable natural exergy resources as a measure of the ecological cost, Energy Convers. Manag. 43 (9–12) (2002) 1149–1163, https://doi.org/10.1016/S0196-8904(02)00005-5.
[38] L. Czarnowska, „Thermo-ecological Cost of Products with Emphasis on External Environmental Costs (Koszt Termo-Ekologiczny Wybranych Produktów Z Uwzględnieniem Zewnętrznych Kosztów środowiskowych.)", Gliwice, 2014.
[39] M. Faist Emmenegger, T. Heck, N. Jungbluth, Erdgas, Sachbilanzen von Energiesystemen: grundlagen für den okologischen Vergleich von Energiesystemen und den Einbezug von Energiesystemen in Okobilanzen für die Schweiz, in: R. Dones (Ed.), Swiss Centre for Life Cycle Inventories CH. Final Report Ecoinvent No. 6-V Swiss Centre for Life Cycle Inventories, 2007. Dübendorf.
[40] J. Szargut, W. Stanek, „Thermo-ecological optimization of a solar collector, Energy 32 (4) (2005) 584–590, https://doi.org/10.1016/j.energy.2006.06.010.
[41] W. Stanek, L. Czarnowska, Environmental externalities and their effect on the cost of consumer products, J. Environ. Sustain. Dev. 11 (1) (2012) 50–63, doi: 10.1504/IJESD.2012.049142.
[42] M. Cellura, V. Grippaldi, Valerio Lo Brano, S. Longo, M. Mistretta, „Life Cycle Assessment of a Solar PV/T Concentrator System" Conference: Life Cycle Management Conference LCM, 2011.
[43] Tin-Tai Chow, Jie Ji, „Environmental life-cycle analysis of hybrid solar photovoltaic/thermal systems for use in Hong Kong, Int. J. Photoenergy 2012 (2012) 1–9, https://doi.org/10.1155/2012/101968. Article ID 101968.
[44] W. Gazda, W. Stanek, „Influence of power source type on energy effectiveness and environmental impact of cooling system with adsorption refrigerator, Energy Convers. Manag. 87 (2014) 1107–1115, https://doi.org/10.1016/j.enconman.2014.05.015.

# Paper II: Thermo-Ecological Cost of various RES energy mix options

Renewable Energy 216 (2023) 119035

Contents lists available at ScienceDirect

Renewable Energy

journal homepage: www.elsevier.com/locate/renene

## Thermo-ecological analysis of the power system based on renewable energy sources integrated with energy storage system

Agnieszka Szostok [a,*], Wojciech Stanek [b]

[a] Environmental Analysis Eko-precyzja, Zaklad Analiz Środowiskowych Eko-Precyzja, Poland
[b] Silesian University of Technology, Department of Thermal Technlogy, Poland

ARTICLE INFO

*Keywords:*
Thermo-ecological cost
Renewable energy
Microgrid
Energy storage

ABSTRACT

Energy systems based on Variable Renewable Energy (VRE) such as solar energy (PV, PV/T) and wind energy (wind turbine) are intermittent by weather and climate conditions. This poses challenges for managing to obtain a stable energy supply. Microgrids based on VRE must accommodate the variability using, for example, energy storage. The second options for adjustment are backup generators or sources with firm capacity cooperating with VRE. The article presents an analysis of individual RES sources PV, PV/T system, wind turbine and biogas plant indicating the advantages of individual components and the possibility of their cooperation in a microgrid. The analysis for the assumed climatic conditions (location: Katowice, Poland) showed the benefits of the combination in the energy mix sources based on solar radiation and wind energy. The analysis also covers the use of the energy stored (based on electrolyser, hydrogen store and fuel cell) and presents the possibilities of using energy storage technology in various options of the energy mix. The most advantageous was a mixed system based on renewable energy sources using solar irradiation and wind energy with the stabilizing participation of a biogas plant - in this case, the capacity of the energy storage was fully used. In the further part of the article an exergo-ecological analysis using the TEC concept (thermo-ecological cost) is presented. TEC indicators for different versions of the energy mix were presented, analysing the systems in terms of natural resource management. The thermo-ecological analysis showed that the best energy mixes in terms of assessing the efficiency of natural resource management are systems that use the advantages of each component, supporting by energy storage.

### 1. Introduction

Conventional power generation (where non-renewable sources are used as coal, gas, oil or coal) is a source of greenhouse gas emissions, which are released into the atmosphere during combustion processes [1–4]. At present converting to energy systems based on renewable energy sources (RES) is the only feasible answer for increasingly depleting fossil fuel resources and the climate crisis [5–7]. However, despite that renewable energy resources have a number of advantages, they are associated with many challenges and provide to redefine the traditional power system operation and planning practices. The main challenges are connected with their sources [8]. Renewable energy sources are driven by natural sources such as sunlight, wind, geothermal heat and the movement of water (depend on weather and climate) and therefore are characterized by a notable temporal and spatial variability [9–13]. Solutions that enable energy generation with reduced greenhouse gas emissions and other environmental impacts, such as renewable energy sources and microgrids, are crucial for sustainable development [14].

In energy systems based on Variable Renewable Energy (VRE) such as solar energy (PV, PV/T) and wind energy (wind turbine), an important factor that must be taken into account is the main sources of renewable generation are intermittent by nature. For this reason taking advantage of the complementarity of the system is fundamental in order to meet the demand and minimize electricity supply risks [15]. Planning of power systems dominated especially by low flexible generation should consider spatial, temporal, and technical details in order to perform harmonized dispatch of generating units. In the absence of predictable generation units (such as conventional power units), the models may overestimate renewable energy sources uptake and underestimate the amount of flexible resources required [16]. The combination of different renewable energy sources operating within a microgrid can be equipped with a smart meter and have the ability to share and trade energy, is called a smart microgrid or smart grid [17].

* Corresponding author.
*E-mail addresses:* agnieszka.szostok@eko-precyzja.eu (A. Szostok), wojciech.stanek@polsl.pl (W. Stanek).

https://doi.org/10.1016/j.renene.2023.119035
Received 13 March 2023; Received in revised form 24 May 2023; Accepted 12 July 2023
Available online 20 July 2023

VRE must accommodate the variability with, for example, energy storage. The second options for adjustment are backup generators or sources with firm capacity, such as nuclear and natural gas, hydroelectricity, bioenergy and geothermal [18]. The first mentioned solution for VRE integration is Energy storage (ES). There are a number of different ways of storing energy. Group of the mechanical storage which include pumped hydro and compressed air storage. Electrochemical storage systems of which advanced lead acid, sodium sulphur, lithium-ion and nickel–sodium-chloride batteries are examples. Hydrogen production from electrolysis and subsequent usage in a fuel cell is also an example of storage energy. In recent years, many new ones have appeared, such as water splitting. New perspectives for renewable energy-based hydrogen production creates catalytically converting bio-ethanol in the presence of steam (CSRE) [19]. Hydrogen-enriched natural gas is also an important issue [20,21]. Ways of storing energy are much more, but this paper focused on the electrolysis/fuel cell system [22,23].

In the analysed system - micro grid, various types of renewable sources were used, such as PV, PV/T, wind turbine, biogas plant and energy storage system. In the article various system arrangements were presented (each presented option contains a different RES arrangement), which are compared with the demand profile (comparing the amount of energy needed and the amount of energy demand expressed in MW). In addition, the thermo-ecological cost TEC is presented for each option. In the case of renewable sources TEC is mainly caused by material inputs to construction, in contrast to conventional systems where emission of harmful substances results in high TEC values [5,6].

## 2. Methodology

### 2.1. Description and characteristic of the analysed PV

The amount of solar radiation converted into electricity by a PV panel can be determined from equation (1)

$$E_{PV} = \eta_{e_{PV}} I_\beta A_{PV} \tag{1}$$

The efficiency of converting solar radiation into energy depends on the amount of radiation falling on the panel and the temperature. Accordingly, the calculations of the values of energy efficiency were made for efficiency ranges commonly found in the literature [24–26]. An exemplary efficiency range is shown in Fig. 1.

### 2.2. Description and characteristic of the analysed collector system

Quantity of transformed a solar radiation into heat by thermal collector can be calculated from equation (2)

$$Q_c = \eta_{th_C} I_\beta A_C \tag{2}$$

Thermal efficiency of collector $\eta_{th_C}$ is calculated from equation (3) [28]:

$$\eta_{th_C} = \eta_{th_{C_0}} - \frac{k_1 \Delta T}{I_\beta} - \frac{k_2 - \Delta T^2}{I_\beta} \tag{3}$$

Where:

The temperature difference $\Delta T$ is calculated from relation (4):

$$\Delta T = T_O - T_C \tag{4}$$

The calculations of the values of energy efficiency were made for efficiency ranges commonly found in the literature [28]. An exemplary efficiency range is shown in Fig. 2.

Efficiency $\eta_{th_{C_0}}$ is designated with the received values of are heat loss coefficients are presented in Table 1.

### 2.3. Description and characteristic of the analysed PV/T system

First for the PV/T system the amount of generated heat from solar radiation is calculated. The heat from PV/T installation is transferred through the exchanger to the water tank. The cooling process begins when the cell temperature exceeds the assumed temperature of 30 °C. Estimate module temperature is calculated using eq. (5):

$$t_{PV} = t_O + \frac{(t_{NOCT} - 20) I_\beta}{800} \tag{5}$$

where $t_{PV}$ is module temperature, $I_\beta$ is solar radiation on the module, $t_O$ is the temperature of the environment and $t_{NOCT}$ is Normal Operating Cell Temperature (44–48 °C) [29–31].

For the purposes of the calculations, the following assumptions where made.

- the cooling process begins when the cell temperature exceeds the assumed temperature of 30 °C,
- cooling water temperature from the domestic hot water tank is constant ($T_{w_{in}} = 10$ °C),
- the refrigerant in the PV/T circuit is ergolide ($c_e = 3.17$ kJ/(kg·K)),
- mass stream of water and ergolide is 0.02 kg/s,
- heat losses in pipelines are ignored.

Fig. 3 presents the simplified diagram of PV/T installations.

The purpose of determining PV/T thermal efficiency is used with features that where created based on [29].

$$\eta_{th} = \eta_0 - \frac{\alpha (T_{eg\ out} - T_O)}{I_\beta} \tag{6}$$

where $\eta_{th}$ is PV/T thermal efficiency; $\eta_0$ is 0.6099. $\alpha$ is heat transfer coefficient ($\alpha = 5.8343\ W/(m^2K)$), $T_{eg\ out}$ is temperature of the working

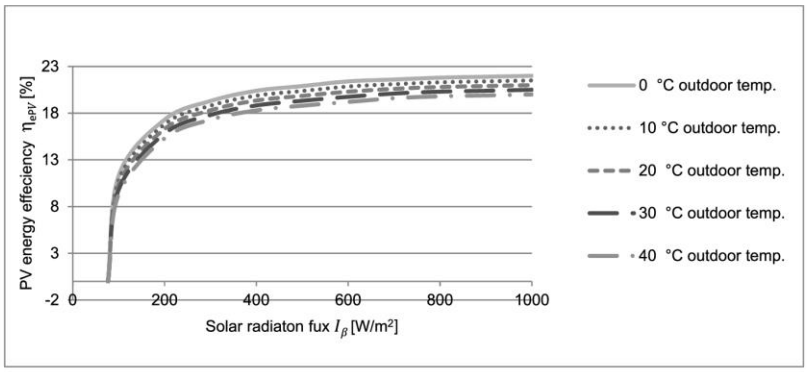


**Fig. 1.** The relation of global radiation, outdoor temperature and energy efficiency of PV panel (based on [17,27]).

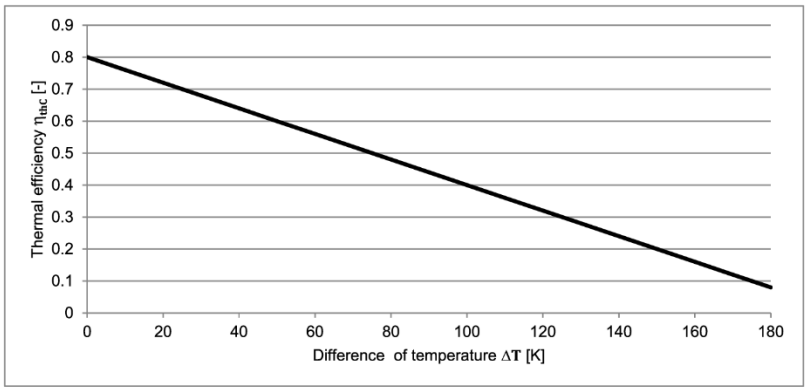


**Fig. 2.** Optical efficiency graph (based on [28]).

**Table 1**
Values of are heat loss coefficients of collector (based on [28]).

| | Heat loss coefficients $k_1$ | Heat loss coefficients $k_2$ |
|---|---|---|
| | W/(m$^2$K) | W/(m$^2$K$^2$) |
| flat-plate collector | 4 | 0.1 |

medium flowing out the PV/T panel (outlet temperature ergolide). Thermal efficiency of PV/T is presented in Fig. 4.

In equation (6). except for the temperature of ergolide, other values are known. The temperature of ergolide at the moment of starting the cooling process is assumed as the ambient temperature, then it is calculated from the heat exchanger analysis using the ε-NTU method (eq. (7)).

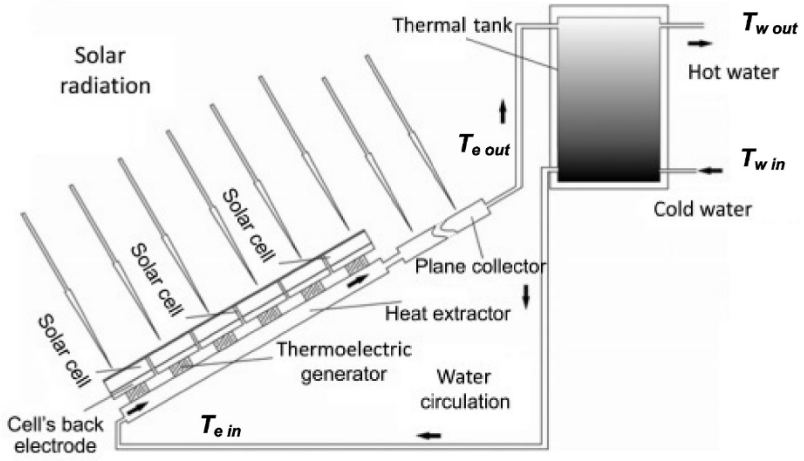


**Fig. 3.** Simplified diagram of PV/T installations (based on [32]).

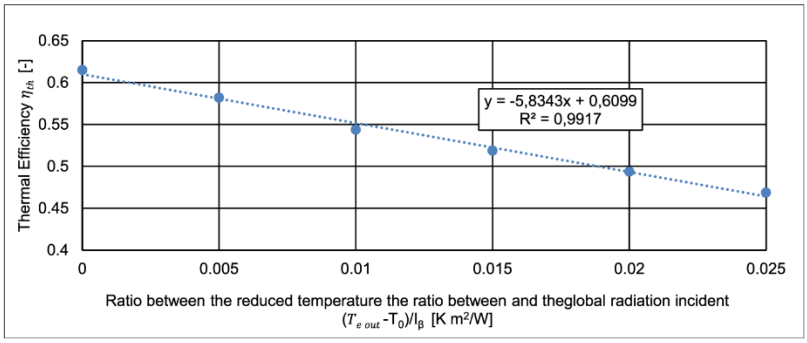


**Fig. 4.** Thermal efficiency of PV/T (based on [17]).

$$\dot{Q}_{PVT} = \eta_{th_{PVT}} I_\beta A_{PVT} \quad (7)$$

where $\eta_{th_{PVT}}$ is thermal efficiency of PV/T, $I_\beta$ is solar radiation and $A_{PVT}$ is PV/T panel surface.

The ε-NTU method is used to determine ergolide and feed water temperatures. The ε-NTU method is one method in which a heat exchanger is analysed. For this purpose, thermal equations in dimensionless form are used. The method enables thermal calculations for the exchanger when the inlet temperatures of the factors and the exchanger parameters are known. The dimensionless parameters R, S, p, φ where determined as presented in Table 2.

The indicators presented in Table 2 contain the heat capacity of streams, which were calculated using equations (8) and (9)

$$\dot{W}_w = \dot{m}_w c_w \quad (8)$$

$$\dot{W}_{eg} = \dot{m}_{eg} c_{eg} \quad (9)$$

Temperatures working medium flowing out the PV/T of calculated using equation (11) (12) and (13)

$$t_{e_{gout}} = \frac{\dot{Q}_{PVT}}{\dot{m}_{eg} * c_{eg}} + t_{eg_{in}} \quad (10)$$

$$t_{eg_{in}} = t_{eg-out} - \varphi(t_{w_{in}} - t_{w_{out}}) \quad (11)$$

$$t_{w_{in}} = const. \quad (12)$$

$$t_{eg_{in}} = p\left(t_{eg\ out} - t_{w_{in}}\right) + t_{w_{in}} \quad (13)$$

where $T_{eg\ out}$ [K] is temperature of the working medium flowing out the PV/T panel (outlet temperature ergolide).

$T_{eg\ in}$ [K] is temperature of the working medium flowing in the PV/T panel (intake temperature ergolide)
$T_{w\ out}$ [K] is temperature of water flowing out the heat exchanger (outlet temperature water)
$T_{w\ in}$ [K]is temperature of water flowing in the heat exchanger (intake temperature water)

Useful heat to support hot water calculated using equation (14)

$$\dot{Q} = \dot{m}_w c_w (t_{w_{out}} - t_{w_{in}}) \quad (14)$$

For the PV/T system, the amount of generated energy from solar radiation is calculated from equation (15):

$$E_{PVT} = \eta_{e_{PVT}} I_\beta A_{PVT} \quad (15)$$

Energy efficiency of PV/T is determined based on Fig. 5 [29,33].

PV/T energy efficiency therefore is calculated from equation (16):

$$\eta_{e_{PVT}} = 0.1464 \frac{T_{eg_{out}} - T_O}{I_\beta} - 0.6828 \quad (16)$$

where $T_O$ is the temperature of the environment and $T_{eg_{out}}$ is temperature of the working medium flowing out the PV/T panel (outlet temperature ergolide).

**Table 2**
Methodology of dimensionless parameters ε-NTU.

| | | |
|---|---|---|
| R | $R = \frac{W_w}{W_{eg}}$ | 1.32 |
| S | $S = k \frac{A_w}{W_{eg}}$ | 1.44 |
| p | $p = \left(\frac{1 - e^{[-s(1-1R)]}}{R - e^{[-s(1-1R)]}}\right)$ | 0.478 |
| φ | $\varphi = pR$ | 0.633 |

### 2.4. Description and characteristic of the analysed wind turbine

Fig. 6 shows the characteristics of a wind turbine, where the dependence of wind speed $v$ on power of wind turbine $P_w$ is presented. The graph is based on the turbine V90–3.0 MW power characteristics [34].

Power of wind turbine is calculated from equation (17):

$$P_w = 0,06136v^5 - 2,81942v^4 4 + 45,26322v^3 - 287,49133v^2 + 789,72637v - 794,68233 \quad (17)$$

where:

$P_w$ –energy of wind turbine [kW]
v – wind speed [m/s]

The following assumptions were used in the calculations:

- Wind turbine cut on: wind speed 5 m/s,
- Wind turbine cut off: wind speed 15 m/s.

### 2.5. Description and characteristic of energy storage - electrolyser and fuel cell

Fig. 7 shows the characteristics of a electrolyser: the relation between the reduced power and the efficiency of the electrolyser.

Mass stream of hydrogen produced in the process of electrolysis is calculated from equation (18):

$$\dot{m}_{h_2} = \frac{\eta_e P_{AC}}{Q_{wH_2}} \quad (18)$$

where:

$\dot{m}_{h_2}$- mass stream of hydrogen produced in the process of electrolysis [kg/h]
$\eta_e$ – electrolyser efficiency [−],
$P_{AC}$- power delivered to the hydrogen generator [kW]
$Q_{wH_2}$ – hydrogen calorific value [kWh/kg].

Fig. 8 shows the characteristics of fuel cell (the relation between the reduced power and the efficiency of the fuel cell).

Power of fuel cell used to meet needs is calculated from equation (19):

$$P_{el} = \eta_{FC} \dot{m}_{h_2} Q_{wH_2} \quad (19)$$

$\eta_{FC}$ – fuel cell efficiency [−].

The excess energy generated in the RES is directed to the electorizer, where hydrogen is produced. Hydrogen is stored and, in case of shortage, is converted into energy in a fuel cell.

### 2.6. Description and characteristic of electricity demand

Hourly data was used in the analysis [36]. An example of the distribution of daily electricity consumption case is presented in Fig. 9.

The maximum instantaneous demand of the system during the analysed year is 15 MW. For the study it was assumed that the total power of the sources generating energy in the system in each option is 15 MW.

## 3. Energy mix options

In paper are presented different energy mix options including different RES systems, which are shown in Fig. 10.

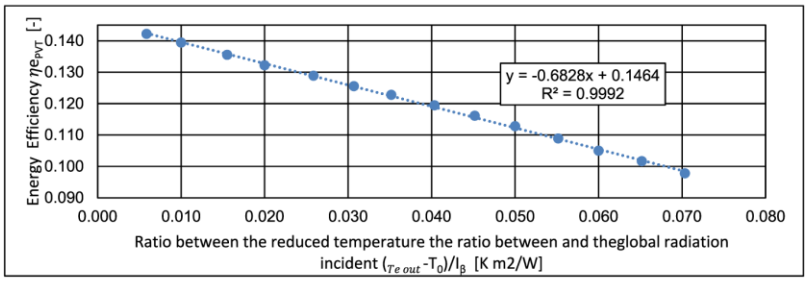


**Fig. 5.** Energy efficiency of PV/T (based on [29,33]).

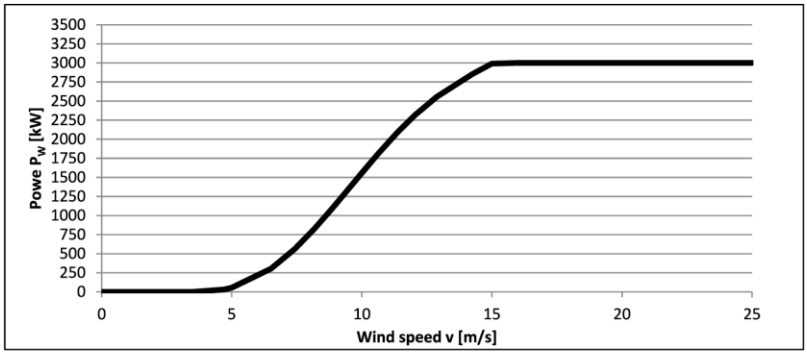


**Fig. 6.** Electric power curve as a function of speed (based on [34]).

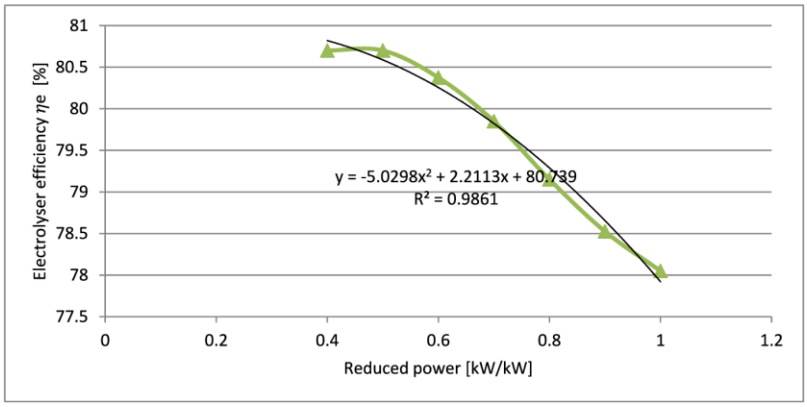


**Fig. 7.** Electrolyser efficiency (based on: [35]).

The system is based on renewable energy sources, the characteristics of which were presented in the previous section of the article. The analysis was conducted hour by hour for the whole year. When energy generation takes place in renewable energy sources, energy is directly consumed. When the generated energy is more than the value of the demand, the energy is directed to the electrolyser where it is converted into hydrogen. Hydrogen is stored in a hydrogen storage and in the event of energy shortages, directed to a fuel cell.

In the case that generation from RES does not take place or it is not enough in relation to the needs (for example due to weather conditions), energy is supplied from the energy storage, and in the event of a lack or too little of the amount of the stored energy, it is supplied from the grid.

The analysis of each renewable energy source and energy storage system was carried out for hourly data. Simulations were performed for climatic data for a selected location in Poland (Katowice) [37]. In the further part of the article, the simulation results will be presented for monthly energy sums, but below are examples of days with generation and demand presented hour by hour.

Fig. 11 shows a winter day with low generation from renewable sources, small amounts of stored hydrogen and high demand. Most of the energy must be supplied from the grid in this case. The opposite case is presented below.

Fig. 12 shows a summer day with a large generation from RE sources. There is no need to supply energy from the grid. In the case of insufficient quantities supplied from the RES (e.g. in the morning or afternoon) the energy is supplied partially from the energy storage.

The results presented above were based on the case where all four renewable sources interact in the energy mix (4,0 MW wind turbine, 4,0

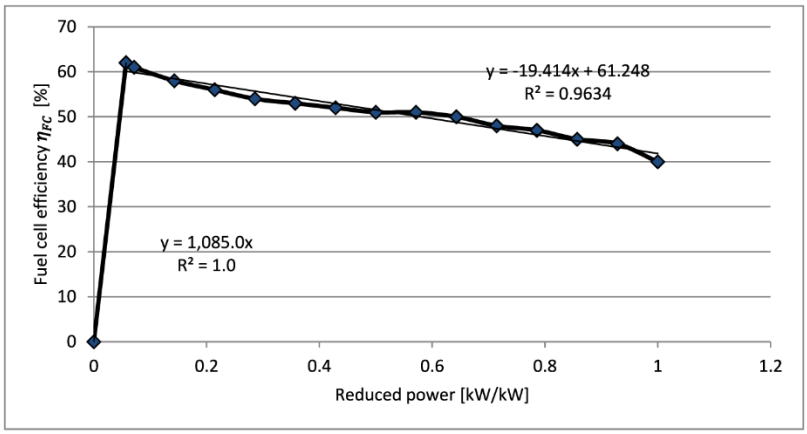


**Fig. 8.** Fuel cell efficiency (based on: [35]).

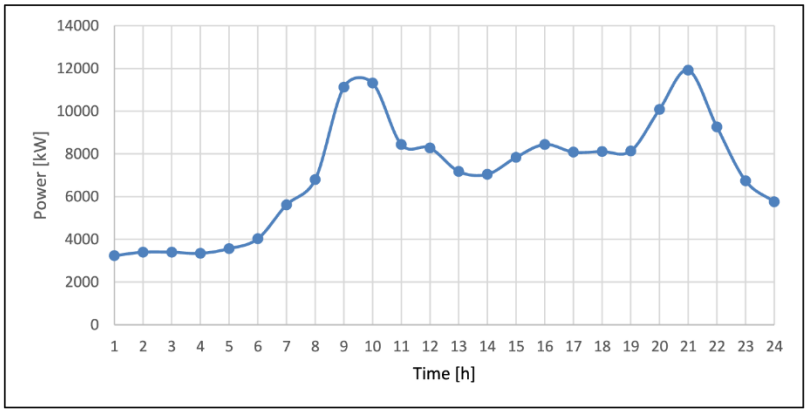


**Fig. 9.** An example of the distribution of daily electricity consumption [36].

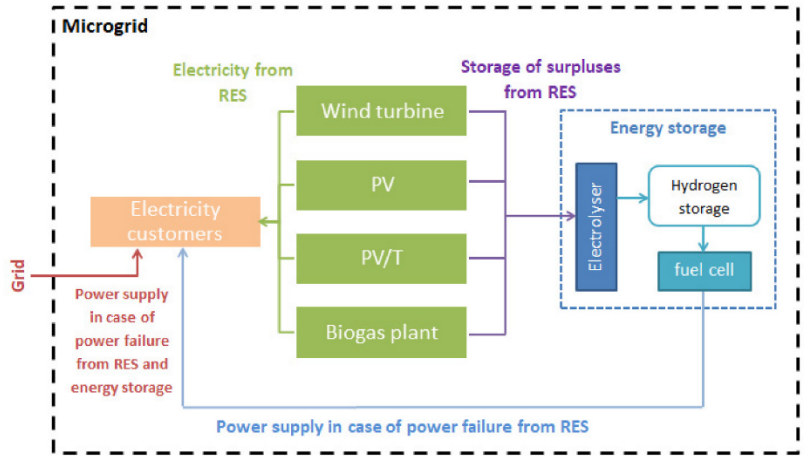


**Fig. 10.** Power system (micro grid) consisting of various renewable sources, storage energy and emergency power supply from the grid.

MW PV/T, 4,0 MW PV, 3,0 MW biogas). In the following part of the article, various configurations of renewable energy sources will be analysed.

### 3.1. *Energy mix options – one RES*

In the first step of analysis the energy mix consists of one source PV,

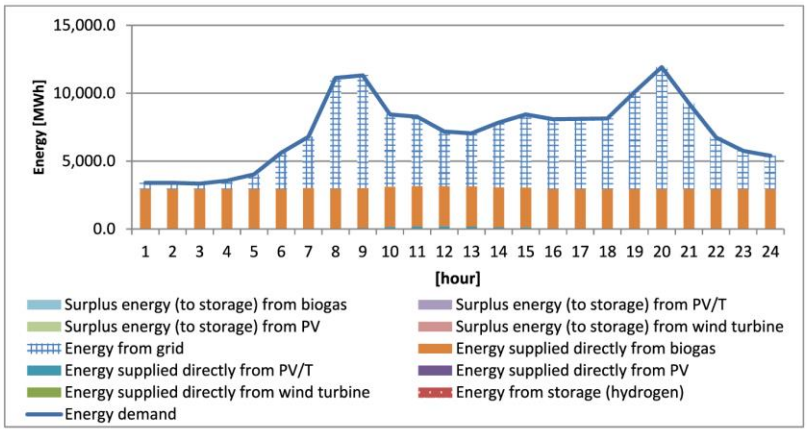


**Fig. 11.** Hour-by-hour consumption and generation for an example day with low renewable generation. (January 3).

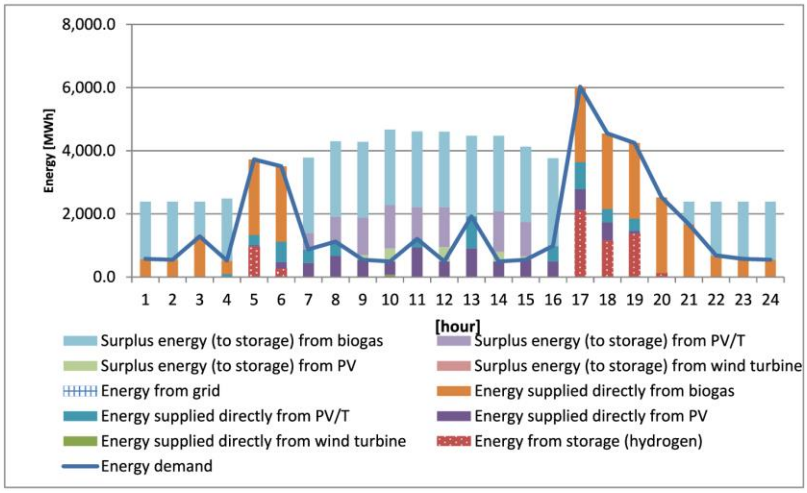


**Fig. 12.** Hour-by-hour consumption and generation for an example day with high renewable generation.

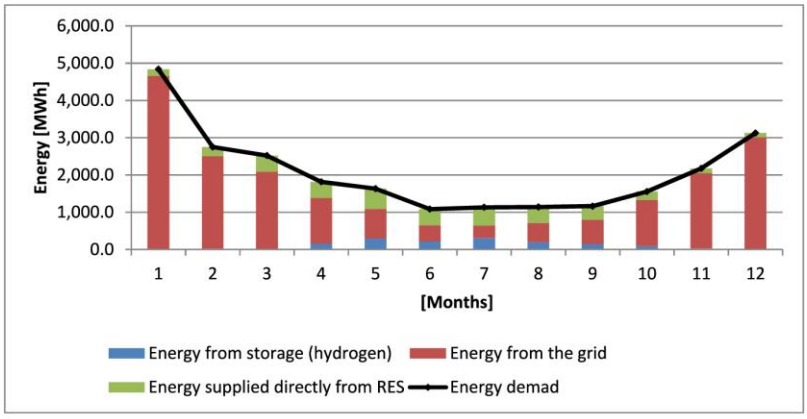


**Fig. 13.** Energy mix option - energy production based only on PV.

PV/T, wind turbine or biogas system. In this case, a single source has a power of 15 MW. Annual charts (with monthly totals) for each RES are presented in the figures below.

Fig. 13 shows the operation of the system in the case of PV operation only. As can be seen, surplus electricity has been accumulated in the energy storage since April and it is possible to cover partial energy shortages in the system. In the summer months, the greatest direct consumption from the RES and the accumulation of energy in the energy storage (due to weather conditions) takes place. Despite this, it is still necessary to supply energy from the grid every month of the year.

Fig. 14 shows the operation of an energy system based only on the PV/T source. The main conclusions of the monthly distribution are the same as for the system based on PV due to the same dependence of generation on weather conditions (insolation, etc.).

However, it can be seen that the higher efficiencies of the PV/T system contribute to the fact that one month of the year (July) is completely covered by renewable energy (through direct consumption and energy storage).

Fig. 15 shows the operation of an energy system based only on the wind turbine. The analysis shows that in this case (for the assumed in the analysis weather conditions) it is very inefficient. Generation occurs mainly in the winter months (December, January, February, March). This may indicate the possible benefits of combining the PV or PV/T mix with wind energy - for presented above systems based on solar energy, generation occurred mainly in the summer months, and in the case of wind energy, we observe the highest production in the winter months. The interaction of these two sources could lead to a better balance of the power system. Further considerations in this aspect will be presented later in the article.

In the case of a system based on biogas plants, which is presented in Fig. 16, the total demand is covered from a renewable source. The biogas plant is the most stable source of energy, least dependent on weather fluctuations from the presented RES. However it should be also emphasized that the process of generating energy in this unit is based on the combustion of biogas, and thus causes the emission of gases such as carbon dioxide, which is a greenhouse gas. Based on Fig. 16, it can also be concluded that the power of the system is too high (power of the biogas plant). All needs are covered directly from RES, very little from energy storage, so the potential of the energy storage is not used in this case.

### 3.2. Energy mix options – mix of two RES

In the second step of analysis the energy mix consists of two source. Below are presented exemplary energy mixes (out of available combinations):

- Energy production based only on PV + wind turbine (7,5 MW PV/T, 7,5 MW wind turbine)
- Energy production based only on biogas + PVT (0,5 MW biogas, 14,5 MW PV/T)
- Energy production based only on biogas + wind turbine (0,5 MW biogas, 14,5 MW wind turbine)

Three sample mixes were selected for the analysis, based on the observed properties of individual sources presented in the above subsection. The selection was made taking into account possible benefits from the interaction of individual sources.

Fig. 17 shows the cooperation of two sources: PV/T and wind turbines. Potential benefits can be seen in the interplay of these two RES - maximum energy generation levels in different seasons. The analysis also indicates that the power of the PV/T systems and the wind turbine is too low. Due to the limited operation time, the selected powers must be much higher to meet the needs of the system.

In the next step, the cooperation of the PV/T system and the biogas plant was analysed (Fig. 18). As can be seen, the discussed mix, due to the increase in the power of the PV/T installation and the presence of a stable source (biogas) works without the supply of energy from the grid for most of the year (except for the first months, when the demand is high and the energy storage does not contain sufficient amounts of energy to cover the missing demand).

In the energy mix (wind turbine + biogas) presented in Fig. 19, it can be seen again that wind energy is less profitable for the assumed weather conditions than other presented RES. Despite the cooperation with a stable source (biogas plant), there are significant energy shortages that must be supplied from the grid. The self-sufficiency of the system (RES and energy storage) is only observed between June and October.

### 3.3. Energy mix options – mix of three RES

In the second step of analysis the energy mix consists of two source. Below are presented exemplary energy mixes:

- Energy production based only on wind turbine + PV/T + biogas (7,5 MW wind turbine, 7,0 MW PV/T, 0,5 MW biogas),
- Energy production based only on wind turbine + PV/T + PV (5,0 MW wind turbine, 5,0 MW PV/T, 5,0 MW PV),
- Energy production based only on PV + PV/T + biogas (6,0 MW PV, 6,0 MW PV/T, 3,0 MW biogas).

As before, selected examples of energy mixes were presented in order to evaluate the best options for cooperation between individual renewable energy sources and energy storage in the microgrid.

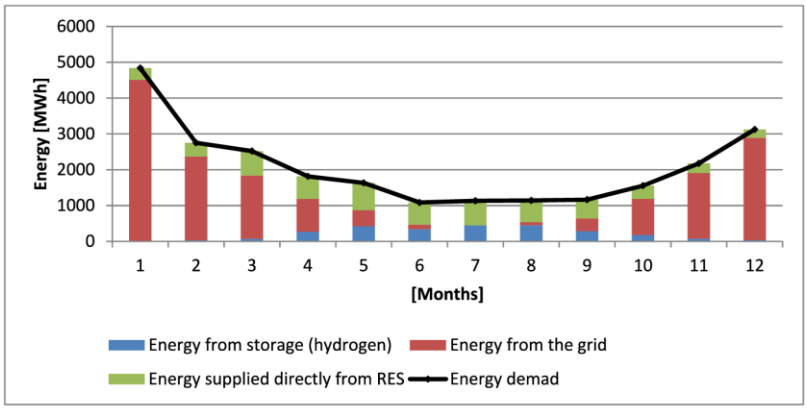


**Fig. 14.** Energy mix option - energy production based only on PV/T.

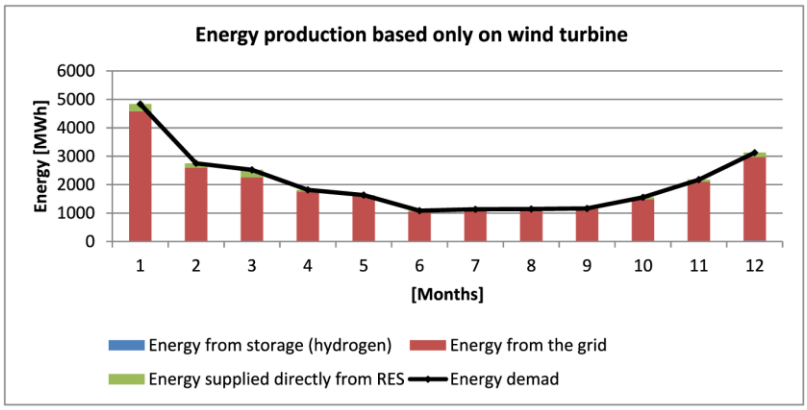


**Fig. 15.** Energy mix option - energy production based only on wind turbine.

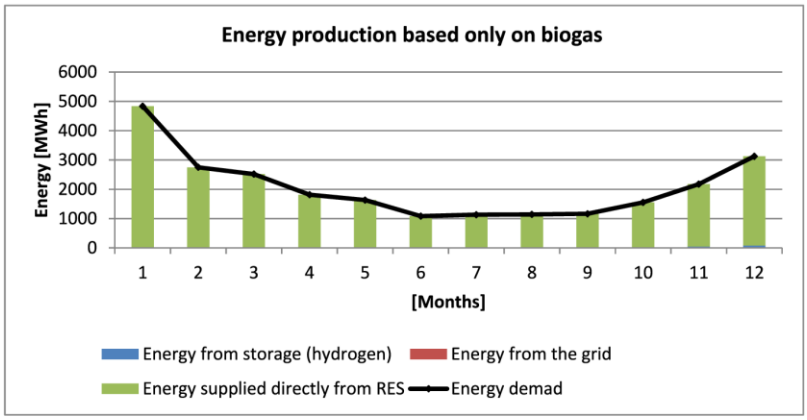


**Fig. 16.** Energy mix option - energy production based only on biogas plant.

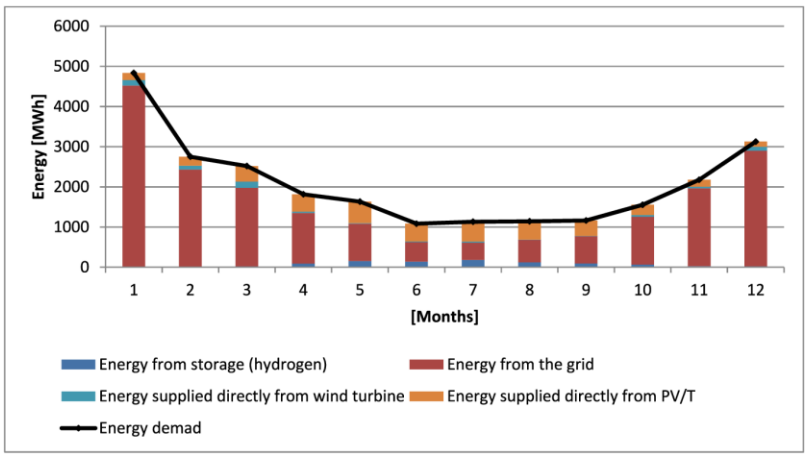


**Fig. 17.** Energy mix option - energy production based on mix of two renewable energy sources (7,5 MW PV/T, 7,5 MW wind turbine).

The energy mix of three renewable energy sources: wind turbine, PV/T and biogas (Fig. 20) shows well the possibilities of cooperation between wind and solar energy, however, the assumed installed power should be higher to cover the demand in the winter months (increasing the power of wind turbines). Through the interaction of random RES with a stable source (biogas plant) some months are based only on renewable energy (directly from RES and energy storage).

In the case of a wind turbine with a PV system (Fig. 21: energy mix

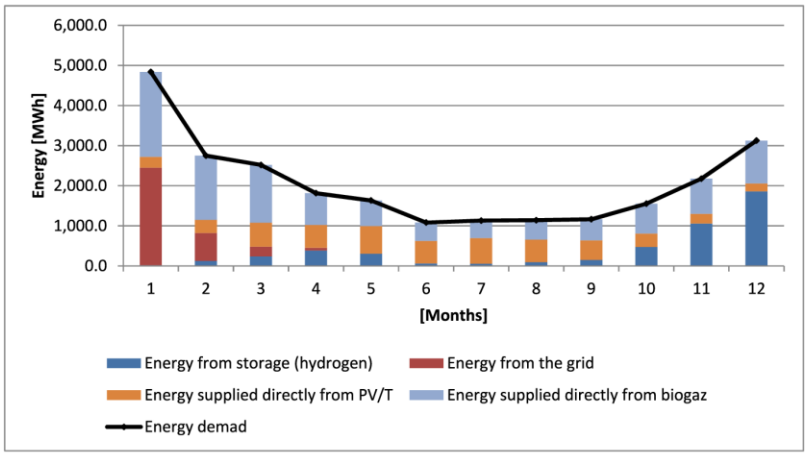


**Fig. 18.** Energy mix option - energy production based on mix of two renewable energy sources (3,0 MW biogas, 12,0 MW PV/T).

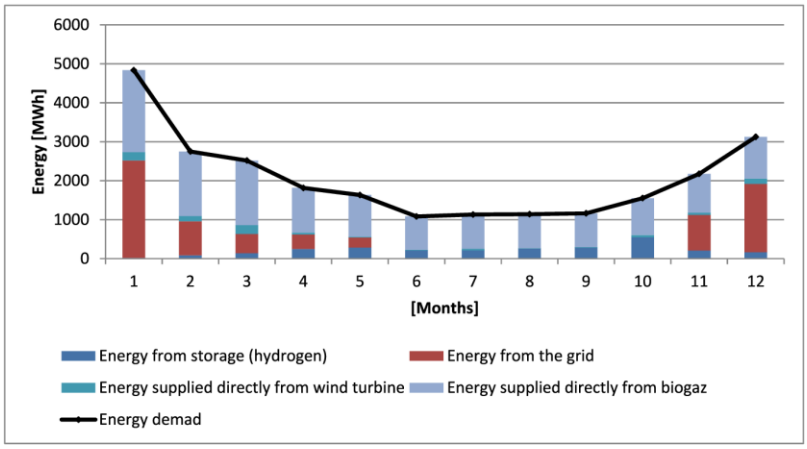


**Fig. 19.** Energy mix option - energy production based on mix of two renewable energy sources (3,0 MW biogas, 12,0 MW wind turbine).

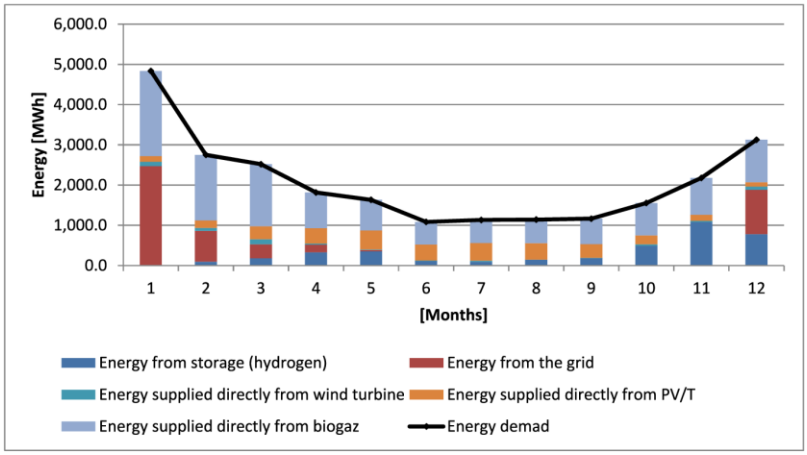


**Fig. 20.** Energy mix option - energy production based on mix of three renewable energy sources wind turbine, PV/T and biogas (6,0 MW wind turbine, 6,0 MW PV/T, 3,0 MW biogas).

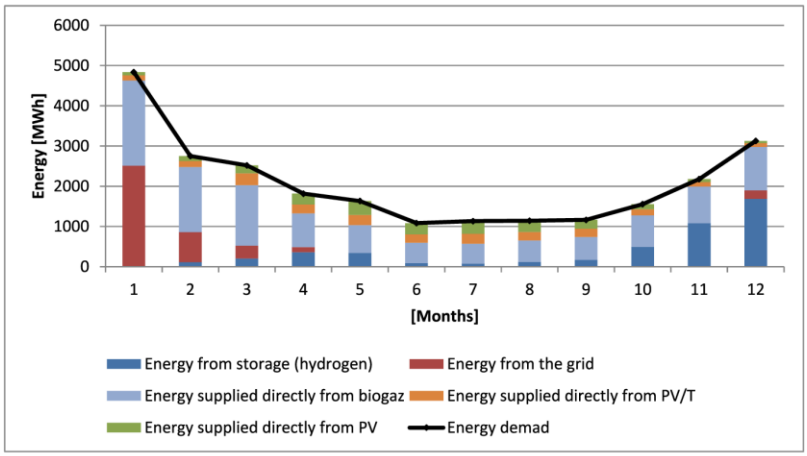


**Fig. 21.** Energy mix option - energy production based on mix of three renewable energy sources PV, PV/T and biogas (6,0 MW PV, 6,0 MW PV/T, 3,0 MW biogas).

based on PV, PV/T, biogas), the self-sufficiency of the system increases even more. Supplying energy from the grid is smaller than in the case of the mix presented in Fig. 20.

The energy mix based on wind turbine, PV/T and PV (Fig. 22) shows that for Variable Renewable Energy (VRE) there is a need for a significant excess installed capacity. In this case, in all months of the year, there is a need for supplementary energy from the grid.

### 3.4. *Energy mix options – mix of four RES*

In the four step of analysis are chosen a mix of four renewable energy sources to generate energy:

- Energy production based on wind turbine + PV/T + PV + biogas (4,0 MW wind turbine, 4,0 MW PV/T, 4,0 MW PV, 3,0 MW biogas)

Fig. 23 shows the cooperation of four sources: wind turbine + PV/T + PV + biogas. The needs to supply energy from the grid appear in the first months of the year, when the energy storage is not sufficiently filled to cover energy shortages, and at the end of the year, when the hydrogen reserves accumulated in the summer months are exhausted.

## 4. Thermo-ecological cost (TEC) – methodology

The yearly thermo-ecological cost (TEC) is an evaluation tool used to measure the efficiency of natural resource management. TEC includes exergy (as an indicator of resource quality) and cumulative calculus and can be a measure of global exergy-ecological performance by representing non-renewable resources through cumulative exergy consumption [38–40]. It should also be emphasized that thermo-ecological cost as a systems approach plays a crucial role in comparing different energy systems. One of the possibilities how to present the physical and ecological cost of each product (which is responsible for the total consumption of natural resources at the level of their extraction from nature) is TEC - thermo-ecological cost.

The thermo-ecological cost covers the exergy use of non-renewable resources derived directly from nature, for example freshwater, fuels and mineral ores. TEC can be defined (according to Szargut [41]) as: "cumulative consumption of non-renewable exergy related to the production of a given product with additional consideration of the consumption resulting from the need to compensate for environmental losses caused by the rejection of harmful waste substances into the environment". Among the most important applications of TEC should be highlighted:

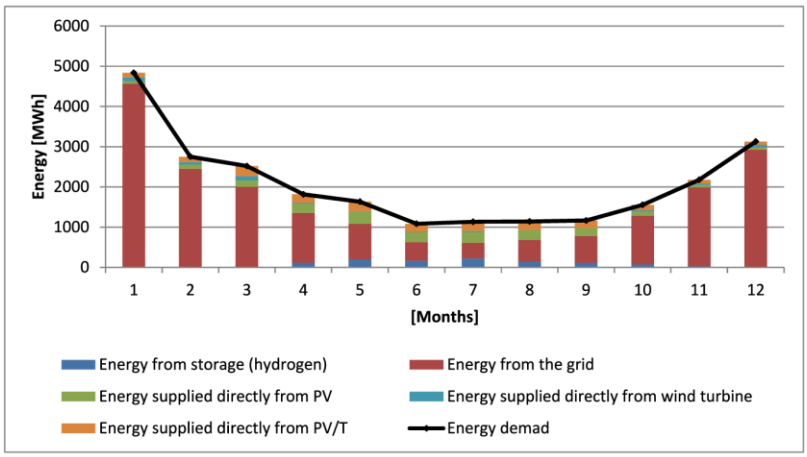


**Fig. 22.** Energy mix option - energy production based on mix of three renewable energy sources wind turbine, PV/T and PV (5,0 MW wind turbine, 5,0 MW PV/T, 5,0 MW PV).

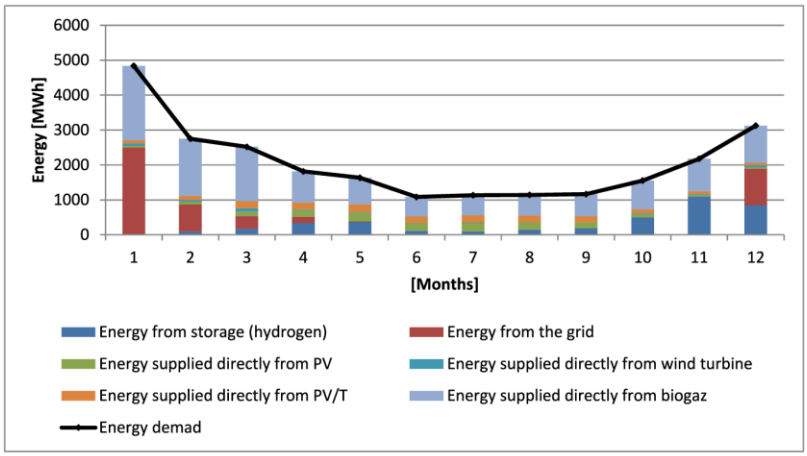


**Fig. 23.** Energy mix option - energy production based on mix of four renewable energy sources wind turbine + PV/T + PV + biogas (4,0 MW wind turbine, 4,0 MW PV/T, 4,0 MW PV, 3,0 MW biogas).

- Evaluation of the impact of operating parameters of energy systems on the depletion of fossil fuel resources.
- Estimation of the impact of introducing harmful substances into the environment on the depletion of non-renewable resources.
- Optimization of operating parameters, structure of production of a given utility product and designing parameters that provide to minimization of the depletion of non-renewable resources.
- Selection of technology ensuring minimum depletion of non-renewable resources.
- Analysis of the impact of cross-regional exchange on the depletion of non-renewable resources.
- Estimating the sustainable development degree.
- Determining the impact of individual consumer goods on the depletion of non-renewable resources during their full life cycle.
- Determining amount of the pro-ecological tax replacing the existing taxes [41–43].

TEC can also be increased due to the consumption of by-products which are exchanged between the branches of the system. In this regard, the thermo-ecological cost of pollutants is not computed as chemical exergy, and as the quantity of energy needed to prevent the pollutant from being released into the environment. An example is the use of exergy in emission reduction installations. If it is impossible to prevent the release of these pollutants into the environment, the thermo-ecological cost should be defined as the amount of exergy needed to reduce the negative effects caused by discards introduced into the environment [44,45]. In some processes, by-products can replace the main in other processes, and thus the value of TEC of the main product under consideration is reduced [46–48]. The specific thermo-ecological cost we can define by three components (eq. (18)):

- The component related to exergy of non-renewable natural resources immediately consumed in the process $b_{sj}$.
- The component contains the thermo-ecological cost of harmful substances $\zeta_k$ of the described process. Both of the mentioned elements increase the volume of TEC.
- The last component of specific thermo-ecological cost described specific thermo-ecological of by-products $f_{ij}$ can reduce volume of the index of operational TEC $\rho_i$ or increase when the consumption of i-th material per unit of j-th main product is high [41–43,46,49].

$$\rho_j = \sum_s b_{sj} + \sum_k p_{kj}\zeta_k - \sum_i (f_{ij} - a_{ij})\rho_i \tag{18}$$

where:

$b_{sj}$ exergy of $s$-th non-renewable natural resource immediately consumed in the process under consideration per unit of $j$-th product, MJ/kg,
$\zeta_k$ thermo-ecological cost of $k$-th harmful substance, MJ/kg.
$p_{kj}$ amount of $k$-th harmful substance from $j$-th process, kg.
$f_{ij}$ coefficient of by-production of $i$-th product per unit of $j$-th main product, e.g. in kg/kg or kg/MJ.
$a_{ij}$ coefficient of consumption of $i$-th material per unit of $j$-th main product, e.g. in kg/kg or kg/MJ.
$\rho_i$ specific thermo-ecological cost of $i$-th product, e.g. in MJ/kg.

The balance of the thermo-ecological cost (TEC) is schematically presented in Fig. 24.

However, it should be mentioned that the above equation only describes the operational part, but when we take into consideration power technologies, other phases of the life cycle may also be important. The general equation to calculate TEC in the whole life cycle (formulated by Szargut [41] and used in analysing the exergetic life cycle of solar collector system by Szargut and Stanek [46]) is presented by eq. (19):

$$\rho_j^{LCA} = \theta_n\left(\sum_i \dot{G}_i\rho_i + \sum_k \dot{P}_k\zeta_k - \sum_u \dot{G}_u\rho_j s_{ju}\right) + \frac{1}{\tau_j}\left(\sum_l G_l\rho_l(1-u_l) + \sum_r G_r\rho_r\right) \tag{19}$$

where:

$\theta_n$ average annual time of exploitation of $j$-th considered machine, device, installation or building, in other words annual operation time with nominal capacity, h/year.
$\dot{G}_i$ nominal stream of $i$-th material used in $j$-th production process, kg/h.
$\dot{P}_k$ nominal stream of $k$-th waste product released to the environment from $j$-th production process, kg/h.
$\dot{G}_u$ nominal stream of $u$-th by-product manufactured simultaneously with $j$-th product within the production process, kg/h.
$s_{ju}$ replacement index of by-product $u$ by main product $j$.
$\tau_j$ nominal lifetime of $j$-th machine, device, installation or building, years.

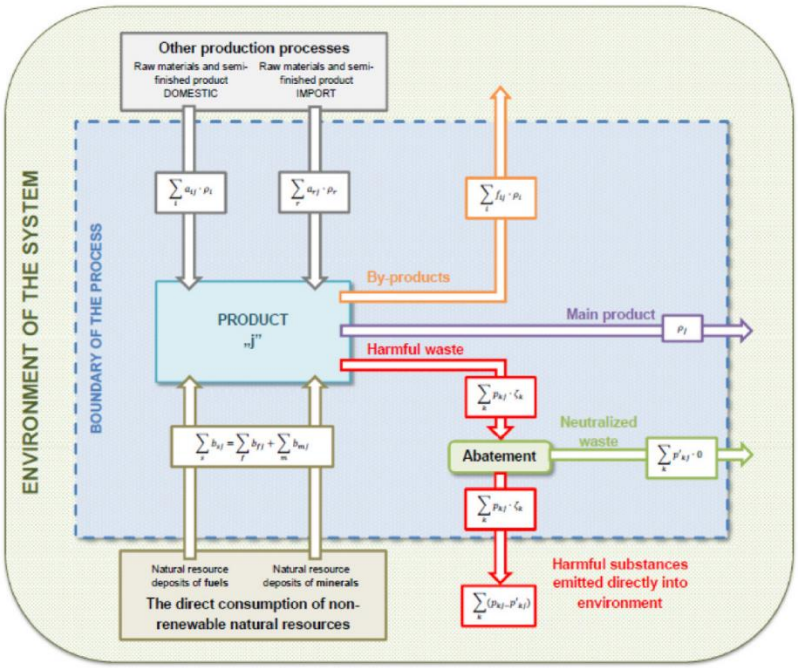


**Fig. 24.** Idea of TEC balance equation.

$G_l$ amount of $l$-th material used for the construction of $j$-th considered machine, device, installation or building, kg.
$u_l$ expected recovery rates of $l$-th material after the end of operation phase of $j$-th considered machine, device, installation or building, kg/kg.
$G_r$ amount of $r$-th material used for the maintenance of $j$-th considered machine, device, installation or building, kg.

## 5. Thermo-ecological cost (TEC) of presented energy mix options

The TEC values presented in the table below (Table 3) were used for the calculations of:

- TEC of energy from the RES – eq. (20):

$$TEC_{RES} = \frac{TEC_{RESref} E_{RES}}{E_d} \tag{20}$$

where:

$TEC_{RES}$ Thermo-Ecological Cost of the energy from the RES, MW/MW.
$TEC_{RESref}$ Reference Thermo-Ecological Cost of the RES, MW/MW.
$E_{RES}$ Total annual amount of energy from RES, MWh.
$E_d$ Total annual amount of system energy demand, MWh.

**Table 3**
Thermo-Ecological Cost (TEC) of energy sources in the mix (based on: [23]).

| Source | $TEC_{ref}$ |
|---|---|
| Polish grid energy mix | 2,81 |
| Photovoltaic power plant | 0,29 |
| PV/T | 0,15 |
| Wind power plant | 0,10 |
| Biogas power plant | 0,12 |

- TEC of energy from the gird – eq. (21):

$$TEC_G = \frac{TEC_{Gref} E_G}{E_d} \tag{21}$$

where:

$TEC_G$ Thermo-Ecological Cost of the energy from the grid, MW/MW.
$TEC_{Gref}$ Reference Thermo-Ecological Cost of the grid, MW/MW.
$E_G$ Total annual amount of energy from grid, MWh.
$E_d$ Total annual amount of system energy demand, MWh.

- TEC of stored energy – EQ. (22):

$$TEC_S = \frac{TEC_{RESref} E_S}{E_d} \tag{22}$$

where:

$TEC_S$ Thermo-Ecological Cost of the energy from the energy storage, MW/MW
$TEC_{Sref}$ Reference Thermo-Ecological Cost of the energy storage, MW/MW
$E_S$ Total annual amount of energy from energy storage, MWh
$E_d$ Total annual amount of system energy demand, MWh

In the next part of the article, the thermo-ecological assessment of the systems discussed in point 3 of the article is presented.

### 5.1. Thermo-ecological cost (TEC) - one RES

In the first step, the thermo-ecological cost of system with one RES was analysed: PV, PV/T, wind turbine or biogas system. The individual cases are presented below.

In the case of a PV-based system (Fig. 25), the lowest TEC values are observed in the summer months (June, July, August) due to the high share of RES (both direct consumption from RES and energy storage).

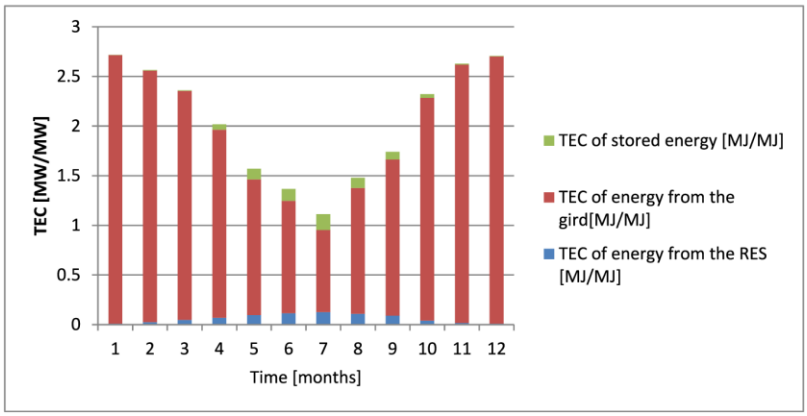


**Fig. 25.** Thermo-Ecological Cost (TEC) - energy production based only on PV.

The situation is similar in the case of a system based on PV/T, which is presented in Fig. 26. However, the values for the summer months are much higher, due to the greater generation of the PV/T system than the PV system (resulting, among others, from the higher efficiency of the system).

In the case of systems based on PV and PV/T, the highest TEC values were observed in the winter months due to low generation from renewable sources. In the case of a wind power system (Fig. 27), high TEC values can be seen throughout the year. The lowest TEC value for this system was determined for March due to the highest RES production for that month.

Fig. 28 is for a system based on a biogas plant only. The TEC values are the lowest compared to the previous options because all energy is supplied from the RES. In the last months of the year, the RES values increase because the energy is partly supplied from the energy storage. Although the energy stored in the bag storage comes from the biogas plant, its TEC increases due to the efficiency of the storage system (electric generator, fuel cell).

### 5.2. Thermo-ecological cost (TEC) - mix of two RES

In the second step, the thermo-ecological cost of system based on a mix of two renewable energy sources to generate energy. Below are presented exemplary energy mixes (out of available combinations):

- Energy production based on mix of two renewable energy sources: PV and wind turbine (7,5 MW PV/T, 7,5 MW wind turbine).
- Energy production based on mix of two renewable energy sources: PV/T and biogas (12,0 MW PV/T, 3,0 MW biogas).
- Energy production based on mix of two renewable energy sources: wind turbine and wind turbine (12,0 MW wind turbine, 3,0 MW biogas).

Fig. 29 shows thermo-ecological cost of power system based on mix of two renewable energy sources: PV/T and wind turbine. The TEC value is very high because there is a need for supply from the mains during lots of days during the year. The lowest TEC values are observed in the summer months due to the production of energy from PV/T.

For the system based on mix of two renewable energy sources: PV/T and biogas (Fig. 30) TEC is high at the beginning of the year, and then successively decreases, because the demand is covered by the RES (directly and from the energy storage).

In the case of a system based on wind turbine and biogas (Fig. 31) TEC is lowest for the summer months because demand is lowest. Low TEC values are observed also in September and October because the energy stored during the summer months is used.

### 5.3. Thermo-ecological cost (TEC) - energy mix options – mix of three RES

In the third step, the thermo-ecological cost of system based on a mix of three renewable energy sources to generate energy. Below are presented exemplary energy mixes (out of available combinations):

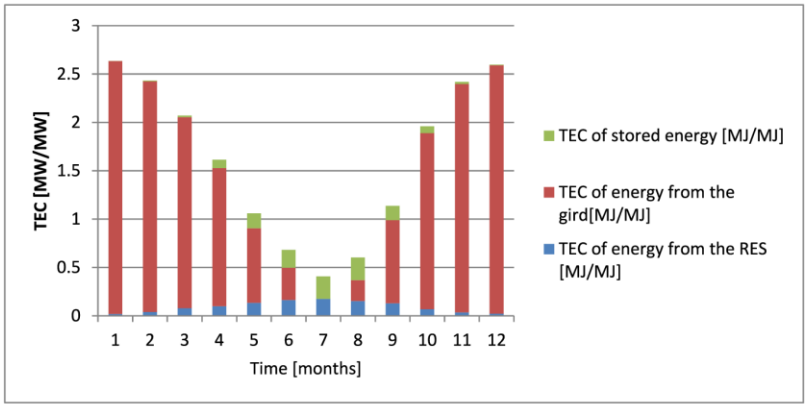


**Fig. 26.** Thermo-Ecological Cost (TEC) - energy production based only on PV/T.

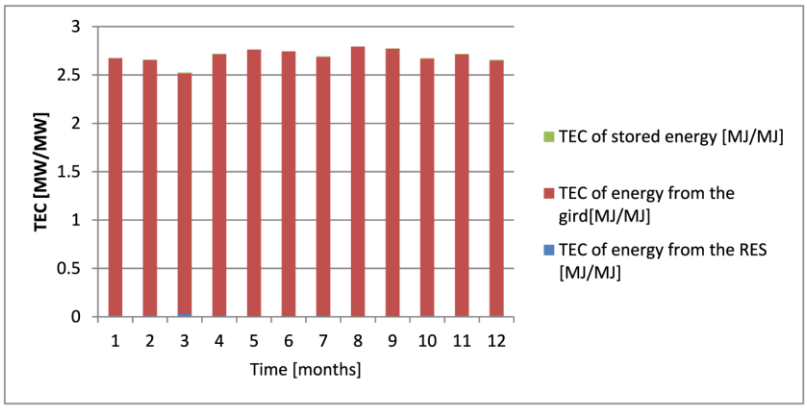


**Fig. 27.** Thermo-Ecological Cost (TEC) - energy production based only on wind turbine.

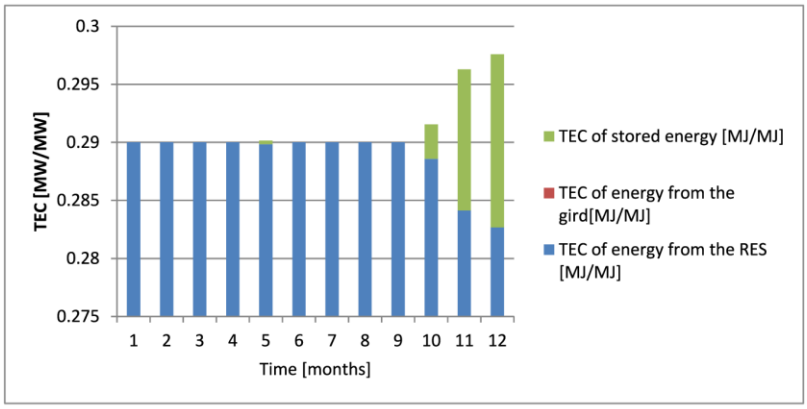


**Fig. 28.** Thermo-Ecological Cost (TEC) - energy production based only on biogas plant.

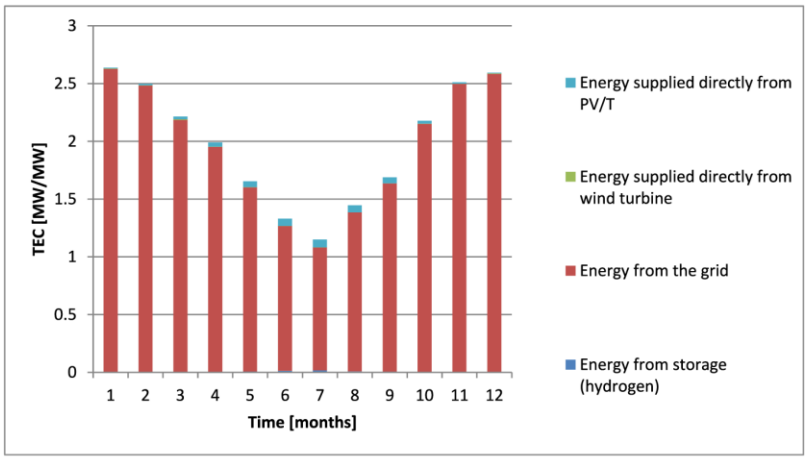


**Fig. 29.** Thermo-Ecological Cost (TEC) - energy production based on mix of two renewable energy sources: PV/T and wind turbine (7,5 MW PV, 7,5 MW wind turbine).

- Energy production based on mix of three renewable energy sources: wind turbine, PV/T and biogas (6,0 MW wind turbine, 6,0 MW PV/T, 3,0 MW biogas).
- Energy production based only on mix of three renewable energy sources: wind turbine, PV/T and PV (5,0 MW wind turbine, 5,0 MW PV/T, 5,0 MW PV).

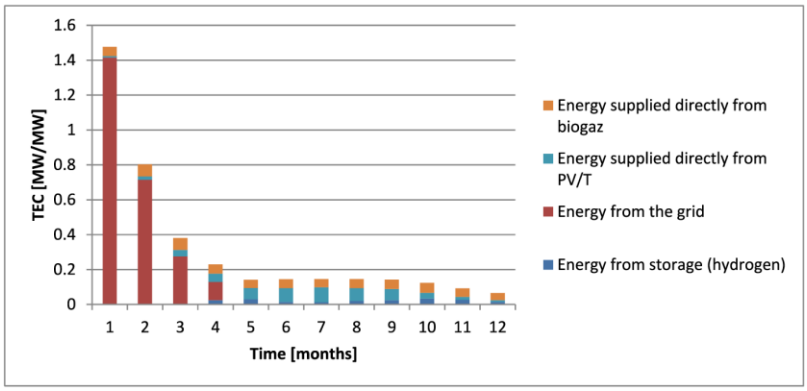


**Fig. 30.** Thermo-Ecological Cost (TEC) - energy production based on mix of two renewable energy sources: PV/T and biogas (12,0 MW PV/T, 3,0 MW biogas).

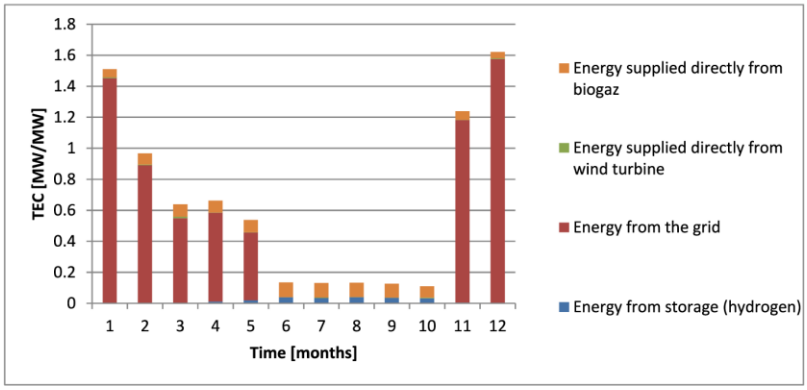


**Fig. 31.** Thermo-Ecological Cost (TEC) - energy production based on mix of two renewable energy sources: wind turbine and biogas (12,0 MW wind turbine, 3,0 MW biogas).

- Energy production based only on mix of three renewable energy sources: PV, PV/T and biogas (6,0 MW PV, 6,0 MW PV/T, 3,0 MW biogas).

In the mix based on mix of three renewable energy sources: wind turbine, PV/T and biogas (Fig. 32), the TEC value for monthly totals falls below 1 for 10 months (February to November). This is due to the interaction of various RES sources and energy storage.

Fig. 33 shows the TEC for the system based on wind turbine, PV/T and PV. IN this case, due to the large share of energy from the TEC network for all months.

For the system based on mix of three renewable energy sources: PV,

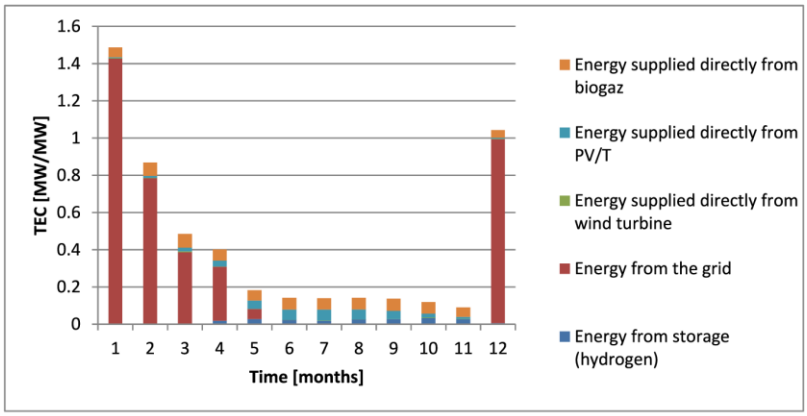


**Fig. 32.** Thermo-Ecological Cost (TEC) - energy production based on mix of three renewable energy sources: wind turbine, PV/T and biogas (6,0 MW wind turbine, 6,0 MW PV/T, 3,0 MW biogas).

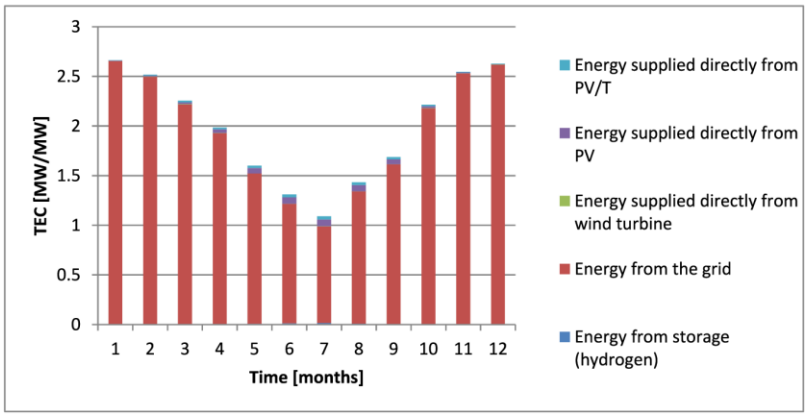


**Fig. 33.** Thermo-Ecological Cost (TEC) - energy production based on mix of three renewable energy sources: wind turbine, PV/T and PV (5,0 MW wind turbine, 5,0 MW PV/T, 5,0 MW PV).

PV/T and biogas the (Fig. 34) TEC values are less than 1 for 11 months. The lowest TEC values are observed between May and November (below 0.2).

### 5.4. *Thermo-ecological cost (TEC) - energy mix options –mix of four RES*

In the fourth step, the thermo-Ecological Cost of system based on a mix of three renewable energy sources to generate energy:

- Energy production based on wind turbine + biogas + PV + PV/T (4,0 MW wind turbine, 4,0 MW PV/T, 4,0 MW PV, 3,0 MW biogas)

Fig. 35 shows the mix of four renewable energy sources wind turbine + biogas + PV + PV/T. TEC falls below 1 in all months except January. In January, due to the high share of energy supplied from the grid, TEC reached a value above 1.5. In December, the TEC is close to 1 because the energy stored in the hydrogen storage is exhausted and is supplied from the grid.

## 6. Summary and conclusions

Main conclusions from the analysis:

- Individual renewable energy sources have different characteristics, and their appropriate combination in the energy mix affects the stabilization of energy production in the microgrid.
- Compared to previous RESs (based on wind and solar energy), the biogas plant is a stable source of energy producing comparable amounts of electricity throughout the year.
- Analysing the cooperation of biogas plant as one of the components of the microgrid it was observed that the biogas plant is an important element stabilizing the continuity of electricity production.
- From the point of view of full use of the energy storage capacity, the most advantageous was a mixed system based on renewable energy sources using solar irradiation and wind energy with the stabilizing participation of a biogas plant.
- For solar-based sources, the lowest TECs were observed in the summer months.
- The lowest TEC values of microgrid based on wind turbines production were observed in the winter months.
- Analysing biogas plants, the TEC increased in the months when the energy from the energy storage was used.
- The thermo-ecological analysis showed that the best energy mixes in terms of assessing the efficiency of natural resource management are systems that use the advantages of each component, supporting by energy storage.

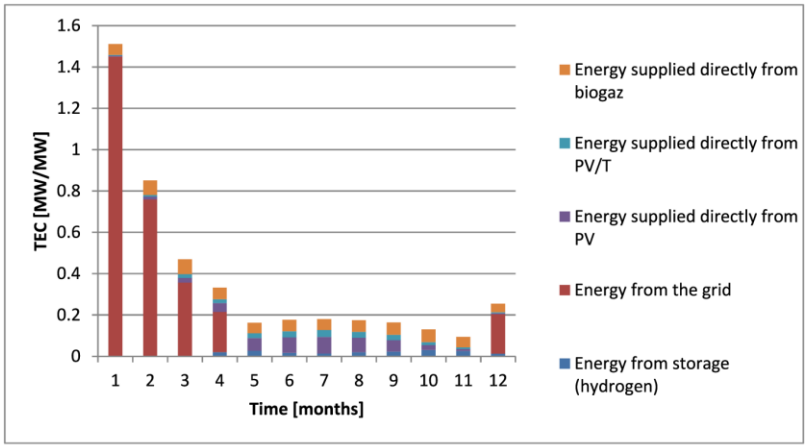


**Fig. 34.** Thermo-Ecological Cost (TEC) - energy production based on mix of three renewable energy sources: PV, PV/T and biogas (6,0 MW PV, 6,0 MW PV/T, 3,0 MW biogas).

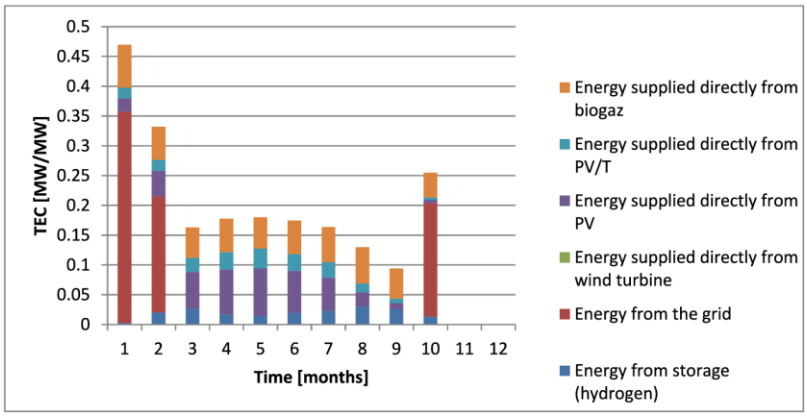


**Fig. 35.** Thermo-Ecological Cost (TEC) - energy production based on mix of four renewable energy sources wind turbine + biogas + PV + PV/T (4,0 MW wind turbine, 4,0 MW PV/T, 4,0 MW PV, 3,0 MW biogas).

- Thanks to the combination of sources with different characteristics (time of energy production during the year, stability, etc.), the best values of the thermo-ecological cost indicator were obtained.

The analysis showed that individual renewable energy sources have different characteristics, and their appropriate combination in the energy mix affects the stabilization of energy production in the microgrid. In the case of renewables based on solar radiation, the highest energy production was observed in the summer, and due to higher efficiencies, the PV/T system showed higher electricity production than the PV system operating under the same conditions. Wind conditions allowed for the largest production of energy in wind turbines in the winter and spring months. Further analysis of the combination of sources based on solar radiation and wind energy in the energy mix showed the benefits of this combination - the largest amounts of energy produced in PV or PV/T systems are in the months when production from wind turbines is low. Similarly, the relationship looks the other way, which is why the cooperation of these two sources of renewable energy seems to be very beneficial in the analysed climatic conditions.

In the further part of the analysis, the operation of the biogas plant was considered. Compared to previous RESs (based on wind and solar energy), the biogas plant is a stable source of energy producing comparable amounts of electricity throughout the year. However it should be stressed, that in comparison to PV, PV/T systems and a wind turbine, a biogas plant during the production of electricity (involving the combustion of biogas) causes gas emissions to the atmosphere. Analysing the cooperation of biogas plant as one of the components of the microgrid it was observed that the biogas plant is an important element stabilizing the continuity of electricity production. Even with significantly lower installed capacity of biogas plants compared to other RES (PV, PV/T, wind turbine) in the microgrid, there is a reduction in the demand of energy from the grid (in comparison of options without biogas plants in the energy mix).

In the presented microgrid, the energy storage was also used (electrolyser, hydrogen store and fuel cell). The surplus of energy produced was converted into hydrogen, stored and used in the event of a shortage of energy. In the case of systems based only on sources using solar radiation (PV, PV/T), the largest production of hydrogen occurred in the summer months and was consumed on an ongoing basis (during hours with low availability or no solar radiation). In the case of a wind turbine, there was a similar relationship: the stored surplus energy was consumed in a short time after its storage. Taking into account the biogas plant (non-cooperating with other RES), the use of the energy storage was only partly justified (the biogas plant unit ensures a stable and most hours of the year, the system does not require replenishment energy from the energy storage). From the point of view of full use of the energy storage capacity, the most advantageous was a mixed system based on renewable energy sources using solar irradiation and wind energy with the stabilizing participation of a biogas plant.

In the further part of the article, the energy mixes were analysed in the context of the efficiency of natural resource management. For this purpose, the TEC (thermo-ecological cost) indicator was used. For solar-based sources, the lowest TECs were observed in the summer months. In the rest of the year a high share of grid power was recorded, which significantly inflates TECs. In the case of production from a wind turbine, a decrease in TEC was also observed in the months with the lowest energy consumption from the grid. The lowest TEC values of microgrid based on wind turbines production were observed in the winter months. Analysing biogas plants, the TEC increased in the months when the energy from the energy storage was used. Although the stored energy was generated in the biogas plant through storage (e.g. efficiency equipment electrolyser, hydrogen store, fuel cell) TEC increases. The thermo-ecological analysis showed that the best energy mixes in terms of assessing the efficiency of natural resource management are systems that use the advantages of each component, supporting by energy storage. Thanks to the combination of sources with different characteristics (time of energy production during the year, stability, etc.), the best values of the thermo-ecological cost indicator were obtained.

## CRediT authorship contribution statement

**Agnieszka Szostok:** development or design of, Methodology, Writing – original draft, preparation, creation, presentation of the published work. **Wojciech Stanek:** formulation or evolution of overarching research goals and aims, development or design of, Methodology, Writing – review & editing, preparation.

## Declaration of competing interest

The author declare that they have no known competing financial interests or personal relationships that could have appeared to influence the work reported in this paper. Authors declare that there are no conflicts of interest.

## Acknowledgements

This work has been developed thanks to the support from the statutory research fund SUBB of the Faculty of Power and Environmental Engineering of Silesian University of Technology.

## Nomenclatures

| | |
|---|---|
| E | - energy [kW] |
| $I_\beta$ | - solar radiation[kW/m$^2$] |
| A | - surface [m$^2$] |
| Q | - heat [kW] |
| k | - heat loss coefficients[-] |
| T | - temperature [K] |
| t | - temperarure[°C] |
| $\dot{W}$ | - heat capacity of stream [kW/s] |
| $\dot{m}$ | - mass stream[kg/s] |
| P | - power[kW] |
| k | - heat transfer coefficient in the exchanger[W/(m2·K)] |
| B | - exergy[MJ] |
| TEC | - cost of thermo-ecological[MJ/MJ] |
| ΔT | - difference of temperature [K] |

*Greek symbols*

| | |
|---|---|
| $\eta$ | - efficiency |
| τ | - time, hours |

*Indices*

| | |
|---|---|
| C | - applies to the collector |
| PV | - applies to the PV system |
| PV/T | - applies to the PV/T system |
| W | - applies to the wind turbine |
| E | - applies to the electrolyser |
| FC | - applies to the fuel cell |
| G | - applies to the grid |
| 0 | - applies to the environment |
| ref | - reference |
| d | - demand |
| s | - stored |
| b | - exergy |
| e | - energy |
| th | - thermal |

## References

[1] The European Youth Portal, What is climate change?. https://europa.eu/youth/get-involved/sustainable%20development/what-climate-change_pl, 08/08/2021.
[2] Intergovernmental Panel on Climate Change, Climate change 2021. The physical science basis". https://www.ipcc.ch/report/ar6/wg1/downloads/report/IPCC_AR6_WGI_Full_Report.pdf, 2021.
[3] bp p.l.c, Statistical review of world energy. https://www.bp.com/en/global/corporate/energy-economics/statistical-review-of-world-energy.html, 2021.
[4] Cong Chao, Yimin Deng, Raf Dewil, Baeyens Jan, Xianfeng Fan, Post-combustion carbon capture, Renew. Sustain. Energy Rev. 138 (2021), 110490, https://doi.org/10.1016/j.rser.2020.110490". ISSN 1364-0321.
[5] Tomas Gomez-Navarro, Tommaso Brazzini, David Alfonso-Solar, Carlos Vargas-Salgado, „Analysis of the Potential for PV Rooftop Prosumer Production: Technical, Economic and Environmental Assessment for the City of Valencia (Spain)", Renewable Energy, 2021.
[6] Piero Bevilacqua, Stefania Perrella, Roberto Bruno, Natale Arcuri, „An Accurate Thermal Model for the PV Electric Generation Prediction: Long-Term Validation in Different Climatic Conditions", Renewable Energy, 2020.
[7] Intergovernmental Panel on Climate Change, Climate change 2021. The physical science basis. https://www.ipcc.ch/report/ar6/wg1/downloads/report/IPCC_AR6_WGI_Full_Report.pdf, 2021.
[8] Partha Das, Kanudia Amit, Rohit Bhakar, Jyotirmay Mathur, Intra-regional renewable energy resource variability in long-term energy system planning, Energy 245 (2022), 123302, https://doi.org/10.1016/j.energy.2022.123302. ISSN 0360-5442.
[9] J. Jurasz, F.A. Canales, A. Kies, M. Guezgouz, A. Beluco, A review on the complementarity of renewable energy sources: concept, metrics, application and future research directions, Sol. Energy 195 (2020) 703–724, https://doi.org/10.1016/j.solener.2019.11.087. ISSN 0038-092X.
[10] Aike Kan, Yelong Zeng, Xiangyu Meng, Dan Wang, Ji Xina, Xiao Yang, Luobu Tesren, The linkage between renewable energy potential and sustainable development: understanding solar energy variability and photovoltaic power potential in Tibet, China, Sustain. Energy Technol. Assessments 48 (2021), 101551, https://doi.org/10.1016/j.seta.2021.101551. ISSN 2213-1388.
[11] Imane Khamlich, Kuo Zeng, Gilles Flamant, Baeyens Jan, Chongzhe Zou, Jun Li, Xinyi Yang, He Xiao, Qingchuan Liu, Haiping Yang, Qing Yang, Hanping Chen, Technical and economic assessment of thermal energy storage in concentrated solar power plants within a spot electricity market, Renew. Sustain. Energy Rev. 139 (2021), 110583, https://doi.org/10.1016/j.rser.2020.110583. ISSN 1364-0321.
[12] Gilles Flamant, Benjamin Grange, John Wheeldon, Frédéric Siros, Benoît Valentin, Françoise Bataille, Huili Zhang, Yimin Deng, Baeyens Jan, "Opportunities and challenges in using particle circulation loops for concentrated solar power applications, Prog. Energy Combust. Sci. 94 (2023), 101056. ISSN 0360-1285.
[13] D. Fernandes, F. Pitié, G. Cáceres, J. Baeyens, "Thermal energy storage: "How previous findings determine current research priorities", Energy 39 (1) (2012) 246–257, https://doi.org/10.1016/j.energy.2012.01.024. ISSN 0360-5442.
[14] Iván Jiménez-Vargas, M. Juan, Rey German Osma-Pinto, Sizing of hybrid microgrids considering life cycle assessment, Renew. Energy 202 (2023) 554–565, https://doi.org/10.1016/j.renene.2022.11.1.
[15] Aina Maimó-Far, Victor Homar, Alexis Tantet, Drobinski Philippe, The Effect of Spatial Granularity on Optimal Renewable Energy Portfolios in an Integrated Climate-Energy Assessment Model, vol. 54, Sustainable Energy Technologies and Assessments, 2022, 102827, https://doi.org/10.1016/j.seta.2022.102827. ISSN 2213-1388.
[16] A. Jain, S. Yamujala, A. Gaur, P. Das, R. Bhakar, J. Mathur, Power sector decarbonization planning considering renewable resource variability and system operational constraints, Appl. Energy 331 (2023), 120404, https://doi.org/10.1016/j.apenergy.2022.120404.
[17] R. Sitharthan, S. Vimal, Amit Verma, Madurakavi Karthikeyan, Shanmuga Sundar Dhanabalan, Prabaharan Natarajan, M. Rajesh, T. Eswaran, Smart microgrid with the internet of things for adequate energy management and analysis, Comput. Electr. Eng. 106 (2023), 108556, https://doi.org/10.1016/j.compeleceng.2022.108556.

[18] Jacqueline A. Dowling, Katherine Z. Rinaldi, Tyler H. Ruggles, Steven J. Davis, Mengyao Yuan, Tong Fan, Nathan S. Lewis, Ken Caldeira, Role of long-duration energy storage in variable renewable electricity systems, Joule 4 (9) (2020) 1907–1928, https://doi.org/10.1016/j.joule.2020.07.007. ISSN 2542-4351.

[19] Yimin Deng, Shuo Li, Lise Appels, Huili Zhang, Nick Sweygers, Baeyens Jan, Raf Dewil, Steam reforming of ethanol by non-noble metal catalysts, Renew. Sustain. Energy Rev. 175 (2023), 113184, https://doi.org/10.1016/j.rser.2023.113184. ISSN 1364-0321.

[20] Jie Xu, Tao Lv, Xiaoran Hou, Xu Deng, Feng Liu, Provincial allocation of renewable portfolio standard in China based on efficiency and fairness principles, Renew. Energy 179 (2021) 1233–1245, https://doi.org/10.1016/j.renene.2021.07.101. ISSN 0960-1481.

[21] Yimin Deng, Raf Dewil, Lise Appels, Flynn Van Tulden, Shuo Li, Miao Yang, Baeyens Jan, Hydrogen-enriched natural gas in a decarbonization perspective, Fuel 318 (2022), 123680, https://doi.org/10.1016/j.fuel.2022.123680. ISSN 0016-2361.

[22] L. Oliveira, M. Messagie, J. Mertens, H. Laget, T. Coosemans, J. Van Mierlo, "Environmental Performance of Electricity Storage Systems for Grid Applications, a Life Cycle Approach", vol. 101, Energy Conversion and Management, 2015, pp. 326–335, https://doi.org/10.1016/j.enconman.2015.05.063. ISSN 0196-8904.

[23] Jiao Yang, Daniel Månsson, Greenhouse gas emissions from hybrid energy storage systems in future 100% renewable power systems – a Swedish case based on consequential life cycle assessment, J. Energy Storage 57 (2023), 106167, https://doi.org/10.1016/j.est.2022.106167. ISSN 2352-152X.

[24] E. Akyuz, C. Coskun, Z. Oktay, I. Dincer, Hydrogen production probability distributionsfor a PV-electrolyser system, Int. J. Hydrogen Energy 36 (17) (2011) 11292–11299. https://doi.org/10.1016/j.ijhydene.2010.11.125.

[25] W. Stanek, Ocena Efektywności Energetycznej I Ekologicznej Transformacji TETIP Do Elektroprosumeryzmu W Środowisku Paradygmatu Egzergetycznego – Koszt Termoekologiczny: Elektroprosumeryzm vs Energetyka WEK-PK, 2021.

[26] Sarah Newman, Kaymie Shiozawa, b Jim Follum, Emily Barrett, Douville Travis, Trevor Hardy, Solana Amy, A Comparison of PV Resource Modeling for Sizing Microgrid Components, Renewable Energy, 2020.

[27] H.L. Zhang, T. Van Gerven, J. Baeyens, i J. Degrève, Photovoltaics: Reviewing the European Feed-in-Tariffs and Changing PV Efficiencies and Costs, The Scientific World Journal 2014 (2014), https://doi.org/10.1155/2014/404913. Article ID 404913, 10 pages.

[28] Akademia Viessmann Polska, Podręcznik Architekta, Projektanta I Instalatora - Kolektory Słoneczne, Wrosław: Viessmann Werke, Allendorf (Eder), 2013.

[29] T.N. Anderson, M. Duke, G.L. Morrison, J.K. Carson, Performance of a building integrated photovoltaic/thermal (BIPVT) solar collector, Solar Energy 83 (4) (2020) 445–455. ISSN 0038-092X, https://doi.org/10.1016/j.solener.2008.08.013.

[30] Antonio Gagliano, Giuseppe M. Tina, Francesco Nocera, , Alfio Dario Grasso, Stefano Aneli, Description and Performance Analysis of a Flexible Photovoltaic/thermal (PV/T) Solar System", Renewable Energy, 2017.

[31] Jie Ji, Tin-Tai Chow, Environmental life-cycle analysis of hybrid solar photovoltaic/thermal systems for use in Hong Kong, International Journal of Photoenergy 2012 (2012), https://doi.org/10.1155/2012/101968. Article ID 101968, 9 pages.

[32] Mahdi Shakouri, Hossein Ebadi, Shiva Gorjian, Chapter 4 - solar photovoltaic thermal (PVT) module technologies, Photovolt. Solar Energy Conv. Technolo. Appl. Environ. Impacts (2020) 79–116.

[33] C.U.C.E. Pinar Mert, Novel, practical and reliable analytical models to estimate electrical efficiency of buildingintegrated photovoltaic/thermal (BIPVT) collectors and systems, Uludag Univ. J. Facult. Eng. 23 (No. 3) (2018).

[34] Śmigielski Zbigniew, Zespół elektrowni wiatrowych [Online] 11 01 2020, http://zet10.ipee.pwr.wroc.pl/record/18/files/Wind%20Farm.doc.pdf.

[35] J. Kotowicz, M. Jurczyk, D. Węcel, W. Ogulewicz, Analysis of hydrogen production in alkaline electrolyzers, J. Power Technol. 96 (3) (2016) 149–156.

[36] EKONTROL, Ekontrol [Online] 11 01 2020, https://ekontrol.pl/pl/demo/8.

[37] Data Bank of the institute of meteorology and water management. https://bank-danych.imgw.pl/home, 08/08/2021.

[38] Wojciech Stanek, Wiesław Gazda, Wojciech Kostowski, Thermo-ecological assessment of CCHP (combined cold-heat-and-power) plant supported with renewable energy, Energy, Energy 92 (3) (2015) 279–289. ISSN 0360-5442, https://doi.org/10.1016/j.energy.2015.02.005.

[39] Wojciech Stanek, Analiza Egzergetyczna W Teorii I Praktyce, Wydawnictwo Politechniki Śląskiej, 2016.

[40] Wojciech Stanek, Lucyna Czarnowska, Thermo-ecological cost – szargut's proposal on exergy and ecology connection, Energy Volume 165 (2018) 1050–1059, https://doi.org/10.1016/j.energy.2018.10.040. Part B.

[41] J. Szargut, Exergy Analysis: Technical and Ecological Applications, 2005.

[42] W. Stanek, Method of Evaluation of Ecological Effects in Thermal Processes with the Application of Exergy Analysis, Silesian University of Technology Press, 2009 (in Polish).

[43] J. Szargut, A. Ziębik, W. Stanek, Depletion of the non-renewable natural exergy resources as a measure of the ecological cost, Energy Convers. Manag. 43 (9–12) (2002) 1149–1163.

[44] L. Czarnowska, Thermo-ecological Cost of Products with Emphasis on External Environmental Costs (Koszt Termo-Ekologiczny Wybranych Produktów Z Uwzględnieniem Zewnętrznych Kosztów Środowiskowych, 2014.

[45] M. Faist Emmenegger, T. Heck, N. Jungbluth, "Erdgas. In: sachbilanzen von Energiesystemen: grundlagen für den okologischen Vergleich von Energiesystemen und den Einbezug von Energiesystemen in Okobilanzen für die Schweiz, in: R. Dones (Ed.), Swiss Centre for Life Cycle Inventories ", CH. Final Report Ecoinvent No. 6-V Swiss Centre for Life Cycle Inventories, Dübendorf, 2007. Online,, http://www.ecoinvent.org/database/olderversions/ecoinvent-version-2/reports-on-ecoinvent-2/reports-on-ecoinvent2.html.

[46] J. Szargut, W. Stanek, Thermo-ecological optimization of a solar collector, Energy 32 (4) (2007) 584–590, https://doi.org/10.1016/j.energy.2006.06.010. ISSN 0360-5442.

[47] T. Jan, Szargut, "Optimization of the design parameters aiming at the minimization of the depletion of non-renewable resources, Energy 29 (12–15) (2004) 2161–2169, https://doi.org/10.1016/j.energy.2004.03.019. ISSN 0360-5442.

[48] J. Szargut, Exergy Method: Technical and Ecological Applications, 2005.

[49] W. Stanek, L. Czarnowska, Vironmental externalities and their effect on the cost of consumer products, Int. J. Environ. Sustain Dev. 11 (1) (2012) 50–63.

# Paper III: Local and global evaluations of microgrid supported by RES

Contents lists available at ScienceDirect

Energy

journal homepage: www.elsevier.com/locate/energy

## Thermo-ecological assessment of microgrid supported with renewable energy

Wojciech Stanek [a,*], Agnieszka Szostok [b]

[a] Silesian University of Technology, Department of Thermal Technology, Poland
[b] Environmental Analysis Eko-Precyzja, Poland

ARTICLE INFO

Handling editor: Henrik Lund

*Keywords:*
Energy efficiency
Thermo-ecological cost
Renewable energy
Microgrid

ABSTRACT

The current energy policy stresses the need for ongoing technological advancements towards more sustainable energy systems. Microgrids powered by renewable energy are key solutions to achieving this goal. This article presents a detailed Thermo-Ecological Cost (TEC) analysis of a microgrid integrating various renewable resources, such as wind, photovoltaic, photovoltaic-thermal, and biogas CHP plants. It discusses the challenges of evaluating local energy efficiency, which is often inadequate for comparing renewable and non-renewable technologies. A system-wide analysis, based on the global energy balance, provides a more accurate assessment. The paper introduces TEC as a more suitable method for evaluating and comparing the energy and ecological efficiency of diverse systems, with practical examples illustrating both local and system-level TEC evaluations of renewable energy-supported microgrids.

### 1. Introduction

In contemporary societies, energy is regarded as a key driver of progress, playing a crucial role in economic development. It serves as the foundation for human survival and advancement. Ensuring a sustainable energy supply while minimizing environmental pollution has become a global concern, one that is shared by all nations today [1]. Sustainable energy refers to the kind of energy generated and utilized in a manner that fosters human development across social, economic, and environmental aspects. Hence, attaining this objective requires a shift towards affordable, clean, abundant, and renewable sources that are easily accessible and exploitable [2]. The decrease in the costs of renewable energy (RE) technologies in recent years and the incorporation of smart energy systems are pivotal elements that will facilitate a transition toward green energy [3]. As a key component of the electric power industry, microgrids are recognized as one of the most promising approaches to integrating renewable distributed generation. This integration enhances the utilization of renewable energy, minimizes power transmission and distribution losses [4].

A microgrid is an electrical power system that consists of a collection of distributed energy resources and loads. It has the capability to operate in both grid-connected and islanded modes, providing flexibility in its operation depending on the situation [5]. In the grid-connected mode, the capability to function either in connection with the utility grid or autonomously, contingent on the current environmental conditions [6]. This form of network serves as an alternative to conventional power systems and is regarded as a more environmentally friendly choice, primarily attributable to its utilization of renewable sources [7,8]. The microgrid constitutes a vital component of the smart grid, boasting substantial application prospects due to its flexibility, high efficiency, and rapid recovery capability [9]. Nonetheless, energy management is a challenge for microgrids relying on renewable resources, given the intermittent and random nature of production. The inherent imbalance of microgrids, coupled with the probabilistic nature of renewable energy and electricity prices, complicates the energy management process [10]. As a result, the use of energy storage systems and specialized controllers, combined with integrated energy management strategies, is crucial to effectively manage the system and ensure optimal performance [11,12]. Effective management of distributed energy resources is crucial in designing microgrid systems [13].

In energy systems reliant on Variable Renewable Energy (VRE) like solar energy (PV, PV/T) and wind energy (wind turbines), a crucial consideration stems from the inherent intermittency of the primary sources of renewable generation. High shares of Variable Renewable Energy in the power grid imply an increase in adaptability and flexibility of the electricity system [14]. Consequently, harnessing the

* Corresponding author.
*E-mail addresses:* wojciech.stanek@polsl.pl (W. Stanek), agnieszka.szostok@eko-precyzja.eu (A. Szostok).

https://doi.org/10.1016/j.energy.2024.134256
Received 16 July 2024; Received in revised form 20 December 2024; Accepted 21 December 2024

complementarity of the system becomes paramount to effectively fulfil demand and mitigate the risks associated with electricity supply [15]. The planning of power systems, especially those reliant on less flexible generation sources, requires a comprehensive approach that integrates spatial, temporal, and technical considerations. This holistic approach is key to ensuring a well-coordinated dispatch of generating units. In the absence of predictable generation units, such as conventional power plants, models may overestimate the integration of renewable energy sources while underestimating the need for flexible resources. Therefore, careful consideration of these factors is essential for effective power system planning and operation [16]. The combination of different RES operating within a microgrid can be equipped with a smart meter and have the ability to share and trade energy, this is called a smart microgrid or smart grid [17]. VRE must take into account variability related to, for example, energy storage. There are many ways to store energy, but this article focuses on the electrolysis/fuel cell system. Energy is stored by producing hydrogen in the electrolysis process and then using it in a fuel cell [18,19]. There are other solutions. Integrating electric vehicles (EVs) into microgrids through vehicle-to-grid (V2G) and grid-to-vehicle (G2V) models optimizes grid stability and facilitates efficient renewable energy use, addressing challenges of fluctuating supply and demand [20]. Integrating reversible pumped hydro storage into microgrids significantly enhances operational efficiency and system stability, particularly when managed by advanced hybrid optimization methods that address nonlinearities and vibration issues [21]. When combined with passive systems such as Trombe walls and underground air ducts, optimized renewable microgrids significantly reduce energy consumption and help achieve net-zero-energy building goals [22]. Optimally sizing renewable energy sources and battery storage within multi-microgrid systems enhances network reliability and efficiency, particularly when accounting for diverse load patterns and power loss considerations [23]. Optimizing the sizing of renewable resources within microgrids is essential for reducing both costs and dependency on grid power, especially in areas with limited connectivity, e.g. rural areas [24].

Current trends in the design of complex process control systems require an increasing integration of mathematical methods, control engineering techniques, new control structures based on distribution, embedded network control systems, and modern information and communication technologies. Advanced control methods and new distributed embedded control structures represent the most effective tools for achieving high performance in many technological processes. These considerations are also worth exploring in the context of controlling multigeneration microgrids, particularly those based on renewable energy sources, where effective management and resource optimization are crucial for ensuring stability and sustainable development [25].

The paper [26] introduces analysis using TEC (thermo-ecological cost) for a CCHP (combined cold-heat-and-power) trigeneration system, utilizing both renewable and non-renewable resources. It compares TEC with TEA (thermo-economic analysis), emphasizing TEC's advantages, particularly in revealing the true high costs associated with purchased electricity. The article recommends the use of the TEC methodology for evaluating both simple and hybrid energy conversion systems, addressing sustainability concerns such as resource utilization, conversion efficiency, and waste generation across the system's life cycle. The article [27] employs a life cycle thermo-ecological cost (LC-TEC) approach to assess the environmental performance of wind turbines with varying capacities and performance attributes. The study [28] enhances current understanding by providing a comprehensive life cycle assessment (LCA) of electricity generated by micro wind turbines with a vertical axis. For impact assessment, two methods were chosen: the CML-IA and Thermo-Ecological Cost in the whole life cycle (TEC-LC). The study [29] investigates the efficiency of a Carnot Battery and conducts a sustainability analysis based on thermodynamics using various methodologies. It involves utilizing electricity from renewable sources to power a heat pump, followed by exergy-based sustainability and thermo-ecological cost analyses. The primary goals of the study [30] include conducting a dynamic thermo-ecological cost (TEC) assessment and performance analysis of a multi-generation system comprising an internal combustion engine fueled by natural gas, a heat pump, a reverse osmosis desalination plant, and a magnesium-chlorine (Mg–Cl) thermochemical water splitting cycle. The environmental impact of the system is also evaluated using the TEC method. The article concludes that TEC proves to be an effective method for assessing the environmental performance of different energy systems and facilitating comparisons among them. The article [31] presents an exergo-ecological analysis utilizing the TEC concept (thermo-ecological cost). It introduces TEC indicators for various versions of the energy mix and analyses the systems regarding natural resource management. The thermo-ecological analysis reveals that the most efficient energy mixes in terms of natural resource management are those that leverage the advantages of each component, supported by energy storage. The article [32] indicates that local energy analysis focused on resource efficiency alone becomes inadequate since it overlooks the quality of individual energy carriers. Such analysis yields conclusions different from those derived from a global perspective, as evidenced by the results presented in the article. The article [33] explores various scheduling strategies for coordinating an energy storage system with wind turbines. The impact of these strategies is evaluated within both local and global balance boundaries. The article [34] presents findings on the thermo-ecological cost assessment of renewable energy sources, outlining their overall environmental impact. The evaluation includes biogas, wind, and photovoltaic power plants, showcasing their cumulative environmental impacts through the application of the thermo-ecological cost methodology. Articles [26–34] presented the importance of using a global assessment to assess systems powered by renewable energy sources, which was the basis for undertaking a microgrid assessment using TEC.

This study evaluates the ecological efficiency of renewable-integrated microgrids by using the exergy-to-ecological cost ratio, aiming to identify optimal technologies and configurations for resource and cost reduction. Amidst climate change and resource depletion, microgrids offer critical alternatives for minimizing environmental impact and increasing grid independence, especially in regions with unstable energy access.

The study's thermo-ecological framework combines exergy efficiency and ecological impact for a holistic assessment of renewable microgrids. By integrating diverse energy sources and advanced management systems, it highlights resource optimization, load balancing, and system resilience. This approach demonstrates significant emission reduction potential while offering practical insights for sustainable microgrid design.

## 2. Description and characteristic of the analysed system

The analysed system is based on renewable energy sources, with the operating diagram presented in Fig. 1. The designed microgrid integrates various renewable energy sources, including a wind turbine, photovoltaic system, photovoltaic-thermal system, and a biogas Combined Heat and Power (CHP) plant (which generates both electricity and heat from biogas). To enhance the system's resilience against the variability of renewable energy generation, an energy storage system is utilized. In case of shortages, emergency power supply from the grid is also available. Heat generation is provided by the biogas CHP plant, PV/T system, solar collectors, and, in emergencies, by heat pumps (both ground-source and air-source). Cooling is supplied by heat pumps and an adsorption chiller.

Electricity generated from renewable energy sources (RES) is first directed to meet the current consumption demands of end users. Any surplus energy produced by the RES is stored in an energy storage system, which consists of an electrolyser, hydrogen storage, and a fuel cell. When renewable energy sources are insufficient to meet the microgrid's

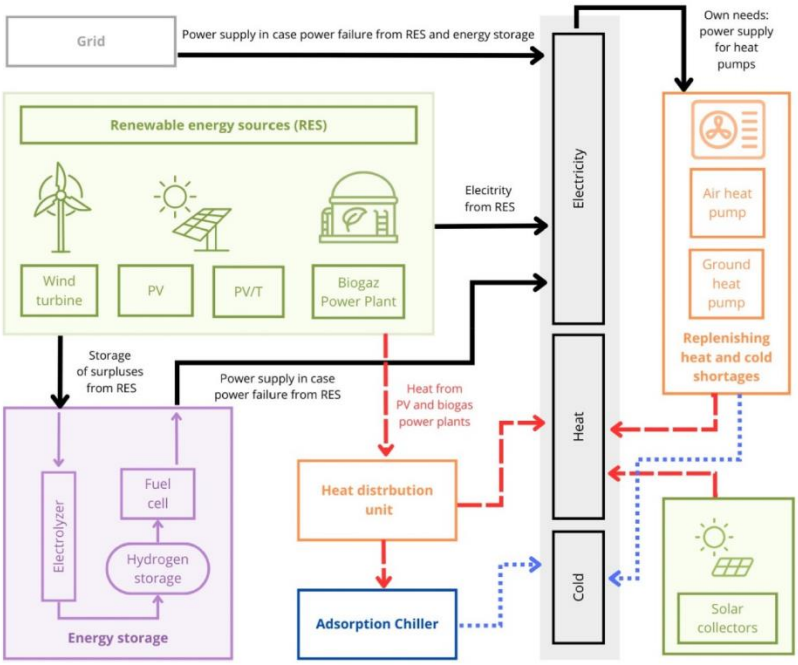


**Fig. 1.** General scheme of analysed system.

current demand, energy is drawn from the storage system. If this is still inadequate and the current consumption exceeds the combined output from the RES and energy storage, power is supplied from the grid.

Heat is also produced within the system, primarily from the PV/T system and the biogas CHP plant. Additionally, solar collectors are incorporated into the system, primarily to produce hot utility water, especially during the summer months. The heat generated by the PV/T system and the biogas CHP plant can also be utilized for cooling, thanks to the adsorption chiller integrated into the system. When the heat generated within the system does not meet current demand, the heat pump system, consisting of air-source and ground-source heat pumps, is employed. These heat pumps enable the generation of heat and cooling, helping to balance any shortages in the system.

A variety of different devices were utilized in the system to analyse the different operating scenarios of the microgrid. The cases considered included both the interaction of all system elements and only their parts. The graphs below illustrate the production of electricity, heat and cooling when all the elements of the system are functioning together. (Figs. 2–4). In the summer, solar radiation—primarily from PV and PV/T systems—accounted for a significant share of energy (Fig. 2). In December, the wind turbine generated the largest share of energy.

Heat production (Fig. 3) varies throughout the year. During winter, spring, and autumn, low outdoor temperatures drive high heat demand, met by the biogas plant and heat pumps (both ground-source and air-source). In summer, heat demand is mainly for domestic hot water, with high solar radiation allowing solar collectors and PV/T systems to generate most of the heat.

Cooling demand (Fig. 4) occurs only in summer. Heat from the biogas plant is used for cooling via an adsorption chiller, with heat pumps (ground-source and air-source) providing additional cooling when needed.

The monthly summaries presented were generated using hourly data for the entire year. These values were derived from meteorological data specific to the location of Katowice, Poland. Fig. 5 presents an example of a daily profile.

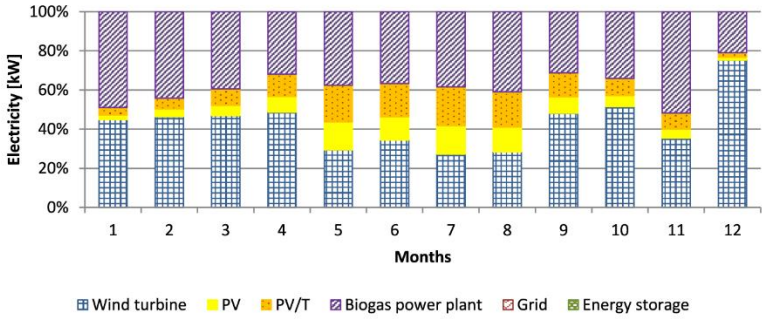


**Fig. 2.** Structure of electricity production in the microgrid.

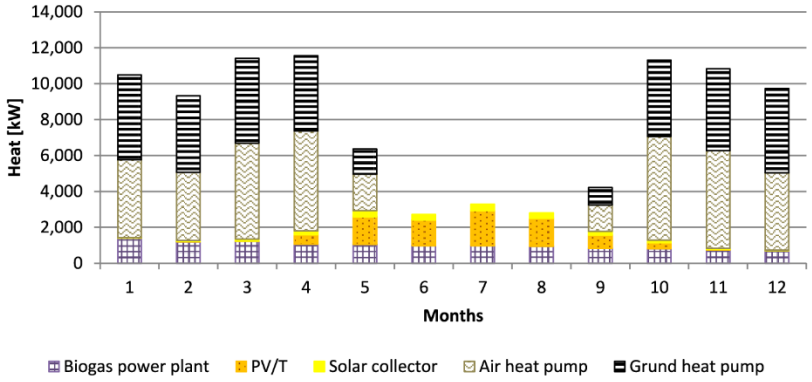


**Fig. 3.** Structure of heat production in the microgrid.

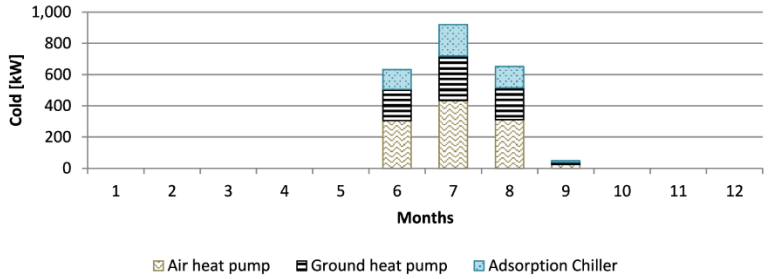


**Fig. 4.** Structure of cold production in the microgrid.

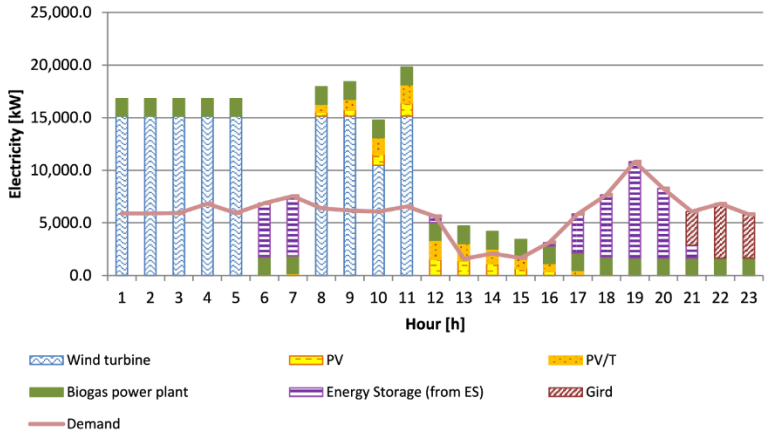


**Fig. 5.** Daily structure of electricity production in the microgrid.

### 2.1. Photovoltaics

The amount of solar radiation converted into electricity by a photovoltaics panel can be determined using the following equation (1)

$$E_{PV} = \eta_{e_{PV}} A_{PV} I_{\beta} \quad (1)$$

The efficiency of converting solar radiation into electricity depends on both the intensity of the radiation incident on the panel and the temperature. Therefore, energy efficiency calculations were performed across efficiency ranges typically reported in the literature [35–37]. An example of efficiency range is shown in Fig. 6.

### 2.2. Collector system

The amount of solar radiation converted into heat by a thermal collector can be determined based on the energy efficiency values, which were calculated using typical efficiency ranges found in the literature [38]. An example of the efficiency range is shown in Fig. 7.

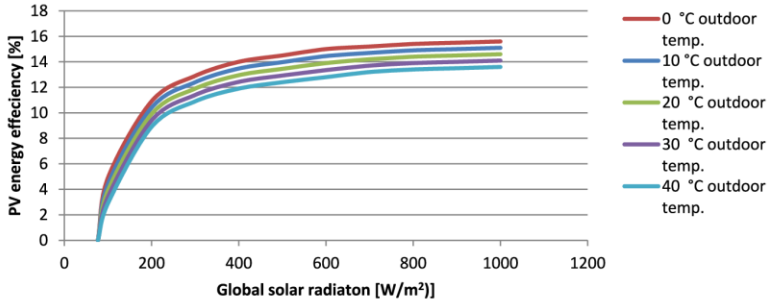


**Fig. 6.** The relation of global radiation, outdoor temperature and energy efficiency of photovoltaics panel.

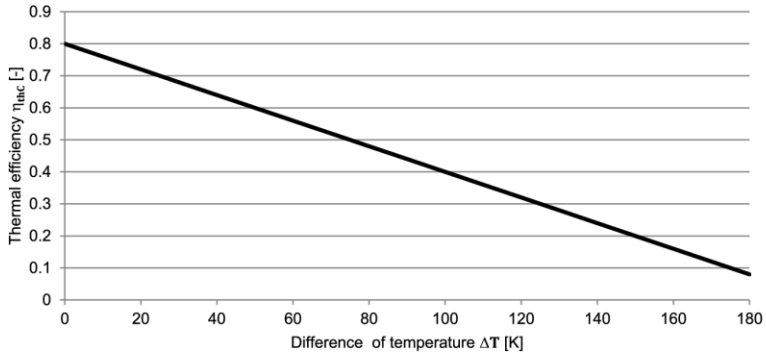


**Fig. 7.** Thermal efficiency characteristic of the collector system (based on [26]).

### 2.3. Photovoltaic/thermal system

Firstly, the amount of generated heat from solar radiation for the photovoltaic/thermal (PV/T) system is calculated. This heat is then transferred via the exchanger to the water tank. The cooling process begins when the cell temperature exceeds the threshold of 30 °C. The PV/T thermal efficiency of the PV/T system is determined using characteristics that were established based on [39,40] (eq. (2)).

$$\eta_{th} = \eta_0 - \frac{\alpha(T_{eg\ out} - T_O)}{I_\beta} \tag{2}$$

Where:

$\eta_0$ is 0.6099,

$\alpha$ is heat transfer coefficient ($\alpha = 5.8343\ W/(m^2K)$),

$\eta_{th}$ is PV/T thermal efficiency,

$T_{eg\ out}$ is the temperature of the working medium flowing out the photovoltaic/thermal (PV/T) panel (outlet temperature ergolide).

Thermal efficiency of photovoltaic/thermal (PV/T) system is presented in Fig. 8.

PV/T energy efficiency therefore is calculated from equation (3):

$$\eta_{e_{PVT}} = 0.1464\,\frac{T_{eg\ out} - T_O}{I_\beta} - 0.6828 \tag{3}$$

Where:

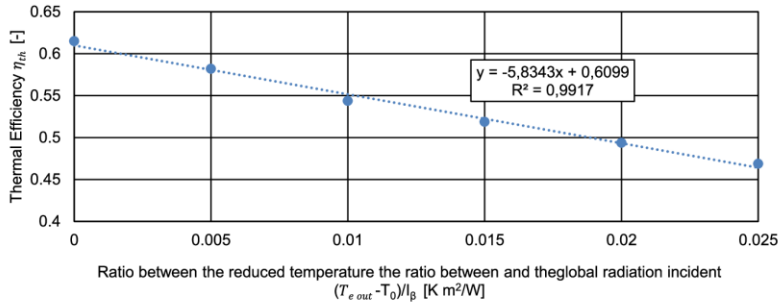


**Fig. 8.** Thermal efficiency of photovoltaic/thermal (PV/T) system.

$T_{eg_{out}}$ is temperature of the working medium flowing out the photovoltaic/thermal (PV/T) system panel (outlet temperature ergolide).

It should be emphasized that hourly solar radiation data were utilized in the calculations for the solar collector, PV, and PV/T systems.

### 2.4. Wind turbine

Fig. 9 illustrates the characteristics of a wind turbine, depicting the relationship between wind speed (v) and the power output ($P_w$) of the wind turbine. The graph is based on the power characteristics of the V90–3.0 MW turbine [41].

### 2.5. Biogas power plant

The ICE module (internal combustion engine) operates on biogas, generating both electricity and heat in the form of hot water. The hot water is produced through heat recovery processes involving the engine's cooling systems (jacket water and oil cooling) as well as the exhaust gases. These gases pass through a heat recovery exchanger before being released into the atmosphere via a stack. The internal combustion engine (ICE) can operate at full load for approximately six months each year. During the remaining five months, its load is limited to about 70 % of its nominal capacity. Under full load operation, the total exergy efficiency of the engine is expressed as [42]:

$$\eta_B = \frac{N_{el} + \Phi \dot{Q}}{\beta \dot{E}_{chem}} \tag{4}$$

Where:

$\Phi$ - Carnot factor,

$\beta$ - exergy to LHV ratio.

### 2.6. Energy storage

Fig. 10 shows the characteristics of an electrolyser, illustrating the relationship between the reduced power and the efficiency of the electrolyser.

The mass stream of hydrogen produced in the process of electrolysis is calculated from equation (5):

$$\dot{m}_{h_2} = \frac{\eta_e P_{AC}}{Q_{wH_2}} \tag{5}$$

where:

$\dot{m}_{h_2}$ - mass stream of hydrogen produced in the process of electrolysis [kg/h]

$\eta_e$ - electrolyser efficiency [−],

$P_{AC}$ - power delivered to the hydrogen generator [kW]

$Q_{wH_2}$ - hydrogen calorific value [kWh/kg].

Fig. 11 shows the characteristics of the fuel cell, illustrating the relationship between the reduced power and the efficiency of the fuel cell.

Power of fuel cell used to meet needs is calculated from equation (6):

$$P_{el} = \eta_{FC}\, \dot{m}_{h_2} Q_{wH_2} \tag{6}$$

where: $\eta_{FC}$ - fuel cell efficiency [−].

The surplus energy generated by the renewable energy sources (RES) is directed to the electrolyzer, where it is used to produce hydrogen. This hydrogen is stored and, in times of energy shortage, is converted back into electricity within a fuel cell.

### 2.7. Air source heat pump

Fig. 12 shows characteristics of air heat pump [44] the relation between the inlet air temperature and heat power and electricity consumption.

Fig. 13 shows characteristics of the air heat pump, illustrating the relationship between the inlet air temperature, cold power and electricity consumption.

### 2.8. Ground-source heat pump

Electricity, heat, and cooling were determined as a function of the heat-transfer agent input temperature (Fig. 14) [45–49].

### 2.9. Adsorption chiller

The adsorption chiller is powered by heat from renewable energy sources. The coefficient of performance (COP) of the device depends on the temperature of the water supplying the adsorption chiller (Fig. 15) [51].

The calculations assumed a constant COP value, and the cooling output was determined using equation (7):

$$Q_{Ads} = COP\, Q_{ads-in} \tag{7}$$

$Q_{Ads}$ – cold produced in an adsorption chiller [kW],

$Q_{ads\text{-}in}$ – heat directed to an adsorption chiller [kW].

### 2.10. Electricity demand

Hourly data were used in the analysis to ensure a detailed and accurate representation of the system's performance over time [52]. An example of the daily distribution of electricity consumption is presented in Fig. 16.

The maximum instantaneous demand of the system during the analysed year is 15 MW. For the study, it was assumed that the total power

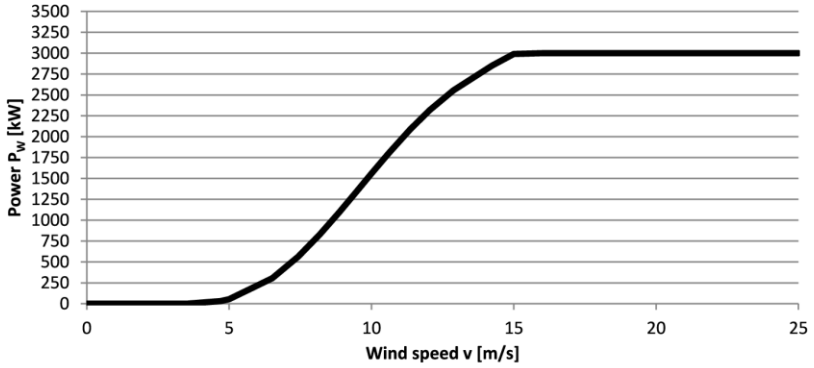


**Fig. 9.** Electric power curve as a function of speed (based on [41]).

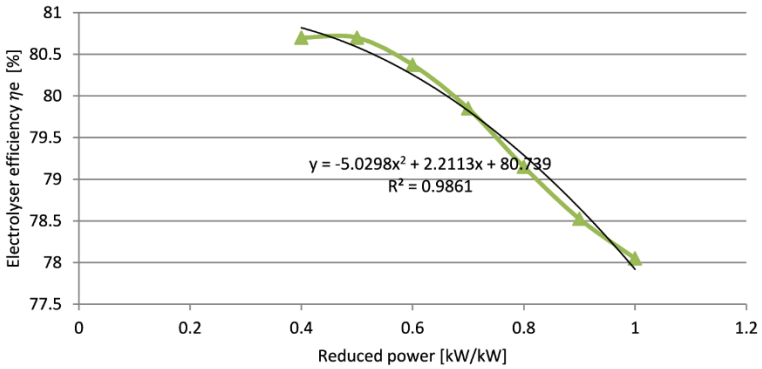


**Fig. 10.** Electrolyser efficiency (based on: [43]).

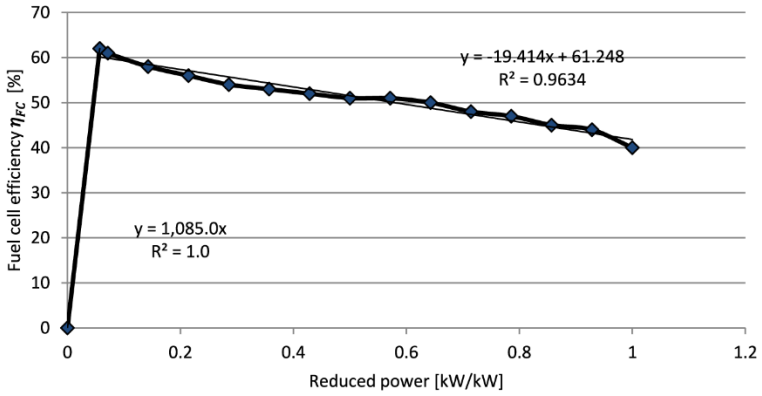


**Fig. 11.** Fuel cell efficiency (based on: [43]).

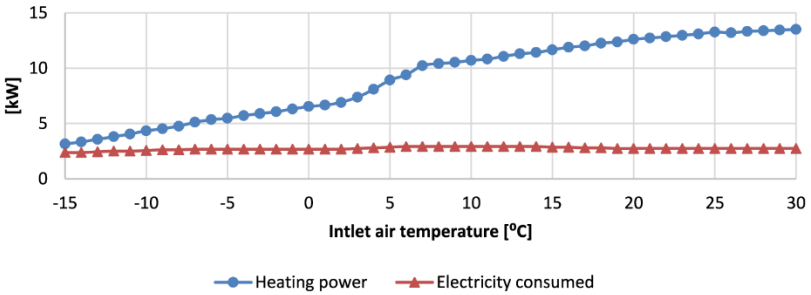


**Fig. 12.** *Characteristics of the air heat pump - heating (based on* [44]).

of the energy-generating sources in the system is 15 MW.

### 2.11. Heat and cold demand

The heat demand for central heating is calculated as presented in eq. (8).

$$\frac{Q_g}{Q_{gmax}} = \frac{t_w - t_z}{t_w - t_{zmin}} \tag{8}$$

Where:

$Q_g$ – heat [kW],
$Q_{gmax}$ – maximum heat [kW], data from calculations in PURMO,
$t_w$ – inside temperature[kW],
$t_z$ – outside temperature [°C],
$t_{zmin}$ – minimum outside temperarure [°C].

Domestic hot water was assumed to follow a daily, repeatable profile based on typical consumption pattern [53], as shown in Fig. 17.

Totality amount of heat is calculated from eq. (9).

$$Q = Q_g + Q_{hotwather} \tag{9}$$

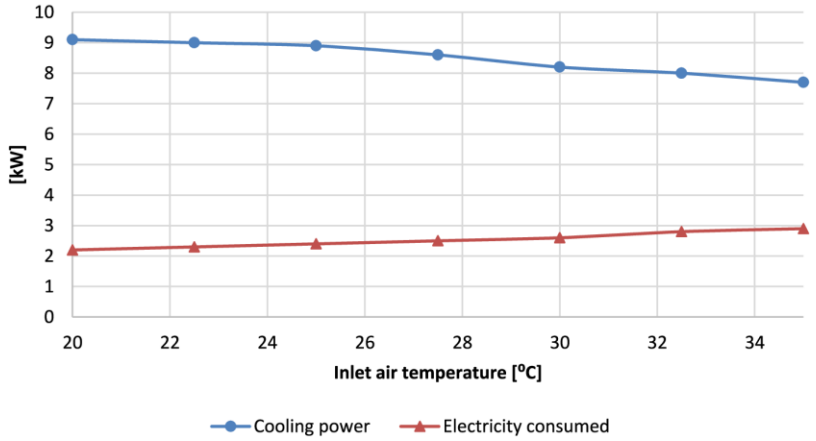


**Fig. 13.** *Characteristics of the air heat pump - cooling (based on* [44]).

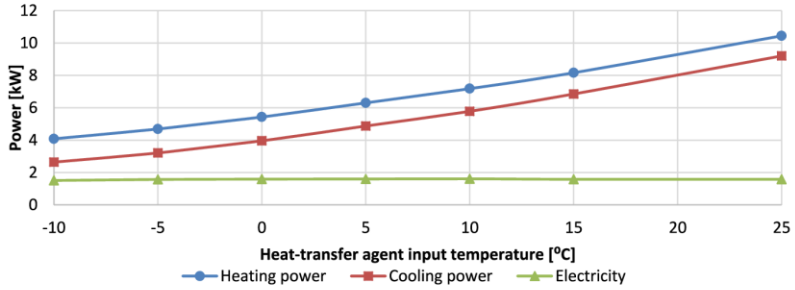


**Fig. 14.** *Characteristics of the heat ground pump (based on* [50]).

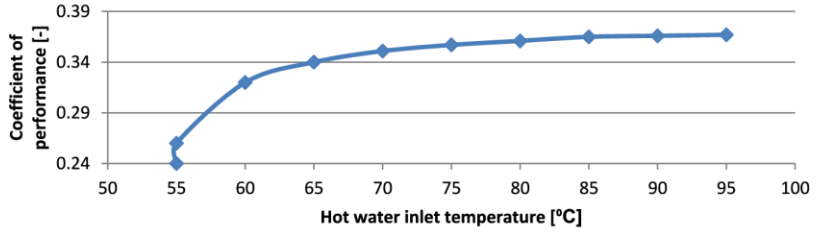


**Fig. 15.** Adsorption chiller characteristic (based on [51]).

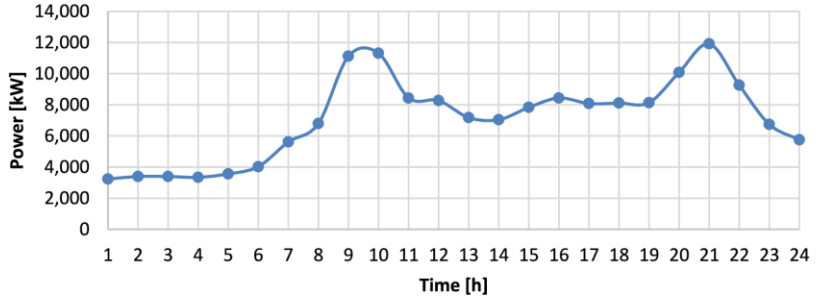


**Fig. 16.** An example of the distribution of daily electricity consumption [52].

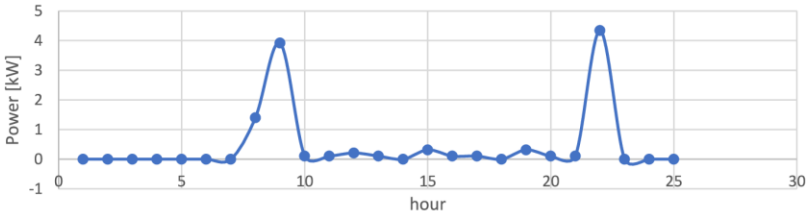


**Fig. 17.** Domestic hot water (DHW) profile.

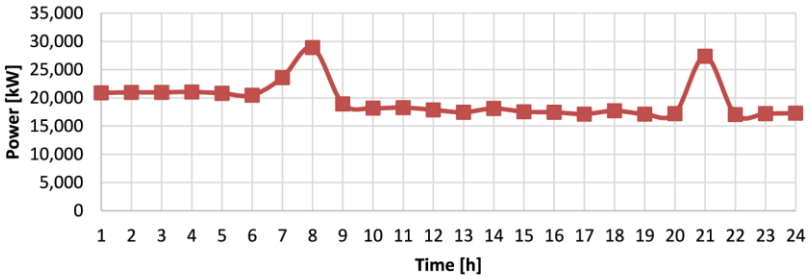


**Fig. 18.** An example of the distribution of daily heat consumption [52].

An example of the distribution of daily heat consumption is shown in Fig. 18.

Cooling demand is calculated using eq. (10).

$$\sum Q_{ji} = Q_{jL} + Q_{oc} + Q_{r,i} + Q_{ps,i} + Q_{losses,i} \tag{10}$$

$Q_{jL}$ - rate of heat flow from people [kW],

$Q_{oc}$ - rate of heat flow from machines and lighting [kW],

$Q_{r,i}$ - rate of heat flow from solar radiation (depending on the total intensity of total radiation in a hour of the year),

$Q_{ps,i}$ - rate of heat flow from fresh air [kW],

$Q_{strat,i}$ - heat losses through partitions depending on the outside temperature $t_{ab}$ [kW],

An example of the distribution of daily cold consumption is shown in Fig. 19.

## 3. Thermo-ecological cost – methodology

In the article employs TEC method - the yearly thermo-ecological cost. It serves as an assessment metric employed for gauging the effectiveness of natural resource utilization. TEC integrates exergy, serving as an indicator of resource quality, along with cumulative calculus, providing a means to evaluate the overall exergy-ecological performance. This encompasses the representation of non-renewable resources through cumulative exergy consumption [26,54,55]. It is important to highlight that the thermo-ecological cost, as a systemic approach, holds significant importance in comparing various energy systems. One way to illustrate the physical and ecological cost of each product, encompassing the total consumption of natural resources from their extraction, is through the Thermo-Ecological Cost (TEC) method. This approach integrates both the energy and environmental impacts, providing a comprehensive evaluation of resource use and ecological effects throughout the product's lifecycle.

The thermo-ecological cost encompasses the exergy utilization of non-renewable resources obtained directly from nature, such as freshwater, fuels, and mineral ores. Highlighted among the most crucial applications of TEC are.

- Assessing the effect of introducing harmful substances into the environment on the depletion of non-renewable resources.
- Assessing the influence of operational parameters of energy systems on the depletion of fossil fuel reserves.
- Optimizing operational parameters, production structures of a specific utility product, and design parameters to minimize the depletion of non-renewable resources.
- Selection of technology ensuring minimum depletion of non-renewable resources.
- Estimating the degree of sustainable development.
- Analysis of the impact of cross-regional exchange on the depletion of non-renewable resources.
- Calculating the amount of pro-ecological tax to replace existing taxes.
- Assessing the impact of individual consumer goods on the depletion of non-renewable resources throughout their entire life cycle [56–58].

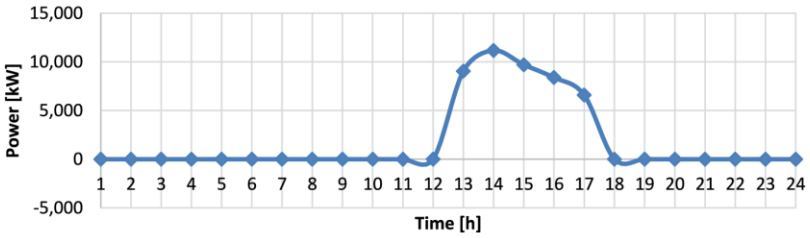


**Fig. 19.** An example of the distribution of daily heat consumption [52].

TEC can increase due to the consumption of by-products exchanged within the system. In this case, the thermo-ecological cost of pollutants is measured by the energy needed to prevent their release into the environment, such as the exergy used in emission reduction systems. If preventing the release is not possible, the TEC should reflect the exergy required to mitigate the environmental impact of these pollutants [59,60]. In certain processes, by-products can substitute for the main product in other processes, consequently reducing the TEC value of the main product under consideration [57,61,62]. We can define the specific thermo-ecological cost using three components (eq. (10)) [56–58,61,63].

$$\rho_j = \sum_n b_{nj} + \sum_k p_{kj}\zeta_k - \sum_e \left(f_{ej} - a_{ej}\right)\rho_e \tag{11}$$

where:

$\zeta_k$ - thermo-ecological cost of $k$-th harmful substance, [MJ/kg].

$b_{nj}$ - exergy of $n$-th non-renewable natural resource immediately consumed in the process under consideration per unit of $j$-th product, [MJ/kg],

$p_{kj}$ - amount of $k$-th harmful substance from $j$-th process, [kg].

$a_{ej}$ - coefficient of consumption of e-th material per unit of $j$-th main product, e.g. in kg/kg or [kg/MJ].

$f_{ej}$ - coefficient of by-production of $e$-th product per unit of $j$-th main product, e.g. in kg/kg or [kg/MJ].

$\rho_e$ - specific thermo-ecological cost of $e$-th product, e.g. in [MJ/kg].

Key assumptions guiding the TEC methodology include.

- Exergy as a measure of resource quality: TEC assumes exergy—representing the useful portion of energy capable of performing work—reflects resource quality and environmental impact, particularly in relation to the depletion of non-renewable resources.
- Cumulative exergy consumption: TEC assumes cumulative exergy consumption accurately represents the total environmental impact across a resource's life cycle, integrating all stages from extraction to disposal.
- System boundaries and pollutant accounting: TEC assumes well-defined system boundaries and effective pollutant management strategies (e.g., emission control and waste treatment).
- By-product substitution and resource efficiency: TEC assumes by-products can replace primary products in processes, reducing non-renewable resource consumption and lowering ecological costs.
- Thermo-Ecological Cost as a proxy for sustainability: TEC assumes minimizing thermo-ecological cost aligns with sustainable development goals, focusing on reducing non-renewable resource use and pollutant emissions, though it may not capture all sustainability dimensions [57,64].

A detailed explanation of how exergy analysis is applied to assess the quality of non-renewable natural resources, including considerations for reference states, resource depletion, and system by-products, can be found in studies such as Domínguez et al. (2014) [65] and Valero et al. (2018) [66].

Limitations of TEC concept include.

- The effectiveness of the thermo-ecological analysis depends on the specific availability of renewable resources like solar and wind energy. This availability varies based on geographical and seasonal factors, making the results location-specific and less generalizable across different climates or regions.
- The study acknowledges the intermittency and variability of renewable energy sources, which complicates consistent energy management within the microgrid. This limitation requires advanced storage solutions or backup sources, impacting both the reliability and cost-effectiveness of the system.
- While exergy analysis is valuable, it does not encompass all ecological impacts, such as those associated with pollutants. The model assumes that pollutants' thermo-ecological costs are limited to the energy required to prevent or mitigate their environmental impact, which may overlook broader environmental and social costs.
- The analysis focuses primarily on ecological costs and technical efficiency, but does not address the socio-economic impacts on local communities or cost-sharing mechanisms. This oversight limits the applicability of the findings in policy and practical implementation contexts [67,68].

The integration of Life Cycle Assessment (LCA) with Thermo-Ecological Cost (TEC) methodology has been effectively demonstrated in previous research. For example, Czarnowska et al. (2014) evaluated the environmental quality of fossil fuels by combining these approaches [69]. Similarly, Stanek et al. (2015) conducted a detailed analysis of the thermo-ecological cost of hard coal across its entire life cycle [70]. These studies highlight the potential of combining LCA and TEC for a more comprehensive assessment of resource and environmental impacts.

## 4. Thermo-economic analysis – methodology

The objective of thermo-economic analysis is to assess, optimize, and diagnose energy-intensive systems. This approach combines considerations of exergy (based on the second law of thermodynamics) and cost (economic factors) [71–73].

The first step in TEA is defining system boundaries and identifying all components, such as turbines, boilers, and compressors. Each component is modelled based on its input-output relationships for energy, exergy, and cost. Defining the scope is crucial for setting clear boundaries in the economic and energetic analysis. TEA uses exergy analysis, grounded in the Second Law of Thermodynamics, to assess how efficiently each component utilizes available energy. This analysis identifies losses due to irreversibilities (e.g., friction, heat loss) by assigning exergy values to inputs and outputs, which are then used to calculate exergy "cost" and "product" for each component.

Central concepts in thermo-economics involve the notions of fuel and product. The product of a component is derived from the objective of its operation, while the fuel is connected to the resources utilized to fulfil this objective. Consider a steam turbine, where the reduction in steam exergy represents the fuel, and this is harnessed to generate work, constituting the product. In every component (i) within a system, the fuel always exceeds the product, and the disparity accounts for irreversibility, such as losses or external inefficiencies.

$$F_i = P_i + I_i \tag{12}$$

Where:

$F_i$ – fuel of component (i), [W],

$P_i$ – product of component (i), [W],

$I_i$ – irreversibility rate, of component (i), [W],

The depiction of fuel and product flows for all plant components in a graphical format constitutes the productive structure of the microgrid. It's important to emphasize that the exergy cost specifically quantifies the exergy entering the analysed system. Consequently, it does not account for transformation processes situated upstream of the local system, distinguishing it notably from thermo-ecological cost.

In TEA, the economic cost of exergy destruction (or losses) is evaluated to understand how much the inefficiencies in each component contribute to the overall system cost. The exergetic cost can be defined as the total exergy consumed to produce the useful product. It is calculated from the following equation: 13 [74]:

$$k^* = \frac{B_F}{B_P} \tag{13}$$

Where:

$k^*$ - exegetic cost, [–],
$B_P$ – exergy of product [MJ],
$B_F$ – exergy of fuel [MJ].

TEA results can identify inefficiencies and guide decisions on system modifications, such as design changes, operational adjustments, or cost restructuring to improve performance. Optimization may focus on minimizing total costs, exergy destruction, or balancing both. TEA is particularly valuable in high-energy sectors, like power plants, where reducing exergy losses and optimizing costs can enhance efficiency and sustainability. By quantifying irreversibility and resource usage, TEA aids in designing systems that align with both economic and environmental goals, promoting resource conservation and pollution reduction for sustainable development [75,76].

## 5. TEC and TEA analysis of presented energy mix options

The analysed system is illustrated in Fig. 20. Flow 1, entering the water turbine, corresponds to the wind force. Flows 2, 3, and 7, entering the system, are associated with solar radiation and are sequentially directed to the PV, PV/T, and solar collector systems. Flow 4 represents the chemical energy utilized in the biogas plant, including the cogeneration generator. Flows 5 and 6 are linked to the lower heat source of the heat pumps, with the exergy in Flow 6 for the air heat pump assumed to be 0. The final flow entering the system, Flow 8, represents the emergency power supply from the grid.

Electricity from the wind turbine, PV, PV/T, and biogas plants (Flows 9, 10, 11, 12) is directed to Component 8 (energy distribution). Energy distribution generates flows that serve the system's internal needs: heat pumps (Flows 16 and 17) and energy storage (Flow 13). In case of an energy shortage, Flow 14 (previously stored energy) is directed to energy distribution. Flow 15 represents electricity supplied to consumers.

Component 10 (heat distribution) is fed by flows from the PV/T, biogas CHP plant, ground-source heat pump, air heat pump, and solar collector (Flows 18, 19, 20, 21, 22). From the heat distribution, heat flows are directed to consumers (Flow 23) and to the adsorption chiller (Flow 25). The adsorption chiller produces cold, which is directed to cold distribution, also powered by heat pumps (Flows 26 and 27). From cold distribution, cold energy flows are directed to the consumers.

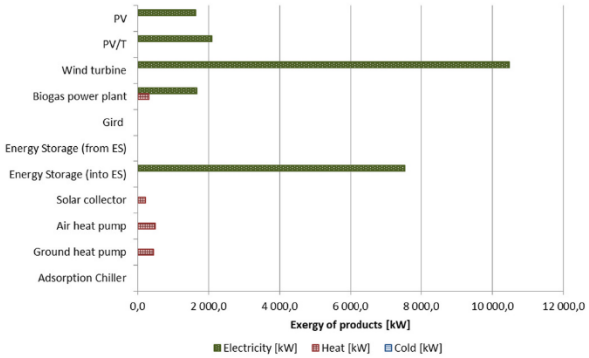


**Fig. 21.** Exergy values for 3rd April, 8 a.m.

The analysis carried out allows for the presentation of the state of the system (values of exergy flows) for each hour of the year. Table 1 below shows data for an example hour of the year (3rd April, 8 a.m.). The table presents two values for energy storage. Energy Storage (from ES) is a stream entering the system from energy storage, i.e., a stream that fills the energy shortages in the microgrid. Energy Storage (into ES) represents the values when the microgrid is powered by energy storage. In this case, the system—renewable energy sources produce more energy than the momentary demand, and the surplus energy is stored in energy storage. The table provides a snapshot of how energy and exergy flows are managed at a specific time, reflecting both generation and consumption patterns in the system. These values are crucial for understanding the balance between energy generation, storage, and demand in the microgrid.

For the adopted TEC indicators of the replaced processes, the fuel division indicators for the CHP (Combined Heat and Power) system between individual products (heat and electricity) were determined using the following equation: (14) and (15):

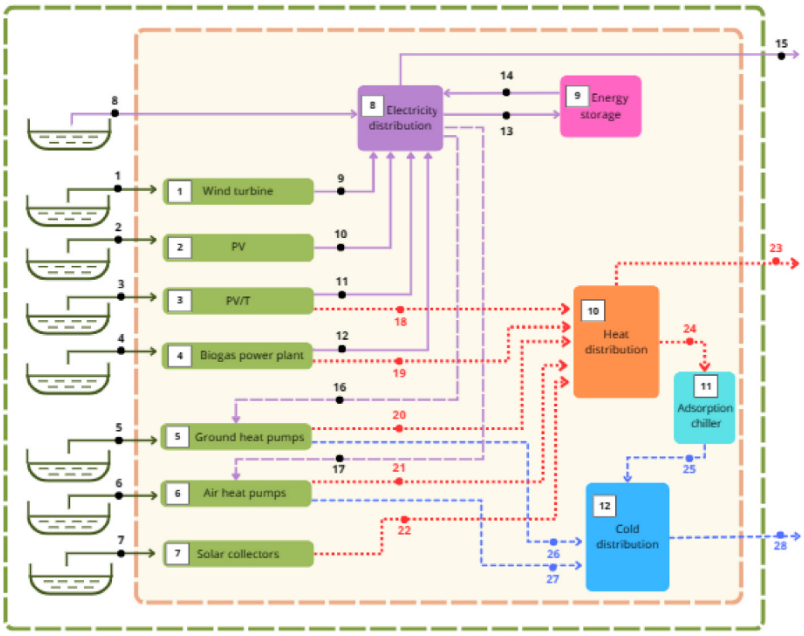


**Fig. 20.** Power system (micro grid) consisting of various renewable sources, storage energy and emergency power supply from the grid.

**Table 1**
Example exergy - 3rd April, 8 a.m.

| Name | F | P | $\eta_B$ | I | k* | (TEC) |
|---|---|---|---|---|---|---|
| – | kW | kW | – | kW | – | – |
| Electricity | | | | | | |
| PV | 13 233,2 | 1 621,5 | 0,1 | 11 611,8 | 8,2 | 0,3 |
| PV/T | 13 233,2 | 2 082,7 | 0,2 | 11 150,6 | 6,4 | 0,2 |
| Wind turbine | 36 087,6 | 10 465,4 | 0,3 | 25 622,2 | 3,4 | 0,1 |
| Biogas CHP plant | 1 459,1 | 830,6 | 0,6 | 628,5 | 1,8 | 0,7 |
| Gird (Polish grid energy mix) | 0,0 | 0,0 | – | – | – | 2,8 |
| Energy Storage (from ES) | 0,0 | 0,0 | – | – | – | 0,3 |
| Energy Storage (into ES) | 9 328,1 | 7 531,5 | 0,8 | 1 796,6 | 1,2 | 0,1 |
| **Heat** | | | | | | |
| PV/T | 0,0 | 0,0 | – | – | – | 0,1 |
| Solar collector | 1 320,0 | 209,2 | 0,2 | 1 110,9 | 6,3 | 0,6 |
| Biogas CHP plant | 505,3 | 305,5 | 0,6 | 199,8 | 1,7 | 0,3 |
| Air heat pump | 2 559,6 | 486,9 | 0,2 | 2 072,7 | 5,3 | 4,0 |
| Ground heat pump | 1 424,4 | 445,4 | 0,3 | 979,0 | 3,2 | 2,4 |
| **Cold** | | | | | | |
| Adsorption Chiller | 0,0 | 0,0 | – | – | – | 4,6 |
| Air heat pump | 0,0 | 0,0 | – | – | – | 0,0 |
| Ground heat pump | 0,0 | 0,0 | – | – | – | 0,0 |

$$\mu_Q = \frac{Q_{CHP} TEC_{Q,rep}}{\left(E_{el,CHP} TEC_{el,rep} + Q_{CHP} TEC_{Q,rep}\right)} \tag{14}$$

$$\mu_{el} = \frac{E_{el,CHP} TEC_{el,zast}}{\left(E_{el,CHP} TEC_{el,zast} + Q_{CHP} TEC_{Q,zast}\right)} \tag{15}$$

Where:

$u_Q$ – share of heat production in fuel consumption in CHP, [−],

$u_{ele}$ – share of electricity production in fuel consumption in CHP, [−],

$TEC_{Q,rep}$ – TEC of heat produced in CHP (of the replaced processes), [MJ/MJ] [77]

$TEC_{ele,rep}$ – TEC of electricity produced in CHP(of the replaced processes), [MJ/MJ] [77],

Specific fuel consumption rates with TEC distribution for individual products are calculated using the following eqs. (16) and (17):

$$x_Q = \frac{\mu_Q E_{ch,CHP}}{Q_{CHP}} \tag{16}$$

$$x_{el} = \frac{\mu_{el} E_{ch,CHP}}{E_{el,CHP}} \tag{17}$$

Where:

$x_Q$ - specific fuel consumption indicator with TEC section for heat, [−],

$x_{ele}$ - specific fuel consumption indicator with TEC section for electricity, [−],

$E_{ch,CHP}$ - chemical energy consumed by CHP, [kW].

The next part of the analysis presents exergy charts for sample days (hours) across each season. Figs. 21 and 22 display the results for 3rd April, 8 a.m.

For the determined $x_Q$ and $x_{ele}$ TEC indicators for heat and electricity, we calculate from eqs. (18) and (19).

$$TEC_{Q,CHP} = x_Q TEC_{FUEL} \tag{18}$$

$$TEC_{el,CHP} = x_{el} TEC_{FUEL} \tag{19}$$

Where:

$TEC_{FUEL}$ – TEC of CHP fuel, [MJ/MJ],

As evident, the primary source of electricity during spring production is the wind turbine. There is an excess of energy at this particular time of the year, which is then stored in the energy stratum. For heating purposes, energy is acquired through heat pumps. The system does not generate cold as there is no demand for it during the analysed period.

As shown in Fig. 22, at the analysed moment of the year, a significantly larger amount of exergy flows into the system than exits it, leading to an accumulation of energy through energy storage.

For the summer period, an example for July 28 at 2:00 p.m. was chosen, and the results are presented in Fig. 23.

In the summer example, the production is primarily generated by the PV and PV/T systems. It can be observed that the electricity produced is accumulated in the energy storage. The heat generated by the PV/T, solar collector, and biogas plant is utilized for domestic hot water production and directed to the adsorption chiller to produce cooling. Additionally, heating is supported by the district heating system and ground heat pump.

As shown in Fig. 24, the energy streams entering the system are primarily sourced solar radiation. Similar to the spring case discussed earlier, exergy is accumulated in the system through the use of energy storage.

For the autumn case, October 6th, 12 p.m. was chosen. The exergy flows for this period are presented in Fig. 25.

Electricity production occurs in the PV/T, PV, and biogas plants. However, unlike in the previous cases, the production is insufficient to meet the demand. As a result, electricity stored in the energy storage system is used. Unfortunately, the energy storage does not fully cover the needs, and the remaining shortages are supplemented by electricity from the grid. Heat is generated by the PV/T, biogas CHP plant, and solar collector, with any gaps being filled by ground source heat pumps.

In Fig. 26, the exergy streams entering and leaving the system during the autumn case are shown. The incoming fluxes are primarily the exergy of solar radiation. In this scenario, there is no accumulation of energy in the energy storage system.

For the winter case, night-time was selected for analysis to examine

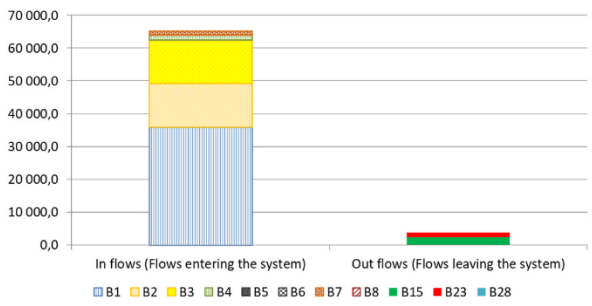


**Fig. 22.** In flows and out flows for 3rd April, 8 a.m.

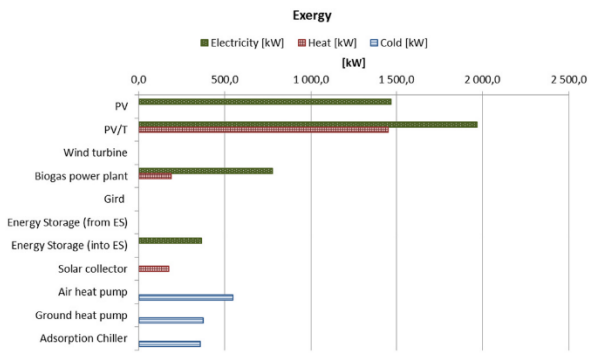


**Fig. 23.** Exergy values for 28th July, 2 p.m.

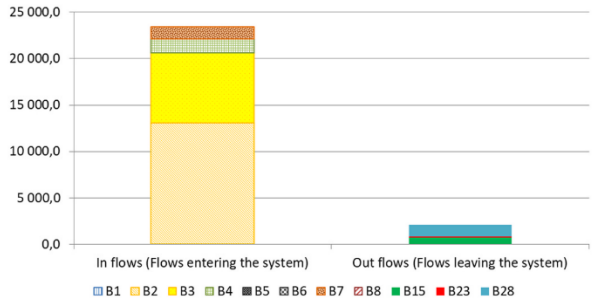


**Fig. 24.** In flows and out flows for 28th July, 2 p.m.

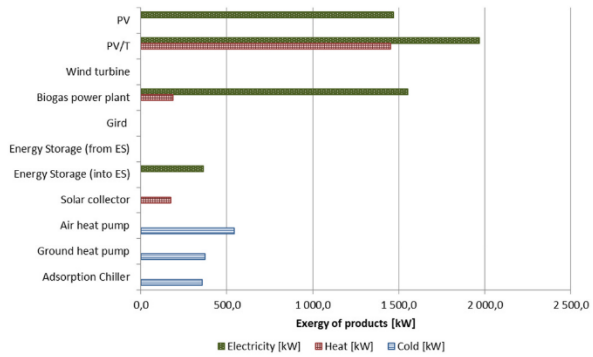


**Fig. 25.** Exergy values for October 6th, 12 p.m.

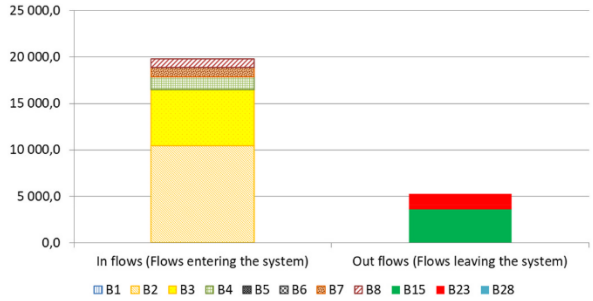


**Fig. 26.** In flows and out flows for October 6th, 12 p.m.

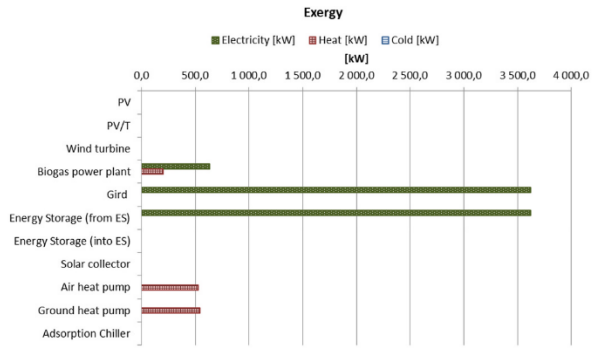


**Fig. 27.** Exergy values for 15th December, 10 p.m.

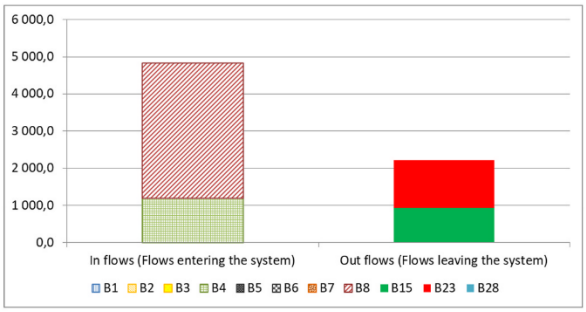


**Fig. 28.** In flows and out flows for 15th December, 10 p.m.

how the system functions under these conditions. Fig. 27 illustrates the exergy flows for 15th December at 10 p.m.

For the analysed period, electricity is generated solely by the biogas plant. However, this production is clearly insufficient to meet the demand, so the gaps are supplemented by energy from storage and grid.

As shown in Fig. 28, the system's incoming streams are primarily electricity from the grid, along with electrical and chemical energy from the biogas plant's substrate. The outgoing flow is lower than the incoming flow (even with the use of energy stored in the energy storage), which is attributed to the system's internal demands, particularly for powering the heat pumps that generate heat.

## 6. Conclusions

The study presented highlights the significance of understanding the origin of resources provided to the microgrid. While the traditional Thermo-Economic Analysis (TEA) proves effective in minimizing internal plant irreversibilities, it is not the suitable approach for evaluating systems with different external resource inputs (especially when we are dealing with renewable energy sources). Adopting a unity exergy cost at the system boundary can yield misleading conclusions. In hybrid systems, TEA outcomes may inaccurately suggest maximizing external resource utilization (without considering their origin) and minimizing energy processing within the system.

Conversely, the proposed Thermo-Ecological Cost (TEC) provides a clear evaluation of the resources provided to the system. In the discussed case, the microgrid contains locally consumed renewables (solar radiation, wind, biogas etc.) and hybrid external resources (electricity, primarily sourced from the coal-based Polish mix). Consequently, the cost associated with the three products generated in the system (electricity, heat, and cold) is directly tied to the input cost of the distinct resources supplied to the microgrid and to the intrinsic quality of the system. This relationship influences the incremental cost along the productive structure.

The study demonstrated that, in both the cases of electricity and heat, it is feasible to achieve a Thermo-Ecological Cost (TEC) below unity. This implies that the exergy of resources utilized to generate the product is lower than the exergy value of that specific product. Due to the persistent presence of non-renewable resources in the final product and the impacts of pollutants and life cycle considerations, achieving a Thermo-Ecological Cost (TEC) of 0 for the final product, an ideal scenario, is not currently feasible.

The analysis was performed for hourly data for the entire year. Data for four days in different seasons: spring, summer, autumn and winter are presented as sample results. It can be observed how variability affects the TEA and TEC results of the system. This is primarily related to the variability of weather conditions and, consequently, the production of electricity, heat and cold. Also, the demand for energy, heat and cold varies depending on external conditions. This means that it is impossible to find similar values for the system within a year. It is changeable and

dynamic. In conditions with good sunlight, we can observe high production values from sources powered by this source, i.e. PV, PV/T and solar collector. In the case of windy days, high electricity production values are recorded at the wind turbine. Similarly for other energy sources. The most stable source is a biogas plant that produces comparable amounts of electricity and heat per year. The element that helps stabilize the system is the energy store. Energy storage clearly affects the energy security of the microgrid, but there are times during the year when it is insufficient and then power from the grid is needed. Then the values in the TEC analysis are clearly higher, because electricity from the grid is sourced from the coal-based Polish mix.

This study emphasizes the importance of understanding the origin and efficiency of resources used in microgrid systems. It compares the Thermo-Ecological Cost (TEC) methodology with traditional Thermo-Economic Analysis (TEA), highlighting TEC's advantage, especially for hybrid systems with diverse resource inputs. TEC links the cost of the microgrid's products (electricity, heat, and cold) to the intrinsic quality and origin of input resources, which is crucial for integrating renewable energy sources. Key findings include.

- Seasonal variability and resource performance:
  - Summer: High solar radiation enabled substantial production of electricity and heat from PV, PV/T, and solar collectors, while renewable energy-supported adsorption chillers met cooling needs.
  - Winter: Wind turbines generated the most renewable electricity, but demand often exceeded supply, requiring grid power.
- Role of energy storage - the inclusion of energy storage improved microgrid stability by addressing renewable intermittency, storing surplus summer energy for later use. However, during peak winter demand, storage was insufficient, leading to higher TEC values due to coal-based grid power reliance.
- Resource efficiency - the microgrid demonstrated TEC values below unity for electricity and heat, indicating efficient resource use, with exergy inputs lower than the exergy value of outputs. This highlights the system's resilience under favourable conditions.
- Challenges in achieving ideal sustainability - despite efficient renewable use, achieving a TEC of 0 is unfeasible due to reliance on non-renewable resources and environmental costs. Further optimization of renewable integration and storage technologies is needed to close this gap.
- System adaptability and policy implications - seasonal dynamics highlight the need for adaptable systems. Surplus energy in summer contrasted with winter challenges, emphasizing the importance of diversifying renewable sources, improving storage, and reducing grid dependency. These findings are especially relevant for regions like Poland, where coal reliance exacerbates environmental costs. A resource-efficient approach focusing on local renewables and advanced storage can enhance sustainability.

Incorporating these insights, the study demonstrates TEC's potential as a powerful tool for assessing and optimizing renewable energy systems. It provides practical guidance for designing sustainable microgrids, reducing environmental impact, and improving energy security.

Nomenclatures

| | | |
|---|---|---|
| E | – | energy |
| $I_\beta$ | – | solar radiation |
| A | – | surface |
| Q | – | heat |
| k | – | heat loss coefficients |
| T | – | temperature |
| t | – | temperarure |
| $\dot{W}$ | – | heat capacity of stream |
| $\dot{m}$ | – | mass stream |
| P | – | power |
| B | – | exergy |
| $\Delta T$ | – | difference of temperature |
| $\eta$ | – | efficiency |
| $\tau$ | – | time, hours |
| Indices | | |
| C | – | collector |
| PV | – | PV system |
| PV/T | – | system |
| W | – | turbine |
| E | – | electrolyser |
| FC | – | fuel cell |
| G | – | grid |
| 0 | – | environment |
| ref | – | reference |
| b | – | exergy |
| e | – | energy |
| th | – | thermal |

(continued on next column)

(continued)

## CRediT authorship contribution statement

**Wojciech Stanek:** Writing – review & editing, Supervision, Methodology, Formal analysis. **Agnieszka Szostok:** Writing – original draft, Methodology, Formal analysis, Data curation.

## Declaration of competing interest

The author declare that they have no known competing financial interests or personal relationships that could have appeared to influence the work reported in this paper. Authors declare that there are no conflicts of interest.

## Acknowledgements

This work has been developed thanks to the support from the statutory research fund SUBB of the Faculty of Power and Environmental Engineering of Silesian University of Technology.

## Data availability

The data that has been used is confidential.

## References

[1] Yang J, Su C. Robust optimization of microgrid based on renewable distributed power generation and load demand uncertainty. Energy 2021;223:120043. https://doi.org/10.1016/j.energy.2021.120043. Elsevier.
[2] Østergaard PA, Duic N, Noorollahi Y, Kalogirou S. Advances in renewable energy for sustainable development. Renew Energy 2023;219(Part 1):119377. https://doi.org/10.1016/j.renene.2023.119377. ISSN 0960-1481.
[3] García AM, Gallagher J, Díaz JAR, McNabola A. An economic and environmental optimization model for sizing a hybrid renewable energy and battery storage system in off-grid farms. Renew Energy 2024;220:119588. https://doi.org/10.1016/j.renene.2023.119588. ISSN 0960-1481.
[4] Long Y, Liu X. Optimal green investment strategy for grid-connected microgrid considering the impact of renewable energy source endowment and incentive policy. Energy 2024;295:131073. https://doi.org/10.1016/j.energy.2024.131073. Elsevier.
[5] Mansouri SA, Ahmarinejad A, Nematbakhsh E, Javadi MS, Esmaeel Nezhad A, Catalão JPS. A sustainable framework for multi-microgrids energy management in automated distribution network by considering smart homes and high penetration of renewable energy resources. Energy 2022;245:123228. https://doi.org/10.1016/j.energy.2022.123228. Elsevier.
[6] Thomas J, Sarantakos I, Teo TT. Tackling different services of an energy storage system in a grid-connected microgrid. Renew Energy 2022;195:357–65. https://doi.org/10.1016/j.renene.2022.06.035.
[7] Jiménez-Vargas I, Rey JM, Osma-Pinto G. Sizing of hybrid microgrids considering life cycle assessment. Renew Energy 2023;202:554–65. https://doi.org/10.1016/j.renene.2022.11.103. ISSN 0960-1481.
[8] Hirsch A, Parag Y, Guerrero J. Microgrids: a review of technologies, key drivers, and outstanding issues. Renew Sustain Energy Rev 2018;90:402–11. https://doi.org/10.1016/j.rser.2018.03.040. ISSN 1364-0321.
[9] Liu F, Mo Q, Zhao X. Two-level optimal scheduling method for a renewable microgrid considering charging performances of heat pump with thermal storages. Renew Energy 2023;203:102–12. https://doi.org/10.1016/j.renene.2022.12.031. ISSN 0960-1481.

[10] Zandrazavi SF, Guzman CP, Pozos AT, Quiros-Tortos J, Franco JF. Stochastic multi-objective optimal energy management of grid-connected unbalanced microgrids with renewable energy generation and plug-in electric vehicles. Energy 2022;241:122884. https://doi.org/10.1016/j.energy.2021.122884. Elsevier.
[11] Ouédraogo S, Faggianelli GA, Notton G, Duchaud JL, Voyant C. Impact of electricity tariffs and energy management strategies on PV/Battery microgrid performances. Renew Energy 2022;199:816–25. https://doi.org/10.1016/j.renene.2022.09.042. ISSN 0960-1481.
[12] Restrepo M, Cañizares CA, Simpson-Porco JW, Su J, Taruc J. Optimization- and rule-based energy management systems at the Canadian renewable energy laboratory microgrid facility. Appl Energy 2021;290:116760. https://doi.org/10.1016/j.apenergy.2021.116760. ISSN 0306-2619.
[13] Tooryan F, HassanzadehFard H, Collins ER, Jin S, Ramezani B. Smart integration of renewable energy resources, electrical, and thermal energy storage in microgrid applications. Energy 2020;212:118716. https://doi.org/10.1016/j.energy.2020.118716. Elsevier.
[14] Gomes G, Xu HJ, Yang Q, Zhao CY. An optimization study on a typical renewable microgrid energy system with energy storage. Energy 2021;234:121210. https://doi.org/10.1016/j.energy.2021.121210. Elsevier.
[15] Maimó-Far A, Homar V, Tantet A, Drobinski P. The effect of spatial granularity on optimal renewable energy portfolios in an integrated climate-energy assessment model. Sustain Energy Technol Assessments 2022. https://doi.org/10.1016/j.seta.2022.102827.
[16] Jain A, Yamujala S, Gaur A, Das P, Bhakar R, Mathur J. Power sector decarbonization planning considering renewable resource variability and system operational constraints. Appl Energy 2023;331:120404. https://doi.org/10.1016/j.apenergy.2022.120404.
[17] Sitharthan R, Vimal S, Verma A, Karthikeyan M, Sundar Dhanabalan S, Prabaharan N, Rajesh M, Eswaran T. Smart microgrid with the internet of things for adequate energy management and analysis. Comput Electr Eng 2022. https://doi.org/10.1016/j.compeleceng.2022.108556.
[18] Oliveira L, Messagie M, Mertens J, Laget H, Coosemans T, Van Mierlo J. Environmental performance of electricity storage systems for grid applications, a life cycle approach. Energy Convers Manag 2015;101:326–35. https://doi.org/10.1016/j.enconman.2015.05.063. ISSN 0196-8904.
[19] Jiao Y, Månsson D. Greenhouse gas emissions from hybrid energy storage systems in future 100% renewable power systems – a Swedish case based on consequential life cycle assessment. J Energy Storage 2023;57:106167. https://doi.org/10.1016/j.est.2022.106167. ISSN 2352-152X.
[20] Güven AF. Integrating electric vehicles into hybrid microgrids: a stochastic approach to future-ready renewable energy solutions and management. Energy 2024;303:131968. https://doi.org/10.1016/j.energy.2024.131968.
[21] Alharbi T, Abo-Elyousr FK, Abdelshafy AM. Efficient coordination of renewable energy resources through optimal reversible pumped hydro-storage integration for autonomous microgrid economic operation. Energy 2024;304:131910. https://doi.org/10.1016/j.energy.2024.131910.
[22] Sady H, Rashidi S, Rafee R. Towards a net-zero-energy building with smart control of Trombe walls, underground air ducts, and optimal microgrid composed of renewable energy systems. Energy 2024;294:130703. https://doi.org/10.1016/j.energy.2024.130703.
[23] Ibrahim NN, Jamian JJ, Md Rasid M. Optimal multi-objective sizing of renewable energy sources and battery energy storage systems for formation of a multi-microgrid system considering diverse load patterns. Energy 2024;304. https://doi.org/10.1016/j.energy.2024.131921.
[24] Roldán-Blay C, Escrivá-Escrivá G, Roldán-Porta C, Dasí-Crespo D. Optimal sizing and design of renewable power plants in rural microgrids using multi-objective particle swarm optimization and branch and bound methods. Energy 2023;284:129318. https://doi.org/10.1016/j.energy.2023.129318. Elsevier.
[25] Kozák Š. State-of-the-art in control engineering. Journal of Electrical Systems and Information Technology 2014;1:1–9. https://doi.org/10.1016/j.jesit.2014.03.002.
[26] Stanek W, Gazda W, Kostowski W. Thermo-ecological assessment of CCHP (combined cold-heat-and-power) plant supported with renewable energy. Energy 2015;92:279–89.
[27] Mendecka B, Lombardi L, Stanek W. Analysis of life cycle thermo-ecological cost of electricity from wind and its application for future incentive mechanism. Energy Convers Manag 2018;170:73–81. https://doi.org/10.1016/j.enconman.2018.05.084.
[28] Lombardi L, Mendecka B, Carnevale E. Environmental impacts of electricity production of micro wind turbines with vertical axis. Renew Energy 2017;128(B):553–64. https://doi.org/10.1016/j.renene.2017.07.010.
[29] Tosun DC, Açıkkalp E, Altuntas Ö, Hepbasli A, Palmero-Marrero AI, Borge-Diez D. Dynamic performance and sustainability assessment of a PV-driven Carnot battery. Energy 2023;278:127769. https://doi.org/10.1016/j.energy.2023.127769.
[30] Ünal C, Açıkkalp E, Balta MT, Hepbasli A. Dynamic thermo-ecological cost assessment and performance analyses of a multi-generation system. Int J Hydrogen Energy 2021;46(40):21198–211. https://doi.org/10.1016/j.ijhydene.2021.03.208.
[31] Szostok A, Stanek W. Thermo-ecological analysis of the power system based on renewable energy sources integrated with energy storage system. Renew Energy 2023;216:1–20. https://doi.org/10.1016/j.renene.2023.119035.
[32] Szostok A, Stanek W. Thermo-ecological analysis – the comparison of collector and PV to PV/T system. Renew Energy 2022;200:10–23. https://doi.org/10.1016/j.renene.2022.09.070.
[33] Simla T, Stanek W. Reducing the impact of wind farms on the electric power system by the use of energy storage. Renew Energy 2020;145:772–82. https://doi.org/10.1016/j.renene.2019.06.028.
[34] Stanek W, Czarnowska L, Gazda W, Simla T. Thermo-ecological cost of electricity from renewable energy sources. Renew Energy 2018;115:87–96. https://doi.org/10.1016/j.renene.2017.07.074.
[35] Akyuz E, Coskun C, Oktay Z, Dincer I. Hydrogen production probability distributions for a PV-electrolyser system. Int J Hydrogen Energy 2010.
[36] Stanek W. Assessment of energy efficiency and ecological transformation of TETIP to electro-prosumerism in the environment of the exergetic paradigm – thermoecological cost: electro-prosumerism vs. energetics. https://ppte2050.pl/platforma; 2021.
[37] Newman S, Shiozawa K, Follum J, Barrett E, Douville T, Hardy T, Solana A. A comparison of PV resource modeling for sizing microgrid components. Renew Energy 2020.
[38] Viessmann Polska Academy. Architect, designer and installer's manual – solar collectors. 2013 [in Polish], Viessmann Werke, Allendorf (Eder).
[39] Anderson TN, Duke M, Morrison GL, Carson JK. Performance of a building integrated photovoltaic/thermal (BIPVT) solar collector. International Solar Energy Society 2020.
[40] Gagliano A, Tina GM, Nocera F, Grasso AD, Aneli S. Description and performance analysis of a flexible photovoltaic/thermal (PV/T) solar system. Renew Energy 2017.
[41] Śmigielski Z. Wind power plant complex [in Polish], available online: http://zet10.ipee.pwr.wroc.pl/record/18/files/Wind%20Farm.doc.pdf; 2020.
[42] Stanek W, Gazda W, Kostowski W. Thermo-ecological assessment of CCHP (combined cold-heat-and-power) plant supported with renewable energy. Energy 2015;92:279–89 [Online].
[43] Kotowicz J, Jurczyk M, Węcel D, Ogulewicz W. Analysis of hydrogen production in alkaline electrolyzers. Journal of Power Technologies 2016;96(3):149–56.
[44] Viessmann. Vitocal 242-S typ AWT-AC. available online: http://www.viessmann.com/web/poland/PDF-90.nsf/7a38371490532f7bc125727b002d5e9e/8668cc3dc77c947ac1257b48001ff04f/$FILE/WP%20Vitocal%20200-S,%20222-S,%20242-S%20(05-2011).pdf; 2011.
[45] Liang LL, Riveros-Iregui DA, Emanuel RE, McGlynn BL. A simple framework to estimate distributed soil temperature from discrete air temperature measurements in data-scarce regions. https://agupubs.onlinelibrary.wiley.com/doi/epdf/10.1002/2013JD020597; 2020.
[46] Boryszew ERG. Antifreezes for refrigeration systems [in Polish], available online: https://www.boryszewerg.com.pl/wp-content/uploads/2019/05/dlaczej-warto-stosowac%CC%81-ergolid.pdf; 2019.
[47] Viessmann. Vitocal 222-G. available online: https://www.viessmann.pl/pl/budynki-mieszkalne/pompy-ciepla/pompy-ciepla-powietrzewoda-w-wersji-split/vitocal-222s.html; 2020.
[48] Kopeć P. Calculations and selection of a ground heat exchanger for a heat pump. Journal of Civil Engineering, Environment and Architecture 2015;XXXII(62):167–77 [in Polish].
[49] PKN. Methods for calculating energy losses in buildings caused by ventilation and air infiltration [in Polish], available online: https://sklep.pkn.pl/pn-en-15241-2011p.html; 2011.
[50] Romicki Eko. Ground heat exchangers [in Polish], available online: http://romicki-ekosystem.pl/pl; 2020.
[51] Gado M, Elgendy E, Elsayed K, Fatouh Md. Parametric study of an adsorption refrigeration system using different working pairs. Aerospace Sciences & Aviation Technology, ASAT-17 2017;17. Cairo, Egypt.
[52] EKONTROL. Management of devices and installations [in Polish], available online: https://ekontrol.pl/pl/demo/8; 2020.
[53] Federal Heat Pump Association (BWP) e.V. Guide to preparing hot water [in Polish], available online: https://www.teraz-srodowisko.pl/media/pdf/aktualnosci/1406-Poradnik-przygotowania-cieplej-wody.pdf; 2020.
[54] Stanek W. Exergy analysis in theory and practice. Silesian University of Technology Press; 2016 [in Polish].
[55] Stanek W, Czarnowska L. Thermo-ecological cost – szargut's proposal on exergy and ecology connection. Energy 2018;165(part B):1050–9. https://doi.org/10.1016/j.energy.2018.10.040.
[56] Stanek W. Method of evaluation of ecological effects in thermal processes with the application of exergy analysis. Silesian University of Technology Press; 2009 [in Polish].
[57] Szargut J. Exergy Method: technical and ecological applications. Southampton: WITpress; 2005.
[58] Szargut J, Ziębik A, Stanek W. Depletion of the non-renewable natural exergy resources as a measure of the ecological cost. Energy Convers Manag 2002;43(9–12):1149–63.
[59] Czarnowska L. Thermo-ecological cost of products with emphasis on external environmental costs [in Polish], available online: https://repolis.bg.polsl.pl/publication/24989; 2014.
[60] Faist Emmenegger M, Heck T, Jungbluth N. Erdgas. In: Dones R, editor. Swiss centre for life cycle inventories, final report ecoinvent No. 6-V. Dübendorf: Swiss Centre for Life Cycle Inventories; 2007. Available online: http://www.ecoinvent.org/database/olderversions/ecoinvent-version-2/reports-on-ecoinvent-2/reports-on-ecoinvent2.html.
[61] Szargut J, Stanek W. Thermo-ecological optimization of a solar collector. Energy 2007;32(4):584–90. https://doi.org/10.1016/j.energy.2006.06.010.
[62] Szargut J. Optimization of the design parameters aiming at the minimization of the depletion of non-renewable resources. Energy 2004;29(issues 12–15):2161–9. https://doi.org/10.1016/j.energy.2004.03.019.
[63] Stanek W, Czarnowska L. Environmental externalities and their effect on the cost of consumer products. Int J Environ Sustain Dev 2012;11(1):50–63.

[64] Sciubba E. Thermodynamic measure of sustainability. Frontiers in Sustainability 2021;2. https://doi.org/10.3389/frsus.2021.739395.
[65] Domínguez A, Czarnowska L, Valero A, Stanek W. Thermo-ecological and exergy replacement costs of nickel processing. Energy 2014;72:103–14. https://doi.org/10.1016/j.energy.2014.05.013.
[66] Valero A, Stanek W. Assessing the exergy degradation of the natural capital: from Szargut's updated reference environment to the new thermoecological-cost methodology. Energy 2018;163:1140–9. https://doi.org/10.1016/j.energy.2018.08.091.
[67] Lund H, et al. Renewable energy systems: a smart energy systems approach to the choice and modeling of 100% renewable solutions. Academic Press; 2014.
[68] Farghali M, Osman AI, Chen Z, et al. Social, environmental, and economic consequences of integrating renewable energies in the electricity sector: a review. Environ Chem Lett 2023;21:1381–418. https://doi.org/10.1007/s10311-023-01483-5.
[69] Czarnowska L, Stanek W, Pikoń K, Nadziakiewicz J. Environmental quality evaluation of fossil fuels using LCA and Exergo-Ecological Cost methodology. Chem Eng Trans 2014;42:139–44 [Online].
[70] Stanek W, Czarnowska L, Pikoń K, Bogacka M. Thermo-ecological cost of hard coal with inclusion of the whole life cycle chain. Energy 2015;92:341–8. https://doi.org/10.1016/j.energy.2015.05.042 [Online].
[71] Valero A, Lozano MA, Serra L, Tsatsaronis G, Pisa J, Frangopoulos CA, et al. CGAM problema: definition and conventional solution. Energy 1994;19(3):279–86.
[72] Valero A, Torres C. Thermoeconomic analysis. Oxford UK: EOLSS Publishers; 2006 [accessed Dec 2013].
[73] Tsatsaronis G, Winhold M. Exergoeconomic analysis and evaluation of energy conversion plants e I. A new general methodology. Energy 1985;10:69–80.
[74] Gazda W, Stanek W. Influence of power source type on energy effectiveness and environmental impact of cooling system with adsorption refrigerator. Energy Convers Manag 2014.
[75] Tsatsaronis G. Exergoeconomics and Exergoenvironmental Analysis. Cambridge University Press; 2011. p. 377–401 [Online].
[76] Bejan A, Tsatsaronis G, Moran M. Thermal Design and Optimization. Wiley; 1996 [Online].
[77] Gładysz P, Saari J, Czarnowska L. Thermo-ecological cost analysis of cogeneration and polygeneration energy systems - case study for thermal conversion of biomass. Renew Energy 2020;145:1748–60. https://doi.org/10.1016/j.renene.2019.06.088. ISSN 0960-1481.